Technical Report Documentation Page

1. Report No. FHWA/TX-10/0-5517-1	2. Government Accession No.	3. Recipient's Catalog No.
4. Title and Subtitle Mechanical Properties of Tire Bales for Highway Applications		5. Report Date October 2008; Revised December 2009
		6. Performing Organization Code
7. Author(s) Brian Freilich, Jorge G. Zornberg		8. Performing Organization Report No. 0-5517-1
9. Performing Organization Name and Address Center for Transportation Research The University of Texas at Austin 3208 Red River, Suite 200 Austin, TX 78705-2650		10. Work Unit No. (TRAIS) 11. Contract or Grant No. 0-5517
12. Sponsoring Agency Name and Address Texas Department of Transportation Research and Technology Implementation Office P.O. Box 5080 Austin, TX 78763-5080		13. Type of Report and Period Covered Technical Report September 07–August 09 14. Sponsoring Agency Code

15. Supplementary Notes
Project performed in cooperation with the Texas Department of Transportation and the Federal Highway Administration.

16. Abstract

Scrap tire bales are typically treated as discrete elements that consist of approximately one hundred (100) scrap tires compressed into a 4.5 foot by 5 foot by 2.5 foot block. The advantage of baling tires is that a volume reduction of approximately ten (10) is achieved, and handling bales is much simpler, and therefore cheaper, than whole tire or tire shreds. The use of tire bales in highway structures, however, requires that the mechanical properties of the tire bales are known. Determining these properties is vital to the proper design and construction of the tire bale structures. A literature review indicated the lack of material properties that are available for tire bales. A laboratory testing program was designed and implemented to determine the strength and compressibility properties of the bales required for design. Field testing to determine the unit weight and permeability of the tire bale mass was also conducted. Analytical studies and cost benefit analyses highlighting the benefits of using tire bales already assembled were also conducted for a series of tire bale case histories. The following document outlines all the work conducted as part of this, as well as previous, testing programs to determine the properties needed for design of tire bales structures, as well as economical aspects of reusing the tires as opposed to throwing them away.

17. Key Words	18. Distribution Statement
Scrap Tires, Tire Bales, Lightweight Fill, Drainage, Reinforcement, Tire Disposal	No restrictions. This document is available to the public through the National Technical Information Service, Springfield, Virginia 22161; www.ntis.gov.

19. Security Classif. (of report)	20. Security Classif. (of this page)	21. No. of pages	22. Price
Unclassified	Unclassified	300	

Form DOT F 1700.7 (8-72) Reproduction of completed page authorized

Mechanical Properties of Tire Bales for Highway Applications

Brian Freilich, MSE, EIT
Jorge G. Zornberg, PhD, PE

CTR Technical Report:	0-5517-1
Report Date:	October 2008; Revised December 2009
Project:	0-5517
Project Title:	Beneficial Use of Scrap Tire Bales in Highway Projects
Sponsoring Agency:	Texas Department of Transportation
Performing Agency:	Center for Transportation Research at The University of Texas at Austin

Project performed in cooperation with the Texas Department of Transportation and the Federal Highway Administration.

Center for Transportation Research
The University of Texas at Austin
3208 Red River
Austin, TX 78705

www.utexas.edu/research/ctr

Disclaimers

Author's Disclaimer: The contents of this report reflect the views of the authors, who are responsible for the facts and the accuracy of the data presented herein. The contents do not necessarily reflect the official view or policies of the Federal Highway Administration or the Texas Department of Transportation (TxDOT). This report does not constitute a standard, specification, or regulation.

Patent Disclaimer: There was no invention or discovery conceived or first actually reduced to practice in the course of or under this contract, including any art, method, process, machine manufacture, design or composition of matter, or any new useful improvement thereof, or any variety of plant, which is or may be patentable under the patent laws of the United States of America or any foreign country.

Engineering Disclaimer

NOT INTENDED FOR CONSTRUCTION, BIDDING, OR PERMIT PURPOSES.

Project Engineer: Jorge G. Zornberg
Professional Engineer License State and Number: CA C 056325
P. E. Designation: Research Supervisor

Acknowledgments

The authors express appreciation for the invaluable guidance of the TxDOT Project Director, Mr. Richard Williammee. We are also thankful for the input by members of the PMC, including Randy Hopmann, Woody Raine, John Delphia, Gus Khankarli, Stanley Yin, Darlene Goehl, John Forehand, Claudia Izzo, George Villarreal, Tomas Saenz, and Bill Prikryl. RTI's excellent support by Duncan Stewart and Sylvia Medina is much valued. Finally, the effort of Christine Weber, Jeff Kuhn, and Kuo-Hsin Yang is appreciated.

Table of Contents

List of Figures

List of Tables

Chapter 1. Introduction

Highway structures are typically created using materials that can readily be found at or near the construction site. If the nearby materials cannot maintain the required stability for the structure, engineers must find other cost effective alternatives. In projects where costs need to remain low and space must be conserved, innovative fill materials may be required in order to build the structure at a reasonable cost. Recently, the need for this suitable construction material has forced the Department of Transportation to use readily available scrap tires as the fill material, solving the need for a cheap material as well as a need to properly and safely dispose of the tires.

There have been numerous uses for scrap tires in highway projects, usually in the form of tire shreds or chips. Tire shreds have been commonly used as reinforcement elements mixed with soils, fill material for embankments, and as a fill material for asphalt pavements. Recent environmental and safety concerns regarding the combustion of large tire shred embankments have led to a significant reduction in their use in soil structures (Wappett 2004). Tire bales have recently emerged as an alternative scrap tire fill material for engineering applications because the bales use a significant amount of whole scrap tires, as well as the ease of constructing the tire bale structures as compared to tire shreds. Previous cost benefit analyses have indicated a tax payer savings of $1.60 per tire when used as bales in highway applications rather than disposed of in landfills (Zornberg et al. 2004). Although there is interest in using tire bales as a fill material, the lack of material properties and cost data, and a fear of potential combustion within tire structures have hindered the use of tire bales as a viable alternative.

The overall objectives of this research program are to (1) define and measure the needed tire bale properties for design, (2) determine the feasibility of using tire bales in highway structures, including cost and stability considerations, and (3) develop specifications for the construction and use of tire bales in highway structures. The research program consisted of a series of laboratory and field testing programs to determine the mechanical and index properties of the tires bales. The laboratory testing was completed using innovative and large scale testing setups constructed specifically for this research program. Numerous design considerations, based upon the case history uses of tire bales, were modeled with the testing setups to determine the mechanical properties of the tire bales needed for future design. In addition, a literature review was conducted to determine the environmental impacts of the tire bales in soil structures, including groundwater contamination and the potential for exothermic reactions leading to combustion of the tire bale structure.

Results from the laboratory testing program were then used to study the stability of current scrap tire bale projects to ensure a satisfactory factor of safety. A cost benefit analysis was coupled with the analytical study to illustrate both the economical and mechanical advantages of reusing scrap tire bales in highway structures. A complete set of material characteristics of tire bales, specifications for the use of tire bales in highway structures, and cost benefit analyses will all be presented in the following document.

1.1 Document Outline

The following document covers the research conducted at the University of Texas at Austin over the past two years regarding the use of tire bales in highway structures. The layout of the document is divided into four main themes:

I. Literature review for laboratory and field characterization of tire bales, as well as documented uses of tire bales in case histories,

II. Mechanical and Index properties of tire bales determined from this testing program, coupled with field measurements at the IH 30 tire bale slope,

III. Cost benefit analysis and analytical study conducted using tire bale properties obtained during this testing program, and

IV. Compilations of guidelines and specifications for the use of tire bales in highway structures.

Chapters 2 and 3 present a detailed outline of the literature reviews conducted for this project. Chapter 2 includes a summary of the laboratory data presented for tire bales, as well as outlines the case histories of tire bales in highway applications. A thorough outline and review of the environmental aspects of using tire bales in highway structures is provided in Chapter 3. Contamination potential, durability, and exothermic reactions are all covered in the chapter.

Brief outlines of the materials used throughout the testing programs are outlined in Chapter 4. Chapters 5 through 10 contain all the testing procedures and results from this testing program. The index properties of the tire bales, such as the unit weight and permeability, are presented in Chapter 5. The shear strength of the tire bale structure for dry, wet, and soil infill conditions is presented in Chapter 6. The compressibility of the tire bale structure (tire bale only structures) is presented in Chapter 7.

In Chapter 8, a detailed cost benefit analysis and analytical study are presented for a series of tire bale case histories. Included is a cost comparison and stability/deformation analysis of the tire bale structure compared with other construction alternatives. The cost benefit of using tire bales in regards to the Department is also presented throughout the chapter.

In Chapter 9, results from the field monitoring of the IH 30 tire bale embankments is outlined and compared with data determined from the laboratory component of the project. Both internal and external deformation measurements are presented and compared with the predicted behavior of the tire bale embankment structure presented in Chapter 8.

A summary of the results and conclusions from the analyses is presented in Chapter 11. Specifications for the use of tire bales in highway structures are presented in Appendix A, and an outline of the tire bale construction process is presented in Appendix B. Finally, an outline of all the data obtained during the laboratory and field testing programs is presented in Appendices C through G.

Chapter 2. Literature Review—Tire Bale Properties and Case Histories Reported in the Literature

Properties of tire bales reported from previous research programs can be summarized into three categories:

i. Index Properties (unit weight, volume, specific gravity, etc.)

ii. Mechanical Properties (interface shearing strength, compressibility, creep, etc.)

iii. Hydraulic Properties (hydraulic conductivity, water storage potential, porosity, etc.)

A brief outline of these properties is presented in the following chapter. In addition, construction practices and design of tire bale highway structures is presented to illustrate the state of the practice of tire bale use. At the end of the chapter, a brief discussion of the research topics still required for design is presented.

2.1 Index Properties of Scrap Tire Bales

The index properties of a material are those properties that define the physical attributes of the material. The most basic index properties include the volume and weight. For scrap tire bales, any index property is difficult to define and measure because of the large size, irregular shape, and variability between the different bales. In order to correctly define and measure the properties of a tire bale, as well as have consistency among numerous researchers, the standard form of the bale must first be defined. The standard scrap tire bale, as defined by Zornberg et al. (2005), LaRocque (2005), and Winter et al. (2006), is a mass of approximately 100 whole tires compressed into a block with dimensions of approximately 2.5(height) x 4.5(length) x 5(width) feet (Figure 2.1). Bales have been traditionally held together by five 7-gauge galvanized steel wires. The standard tire baling machine, such as the Encore Systems Baler (www.tirebaler.com), compresses the tires with a hydraulic ram that can reach up to 65 tons of load.

Figure 2.1: Photograph of a Traditional Scrap Tire Bale

The length of the bale is defined as the dimension of the bale parallel to the baling wires, and the width perpendicular (Figure 2.2). The bale volume varies significantly based on how these dimensions are measured. If average values of the length, width, and height are measured,

then the average volume of the bale is defined. When the maximum dimensions are measured, the maximum enclosing cuboid (maximum volume or MEC) is defined. The actual volume cannot be simply measured and must be back calculated from the buoyancy force of a bale submerged (wrapped in an impermeable material) in a water bath (Simm et al. 2004). An outline of the standard tire bale average volumes reported in the literature is provided in Table 2.1.

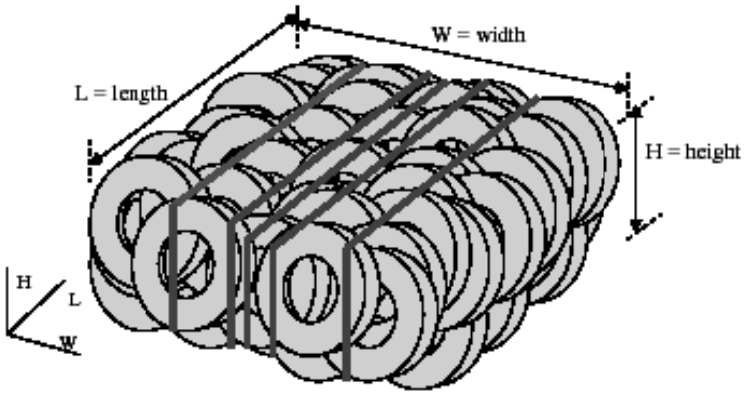

Figure 2.2: Standard Bale Coordinate (Axes) System (LaRocque 2005)

The weight of the standard tire bale is usually assumed to be approximately 2000 pounds (1 ton). However, a significant amount of variability is present since the number and size of the tires used within the bale varies. The weight of standard tire bales, as reported in the literature, ranges from 1630 to 2300 pounds (Zornberg et al. 2005, LaRocque 2005).

The unit weight of the tire bale has been defined as the weight of the tire bale divided by the average volume of the bale. Three unit weights are commonly reported; the as received dry unit weight (no water in the tire bale), the submerged unit weight (tire bale completely submerged), and the wet unit weight (tire bale with water storage), as provided in Table 2.1.

Table 2.1: Average Volume and Unit Weight Values Reported in the Literature

Reference	Volume (ft^3)	Unit Weights (pcf)		
		Dry	Submerged	Wet
Zornberg et al. (2005)	56 ± 3	36.5 ± 3	4.3 ± 1.5	39.5 ± 2
LaRocque (2005)	57.4 ± 5	36.7 ± 4	5.6 ± 1.5	47.1 ± 5
Winter (2006)	57.6	34.5	-	-
Simm et al. (2004)	41.4*	47.4	-	-

* actual volume

It is evident from data reported by Simm et al. (2004) that the bale volume used to determine the unit weight can have a significant effect on the value. The average volume, in general, does not accurately represent the tire bale geometry since it includes voids present along the surface of the tire bale, as illustrated in Figure 2.3. Winter et al. (2006) suggested that the

actual bale volume be used in the unit weight calculations since the effects of submergence and soil infill could easily be taken into account using the following equation:

$$\text{Unit Weight} = 0.72 \cdot \gamma_T + 0.28 \cdot \gamma_S \quad (2.1)$$

where γ_T is the unit weight of the bale using the actual volume and γ_S is the unit weight of the material surrounding the bale (soil, water, etc.). The equation was derived from the observation that 72% of the volume taken up by a bale in a structure is occupied by the tire bale and 28% is void space present around the bale due to the irregular geometry.

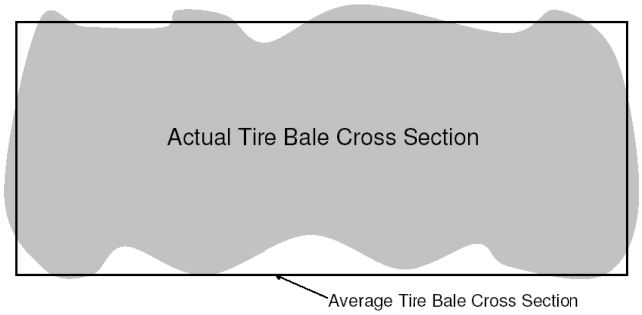

Figure 2.3: Two-Dimensional Illustration of the Average and Actual Volume of a Standard Tire Bale

The specific gravity is defined as the unit weight of solids within the bale, divided by the unit weight of water. The specific gravity was initially calculated to determine if the value was less than one (1) for the tire bale, indicating that the bale would float and therefore would not be suitable for submerged structures. LaRocque (2005) determined the specific gravity by measuring the weight of the dry tire bale (weight of the solids) and of a submerged tire bale, which was used to calculate the volume of solids from the buoyancy force. The specific gravity was therefore defined as the weight of the tires divided by the volume of water displaced times the unit weight of water. Typical values for the specific gravity of tire bales and tire shreds are provided in Table 2.2. It is evident that the form of the tires (whether baled or shredded) does not change the value of the specific gravity since no change to the tire material has been made.

Table 2.2: Typical Values of Specific Gravity for Standard Tire Bales and Tire Shreds

Source Paper	Specific Gravity	Material
LaRocque (2005)	1.14 - 1.23	Tire Bale
Zornberg et al. (2004)	1.07 - 1.14	Tire Bale
Humphrey and Manion (1992)	1.05	Tire Chips
Moo-Young et al. (2003)	1.06 - 1.1	Tire Shreds

2.2 Mechanical Properties of Scrap Tire Bales

The mechanical properties of the tire bale are those properties that can be used to predict the performance of a tire bale structure due to applied loads. The three main properties that have

been reported in the literature are the tire bale interface strength, the compressibility of the tire bale, and deformations associated with sustained loading (creep).

Assuming that the tire bale remains intact during the life of the structure, the most critical weak planes exist along the perimeter of the bale. Simm et al. (2004) estimated the strength along the bale interface by stacking two bales, holding the bottom bale in place, and dragging the top bale along the bottom bale. It was calculated that the friction angle along the interface was approximately 35^{o} based on the normal load along the interface (the weight of one bale) and the shearing load applied to the bale. A series of similar direct shear tests were reported by Zornberg et al. (2005) in which two bales were stacked upon each other, and placed on top of a steel plate supported by steel rollers (Figure 2.4). The normal load was varied along the top bale which was held in place, and the force required to pull the bottom bale out of the arrangement was measured. The authors mention that the test did not perform as expected and that the two bales tended to rotate rather than the bottom bale displacing relative to the top bale. Linear failure envelopes (shearing stress by the normal load) presented by the authors were characterized with Mohr-Coulomb parameters; a friction angle of 25^{o}–30^{o} and a cohesion of 50 psf.

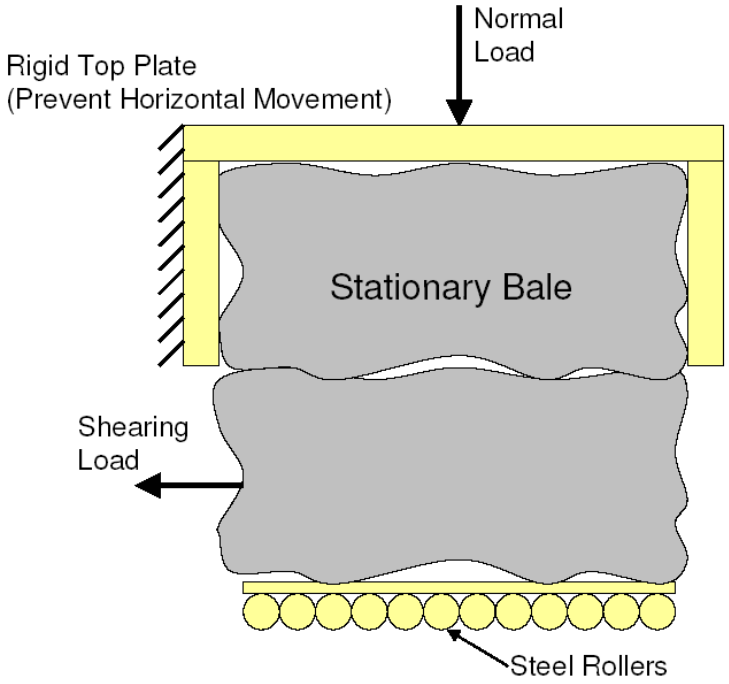

Figure 2.4: Illustration of the Testing Setup for Zornberg et al. (2005)

A more stable testing setup was designed by LaRocque (2005), which consisted of stacking three bales in a pyramid arrangement, applying a variable normal load to the top bale, and measuring the force required to push the top bale past the stationary bottom bales (Figure 2.5). A roller joint was placed at the top of the normal load actuator so that large displacements along the interface could be achieved. Failure was defined as the horizontal load that initiated sliding along the interface, or rigid movement of the top bale. The strength along the interface was defined with a friction angle of 36^{o} and cohesion of 30 psf.

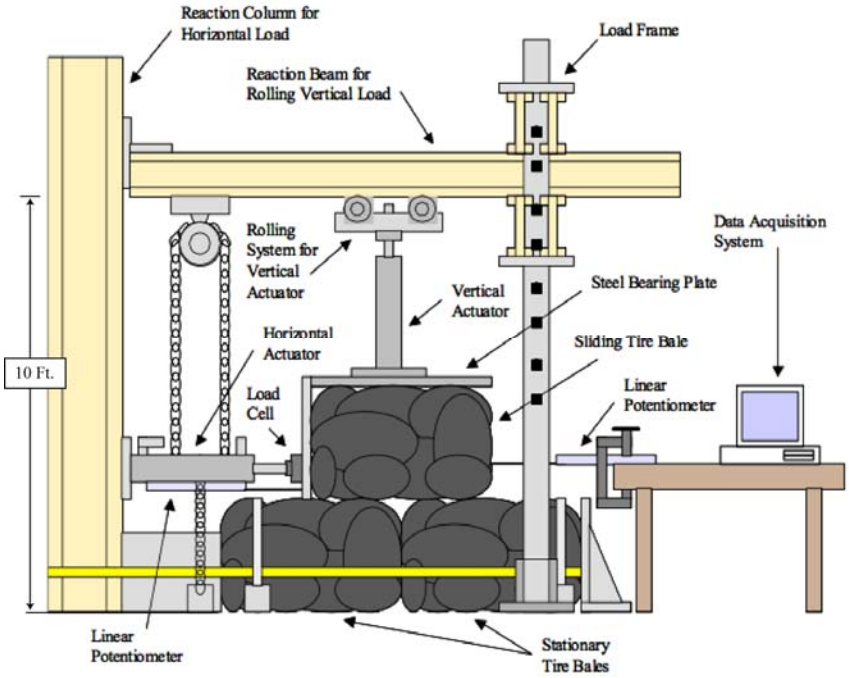

Figure 2.5: Testing Setup for LaRocque (2005)

A summary of the strength parameters from the testing programs is provided in Table 2.3. Although values of the cohesion varied, most likely due to changes in the testing setup, the values of friction angle remained essentially the same.

Table 2.3: Mohr Failure Envelope Parameters from Tire Bale Interface Testing

Reference	Cohesion (psf)	Friction Angle (degrees)
Simm et al. (2004)	0	35
Zornberg et al. (2005)	50	25 - 30
LaRocque (2005)	30	36

The vertical compressibility of a tire bale due to normal loading is another mechanical property that must be considered during the design of the structure. Initial concerns were that large normal loads would cause wire breakage of the bale, and therefore significantly alter the performance of the structure. Jones (2005) reported compression testing conducted at the Colorado School of Mines in which the ultimate normal load (load to cause complete wire breakage) was the variable of interest. Normal loads up to 600,000 pounds (~27,000 psf) were applied to tire bales without ultimate failure; however it was noted that the first wire broke after 150,000 pounds (~7,000 psf) of normal load were applied.

Zornberg et al. (2005) reported compression tests on a single bale in a large compression testing setup (Figure 2.6). Vertical deformations, lateral expansion, and applied load were measured during the testing. The results of the compression testing (Figure 2.7) provided evidence of a non-linear response to loading, with the modulus (stress/strain) increasing

significantly after applied stresses above 4 ksf (4000 psf). The maximum compressive strain exhibited by the bale was 60% at the maximum loads. It is also apparent that there was no ultimate failure of the bales, which was defined as a maximum stress which caused a destruction of the bale or all the wires breaking.

Figure 2.6: Large Compression Test Setup (Zornberg et al. 2005)

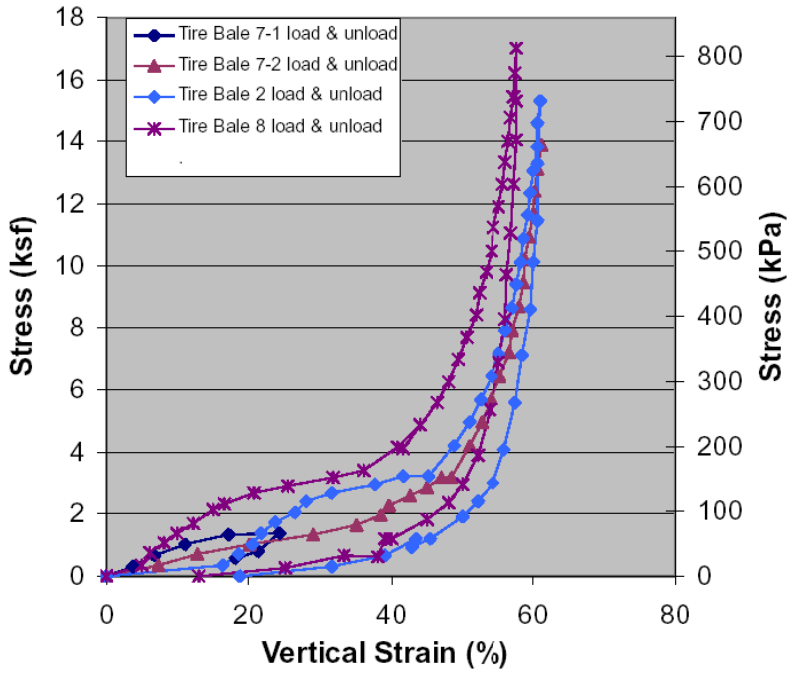

Figure 2.7: Results from One Dimensional Compression Testing (Zornberg et al. 2005)

The influence of soil confinement on the bale compression was determined by surrounding the bale with compacted sand during compression. The presence of the surrounding soil increased the modulus (slope of the stress-strain curve) of the bale by more than 35% (see Figure 2.8).

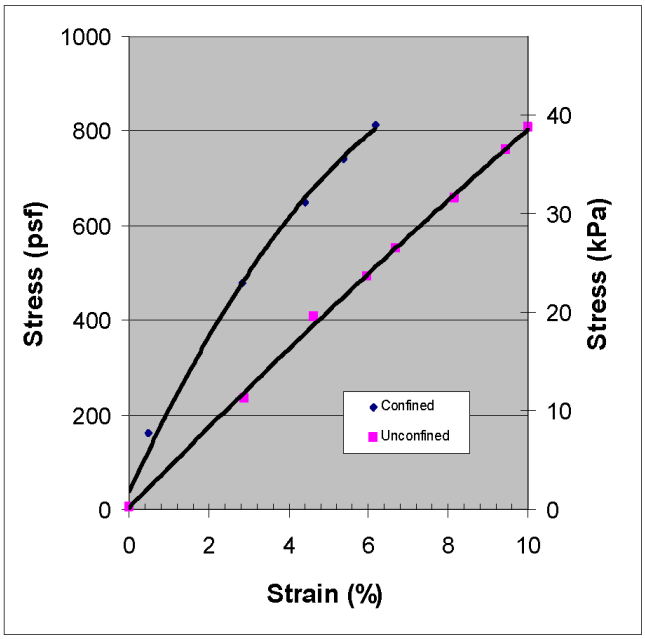

Figure 2.8: Influence of Confinement on Stiffness of a Tire Bale (Zornberg et al. 2005)

LaRocque (2005) also conducted one dimensional compression testing on tire bales under different stacking arrangements and under confined and unconfined conditions. Illustrations of the two stacking conditions are shown in Figure 2.9. Confinement was achieved by hand tightening three nylon cargo straps around the bale. Typical results from the testing are shown in Figure 2.10 for the three bale arrangement.

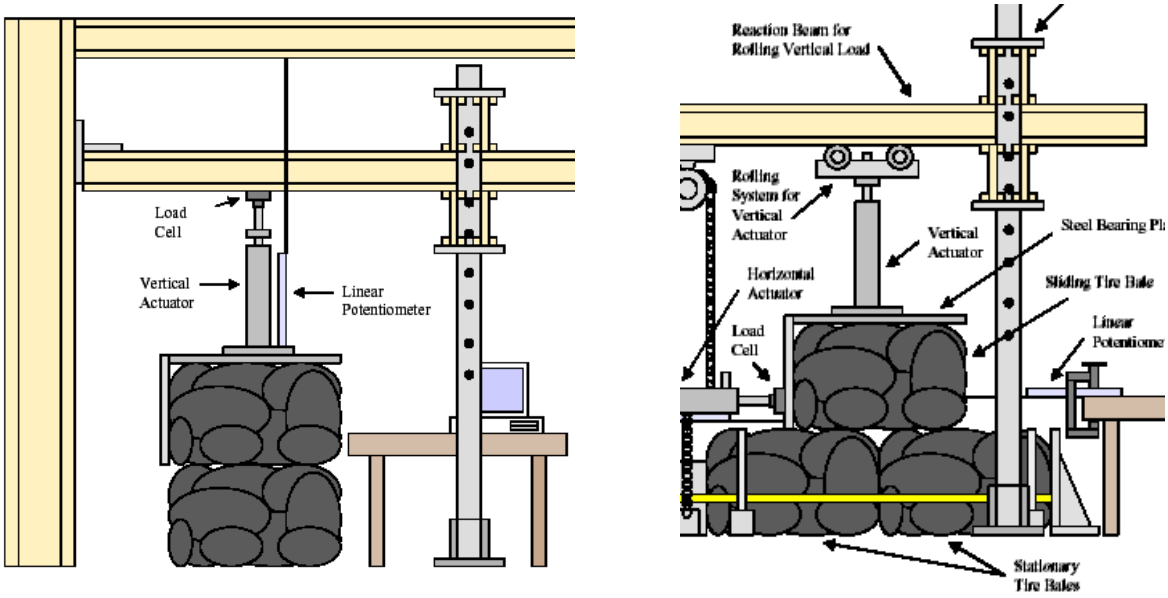

(a) Two Bale Stacking *(b) Three Bale Stacking*

Figure 2.9: Illustration of the Two Different Bale Arrangements (LaRocque 2005)

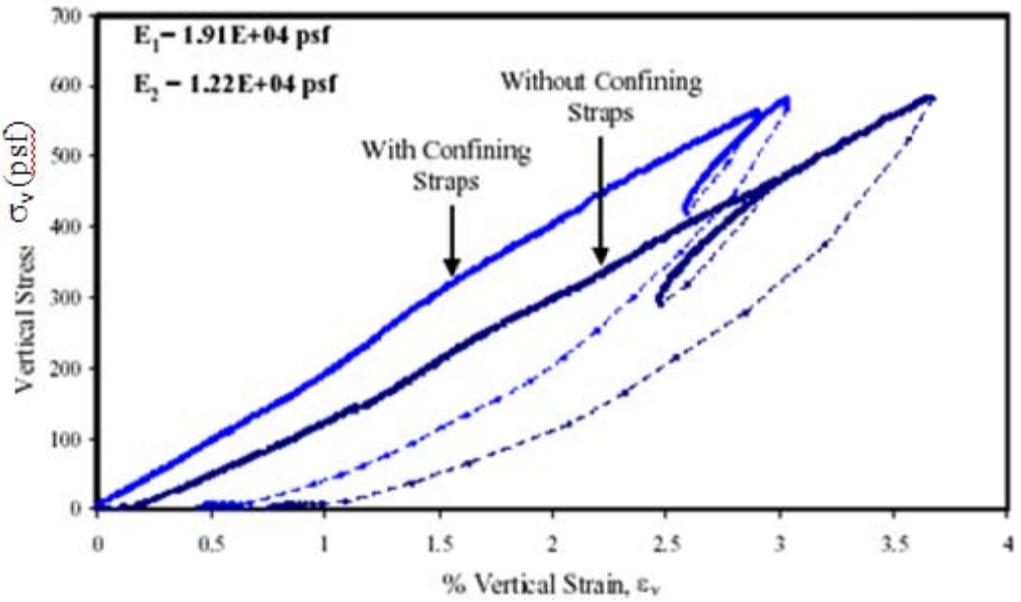

Figure 2.10: Compression Testing Results from the Three Bale Arrangement (LaRocque 2005)

The modulus values, or slopes from the loading curves, from the tests are provided in Table 2.4. Results provided evidence that confinement increased the modulus of the bales, and that the stacking of the bales can significantly influence the stiffness of the mass (two bale structure was stiffer than three bale structure). This influence of the tire bale structure may be related to the change in contact area of the interfaces, in which the contact area of the two bale structure is higher (stresses are lower) than the three bale arrangement (stresses are higher).

Table 2.4: Modulus Values from Compression Testing Reported by LaRocque (2005)

Bale Arrangement	Simulated Confining Pressure	Modulus, E (psf)
3-bale	Yes	1.91E+04
3-bale	No	1.22E+04
2-bale	No	1.35E+04

An important aspect that can be observed in the curves shown in Figures 2.7 and 2.10, and also reported by Jones (2005), is the permanent strain of the bale after the compressive loads are removed. Jones (2005) reported significant plastic deformations of the bales in the lab, but did not measure this phenomenon in the field for bales stacked up to ten bales high. LaRocque (2005) measured permanent strains of 0.5 to 1% for compression tests.

As an extension of the compression testing, sustained loading (creep) tests were conducted by Zornberg et al. (2005) and LaRocque (2005) to determine the amount of vertical deformation caused by sustained normal loading. Typical results from the testing are shown in Figure 2.11 and 2.12 from the research programs. Zornberg et al. (2005) reported that 95% of the compression occurred within the first 24 hours, with creep strains never exceeding 1.5 mm for sustained loadings of 314 and 815 psf. The creep strain rate was estimated to be approximately

0.005% of creep strain per day. LaRocque (2005) reported maximum creep strains of less than 0.053% of the original bale height after 72 hours of sustained loading at 400 psf.

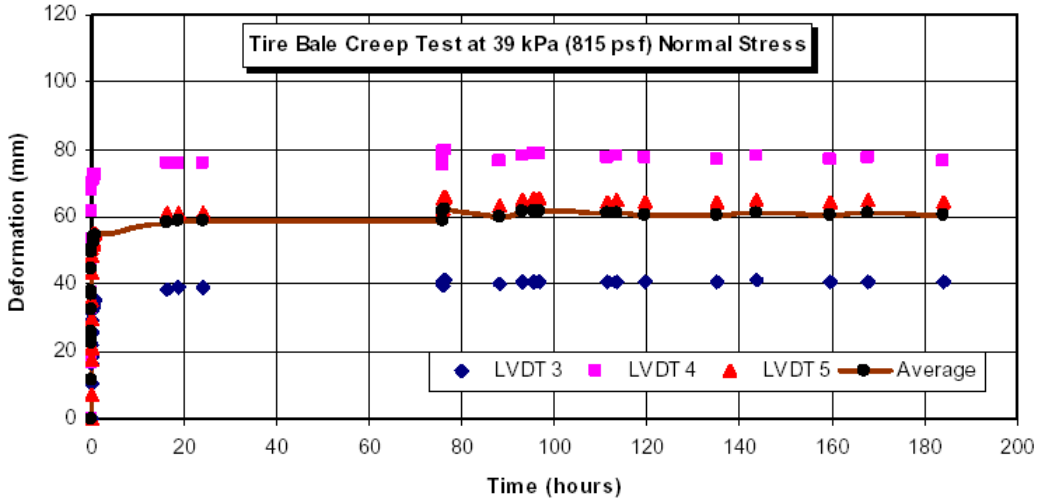

Figure 2.11: Creep Test Results from Single Bale Arrangement (Zornberg et al. 2005)

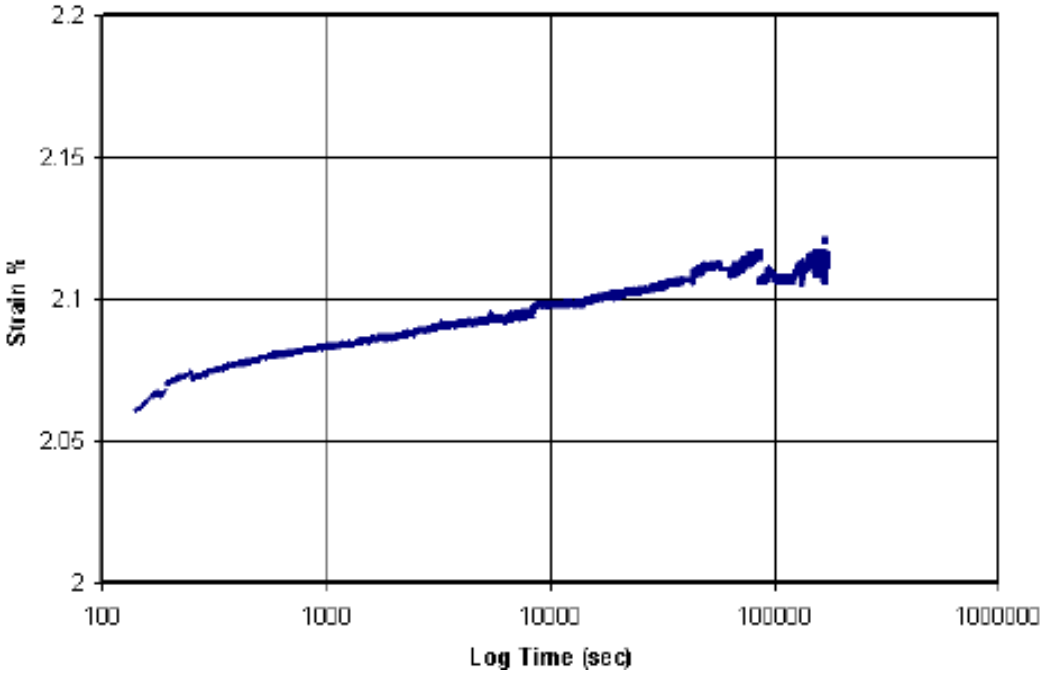

Figure 2.12: Creep Test Results from Three Bale Arrangement (LaRocque 2005)

LaRocque (2005) also conducted a series of sustained shear loading tests to determine the effects of sustained horizontal loading on the interface strength of the tire bales. It is unclear what normal load was applied to the bales (it is assumed the interface normal load was 400 psf). Sustained horizontal (shear) loads of 64.5 (25% of the peak shear stress), 130.9, and 163.7 (75% of the peak shear stress) psf were applied to the mobile tire bale. The horizontal displacement

rate (horizontal displacement with time or horizontal creep) for the bale ranged between 1 to 6.6 inches per day, indicating a significant creep deformation along the interface. The testing method used for the sustained loading may not be appropriate to measure shear creep strains since the creep strains due to normal loading along the interfaces was not isolated.

Zornberg et al. (2005) also reported the results of cyclic compression testing for a single tire bale in which a load of 9000 pounds was applied at a 1±0.5 Hz frequency for 1000 cycles. Bales were tested under both unconfined and confined conditions as described previously. The results of the tests are shown in Figure 2.13. The maximum deformation was reached after approximately 100 cycles for both the unconfined and confined cases. It is evident that the deformations of the confined bale were less than that of the unconfined bale, which is in agreement with the data reported for cyclic testing. The minimum deformations, which represent the permanent deformations of the bales, were similar for both confined and unconfined conditions.

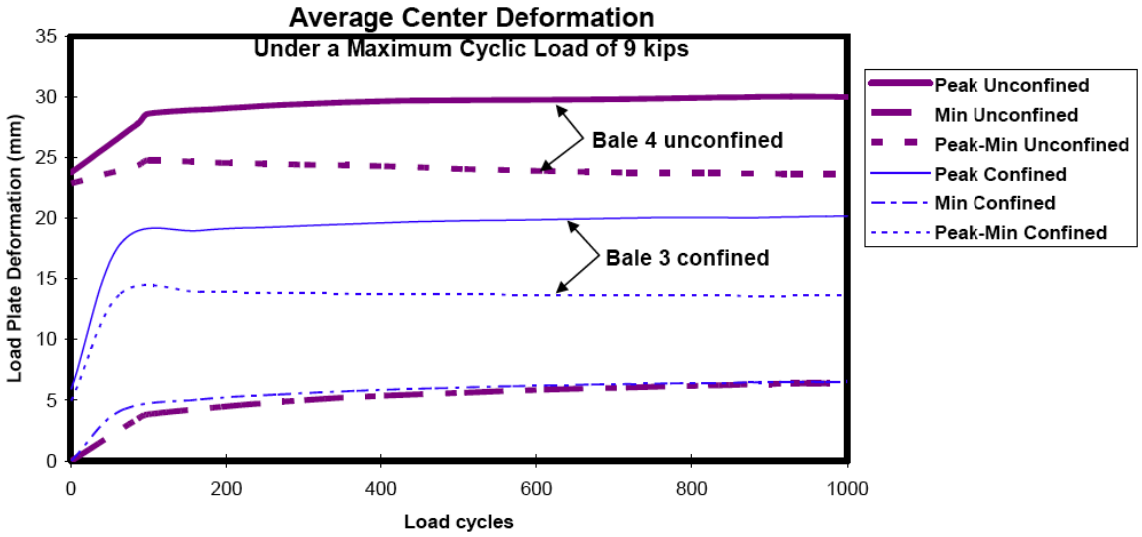

Figure 2.13: Cyclic Compression Testing Results for a Single Bale (Zornberg et al. 2005)

2.3 Hydraulic Properties of Scrap Tire Bales

The ability of the tire bale mass to act as a drainage medium is controlled by the permeability of the mass. Simm et al. (2004) measured the permeability (k) of a single tire bale in a high discharge flume. Permeability was measured along the length of the bale (parallel to the baling wires) and along the width of the bale (perpendicular to the baling wires), with values of k ranging from 4 cm/s and 14 cm/s, respectively. LaRocque (2005) estimated the vertical permeability of the bales by saturating the bales in a water bath and measuring the change in weight with time after the bales were removed (reporting values of permeability of approximately 0.4 cm/s. Zornberg et al. (2005), reported values for the vertical permeability ranging from 0.05 to over 0.1 cm/s).

2.4 Case Histories of Tire Bales in Soil Structures

Although obtaining lab data is an important aspect of engineering design, valuable lessons and data can be found from the review of case histories in which scrap tire bales have

been used. Four groups of case histories have been identified during the course of the literature review. These case histories have provided a significant insight into the use of tire bales in highways structures. The four groups are briefly outlined in the following sections.

2.4.1 Group 1—Road Foundations over Soft Soils

The simplest application of tire bales in highway engineering is the use of the bales as a base course material for roadways. The use of tire bales is especially advantageous when constructing a roadway over soft soils, in which heavier materials would cause excessive settlement and placing a surcharge or removal of the material would be required (Winter et al. 2006). Care must be taken during construction to ensure that voids between the bales are minimized by placing the bales close together and filling around the bales with course grained soil (typically sand). Drainage from the tire bale layers must also be provided to ensure that the bales do not hold water, especially in areas where freezing can occur. A geotextile is traditionally also placed around the bales to reduce any soil ingress into the bales and to help bind the bales together. Case histories of the use of tire bales as a roadway foundation have been outlined by Winter et al. (2006) and Zornberg et al. (2004), and have been constructed in the UK (Figure 2.14), New York, Pennsylvania (Figure 2.15), and Texas. Winter et al. (2006) notes that one roadway project in the UK has performed satisfactory despite the heavy loadings caused by a large number of logging trucks using the road.

The main advantage of using the tire bales is the cost savings associated with not having to preload the soft ground surface, or removing the existing soils and bringing in an appropriate granular sub-base material (refer to Chapter 8). Zornberg et al. (2004) outlined a cost analysis of a roadway in Chautauqua County, New York in which the cost savings of using tire bales rather than conventional methods was approximately $3,050 per 1000 feet of roadway, and that the taxpayer savings were $1.60 per tire in comparison to disposing the tires.

Figure 2.14: Lightweight Tire Bale Road Construction (www.angloenvironmental.com/tyre_blocks_anglo.php)

Figure 2.15: Use of Tire Bales as Roadway Subgrade in Pennsylvania (www.dep.state.pa.us/dep/deputate/pollprev/starrTirePile/Images/IMG_0193)

General Tire Bale Roadway Construction Sequence

One of the advantages of using tire bales as a subgrade material is the ease of construction as compared to a traditional flexible soil subgrade. Two types of tire bale subgrades have been identified in the literature review (Winter et al. 2006):

- Floating Subgrade—tire bales are placed directly on the ground surface.
- Buried or Excavated Subgrade—an excavation is made into the foundation soils where the tire bales are to be placed.

The only difference in the construction of the two different subgrades is the need for an excavation for the buried tire bales. The general construction sequence of the roadway is illustrated in Figure 2.16. The general construction sequence is as follows:

1. Prepare or excavate the foundation material and provide a flat working surface,
2. Place an appropriate geotextile along the foundation material, making sure that enough material is left along the edges to cover the sides of the bales,
3. Place bales along the roadway, with the alignment of the baling wires parallel to the roadway direction,
4. Compact a soil fill around the bales, typically a dry sand or gravel that can easily be placed in the voids present between bales,
5. Wrap the extra geotextile material around the bales, and
6. Construct the roadway as specified.

Figure 2.16: Photograph of a Roadway with a Single Layer Tire Bale Subgrade (www.lstire.com/images/bale_job_during_resized.jpg)

2.4.2 Group 2—Embankment Remediation/Reinforcement of IH 30 Slope Failures

The second case history outlines the remediation of two sections of embankment failures along IH 30 in Fort Worth, Texas. Phase One of the embankment reconstruction involved placing reinforcing layers of tire bales along the height of the re-compacted soil slope (illustrated in Figure 2.17 a). The orientation of the bales was not specified, and individual bale layers were supposed to be placed 6-8 inches apart so that they could be encapsulated with soil, most likely a method to limit exothermic reactions (LaRocque 2005). The tire bales were, however, placed in contact with each other during the construction, creating a series of planar reinforcement layers of tire bales within the soil embankment. Each tire bale reinforcement layer was then separated with 6-8 inches of compacted soil. It was also noted that the embankment was not completed initially due to the lack of bales available at the site. The availability of tires is also a topic that is covered by Winter et al. (2006), in which the first criterion for using tire bales is that there is a sufficient supply available.

Phase Two of the IH 30 embankment repair was initiated due to slope failures directly adjacent to the previously repaired Phase One repair. The cause of the slope failure was concluded to be water stored in the tire bale reinforcement layers seeping into the adjacent slope (Figure 2.18). The second phase was reconstructed using only a tire bale mass to recreate the slope (a general illustration is shown in Figure 2.17b), with a compacted soil cover and drainage layer beneath the bales. The actual Phase Two embankment consisted of a tire bale mass three bales high, as shown in general construction methods provided in the next section. The tire bales were also covered by a geotextile to prevent flow of soil into the voids of the tire bales.

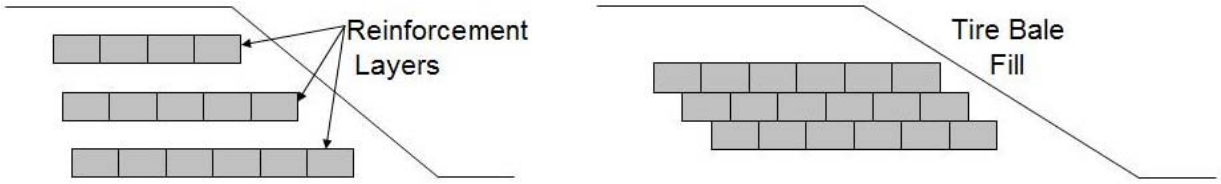

(a) Reinforcement Layers *(b) Slope Fill Material*

Figure 2.17: Illustrated Examples of the Proposed Tire Bale Uses within Soil Embankments

Figure 2.18: Water Flow from the Tire Bale Reinforcement Layers (LaRocque 2005)

Examination of the IH 30 case histories illustrates two methods for the use of tire bales in highway projects. The most notable properties that controlled the stability of the slope were the high permeability of the tire bale mass, and the significant water storage potential of the bales. Phase Two of the slope reconstruction included a drainage layer and horizontal drainage pipe to remove water from the tire bale mass. The addition of the drainage layers is a necessary step for two reasons:

- Removal of water from the bales ensures that seepage from the bale mass into the surrounding soils (especially the compacted soil cover and surrounding soil slopes) is reduced, decreasing stability problems within the soil.
- The submerged unit weight of bales is lower than the dry/wet unit weight (as outlined in Table 2.1), and therefore submerging the bales may decrease the stability of the structure.

General Tire Bale Embankment Construction Sequence

The construction sequence of the tire bale embankment for the IH 30 slope remediation projects illustrates the use of tire bales both as a fill material and a reinforcement material. The construction sequence of both structures is similar; the only difference being the placement of intermediate soil layers between tire bale layers for the reinforced slope. The general construction sequence, which is a review of both of the IH 30 tire bale reinforced and tire bale fill embankment construction projects, is as follows (ftp.dot.state.tx.us/pub/txdot-info/gsd/pdf/baledtires.pdf, LaRocque 2005, and Prikryl et al. 2005):

1. Excavation and removal of the failed soil; preparation of the foundation surface.

2. Placement of a drainage layer, such as a geotextile, gravel rip-rap layer, or both.

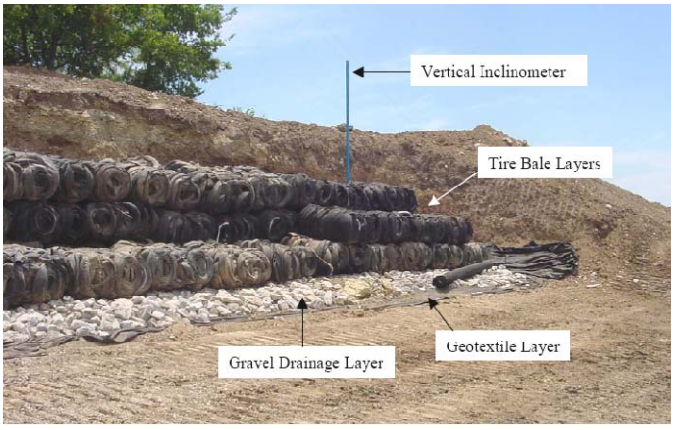

3. Placement of the tire bale layers (usually with random orientations).

4. Placement and compaction of an intermediate soil layer if required.

5. Compaction of a soil cover to protect bales and allow vegetation to grow.

2.4.3 Group 3—Lightweight Earthen Dam/Embankment Fills

In order to construct larger embankments, a large footprint area may be required to provide the required slope stability. However, if the required amount of land is unavailable, excessive settlements are expected, or the needed amount of proper material is not available, a lightweight material alternative is required. Two case histories that exemplify the use of tire bales as a lightweight fill material are the Arkansas dam construction (Rooke 2001, www.eagle-equipment.com/enviroblock.html) and the River Witham flood defense embankment expansion (Simm et al. 2004).

Numerous proposed uses of tire bales used as fill material in earthen dams are reported in the literature. The most notable was a project reported by Rooke (2001) in which tire bales were to be used as a fill material around a compacted clay core dam. It was estimated that approximately 4.5 million tires would be used in the project and the impounded water would improve the communities' fire insurance rating of about $200,000. Data pertaining to the performance or construction of the dam has not yet been found. However, one reference did provide a few photographs of the construction of the dam, which used 1 million scrap tires (www.eagle-equipment.com). A photo of the tire bale fill layers between compacted soil layers, which formed the outer shell of the clay core dam, is shown in Figure 2.19.

Figure 2.19: Tire Bales Used as a Fill Material in the Outer Shell of an Earthen Dam (http://www.eagle-equipment.com/enviroblock.html)

Another proposed use of tire bales as a lightweight fill material was for the expansion of the River Witham flood defense embankments. The thick soft peat materials under the pre-existing embankments (Figure 2.20) required that either a large footprint for the soil embankment was used, or that a lightweight fill material was needed. Tire bales were chosen as the fill material due to:

- The low density of the bales (~1/3 that of soil),
- Steeper slopes could be constructed, saving on required land,
- Larger volumes of bales could be shipped in on barges at one time due to lower weight,
- Bales could be placed no matter the weather conditions, and
- No need to locate potential soils to construct embankment.

The expansion plan of the embankment is shown in Figure 2.21 and actual construction photographs are provided in Figure 2.22. It is important to notice that a geotextile separator is included above and below the bales, and drainage is provided from the bale mass. Approximately 1.2 million whole tires (or 12,000 tire bales) would be needed to complete the project. It was also mentioned that the baling wires were reinforced by geosynthetic straps due to the expected corrosion of the baling wires and the need for a 200 year design life of the bales.

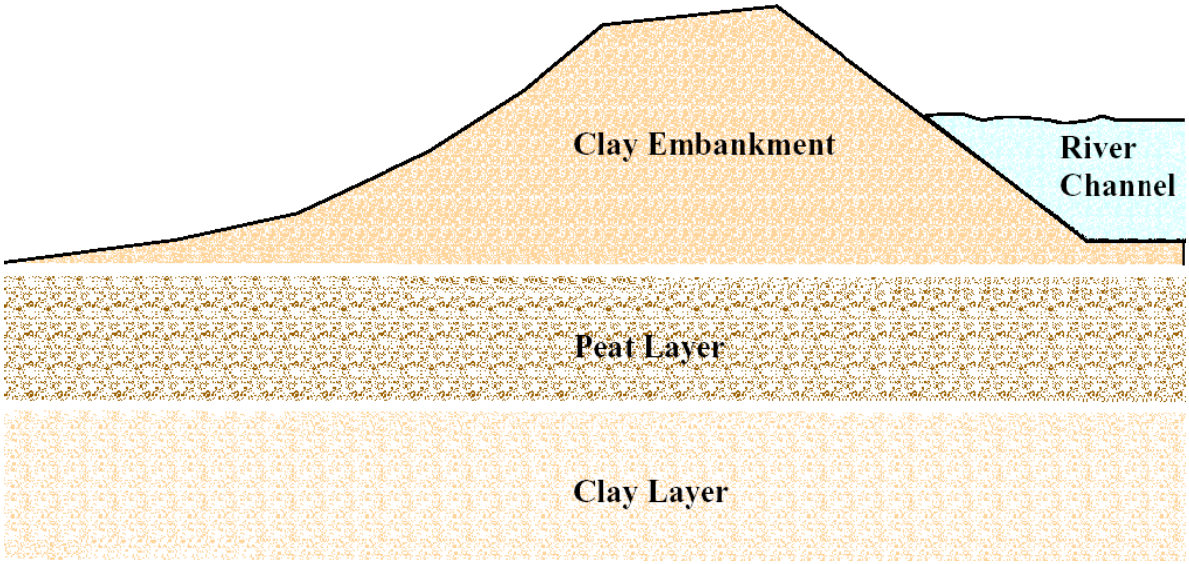

Figure 2.20: Existing Soil Profile under the Flood Embankment (Simm et al. 2004)

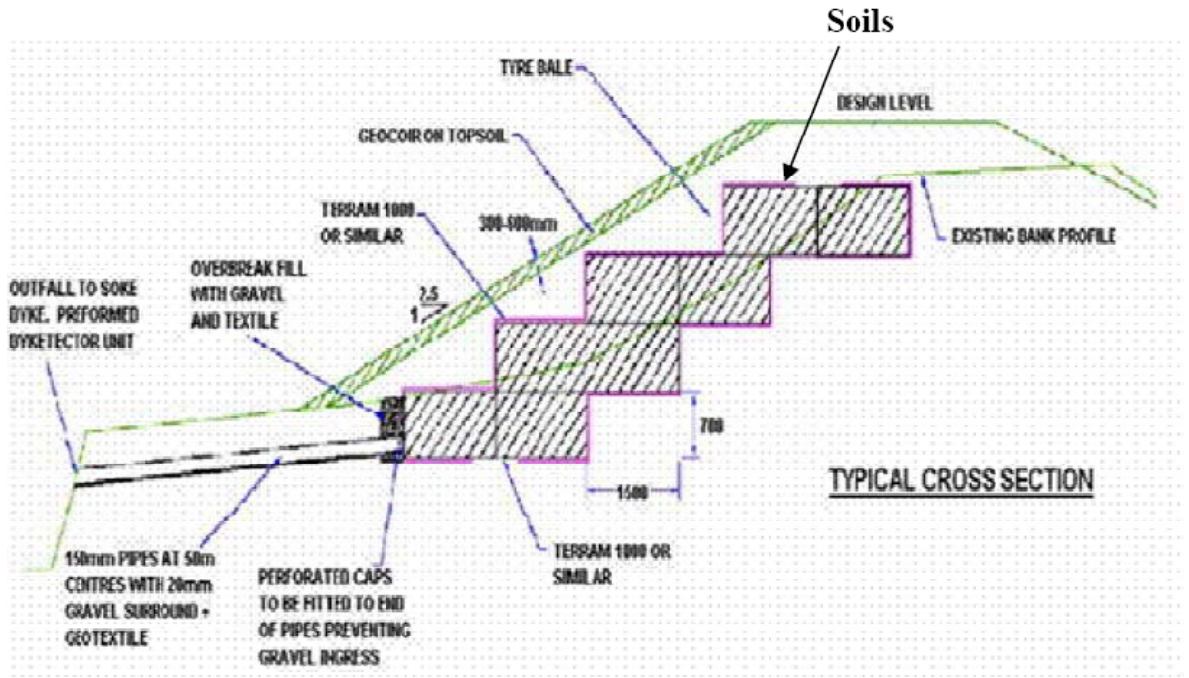

Figure 2.21: Expansion Plans for the Flood Defense Embankment (Simm et al. 2004)

Figure 2.22: Proposed Expansion to Flood Embankment (www.angloenvironmental.com/tyre_blocks_anglo.php)

The main cost-benefit of using tires bales as a lightweight fill is the reduction in the structure footprint and materials needed. Zornberg et al. (2005) estimated the cost benefit of using a tire bale core for a number of Colorado Department of Transportation (CDOT) projects was $2.80 to $7.40 per cubic yard as compared to conventional earthen fill materials.

2.4.4 Group 4—Gabion Gravity Retaining Walls

Tire bales can also be used as modular blocks to construct a gravity retaining wall, as illustrated by numerous retaining walls built by the New Mexico Department of Transportation (Duggan 2007, Hudson 2008). For both walls, the tire bales replaced the expensive gravel fill commonly used in a gabion gravity wall. A schematic of the tire bale wall constructed along US 550 is shown in Figure 2.23. The use of tire bales reduced the weight and size of the wall needed while still providing adequate factors of safety against sliding and overturning. It was also noted that the wall was less labor intensive to build as compared to a traditional gabion wall. In order to reduce the voids between bales, and also limit the movements along the interfaces of the bales, steel bars were used to tighten the layers of tire bales together as well as hold the bales in place, as shown in Figure 2.24.

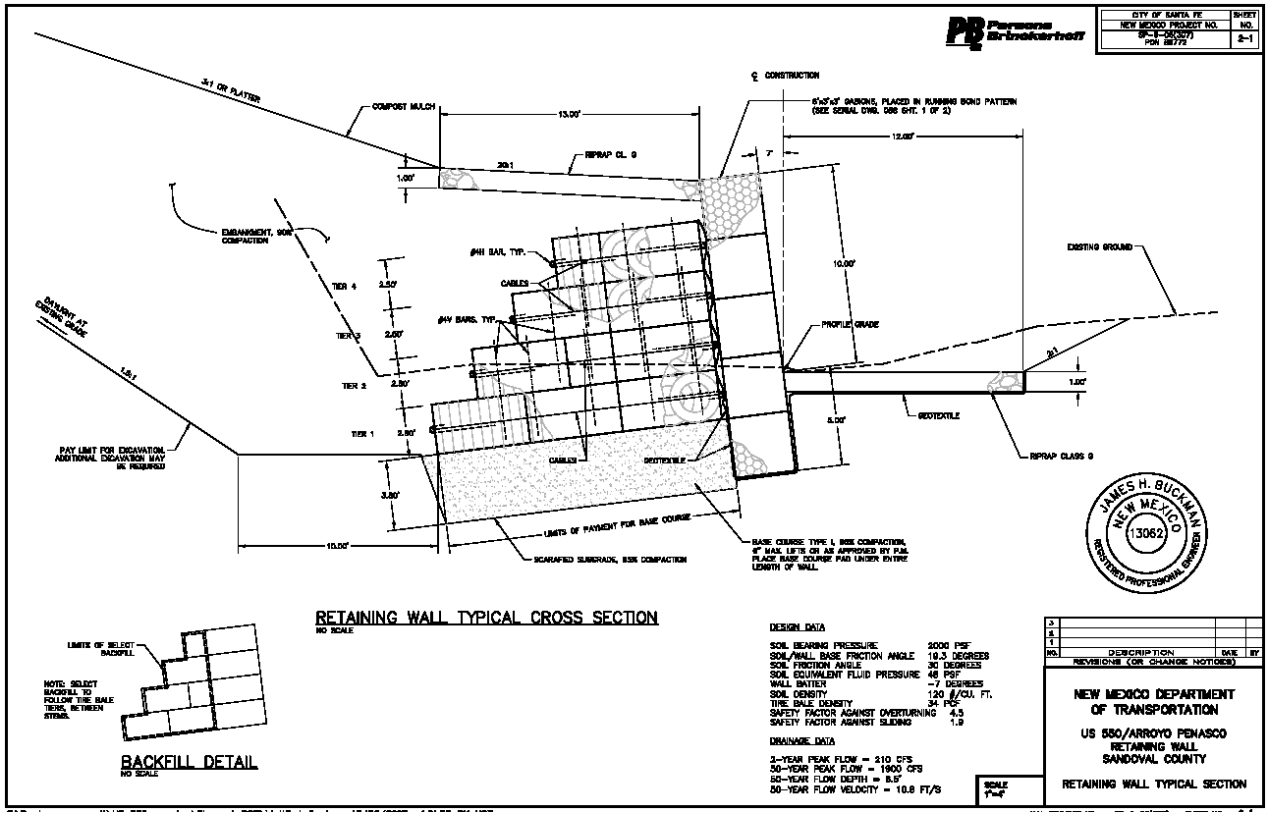

Figure 2.23: First Layer of the Tire Bale Gabion Retaining Wall (Duggan 2007)

Figure 2.24: Design Schematic of the Tire Bale Gabion Retaining Wall (Duggan 2007)

General Tire Bale Embankment Construction Sequence

The use of tire bales in gabion retaining walls replaces the very expensive and labor intensive gravel filled baskets that traditional walls are constructed of. The use of tire bales is therefore much simpler and quicker than the gravel alternative, which requires that gravel is manually placed in each gabion basket. In general, the construction sequence is similar to that of the tire bale embankment and roadway, in that a foundation must be prepared and tire bales placed in a predefined manner. The general construction sequence for a tire bale gabion walls is as follows (all photographs provided by NMDOT, Duggan 2007, and Hudson 2008):

1. Excavate and prepare a flat foundation material. NMDOT reported constructing at least one foundation with a tilt to increase the resistance to sliding along the foundation.

2. Unwrap gabion cage material and place tire bales.

3. Wrap gabion cage around bales and secure.

4. Continue process until wall is complete. Tire bales can be used to create any geometry and curvature of wall.

5. Place retained soil fill behind wall. It is recommended to place some form of gravel or soil cover on the tire bales.

2.4.5 Overview of Design and Construction of Tire Bale Structures

From the brief review of the case histories provided, a basic construction methodology for tire bale structures can be defined. It is important to note that only draft or recommended specifications for the design of tire bale structures were found during the literature review. However, research data and field experience has been reported that supports many of the construction requirements found in the case histories. The general construction methodology for a tire bale structure is as follows:

1. Preparing a flat ground surface, excavating any high areas, and filling any voids along the foundation. The NMDOT specified the excavation/compaction of a slightly tilted foundation, towards the direction of loading, to increase the normal load along the bale interface and therefore increase the shearing resistance along the interface, as well as increasing the compression of the structure.
2. Placement of a suitable geotextile along the ground to prevent soil inflow/outflow from the tire bale mass. Winter et al. (2006) also suggested placement of a thin sand layer over the top of the geotextile to provide protection to the geotextile and a working platform for equipment.
3. Addition of a suitable drainage layer surrounding the tire bale mass. Drainage can be provided by simply placing a horizontal pipe from the bale mass to the surface of the structure. TxDOT installed a gravel drainage base for the IH 30 site in order

to allow the vertical flow from the bales to be collected and removed from the slope.

4. Placement of the bales with the orientation of the bale wires parallel to the direction of loading. The orientation of the bales is usually specified as the length of the bales (parallel to the baling wires) placed in the direction of maximum loading. Winter et al. (2006) suggested that bales be placed in a checkerboard fashion with the baling wire parallel to the direction of maximum loading. It is also important to ensure that the bales are placed close together and that the geometries of the bales are inspected before placement. All testing reported thus far on the strength of the tire bale interface has only considered the strength parallel to the baling wires.
5. The design for the tire bale mass can also specify filling the voids between bales with soil and wrapping a geotextile around the tire bale mass. Filling the voids with soil, although optional, is usually recommended to reduce soil ingress between bales and can also act as a packing between the bales to reduce lateral movements due to normal loading (stiffening the tire bale mass). If no soil infill is used, it is recommended that bales be placed together as tightly as possible to increase confinement and reduce horizontal and vertical deformations. The two functions of the geotextile separator are to reduce soil flow into the voids of the tire bales and to bind the tire bales together.
6. The last stage of constructing the structure is placement of a suitable soil cover over the tire bales. The soil cover protects the tires from UV rays, reduces the temperature changes within the tire bale mass, limits the amount of water and air entering the bale mass, and also prevents damage to the baling wires. The main concern that compels designers to include a soil cover is exothermal reactions within the bale mass that can cause combustion. Humphrey (2004) indicates that a soil cover of at least 3 feet significantly reduced the temperature variations within tire shred embankments, and that tire shred embankments with this minimal soil cover did not show any signs of exothermic reactions. The type of soil cover is not required for tire bale masses but is included as a precautionary measure. No specifications for the soil cover were found and have ranged in design from highly plastic clays to gravel gabion covers.

The benefits of the construction process, which in many aspects is simpler then the construction of the soil structures, is discussed in Chapter 8.

2.5 Discussion of Research Needs

The literature review presented in the previous sections is a broad outline of the research programs and case histories available. Although there have been many uses for tire bales in highway structures, there is still not much lab or field data to support the use in many other situations. From a review of the proposed and actual uses of tire bales, and from data reported in the literature, a general outline of research still required is proposed. The following research needs, as based upon this literature review, are as follows:

- Long term considerations for tire bales: The tire bales are only effective as modular blocks as long as the baling wires are intact. Some testing has been conducted on the expansion of bales after wires have been cut, but no data exists on how this influences shear strength, vertical compressions of the bale and horizontal pressures applied by the bale to surrounding medium. It is important to understand what influence time and surrounding condition has on the effectiveness of bales to act as a solid block.
- Effect of soil and moisture along the tire bale interfaces: Tire bale structures have been constructed under numerous geometries and designs. Two aspects that have not been accounted for are the effects of water and soil infill on the interface strength of the tire bale. Moisture especially can have a detrimental effect on the interface strength and stability of the structure if not taken into account.
- Quality Control and Quality Assurance for production of tire bales: Although a standard tire bale and reduced volume tire bales have been defined, there are no specifications that control the quality of the bales used. Simple specifications can be researched and defined that describe the acceptable range in bale dimensions, bale weight, and even tensions in the baling wires.
- Environmental Concerns of Tire Bales: The use of tires in soil structures leads to the question of whether or not contamination and exothermic reactions should be a concern. This topic will be covered in the next section, however it will be concluded that not much data exists for whole tires. Much of the research presented will be for tire shreds, which is the same material, but in a different form.

Chapter 3. Literature Review—Environmental Impacts of Using Scrap Tires in Highway Structures

A literature review was conducted to obtain data pertaining to the environmental issues of using tire bales in soil structures. Three main topics will be discussed in this chapter:

1. Durability of tires and tire bales in soil structures.
2. Contamination due to the use of tires in soil structures.
3. Exothermic reactions of tires in stockpiles and in soil structures.

Although many of the research programs reported in this chapter deal with the use of tire shreds, the data is still applicable to the use of whole tires and tire bales in the soil structures.

3.1 Durability of Tires

The effect of the environment on the material structure of tires has not been a concern in the design of whole tire and tire shred structures. Tires, in general, are inert materials that do not significantly react with water or soil causing a loss in material structure, or degradation of the tire with time. The following section outlines the degradation concerns of whole tire and tire bales, and design approaches to reduce any degradation that may occur.

3.1.1 Durability of Whole Tires

The main cause of degradation of tires is exposure to UV radiation. Winter et al. (2006) reported field evidence that at least five to ten years of exposure to UV radiation was needed before the effects of the degradation (sidewall cracks and brittle rubber behavior) were observed. Antioxidants added to the rubber to prevent the degradation, such as carbon black, sulphur oxide and zinc oxide, can be leached out over time increasing the degradation rate of the tires. Temperature may also have a slight effect on the degradation process, but is insignificant when compared to UV degradation. In order to reduce the degradation of tire due to temperature and UV radiation, a soil cover is usually placed over any tire mass. The soil cover acts as a shield, separating UV radiation and temperature changes from the tire mass, and also as a medium for vegetation to grow.

Field experience also suggests that the presence of soil and water do not degrade the tires. Zornberg et al. (2005) reported that whole tires removed from a landfill after 50 years were still in good condition. Winter et al. (2006) reported that 60,000 tires submerged and buried along Lake Superior for 40 years did not show any signs of degradation. Although there is not a significant amount of research data collected on the long term behavior of buried tire bales, field experience indicates that tires would not degrade under normal buried or submerged conditions.

3.1.2 Durability of Tire Bales

The durability of tire bales is not controlled by the durability of the tires, but by the durability of the baling wires. Typical tire bales use 7-gauge (0.1443 inch diameter) galvanized steel wires to confine the bales, which are assumed to have corrosion rates of approximately 4 to 15 μm/year and therefore will not provide adequate restraint after some time. The expected

restraint time of the wires is further reduced due to damage during construction and increased degradation due to the placement of surrounding soil infill. For many tire bale structures, the expected lifetime may be more than the restraint time of the baling wires. Therefore, some consideration must be given to the behavior of the bales after wire breakage.

LaRocque (2005) and Winter et al. (2006) both conducted rapid expansion testing of tire bales to determine the behavior of the bales after wire breakage, in which the baling wires were cut and the expansion deformations were measured (Figure 3.1). Winter et al. (2006) conducted the testing immediately after construction of the bales, and found that the length of the bale increased to almost twice the bale length (expansion of over 5 feet). LaRocque (2005) conducted the expansion tests for bales constructed over a year earlier, and measured horizontal expansions of almost 3.3 feet. The results from the two programs indicate that there may be a loss in expansion potential with time, and therefore a reduction in wire tension with time. A more in-depth analysis of the rapid expansion testing will be presented in Chapter 5.

Figure 3.1: Rapid Expansion Testing of Tire Bales (LaRocque 2005)

3.2 Contamination Potential of Tire Structures

Placement of tires underground leads to the concern of the effect of the tires on the ecosystem, most notably the groundwater. Most of the research conducted in this area is concerned with tire shreds, which is considered the worst case condition since shredding increases the surface area of the rubber and exposes the reinforcing steel that would otherwise be covered in tire bales. Significant amounts of research have been conducted to determine what contaminates are introduced to the soil and groundwater due to the tire structure. Data for both whole tires and tire shreds is presented in this section.

3.2.1 Contamination due to Whole Tires

Collins et al. (1995; 2002) presented results for whole tires placed in marine conditions, and concluded that contaminates were only released from the outer surface (a few micrometers) of the tires, and the rate of contaminates released by the tires decreased with exposed time. Zinc was one of the main contaminates of interest that was measured. Hylands and Shulman (2003) conducted a series of lab and field studies of tire structures and reported that all regulated metals

and organics present in the leachate were well below regulatory levels. Only small traces of volatile organics were found, but were 10-100 times less than the regulatory levels.

3.2.2 Contamination due to Shredded Tires

Field and laboratory studies on the effect of tire shreds on water quality have been extensively reported in the literature. Humphrey et al. (1997b) reported contaminate concentration results from a field study of a tire shred embankment above the water table. Leachate from both a tire shred section and a soil only control section had similar metal concentrations for primary drinking water standards. Leachate from the tire shred section did have higher concentrations of manganese and iron (metals in the secondary drinking water standards), which was attributed to the exposed steel. All volatile and semi-volatile organics measured were below detectable limits.

Humphrey and Katz (2001) reported results from a field study in which 1.4 metric tons of tire shreds were buried in a trench below the water table. Contaminate concentrations were measured upstream, downstream, and at the site to determine the effects of the tire shreds. Levels of iron, zinc, and manganese were elevated at the site, but decreased to near background levels with distances of 0.6 to 3 meters downstream. The level of iron also increased slightly with time, most likely due to iron oxide (rust) precipitating into the water. Volatile compounds such as benzene were measured in the groundwater, but were almost non-detectable and much less than the drinking water standards. It was also determined that the environmental conditions influenced the concentration of contaminates found in the groundwater. Higher concentrations of metals were found in acidic environments, while higher concentrations of organics were found for basic environments. All concentrations were still below water and safety standards.

Moo-Young et al. (2003) conducted a series of laboratory tests to determine the effects of flowing and static water on the concentration of contaminates for tire shreds. Tire shreds placed in a tap water bath decreased the pH of the water from 7.95 to 6.98, which was attributed to the acidic interaction between the steel and water. Column flow tests consisting of rain water flowing through a tire shred mass indicated that the effluent water had an increase in organic carbon and iron concentration, a decrease in pH, and an increase in turbidity (increase in particulate matter in the water, attributed to rust particles in the water); all of which decreased after 2-4 days of flow. Results from pause flow testing, in which water was stopped in the column for a period of time, indicated an increase in iron concentration and turbidity with time, attributed to the exposure of the steel belting and formation of rust.

3.2.3 Summary of Contamination Potential—Design of Tire Structures

The research presented in this section has provided sufficient evidence that using tires, whether shredded or whole, in soil structures does not create a contamination problem if proper design guidelines are followed. All metal and organic contaminates found in the groundwater were below drinking water and safety standards for all environments (acidic or basic). However, some design standards have been proposed to further limit the contamination potential due to tire shreds in soil structures. Wappet (2004) listed a few of the design limitations for tire shred structures, which included wrapping the tire shred section with a geomembrane, using tire shreds only above the water table, and limiting the amount of tire shreds that can be used. In the case of tire bales, in which the tires remain whole, it can be assumed that the data collected for whole tires is most applicable and that any contaminants present due to the tires would be insignificant and therefore not a concern.

3.3 Exothermic Reactions within Tire Structures

The potential costs and environmental damage due to the combustion of a tire mass warrants the need for stringent design considerations to reduce the risk of tire fires. In terms of whole tires, fires are usually started due to the ignition of fuel or other contaminates at the site that initiate the actual tire fire. The ignition of these fires is usually some form of arson, lightning strike, adjacent organic fuel, or faulty electrical wiring and can be avoided by properly stockpiling tires. When dealing with tire shreds, a separate phenomenon is encountered in which heat is generated within the tire shred mass, causing combustion of the tires. The following section outlines research conducted to determine the cause of the heat generation within the tire shred embankments, and how the results should influence the design of tire bale structures.

3.3.1 Case Histories of Combustion in Tire Shred Embankments

Prior to 1997, over 70 tire chip fill applications had experienced problems with fumes, heat generation, or even open flames (Humphrey 2004, Winter et al. 2006). Three case histories that highlight the use of thick tire shred fills in engineering structures and the resulting fire problems are presented in the section.

The first case history is a slope remediation project in Il Waco, Washington where tire shreds were used as a lightweight fill material to reconstruct a highway damaged due to a landslide (constructed in 1996). The tire shreds used were 4–6 inches in length and 2 inches wide. The dimension of the tire chip fill was 140 feet long and 25 feet deep (illustration shown in Figure 3.2). The tire chip fill was underlain by a rock fill drainage layer and compacted beneath 4.5 feet of soil and crushed rock fill. It was noted that during construction, 4.8 inches of rain fell onto the tire shred fill (tire shreds became wet). Two months after the completion of the fill, a 75-foot-long crack was observed in the pavement and attributed to settlement of the structure. Three months after completion, heat and steam were observed rising from the tire shred section (Figure 3.3). A monitoring program was initiated (Humphrey 1996) and temperatures of 130^{o}F to 160^{o}F were measured within the tire shred mass.

Five months after the completion of the fill, significant settlements were measured and liquid petroleum products were detected seeping from the base of the tire shred mass. The tire shred section was subsequently removed, with over 13,000 tons of tires and contaminated material removed, at a cost of $3.2 million (WA DOT 2003).

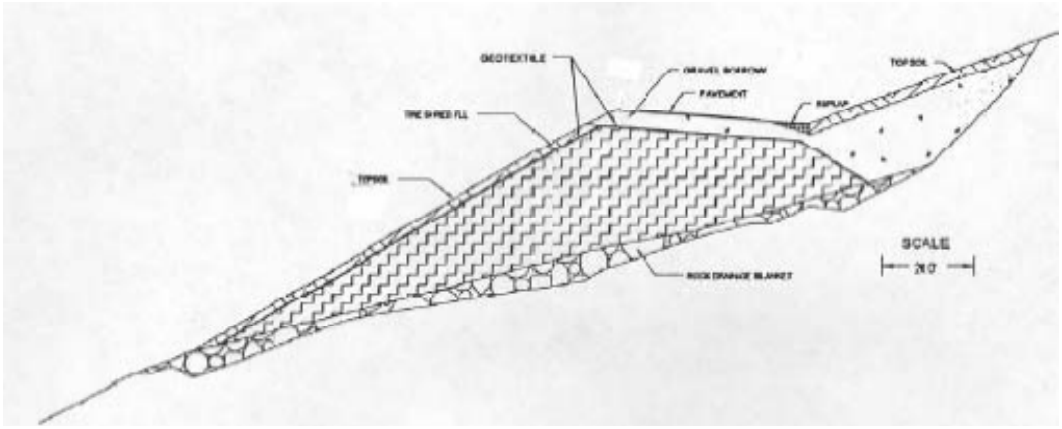

Figure 3.2: Illustration of Tire Shred Fill for Il Waco, Washington Highway Remediation Project (Wappett 2004)

Figure 3.3: Removal of Tire Shred Section from Il Waco, Washington (Wappett 2004)

The second case history is a tire shred embankment contracted across a ravine in Garfield County, Washington in 1995. Tire shreds were used as a lightweight fill to construct the embankment, which was 225 feet long and almost 50 feet in height, with over 16,500 cubic yards of tire shreds used. A flash flood in July 1995 blocked the drainage pipes through the embankment and water ponded behind the embankment to almost 30 feet. Three months later, steam was observed coming from a fissure on the upstream face of the embankment. Within another three months (January 17, 1996) open flames were reported on the embankment face at the base of the structure (Humphrey 1996). Remediation of the embankment cost approximately $2.5 million.

The final case history is a multilevel geogrid reinforced retaining wall constructed using a tire shred backfill (Fitzgerald 2003). Rainfall occurred during the construction of the wall (tire shreds were wet after completion of the wall in 1994). In the summer of 1995, evidence of internal heating of the wall was observed, and in October of 1995 a fire was observed in the 6th level of the retaining wall.

3.3.2 Potential Causes of Combustion in Tire Shred Embankments

The previous case histories of tire shred fires illustrate the favorable conditions in which combustion of tire shreds occur. Conditions present in all three case histories that have been hypothesized to increase the heat generation and subsequent combustion in the structures are:

- Thickness of the tire shred fill—thicker tire shred fills provide higher insulation and limit the air to the lower levels. It has been observed that the combustion of the tire shreds occurs close to the base of the structure, where the insulation is highest and water can potentially pond.
- Particle size—It was noted that for the two case histories in Washington, smaller tire shred sizes were used, increasing the surface area of the tires and also increasing the amount of exposed steel.
- Moisture Conditions—The presence of moisture was present during the construction and life time of the structures.

Humphrey (1996, 2004) outlined potential causes of the heat generation within the tire shred structures based off of observations made from the case histories. The potential causes, as discussed in WA DOT (2003), Fitzgerald (2003), and Wappett (2004), include:

- Oxidation of the exposed steel wires—The iron in the exposed steel undergoes oxidation, which is an exothermic reaction. Approximately 2,623 Btu of energy are released per pound of iron oxidized, which indicates that only 0.095 pounds of steel would be needed to raise the temperature of 1 cubic foot of tire shreds by 10^{o}F (Wappett 2004). The oxidation of the iron increases with temperature (so as heat is generated, the exothermic reaction is increased), acidic conditions, and presence of water.
- Microbes generating acidic conditions—Certain types of bacteria can oxidize the iron in the steel and sulfur in the tire rubber. The oxidation process is exothermic, which contributes to the heat generation, and also increases the acid concentration which can increase the oxidation of the steel wires and increase the heat generation.
- Oxidation of the tire rubber—The oxidation of rubber is an exothermic reaction that occurs at temperatures above 200 to 250^{o}F (Moo-Young et al. 2003). Although unlikely that this temperature would be reached under normal conditions, it is still mentioned as a contributing factor to the heat generation.

3.3.3 Tire Shred Properties that Influence Heat Generation: Lab and Field Studies

The heat generation of the tire shred structure is influenced by the tire shred thermal properties and the design of the structure. Field and Laboratory studies have been conducted on tire shred embankments and stockpiles to determine not only how the heat generation is caused, but how it can be reduced with proper design. The following section outlines research conducted to determine the thermal properties of tire shreds and how design effects the hear generation.

Chen (1996) conducted a series of laboratory experiments to determine the thermal conductivity, or insulating, properties of tire shreds. The thermal conductivity reported (referred to as the apparent thermal conductivity) is a thermal property of the tires that is influenced by the conduction, convection, and radiation heat transfers from the tire shred mass. It was assumed that the convection and radiation heat transfers are too insignificant to measure or separate from the conduction heat transfer, especially in a porous medium. In order to calculate the thermal conductivity, it was assumed that:

1. Heat transfer was one-dimensional and evenly distributed throughout the specimen.
2. The thermal properties were constant throughout the specimen.
3. Heat loss caused by radiation was negligible, as was heat loss due to convection between the tire shred mass and the testing apparatus.

Humphrey et al. (1997 a) summarized the laboratory results and compared them with field measurements of the thermal conductivity of tire shreds. The laboratory measured apparent thermal conductivity of tire shreds decreased from 0.32 to 0.20 W/m^{o}C (Watts per meter degrees Celsius) as the density increased from 0.58 to 0.79 Mg/m^{3}. The thermal conductivity also increased 40% as the temperature gradient increased from 22.3^{o}C/m to 68.5^{o}C/m. The thermal conductivity determined in the field ranged from 0.19 to 0.20 W/m^{o}C. The results from this

testing indicate that at the lower sections of the embankment, where combustion has been found to initiate, the conductivity of the shred mass is lowest. Therefore any heat generated at the base is lost at a much slower rate, or heat is generated faster than it is dissipated.

Shalaby and Khan (2002) conducted field studies of large tire shreds (150–300 mm in length) used as lightweight subgrade fill for a roadway constructed over soft ground. Thermocouples were used to measure temperature with depth in both the tire shred fill and the surrounding soil to determine the thermal gradients. The back-calculated thermal conductivity of the tire shreds for steady-state conditions was approximately 0.2832 W/m^{o}C, almost a fifth of the value of the soil.

Nightingale and Green (1997) conducted laboratory studies to determine the conditions needed for combustion of tire shred layers compacted to a density of 400 kg/m^3. For a 3 meter thick tire shred layer, combustion occurs at temperatures around 70^{o}C. Increasing the layer thickness to 6 meters reduced the combustion temperature to 60^{o}C, indicating an inverse relationship between height of the tire shred mass and the critical temperature at which combustion occurs. The data implies that as the tire shred height increases, the heat generation required to achieve combustion decreases.

In the previous studies, no consideration was given to any heat generation within the tire shred mass, which is the mechanism that initiates any combustion within the structure. Wappett (2004) conducted field studies on a tire shred stockpile and a series of tire shred embankments to determine both the thermal conductivity of the tire shreds as well as measure any heat generated within the different structures. Along with a tire shred only stockpile, three embankments 5 feet in depth and 30 feet long were constructed; a soil only embankment, a soil embankment with 6 inch compacted tire shred layers, and a tire shred-soil mixture embankment with 10% shreds by weight. Temperatures, moisture content, heat flux (at the surface only), and relative humidity were measured with depth in the structures. The apparent thermal conductivity of the tire shred structures were calculated using a finite-difference scheme during dry periods (no rainfall) assuming one-dimensional conduction within the structure and negligible heat transfer due to radiation and convection (Table 3.1). It was noted that the tire shred thermal conductivity was much less than the soil only value, but mixing the tire shreds with the soil actually increased the conductivity.

Table 3.1: Apparent Thermal Conductivities for the Tire Shred Embankments and Stockpile Calculated by Wappett (2004)

	Material			
	Soil Only Embank.	**Layered Embank.**	**Mixed Embank.**	**Tire Shred Stockpile**
Density (pcf)	122	100	112	40
Heat Capacity (Btu/lb ^{o}F)	0.2054	0.1924	0.197	0.1211
Thermal Conductivity	**(Btu/hr ft ^{o}F)**	**(Btu/hr ft ^{o}F)**	**(Btu/hr ft ^{o}F)**	**(Btu/hr ft ^{o}F)**
Dry Period 1	0.981	1.082	1.152	0.518
Dry Period 2	1.196	1.258	1.573	0.151
Dry Period 2	1.252	1.353	1.596	0.31
Average	1.143	1.231	1.44	0.326

The heat generated within the embankments was calculated using the thermal conductivities and mass heat capacities (found in the literature) in Table 3.1 and the equation for one-dimensional heat transfer (Equation 3.1). A finite-difference scheme was then used to incrementally solve for Eq. 1 and the heat generation rate (q, in units of Btu/ft^{3}hr) within the structures with time and depth (Equation 3.2). The heat generation calculated, in general, was defined as a variable that explained any generation of heat within the tires that could not be predicted using the general heat transfer equation in Eq. 3.1 (Note that the q term is the only difference between Eq. 1 and Eq. 2). Integrating over time gives the cumulative heat generated within the structure (in units of Btu/ft^3). Results from both dry and wet conditions for the embankment structures (both soil and tire shred-soil) provide evidence that in general there is a loss of heat within the embankment with time, or an endothermic reaction (Figure 3.4). Wappett hypothesized that this may also be due to heat being removed from the embankment at rates faster than it was being generated.

$$k\frac{\delta^2 T}{\delta z^2} = \rho \cdot C\frac{\delta T}{\delta t} \tag{3.1}$$

$$q = \rho \cdot C\frac{\delta T}{\delta t} - k\frac{\delta^2 T}{\delta z^2} \tag{3.2}$$

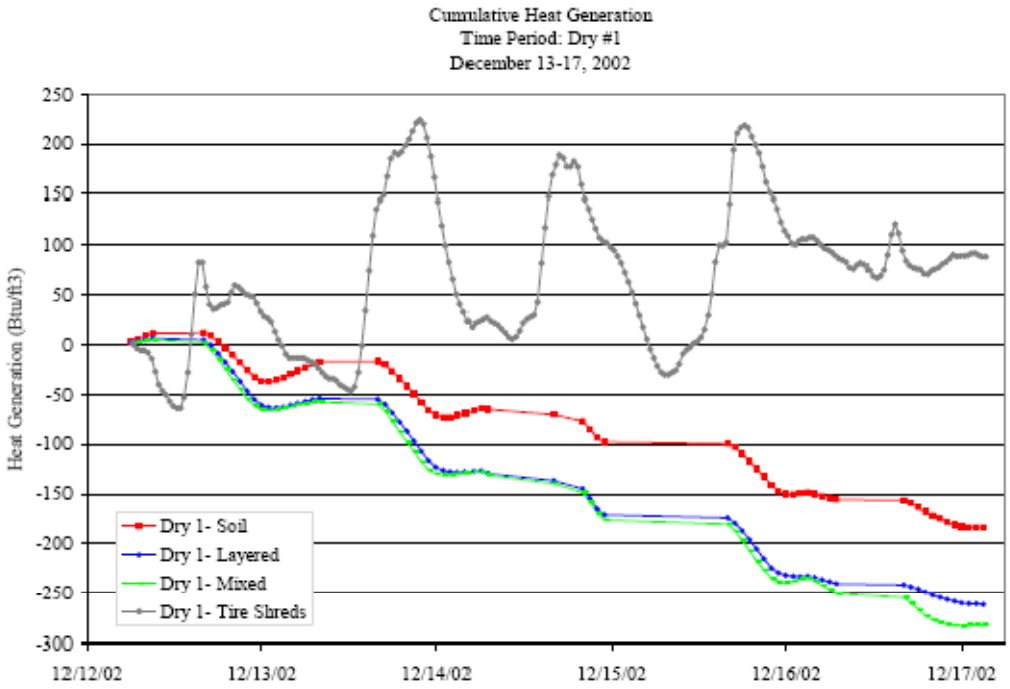

Figure 3.4: Cumulative Heat Generated Within the Tire Shred Embankments and Stockpile with Time for the First Dry Period (Wappett 2004)

Only few time periods show an increase in heat with time, and correlate with the wet and dry periods. Only the tire shred stockpile had an increase in the heat generated with time, or an

exothermic reaction (shown in Figure 3.4). This resulted in temperatures as high as 160°F measured in the tire shred stockpile, while temperatures in the embankments only reached 89°F at maximum. The heat generated within the stockpile was also found to increase with the presence of moisture. Results from this testing program indicated that proper design of the tire shred embankment can significantly decrease, if not completely negate, the exothermic reactions within the structures, limiting the heat generated and significantly reducing the potential for combustion.

Another recent field study on the performance monitoring of two embankments containing tire chips was conducted by Tandon et al. (2007). Embankment 1 was a 20 foot high, 81 foot long structure constructed of a mixture of 50% tire shreds and 50% soil. Embankment 2 was a 206 foot high, 81 foot long structure with a 6 foot thick tire shred fill layer in the center. Temperatures were measured at the surface and along the depth of the embankments for a period of 21 months (Figures 3.5 and 3.6).

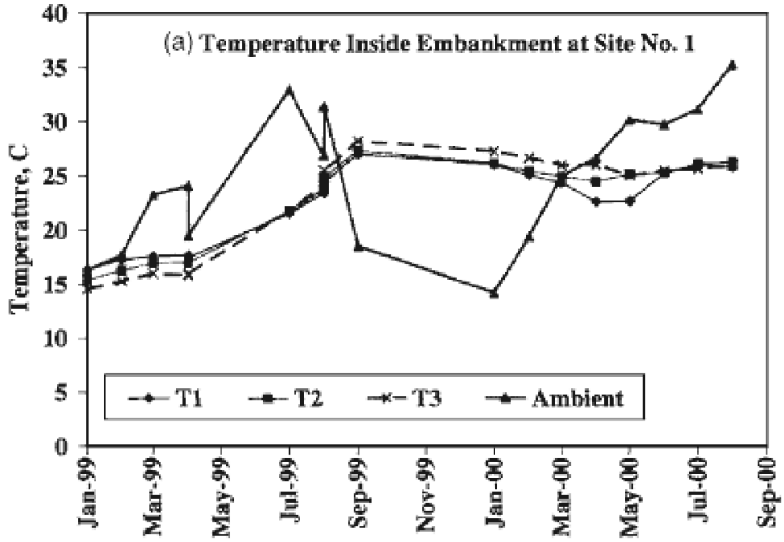

Figure 3.5: Temperatures Measured in Embankment 1 (Tandon et al. 2007)

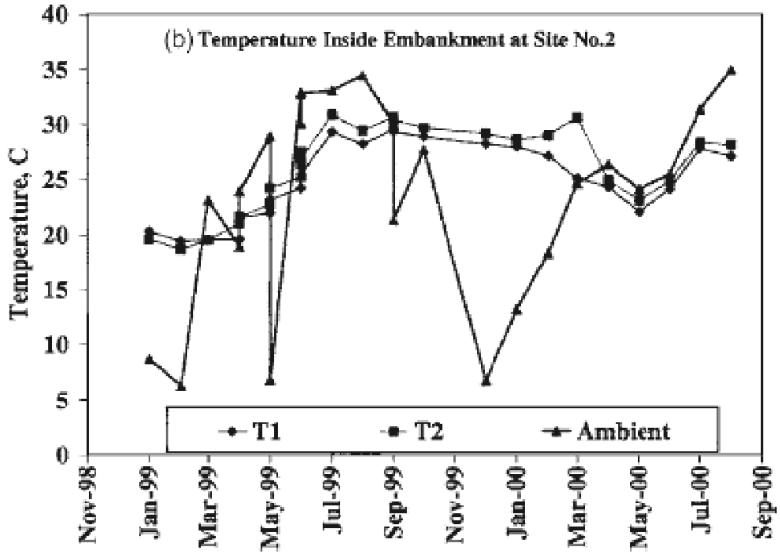

Figure 3.6: Temperatures Measured in Embankment 2 (Tandon et al. 2007)

It was apparent from the results the variation of temperature within the embankment was less than the ambient temperature and in general the internal temperatures were less than ambient values. However, there is a period of time during the winter months (marked in the figures) where the internal temperature within the embankments was higher than the ambient temperature. This was not apparent in any temperature data presented by Wappett (2004) for the tire shred embankments. This may indicate heat generation within the embankments occurring within the tire shreds that have maintained an elevated temperature. However, no signs of combustion or significant heat generation have been noticed at the site.

3.3.4 Potential Combustion of Tire Bales

The literature presents no evidence that suggests there is any significant heat generation or combustion potential from whole tires or tire bales stored above or below the ground. Winter (2006) mentioned tire bale storage sites in Kansas and Colorado containing more than 10 million whole tires (in bale form) that have been stored above and below ground for 9 years with ambient temperatures above 100^{o}F without any signs of combustion.

Simm et al. (2004) and Winter et al. (2006) reported tests carried out by the Fire and Risk Sciences Division of the Building Research Establishment in which a tire bale structure (10 bales long, 4 bales high and 4 bales wade) had to be heated to 370^{o}F before any signs of combustion were present. Actual ignition of the structure took an additional 39 days at the elevated temperature. Additional tests reported indicate that temperatures would have to be in excess of 360^{o}F for a time period of up at least 30 days for the combustion of the tire bale structure, no matter the arrangement or thickness, to occur.

Additional tests reported by Simm et al. (2004) indicate that arson was also an unlikely cause of combustion of the tire bales. A blow torch was used to attempt to ignite the edges of the tire bale, which was unsuccessful. The bale was only ignited after cutting the two inner bale wires and igniting the center of the bale, which required 15 minutes of direct contact with the flame to catch fire. Results indicate that even tire fires caused by arson would be difficult to cause in tire bale structures.

3.3.5 Contamination Potential from Exothermic Reactions and Combustion of Tires

In addition to the cost and danger associated with combustion in tire shred fills, the potential contamination due to the burning of tires also drives the need to stringent design guidelines to reduce the risk of fire. Tire fires generate dangerous air and water pollution that can potentially affect a large area and thousands of people. The pollutants from both whole tire fires above ground and tire shred fires below ground are similar, the only difference being that tire shred fires are not as easily noticed and pollutants may easily enter the groundwater system. A brief literature review was conducted to determine the potential contaminants that can result from tire fires as outlined in this section.

Significant amounts of gas and smoke can be produced during a fire, as exemplified by the smoke plume from the Rhinehart Tire fire, which was over 3,000 feet wide and 50 miles long. Pollutants include methane, ethane, isopropene, butadiene, propane, CO, CO_2, NO_2, and HCl (Wappett 2004). Other pollutants from the Rhinehart Tire Dump Fire, as listed on the EPA website (www.EPA.com), included benzene, acetone, toluene, chromium, nickel, sulphuric acid, arsenic, manganese, iron, and numerous others. Combustion by-products produced by tire fires includes ash, sulfur compounds, polynuclear aromatic hydrocarbons, aromatic nephthenic and paraffinic oils, and PCBs, many of which are carried along with the smoke plume. The intense heat of the fires also leads to pyrolysis, in which organic substances in the tire thermally decompose into hazardous compounds (Wappett 2004). Pyrolytic oil, the result of compounds formed by pyrolysis, is a major contamination concern for groundwater and environmental pollution, with over 55,000 gallons of unburned oil produced per million tires burned.

For tire shreds buried under soil, the flow of the oil and contaminates into the soil and groundwater poses a major health concern, which can be very expensive and difficult to fix. The contamination potential also increases since the exothermic reaction occurs underground may go on without any sign. The cleanup of the sites becomes expensive due to the effort required to put out the fire, remove any contaminated soil, and cleanup any groundwater contamination.

3.4 Design Guidelines for Tire Bale Embankments

Although much of the data presented in the chapter does not directly apply to the use of tire bales in highway applications, the lessons learned have been used to determine the guidelines for design of tire bale structures. Many of these specifications have evolved from tire shred guidelines presented in Humphrey (2004), as well as in previous papers presented by the same author, to limit the potential of combustion in tire shred structures. In general, many of these limitations have been considered too stringent in terms of tire bales, but provide an excellent basis for the limitations for tire bale structures. A brief summary of many of the specifications are as follows:

I. Limiting height of tire structures—tire shred embankments are limited to a maximum height of 10 feet to reduce the insulating effects of tire shreds that lead to excessive heat generation. In terms of tire bales, this specification is considered too stringent and field observations have indicated tire bale walls up to 10 bales high (25 feet) have not experienced any problems.

II. Tires must be free from contaminants—any substance on a tire when placed in the ground can instantly be absorbed into the groundwater to cause contamination problem. Any substance that is flammable could also potentially increase the combustion potential of

the tire structure if enough is present. This is a specification that is always required of both tire shred and tire bale structures.

III. Reduce infiltration and ponding of water—the flow of water into tire structures may not be avoidable, since the tire mass does provide an excellent drainage layer. However, design specifications will require that the infiltration and ponding be reduced by adding drainage out of the tire mass.

IV. Top cover of tire structures—the use of a soil cover on top of the tire mass provides numerous benefits, including UV protection, limiting free access to air and water, and prevents any form of arson or vandalism. The soil cover also allows vegetation growth, which provides a more aesthetically pleasing structure then a tire bale facing.

3.5 Summary

The previous chapter outlined a series of lab and field studies concerned with the environmental impacts of using tire materials in soil structures. Although much of the research presented in this chapter deals with tire shreds, the results have been directly applied to the design of tire bale structures. The applicability of tire shred data to the design of tire bale structures is still uncertain, especially when dealing with the potential combustion of the tire bale mass. The lack of laboratory and field data concerned with the cause of heat generation in tire shreds and whole tires may be causing an over-conservative design approach for tire bales. More research is required to establish the different thermal and heat generation properties of tire bales (as opposed to tire shreds) to determine if there is a need for strict design specifications for tire bale structures.

Chapter 4. Testing Materials

Two main materials were used to determine the mechanical and environmental characteristics of tire bales; standard scrap tires bales and soil infill. The following chapter outlines the material properties needed for the analyses presented in the Results chapters. Testing methods will be briefly introduced in this chapter, and described in more depth as the introduction to the Results chapters.

4.1 Materials

The following section contains a brief description of the materials used during the testing program. Each material was chosen for the testing program based upon the availability in the state and applicability to highway construction.

4.1.1 Standard Scrap Tire Bales

The standard scrap tire bale is a compressed block of approximately 100 tires with dimensions of approximately 4.5 feet in length by 5 feet in width by 2.5 feet in height. The typical dry weight of a tire bale is usually assumed to be approximately 2000 pounds. Eight (8) tire bales were constructed specifically for this testing program at the IDSA Tire Transport and Disposal site (Baxley 2006). The general construction sequences for tire bales are presented in Appendix B. A digital photograph was taken of each tire with a 12.5 inch scale to illustrate the general shape of the bales (Figure 4.1).

Figure 4.1 a
Tire Bale 1

Figure 4.1 b
Tire Bale 2

Figure 4.1 c
Tire Bale 3

Figure 4.1 d
Tire Bale 4

Figure 4.1 e
Tire Bale 5

Figure 4.1 f
Tire Bale 6

Figure 4.1 g
Tire Bale 7

Figure 4.1 h
Tire Bale 8

Figure 4.1: Digital Photographs of the Tire Bales used Throughout the Testing Program

The variability in the tire bale geometry and weight, which can be visually observed from the photos presented, results from the variety of scrap tires used to make the bales. Each tire used in the bales is different, and therefore each bale is slightly different. A range of geometry or volume measurements are therefore generally reported (refer to Chapter 2) to indicate the variability in dimensions from bale to bale. A more detailed analysis of the tire bale dimensions and weight are presented in Chapter 5.

4.1.2 Sand Fill

The sand used for the testing programs was a uniformly graded sand (SP), as defined by the Unified Soil Classification System. This sand is commercially available as fill sand from Travis Aggregates (Location: Manor, Texas, Phone: (512) 276-9900). Results from a sieve analysis on the sand (ASTM D422-63) are presented in Figure 4.2. Results from direct shear tests (ASTM D3080-04) conducted on the sand under dry conditions (water contents less than 4%) are presented in Figure 4.3. The direct shear testing was conducted with a ShearTrac II-D direct shear apparatus (Manufacturer: Geocomp Corporation, Phone: 800-822-2669). The sand was compacted to a dry unit weight 103 pcf, the same weight of the sand used for the tire bale-sand interface testing presented in Chapter 6. Additional direct shear testing was conducted on sand compacted to a unit weight of 93 pcf to determine the effect of remolding on the sand, and to determine the variability of the sand strength with density. The strength of the sand was found to be represented by a friction angle of 21^o for a unit weight of 93 pcf and 30^o for a unit weight of 103 pcf.

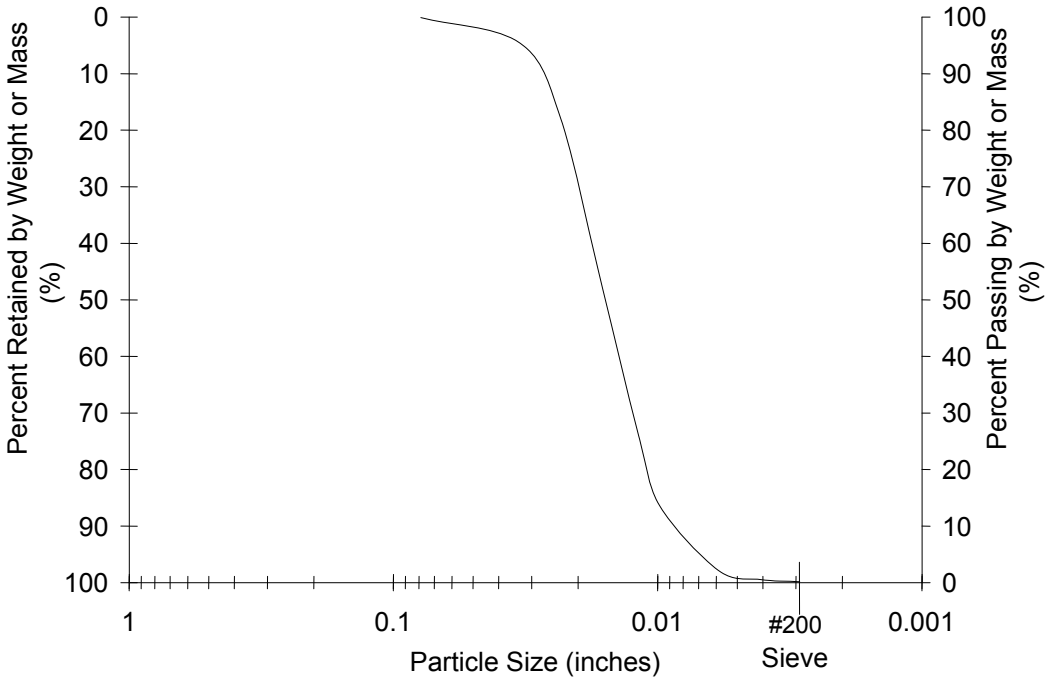

Figure 4.2: Sieve Analysis Results for the Sand Fill

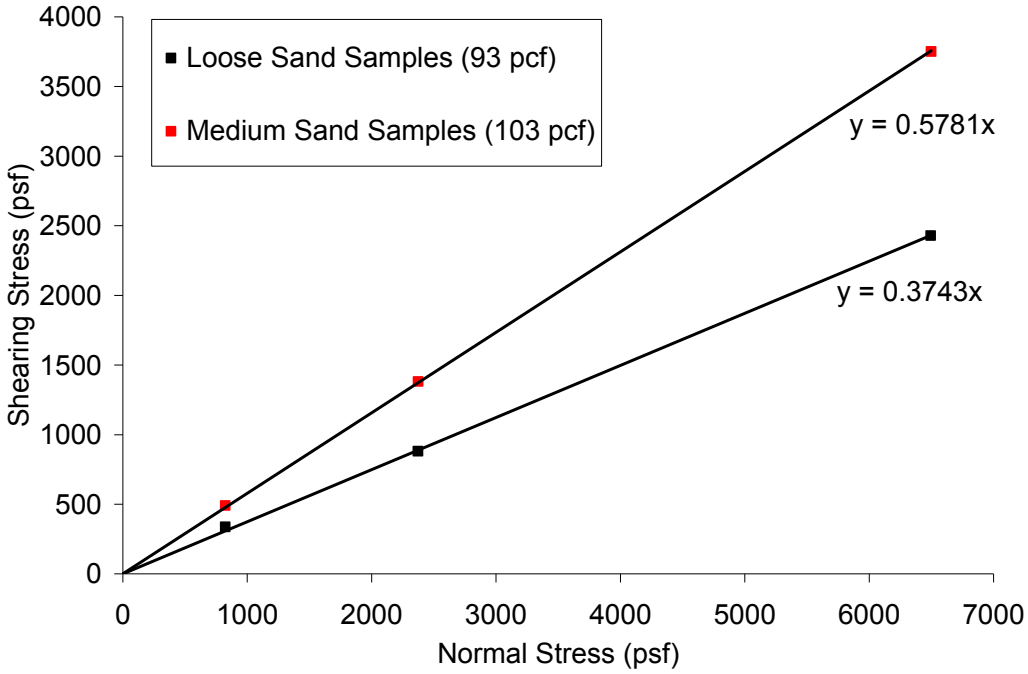

Figure 4.3: Strength Envelopes Obtained from Direct Shear Test of the Sand Fill

4.1.3 Compacted Clay Soil

The compacted clay soil used for the testing program is a gray clay soil obtained from the Elgin Butler Brick Company, (located in Elgin, Texas, Phone: 512-285-3356). The soil is a highly plastic fine grained clay, or CH (ASTM D2487), with a plasticity index of 36 and liquid limit of 59 (ASTM D4318) (Najjir and Rauch 2003). Standard proctor compaction testing (ASTM D 698) indicate an optimum water content of 20% and a corresponding maximum dry unit weight of 108 pcf. Results from unconsolidated-undrained (UU) direct shear testing of the clay compacted at the optimum water content (20%) to a dry unit weight of 102 pcf are shown in Figure 4.4. The undrained strength of the clay is represented by a linear failure envelope with cohesion of 1653 psf and a friction angle of 23^{o}.

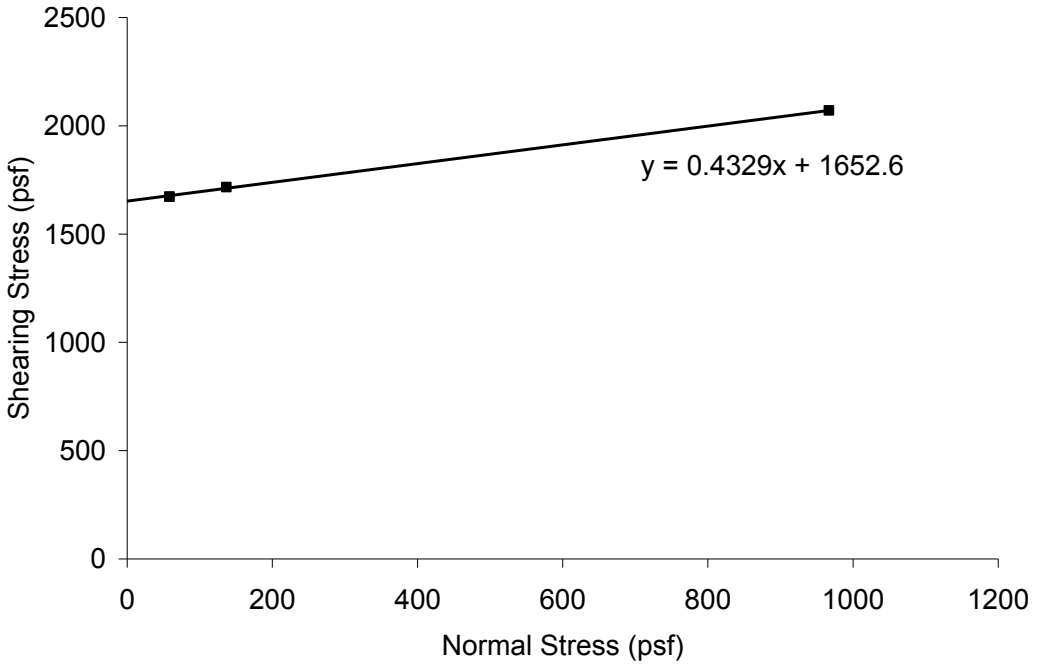

Figure 4.4: Strength Envelope for the Compacted Grey Clay from UU Direct Shear Testing

4.2 Introduction to Testing Methods

The size and weight of the scrap tire bale increased the difficulty of the testing procedures to characterize the bales in the laboratory and in the field. Material characterization tests that are traditionally considered trivial, such as the measurement of the unit weight or water content, become difficult tasks to complete for bales since the material cannot be easily moved or lifted. The development of the testing procedures used to determine the index properties and mechanical characteristics of tire bales are outlined as the introduction to the Results chapters (Chapters 5, 6, 7, and 8). Many of the tests have been modified from testing programs presented by Simm et al. (2004), LaRocque (2005), Zornberg et al. (2005) and Winter et al. (2006).

Chapter 5. Material Characterization of Tire Bales—Index Properties and Hydraulic Permeability

The following chapter outlines the testing program and results of the index properties and hydraulic characterization of standard tire bales. Defining and determining the index properties was difficult due to the irregular shape of the tire bales, as well as the variability of the bales. A hydraulic characterization test was also conducted on the bales to determine the magnitude of the permeability of the bales. All index properties were defined using field testing so that ample space was available for all testing procedures. Descriptions of the testing procedures used to define the index properties are outlined in this chapter. Tire bales 1 through 5 were used to determine the index properties. All results of the index testing are also presented in Appendix C.

5.1 Determination of the Tire Bale Weight

The weight of a tire bale was measured for three different cases; dry, submerged and wet. The measurements of the submerged and wet weights were accomplished with a large water bath (Figure 5.1 b). The general testing procedure to determine the weight of the bales was as follows:

1. Dry Bale Weight—The dry bales were lifted by a load cell system (Figure 5.1 a) and weights recorded (W_{DRY}).
2. Submerged Bale Weight—The bales were submerged in a water bath while connected to the load cell system (Figure 5.1 b) and agitated until air bubbles were no longer noticed, after which weight measurements were recorded (W_{SUB}).
3. Wet Bale Weight—After removing the bale from the water bath, a hydraulic conductivity test was conducted (Chapter 5.5) and any water remaining in the bale after 10 minutes was measured by weighing the bale (W_{WET}).

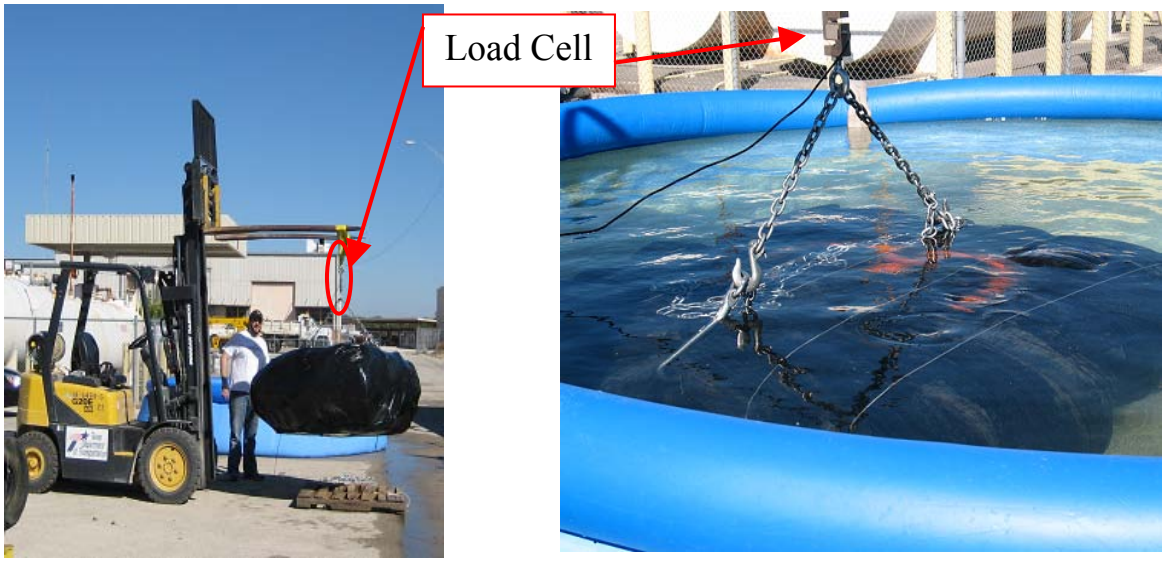

(a) Dry Bale Weight Measurement. (b) Submerged Bale Weight Measurement.

Figure 5.1: Measurement of the Dry and Submerged Tire Bale Weights

Table 5.1 provides the weights measured for each tire bale during the testing program.

Table 5.1: Measured Values of the Tire Bale Weights

Tire Bale	Weight (pounds)		
	Dry	Submerged	Wet
1	2034	240	2188
2	1972	232	2162
3	1884	245	2082
4	1902	215	2056
5	1932	235	2124

The average value of the dry weight is approximately 1950 pounds, which is within 5% of the assumed weight of a standard tire bale. The submerged unit weight is approximately 1/10 of the dry weight, indicating a significant reduction in weight of the tire bale mass if submerged. In general, only 100 to 200 pounds of water remained in the bale after submergence, indicating 1.6 to 3.2 ft^3 of water can be stored in a bale when not submerged. The use of the measured weights in the unit weight calculations will be discussed in Chapter 5.4.

5.2 Determination of the Tire Bale Volume

The irregular shape of the tire bale complicates how the volume of the bale can be defined and measured. Three different bale volumes have been presented in the literature, as follows:

1. Average Bale Volume (V_{AVG}) —Calculated by taking average values of the bale length, width, and height and multiplying the values. This is the most commonly reported volume in the literature.
2. Maximum Enclosing Cuboids (MEC)—Maximum bale dimensions are measured and multiplied to obtain the volume of the smallest box in which the entire bale mass can be contained.
3. Actual Tire Bale Volume (V_{ACT})—The actual volume contained within the bale, measured using submergence testing of a bale wrapped in an impermeable membrane.

Two-dimensional representations of the different bale volumes are shown in Figure 5.2. The average bale volume, although commonly reported in the literature, is difficult to use in analytical studies where soil infill is present or bales are submerged. The maximum enclosing cuboid is useful when determining the volume of the bales during transport (tire bales will not be placed in the most compacted arrangement and will take up the most space).

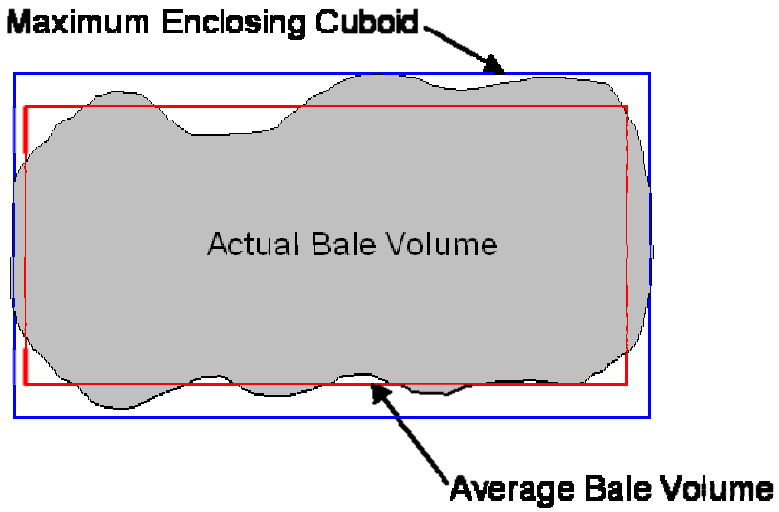

Figure 5.2: Two-Dimensional Representations of the Tire Bale Volumes Measured

The average volume was determined by taking twenty (20) measurements each of the length, width, and height of the bales, calculating the average of each dimension, and multiplying them together ($\forall_{AVG} = L_{AVG} \cdot W_{AVG} \cdot H_{AVG}$). The average dimensions are provided in Figure 5.3 for the tire bales used for the index testing program. For the bales that were used for rapid expansion testing (refer to Chapter 8), the number of tires in each bales was also counted. It was found that on average, the bales only contained between 75 to 85 tires.

Tire Bale 1
Length = 4.67 ft.
Width = 5.01 ft.
Height = 2.38 ft.
No. Tires = 75

Tire Bale 2
Length = 4.66 ft.
Width = 5.1 ft.
Height = 2.57 ft.
No. Tires = 82

Tire Bale 3
Length = 4.7 ft.
Width = 4.98 ft.
Height = 2.49 ft.
No. Tires = Unknown

Tire Bale 4
Length = 4.62 ft.
Width = 5.19 ft.
Height = 2.51 ft.
No. Tires = Unknown

Tire Bale 5
Length = 4.73 ft.
Width = 5.1 ft.
Height = 2.51 ft.
No. Tires = 85

Figure 5.3: Photographs and Average Dimensions of the Five Tire Bales Used for the Index Testing Program

The average dimensions and largest dimensions of the bale measured during this process (used to determine the MEC) are provided in Table 5.2. Visual observations of the tire bales indicate that the bale is not a perfect box, and the rounded edges and irregular shape complicate how the average dimensions and volume are defined and measured. The actual volume, which takes into account the irregular bale shape, is a better representation the bale geometry (Simm et al. 2004, Winter et al. 2006).

Table 5.2: Average Dimensions and Maximum Enclosing Cuboid Dimensions Measured for the Tire Bales

	Average Dimensions (feet)			MEC Dimensions (feet)		
Tire Bale	Length	Width	Height	Length	Width	Height
1	4.67	5.01	2.38	5.21	5.27	2.5
2	4.66	5.1	2.57	5.48	5.4	2.71
3	4.7	4.98	2.49	5.23	5.38	2.73
4	4.62	5.19	2.51	5.13	5.63	2.77
5	4.73	5.1	2.51	5.33	5.73	2.56

The actual volume was determined from wrapping the bales in plastic and submerging the bales in a water bath (Figure 5.4 a). The buoyancy force was used to determine the volume of water displaced, which is equivalent to the actual volume of the bale. The bales did not completely submerge during testing (Figure 5.5), so the volumes of any portion of the bale not submerged were carefully measured and included in the volume. The testing illustrated that submerged bales should not be impermeable since there is a potential for the bales to float. The

three volumes measured during this testing program are provided in Table 5.3, along with values presented in previous studies.

(a) Tire Bale Wrapped in Plastic.

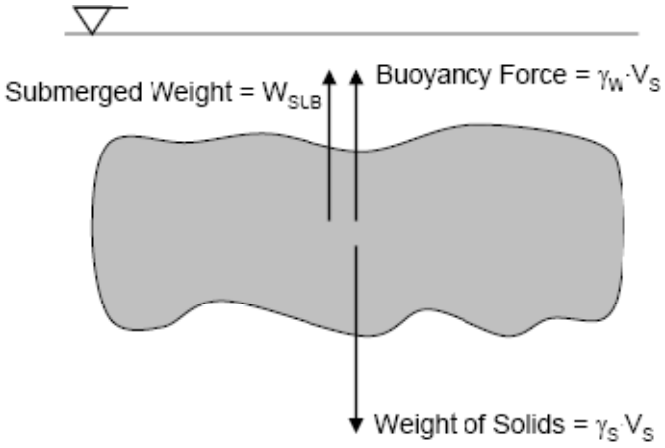

(b) Forces Acting on Submerged Bale.

Figure 5.4: Measurement of the Actual Volume of the Bales from Submergence Testing

Figure 5.5: Submergence of a Wrapped Tire Bale

Table 5.3: Values of the Tire Bale Volumes

Reference	Volume (ft^3)		
	Average	MEC	Actual
Zornberg and Freilich (2008)*	59.2 ± 2.2	76.8 ± 4.5	41.3 - 47.1
Zornberg et al. (2005)	56 ± 3	-	-
LaRocque (2005)	57.4 ± 5	-	-
Winter et al. (2006)	57.6	-	-
Simm et al. (2004)	-	-	41.4

* Indicates results obtained from this testing program.

The average volumes provided in Table 5.3 for all the research programs are in agreement, with an approximate value of 57.6 ft^3. The actual bale volume is much less, with an average value of approximately 44.3 ft^3. The difference between the average and actual volumes indicates that the average volume includes approximately 13 ft^3 of air due to the irregular and rounded shape of the bale, which will significantly influence how the unit weight of the tire bales can be defined and used in design. The MEC volume indicates how much larger the bale is during transportation as compared to the average or actual volume of the bales in a structure.

5.3 Saturated Bale Weight, Void Ratio, and Specific Gravity

The use of tire bales in submerged situations requires that the saturated unit weight of the bale be known so that effective stresses (total weight minus the water pressure) can be calculated. In the previous sections, there has been no attempt to measure the saturated weight because the permeability of the bale is so high; any attempt to saturate the bale and measure the weight will result in the water instantly flowing out. The saturated weight was therefore calculated with data obtained from submergence testing with no impermeable plastic wrapping.

The three forces acting on a submerged tire bale (Figure 5.4 b) are the buoyancy force of the bale (volume of tire solids times the unit weight of water), the total dry weight of the bale (volume of tire solids times the unit weight of the tire solids = W_{DRY}), and the submerged weight of the bale measured with the load cell (W_{BUOY}). Vertical equilibrium of the three forces (Eq. 5.1) allows for the calculation of the volume of solids (V_S).

$$V_S = \frac{W_{DRY} - W_{BUOY}}{\gamma_W} \tag{5.1}$$

Values of the volume of solids, provided in Table 5.4, provide evidence that even though the bales are constructed with a different amount and type of tire, the volume of tires within the bales is still approximately the same, with an average value of 27.5 ft^3.

Table 5.4: Volume of Solids Calculated from Submergence Testing of Tire Bales

Tire Bale	Volume of Solids (ft^3)
1	28.8
2	27.9
3	26.3
4	27.1
5	27.2

The volume of voids (V_V) within the tire bale mass was defined as the average volume of solids subtracted from the actual tire bale volume already measured. The average volume of voids is approximately 19.5 ft^3 for the bales tested.

$$V_V = V_{ACT} - V_S \tag{5.2}$$

The saturated weight of the tire bale was defined as the dry tire bale weight (W_{DRY}) plus the weight of water in the voids (V_V times 62.4 pcf).

$$W_{SAT} = W_{DRY} + (V_V \cdot \gamma_W) \tag{5.3}$$

The average saturated weight of the tire bales is approximately 3,190 pounds. A complete set of the tire bale weights needed for design is provided in Table 5.5.

Table 5.5: Measured and Calculated Tire Bale Weights

	Tire Bale Weight (pounds)
Dry	1945
Submerged	233
Wet	2122
Saturated	3190

A subsequent result of calculating the volumes of solids and voids within the bale allow for the calculation of the tire bale void ratio and specific gravity. The void ratio is defined as the volume of voids divided by the volume of solids (Eq. 5.4), and is significantly affected by the total bale volume used (average or actual).

$$e = \frac{V_V}{V_S} = \frac{V_{BALE} - V_S}{V_S} \tag{5.4}$$

The actual void ratio of the tire bale (using the actual volume) is approximately 0.57. If the average volume is used, the value increases to 1.21. The increase is due to the fact that the average volume includes space around the bale that is only occupied by air, therefore increasing the volume of voids.

The specific gravity of the tire bales is defined as the unit weight of solids divided by the unit weight of water (Eq. 5.5). Values of the dry weight, volume of solids, and unit weight of water are already known.

$$G_S = \frac{\gamma_S}{\gamma_W} = \frac{W_{DRY}}{V_S \cdot \gamma_W} \tag{5.5}$$

The average specific gravity of the tire bales is 1.14. An interesting point is that the reported range of specific gravities for tires is 1.05 to 1.23, and the value of specific gravity of the tire bales (the average specific gravity of the five hundred tires present in the bales) is the

average value of that range. The specific gravity of the tire bales indicates that the bales will not float, but are not much heavier then water (only 14% heavier), and therefore submergence will significantly decrease the unit weight of the tire bale mass.

5.4 Unit Weight of Tire Bales

The unit weight (weight/volume) of the tire bale is very dependent on the volume value used in the calculation. In this section, the unit weight will be calculated using the average and actual volumes, and show the relationship between the two values.

5.4.1 The Average Volume Unit Weight

Traditionally, the unit weight of the tire bales has been defined in reference to the average volume measured, since it is the easiest volume to measure.

$$\gamma_{AVG} = \frac{\text{Weight}}{V_{AVG}} \tag{5.6}$$

The values of the dry, wet, and submerged unit weights calculated using the average volume found from this testing program and from the literature are provided in Table 5.6.

Table 5.6: Dry, Wet, and Submerged Unit Weights Defined in Reference to the Average Bale Volume (γ_{AVG})

Reference	Average Volume (ft^3)	Unit Weights (pcf)		
		Dry	Submerged	Wet
Zornberg and Freilich (2008)*	59.2 ± 2.2	32.9 ± 2.1	3.95 ± 0.5	35.9 ± 1.2
Zornberg et al. (2005)	56 ± 3	36.5 ± 3	4.3 ± 1.5	39.5 ± 2
LaRocque (2005)	57.4 ± 5	36.7 ± 4	5.6 ± 1.5	47.1 ± 5
Winter et al. (2006)	57.6	34.5	-	-

* Indicates results obtained from this testing program.

5.4.2 The Actual Volume Unit Weight

In order to take into account soil infill between the bales, or submergence of the bale structure, a different definition of the unit weight must be used. Winter et al. (2006) therefore suggested defining the unit weight with respect to the actual bale volume (Eq. 5.7), so that the voids present between bales are not taken into account in the value.

$$\gamma_{ACT} = \frac{\text{Weight}}{V_{ACT}} \tag{5.7}$$

The actual unit weight is then plugged into Eq. 5.7, along with the unit weight of any material present within the voids (γ_{FILL}), so that the equivalent unit weight of the tire bale mass is

determined. Winter et al. (2006) presented Eq. 5.8 based from observations that 0.72 of the volume taken up by a tire bale within a structure was the actual bale, and 0.28 of the volume was voids present between bales.

$$\gamma_{EQ} = 0.72 \cdot \gamma_{ACT} + 0.28 \cdot \gamma_{FILL} \tag{5.8}$$

Values of the dry, wet, and saturated actual unit weights are provided in Table 5.7. The unit weight of the tire bale structure is determined by plugging in the appropriate tire bale unit weight and any fill unit weight (including water) into Eq. 5.8.

Table 5.7: Values of the Dry and Saturated Unit Weights for Tire Bales Defined in Reference to the Actual Bale Volume (γ_{ACT})

	Actual Unit Weight (pcf)
Dry	45.6
Wet	48.9
Saturated	66.5

5.4.3 Discussion of the Average and Actual Unit Weights

It can easily be shown that the average volume unit weight (γ_{AVG}) is a specific case of the actual volume unit weight of the tire bale structure (γ_{EQ}) with no fill material. The equivalent unit weight of a dry tire bale mass with no fill material, as defined by Eq 5.8 and Table 5.7, is:

$$\gamma_{EQ} = (0.72 \cdot 45.6\ \text{pcf}) + (0.28 \cdot 0) = 32.8\ \text{pcf} \tag{5.9}$$

The result is the same value as that for the dry average volume unit weight, indicating that the average volume unit weight is a special case of the more general equivalent unit weight. Therefore, γ_{AVG} can only be used for tire bale only structures, and any form of soil infill or submergence (in which water is the infill material and effective stresses are required) requires that we define the equivalent unit weight of the tire bale structure that utilizes the actual tire bale unit weight (γ_{ACT}).

5.5 Estimation of Hydraulic Conductivity of Tire Bales

After submergence testing of the tire bales, a quick, one-dimensional hydraulic conductivity test was conducted in order to estimate the vertical permeability of the tire bales. The vertical permeability has been shown to be the critical, or lowest, value of permeability (Simm et al. 2004). A schematic of the testing procedure is shown in Figure 5.6. Immediately after removal from the water bath (Figure 5.6 a), the tire bale is saturated. After some increment of time, the flow from the bottom of the bale has reduced the mass of water within the bale (Figure 5.6 b). It is assumed that the water is flowing through the bale as a plug, and that a unit gradient (gravity is the only force acting on the water) is always present.

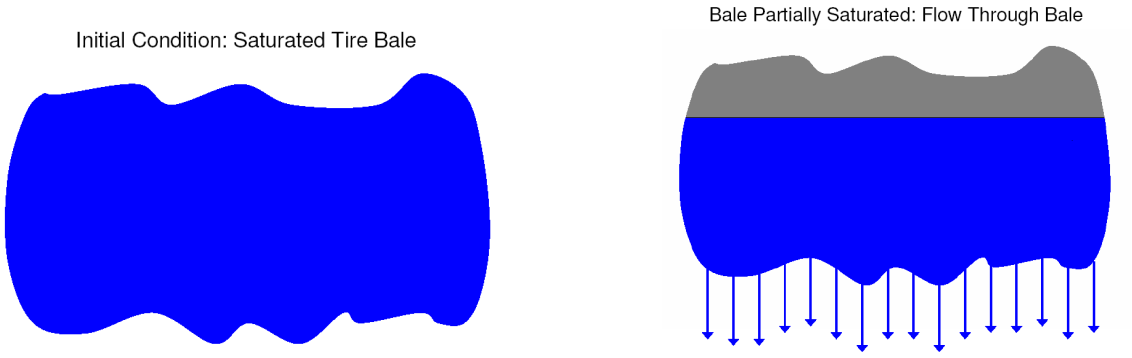

(a) Saturated Tire Bale at t = 0 (b) Tire Bale after some time t > 0

Figure 5.6: Schematic of the Hydraulic Conductivity Testing of Tire Bales

Assuming that Darcy's equation (Eq. 5.10) is valid (which may not be true due to the turbulence of flow), the hydraulic permeability (k) can be estimated from the change in weight of the bale with time. The average footprint of the tire bale (length by width) was used to estimate the area of flow.

$$Q = \frac{V_W}{\Delta t} = k \cdot i \cdot A = k \cdot L_{AVG} \cdot W_{AVG} \qquad (5.10)$$

The load cell system was used to measure the change in weight of the bale with time, which was equivalent to the loss of water with time since no tire material was lost. The volumetric flow rate of water (in units of ft^3/sec) through the bottom of the bale with time can then be calculated by taking the derivative of the tire bale weight versus time curve, and dividing by the unit weight of water. Values can then be plugged into Eq. 5.10 to determine the conductivity (k). The flow rate of water significantly decreases after approximately 15 seconds before reaching a value of zero (0) (Figure 5.7). The maximum values of the conductivity for the first 15 seconds were considered the estimated hydraulic conductivity of the bales, since limited water was present in the bales after that time.

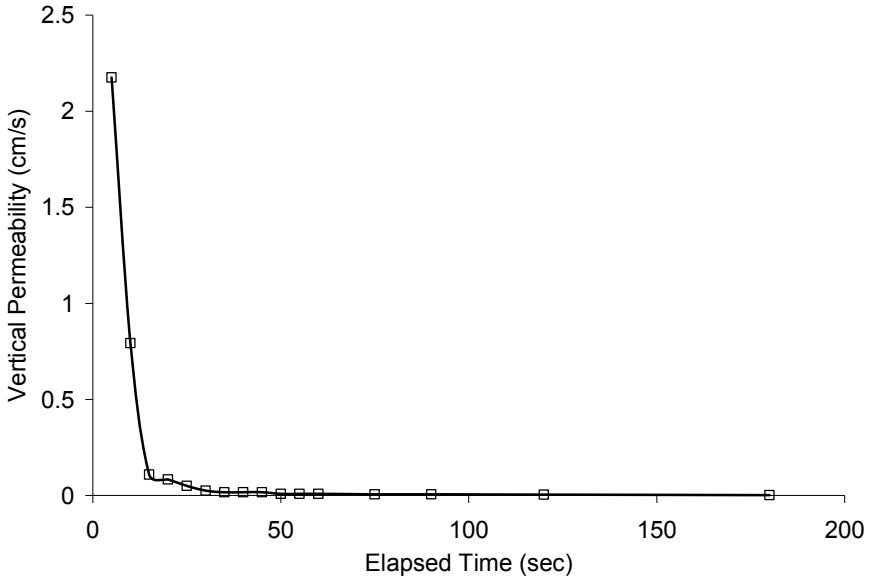

Figure 5.7: Change in the Tire Bale Hydraulic Conductivity with Time

The range in hydraulic conductivity measured in this testing program, as well as other test results reported in the literature, is provided in Table 5.8.

Table 5.8: Estimated Hydraulic Conductivity of Tire Bales

Reference	Hydraulic Conductivity (cm/sec)
This study*	0.5 - 2.0
LaRocque (2005)	0.4
Simm et al. (2004)	14
* Indicates results obtained from this testing program.	

5.6 Bale Behavior after Baling Wire Failure

Degradation of the galvanized steel baling wires has been a concern for tire bales placed in soil structures. Recently, there has been an increased interest in using aluminum wires, nylon cords, or geosynthetic wraps (Figure 5.8) to retain the tire bales.

Figure 5.8: Placement of Extra Geosynthetic Straps around a Tire Bale with Galvanized Steel Baling Wires (www.angloenvironmental.com)

The corrosion of the wires, which is assumed to occur at a rate of approximately four to fifteen micrometers a year (4 to 15 μm/yr), is further increased due to the presence of water, corrosive soil environments, and damage during construction. For the bales within the wet sand fill for the laboratory component of the research program (refer to Chapter 6.5), significant corrosion along the steel wires was observed to occur only after a few weeks after placement (Figure 5.9).

Figure 5.9: Corrosion of the Steel Baling Wires After Placement in a Wet Sand Fill

The following sections present results from the testing of tire bales after wire breakage. Many of the results from this section were used directly in the compilation of the specifications for tire bale construction and construction of the tire bale structures (Appendix A).

5.6.2 Horizontal Displacements of Tire Bale after Wire Failure

Initial concerns with wire breakage were that degradation, and subsequent failure, of the baling wires would lead to a violent expansion of the bale, causing an explosion of the tires out of the structure. Although testing results presented by LaRocque (2005) and Winter et al. (2006) provided evidence that this explosion of the bale does not occur, the deformations associated

with the baling wire breakage may still be an important factor in the design of tire bale structures. A series of rapid expansion tests were conducted after the field testing program to determine the effects of cutting each baling wire on the geometry of the bale, and to provide evidence of the expansion behavior of the bale. Baling wires for three bales were cut in random order, one at a time so that measurements of the change in bale length, width and height could be obtained. The baling wires were numbered (Figure 5.10) and cut in different order so that the effects of random wire breakage could be determined.

Figure 5.10: Tire Bale Wire Numbers and Rapid Expansion Test Setup

After cutting each of the baling wires, the bale was allowed to sit for five (5) minutes and measurements of length and width were then recorded at the left, middle, and right ends of the bale. Only one measurement of the height was taken at the highest point of the bale. The behavior of the bale during wire breakage was also visually observed throughout the test. Photographs and measurements from the rapid expansion testing of Bale 2 are provided in, respectively, Figure 5.11 and Table 5.9.

Table 5.9: Total Change and Incremental Change in Tire Bale Dimensions with Each Wire Breakage for the Rapid Expansion Testing of Tire Bale 2

Total Change in Bale Dimensions								
Wire Cut	**ΔL_{LEFT}**	**ΔL_{MIDDLE}**	**ΔL_{RIGHT}**	**Avg ΔL**	**ΔW_{LEFT}**	**ΔW_{RIGHT}**	**Avg ΔW**	**ΔH**
None	0	0	0	0	0	0	0	0
3	0.25	0.5	0	0.25	-0.25	-0.22	-0.23	-0.5
4	0.8	11	2	4.6	0.25	0.28	0.27	-0.5
2	3.5	18.25	2.5	8.08	-0.25	0.78	0.27	-0.5
1	47	28.75	17	30.92	2.25	0.78	1.52	-2
5	51	39.75	38	42.92	8.75	5.78	7.27	0.5

Incremental Change in Bale Dimensions								
Wire Cut	**ΔL_{LEFT}**	**ΔL_{MIDDLE}**	**ΔL_{RIGHT}**	**Avg ΔL**	**ΔW_{LEFT}**	**ΔW_{RIGHT}**	**Avg ΔW**	**ΔH**
None	0	0	0	0	0	0	0	0
3	0.25	0.5	0	0.25	-0.25	-0.22	-0.23	-0.5
4	0.55	10.5	2	4.35	0.5	0.5	0.50	0
2	2.7	7.25	0.5	3.48	-0.5	0.5	0.00	0
1	43.5	10.5	14.5	22.83	2.5	0	1.25	-1.5
5	4	11	21	12.00	6.5	5	5.75	2.5

Figure 5.12 a
Cut 0: Original Length

Figure 5.12 b
Cut 1:Baling Wire 3

Figure 5.12 c
Cut 2: Baling Wire 4

Figure 5.12 d
Cut 3: Baling Wire 2

Figure 5.12 e
Cut 4: Baling Wire 1

Figure 5.12 f
Cut 5: Baling Wire 5

Figure 5.11: Photographs of Tire Bale 2 after Each Wire Breakage (Rapid Expansion Test)

The tabular results of the other two rapid expansion tests are reported in Tables 5.10 and 5.11 for Bales 1 and 3, respectively. The results from this testing program provide evidence of three important characteristics of the tire bale behavior during wire breakage:

1. A significant portion of the total change in volume is due to the increase in length of the bale, which is the dimension that is directly confined by the baling wires. The changes in width and height are mainly due to tires falling out of the bale, and not an expansion of the tires.
2. The maximum change in length measured was approximately between 40–55 inches in the length, or an increase in the length of approximately 75%–102%.

3. The change in dimensions of the bale is essentially zero until the last one or two baling wires are cut. This is in agreement with the baling wire tensions measured in the previous section, in which cutting one baling wire redistributes the loads into the surrounding wires. Only after more than half of the wires are cut will the bale begin to deform.

Table 5.10: Total Change and Incremental Change in Tire Bale Dimensions with Each Wire Breakage for the Rapid Expansion Testing of Tire Bale 1

Cumulative Change in Dimensions			Incremental Change in Dimensions		
AVG ΔL	AVG ΔW	ΔH	AVG ΔL	AVG ΔW	ΔH
0	0	0	0	0	0
2	0	0	2	0	0
2	0	-0.5	0	0	-0.5
4.5	-1	-0.5	2.5	-1	0
5.5	0.5	-1	1	1.5	-0.5
42	1.5	-1	36.5	1	0

Table 5.11: Total Change and Incremental Change in Tire Bale Dimensions with Each Wire Breakage for the Rapid Expansion Testing of Tire Bale 3

Total Change in Bale Dimensions								
Wire Cut	ΔL_{LEFT}	ΔL_{MIDDLE}	ΔL_{RIGHT}	Avg ΔL	ΔW_{LEFT}	ΔW_{RIGHT}	Avg ΔW	ΔH
None	0	0	0	0	0	0	0	0
1	3.5	-0.25	-3.5	-0.08	0.75	-0.72	0.02	-0.5
5	3.5	0.75	-1	1.08	0.25	-0.72	-0.23	-1
2	11	1.25	-2.5	3.25	0.25	-1.22	-0.48	-1.5
4	11.5	7.75	1	6.75	1.25	-0.72	0.27	-1
3	29.5	40.25	38.5	36.08	0.75	1.28	1.02	1

Incremental Change in Bale Dimensions								
Wire Cut	ΔL_{LEFT}	ΔL_{MIDDLE}	ΔL_{RIGHT}	Avg ΔL	ΔW_{LEFT}	ΔW_{RIGHT}	Avg ΔW	ΔH
None	0	0	0	0	0	0	0	0
1	2.5	-0.5	-0.5	0.5	-0.5	0	-0.25	0.5
5	0	1	2.5	1.17	-0.5	0	-0.25	-0.5
2	7.5	0.5	-1.5	2.17	0	-0.5	-0.25	-0.5
4	0.5	6.5	3.5	3.50	1	0.5	0.75	0.5
3	18	32.5	37.5	29.33	-0.5	2	0.75	2

5.6.3 Horizontal Expansion Pressure of Tire Bale after Wire Failure

In addition to the rapid expansion tests, in which the deformation of the bales was the main variable, a horizontal pressure test was also conducted to determine the pressures applied to the surrounding structure due to wire breakage of a tire bale. The testing setup (Figure 5.12) consisted of a single bale (tire bale 8) confined along the length of the tire bale (the dimension directly confined by the baling wires) by two rigid steel plates. One rigid plate reacted against a reaction wall and the other against a series of load cells to measure the change in force. Therefore, the expansion pressure at one side of the bale is effectively measured in this test. A photograph of the actual test setup is provided in Figure 5.13.

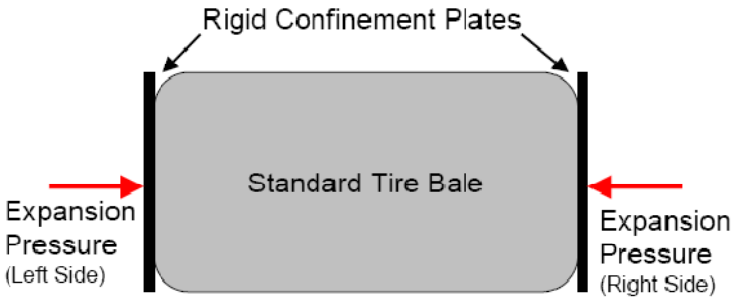

Figure 5.12: Illustration of the Horizontal Pressure Testing Setup

Figure 5.13: Photograph of the Horizontal Pressure Testing Setup

Two load cells were placed at one end of the bale and reacted against a steel plate bolted to the floor to measure the expansion pressure. The horizontal expansion pressure test was conducted by cutting the baling wires (in the order 5, 1, 4, 2, and 3) and measuring the change in pressure after each wire was cut. The change in expansion force with each wire cut is shown in Figure 5.14. The increase in horizontal load (after each wire breakage) is dependent on time, indicating a small creep expansion of the bales after wire breakage. At the end of wire cutting, the total increase in horizontal expansion force for one side of the bale was approximately 2416 lbs, which results in an expansion pressure of approximately 200 psf at each end of the tire bale.

Immediately after the test was completed, the rigid plates were removed and an instant horizontal expansion of 38 inches was measured.

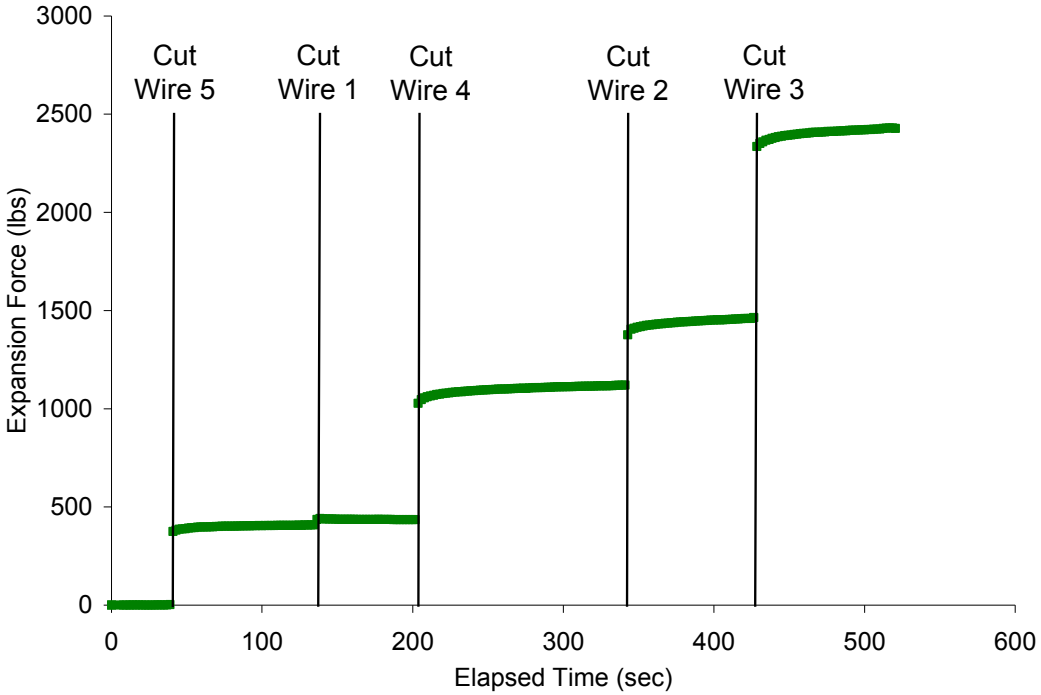

Figure 5.14: Increase in Horizontal Expansion Pressure with Wire Breakage

5.7 Summary

The preceding chapter outlined the testing procedures conducted to calculate the variables needed to define the tire bale unit weight and estimated permeability, as well as to determine the characteristics of the bales after wire breakage. A complete set of the data obtained from the index testing program is provided in Appendix C. Although both the average volume and actual volume unit weights were presented, it is recommended that actual volume unit weight be used in conjunction with Eq. 5.8 to define the equivalent tire bale mass unit weight. Defining the equivalent unit weights allows the designer to consider the effects of soil infill in the weight of the tire bale mass, and also allows for a simple way to calculate the effective stresses (by plugging in the saturated tire bale unit weight and unit weight of water for the fill material) of the tire bale mass when using a limit equilibrium or finite element program. The use of these properties will be further discussed in Chapter 8 for the analytical study of tire bale structures.

The estimated permeability presented in this chapter is the lowest value expected in the field. For tire bale only structures, the permeability will be significantly influenced by voids present between bales, which were not considered in this testing program. Field experience with drainage issues in tire bales indicated that bales are not only a free flowing layer within a structure, but can also store significant amounts of water (tire bale structures can have void ratios as high as 1.2). Drainage from tire bale layers should always be provided, as discussed further in Chapter 9.

Chapter 6. Material Characterization of Tire Bales—Interface Shearing Strength

Proper design of tire bale structures requires that engineers are able to perform stability analyses to ensure an adequate factor of safety. The stability analyses must utilize the strength of the tire bales, which must be properly characterized and known for the conditions of the structure. For short term conditions, it is assumed that the tire bales act as discrete blocks and sliding along the interfaces is the controlling mode of failure. The following chapter outlines the testing procedure and results obtained from a large scale direct shear test developed to determine the interface strength of tire bales for different design conditions (Figure 6.1).

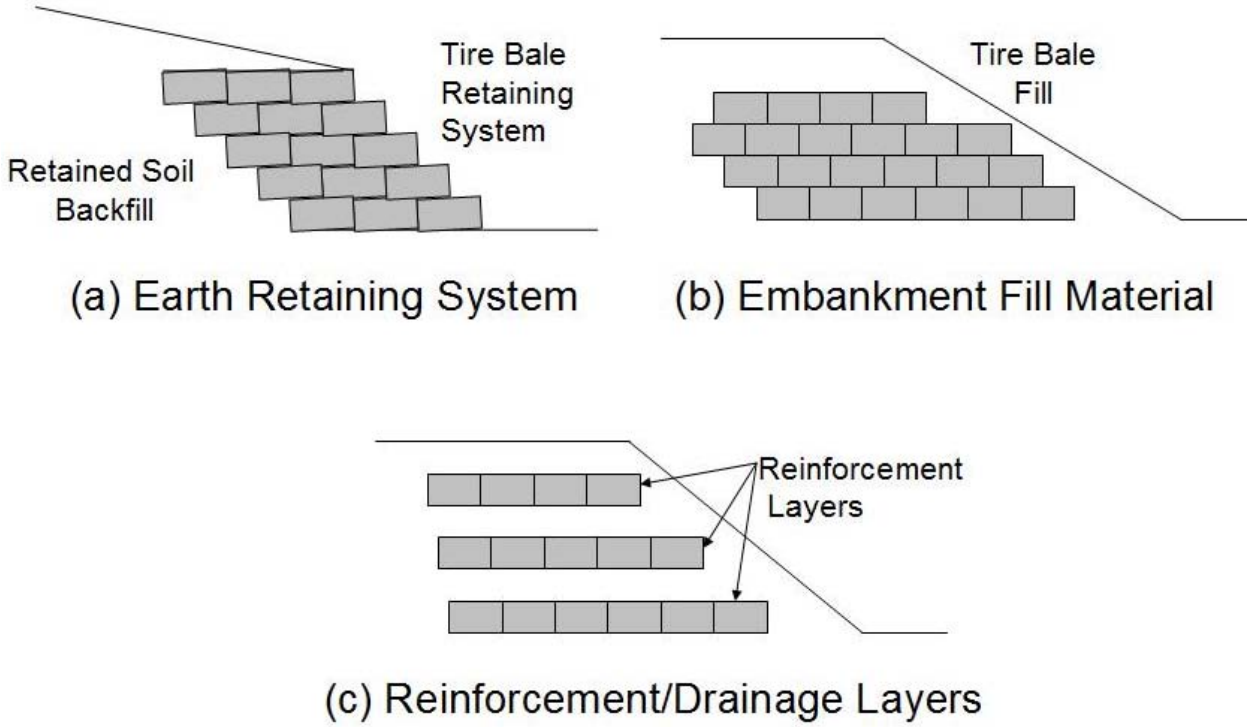

Figure 6.1: Illustrations of Proposed Uses of Tire Bales in Highway Structures

6.2 Development of the Large Scale Direct Shear Test

Any testing procedure to determine the interface strength of the tire bales is a difficult process due to the large size of the bales and loads that must be applied. Initial interface strength testing involved stacking two bales (Figure 6.2) and applying a normal and shear load to one bale while holding the other stationary. This method was found to be too difficult due to instability and rotation of the bales (rather than sliding along the interface) after small displacements (Zornberg et al. 2005). This method of testing also limited the total displacement of the mobile bale to a few inches and made the calculation of the contact area (which changed with displacement) difficult.

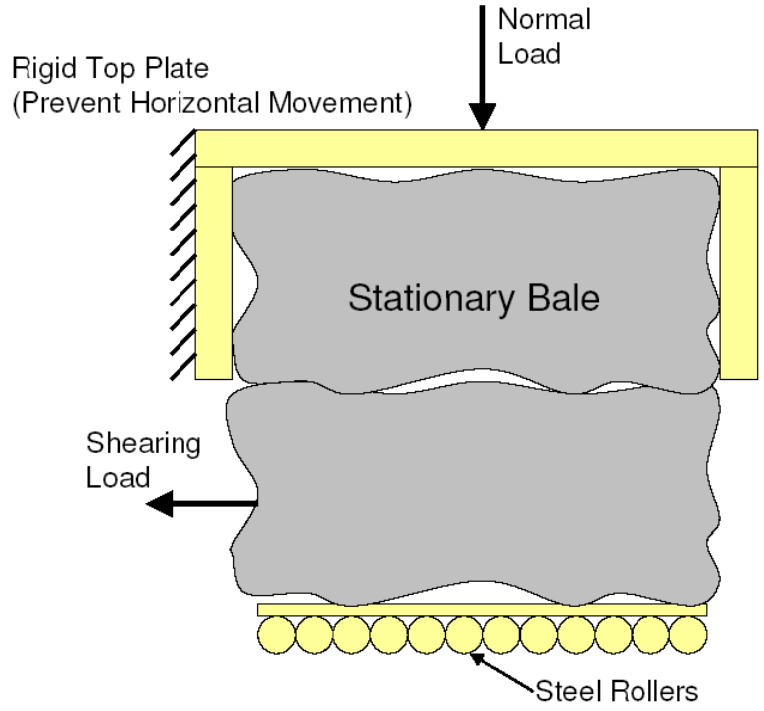

Figure 6.2: Direct Shear Testing of the Tire Bale Interface Using Two Tire Bales

A large scale direct shear testing procedure developed at the University of Texas at Austin (Zornberg et al. 2004, LaRocque 2005) required that the bales be placed in an initial brick, or pyramid, fashion (Figure 6.3). The bottom two bales were held stationary as the top bale was displaced horizontally with a hydraulic piston. This test is similar to that of a soils direct shear test, in which the material is forced to fail horizontally along a defined shear plane.

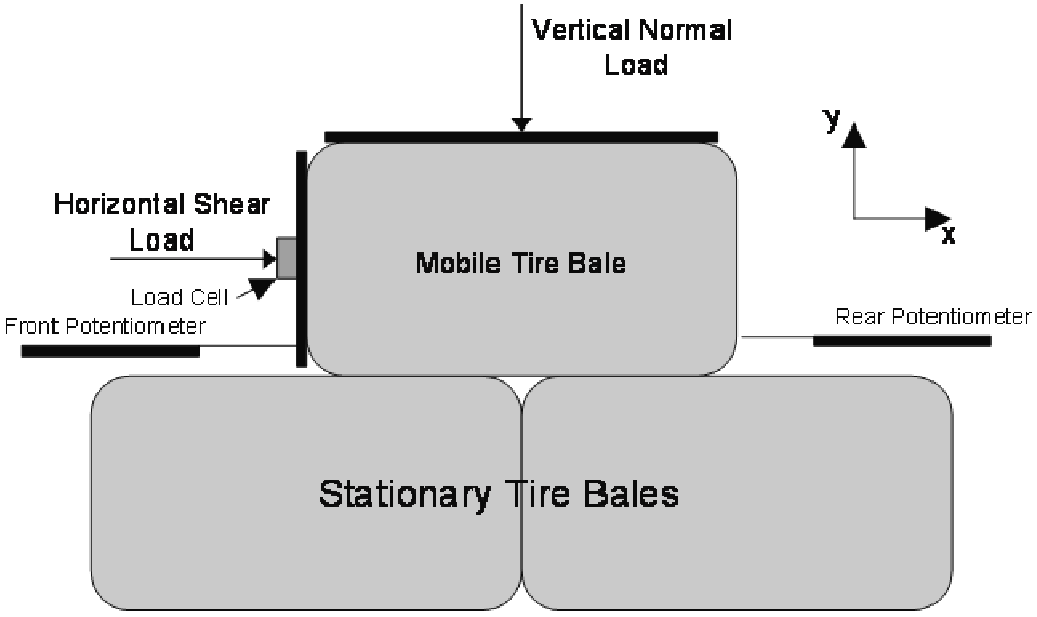

Figure 6.3: Schematic of the Large Scale Direct Shear Test Setup

The normal load was applied by a hydraulic actuator mounted to a rigid top plate and placed on the top mobile bale. The normal load reacts against a roller joint along the load frame so that large displacements (as much as 24 inches) could be achieved (Figure 6.4). Potentiometers were placed at the front and rear of the mobile bale to measure the horizontal displacements, and a load cell was used to measure the vertical shearing load applied to the bale.

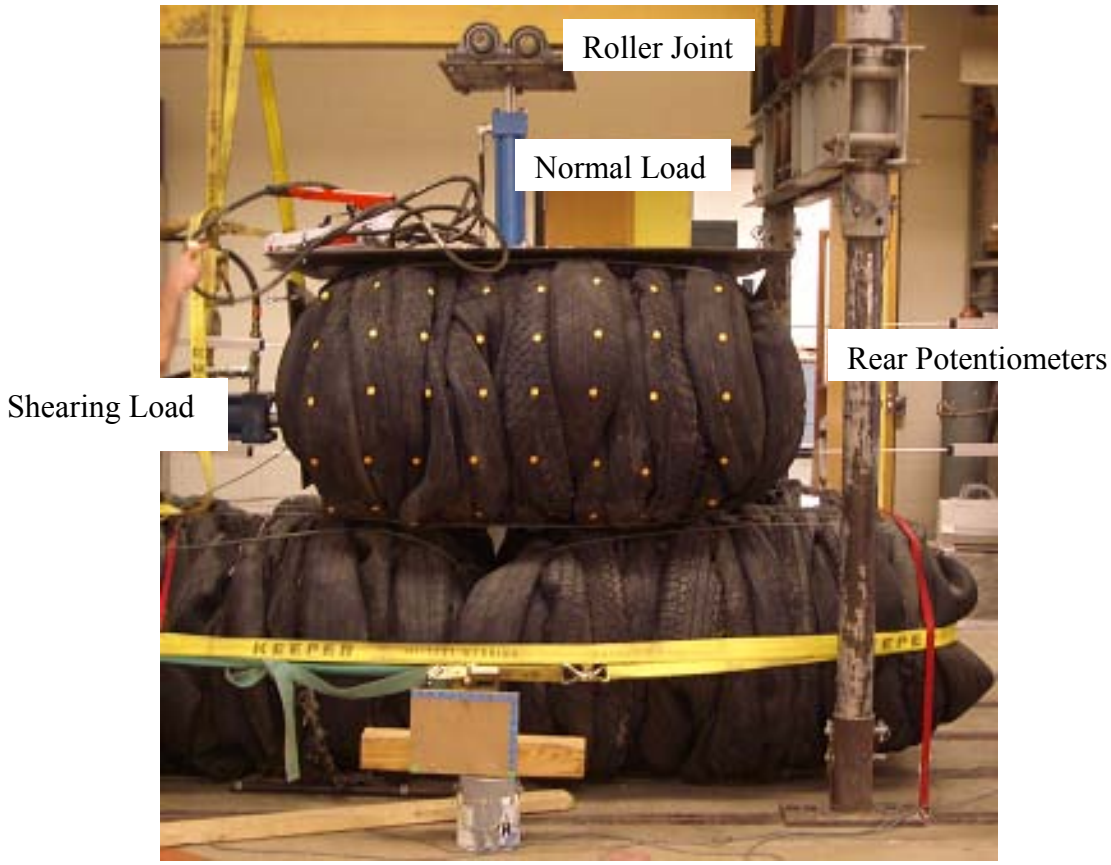

Figure 6.4: Large Scale Direct Shear Test Setup with Instrumentation

The horizontal shear load was applied at a distance of 0.8 feet (1/3 the height of the bale) from the bottom of the mobile bale, which represented the resultant force due to a triangular stress distribution on the tire bale. The location of the shearing load was also found to have a significant effect on the bale behavior (Figure 6.5). For shearing loads applied at the mid-height of the bale, the bale deformation was rotational. Applying the shearing load at the bottom third of the bale produced the sliding failure along the interface that is more representative of failure in a tire bale structure.

The large scale direct shear test setup was also modified so that a soil layer could be compacted beneath the mobile bale to determine the tire bale-soil interface strength. The compacted soil layers were limited to 3 inches in thickness to ensure that failure occurred along the interface and not within the soil mass. An illustration of the soil interface test setup is shown in Figure 6.6. Results from the different interface testing programs are discussed and compared in the following sections.

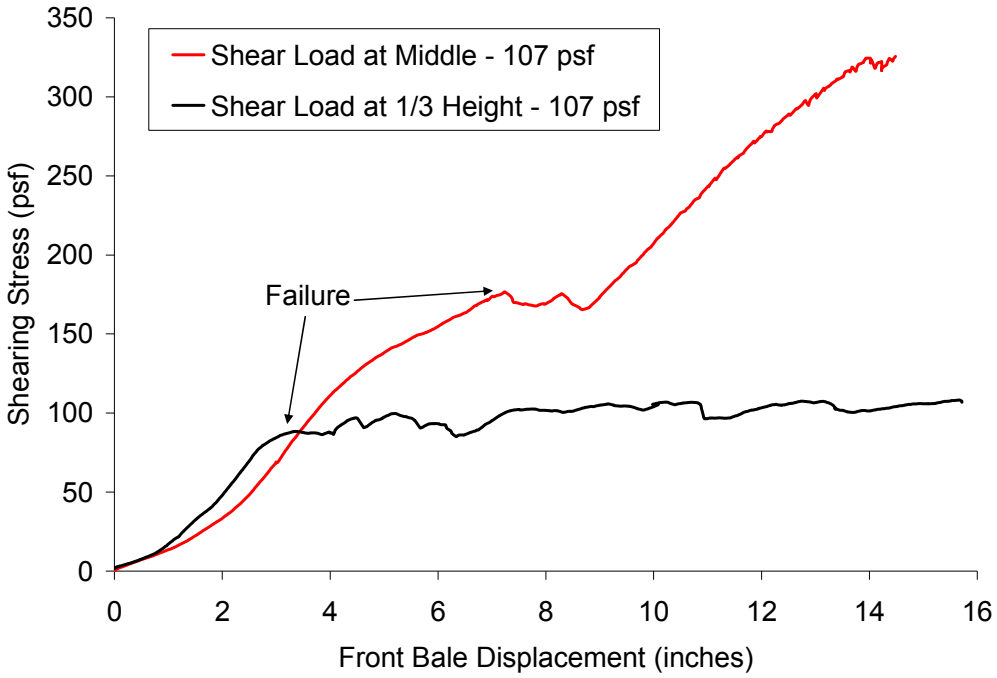

Figure 6.5: Shearing Stress versus Bale Displacement for Shearing Loads Applied at Different Points Along the Height of the Bale

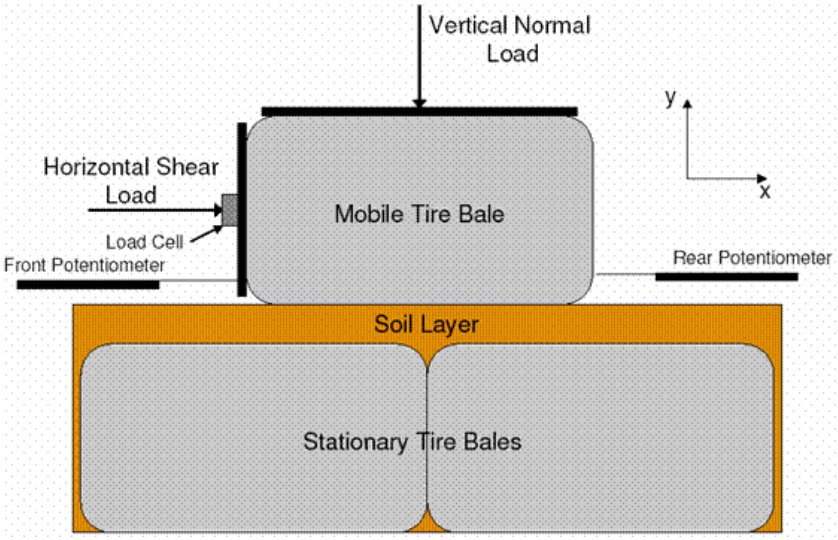

Figure 6.6: Large Scale Direst Shear Test Setup with Compacted Soil Interface Layer

6.3 Definition of the Tire Bale Sections

In the following sections, it will become useful to define the different sections of the tire bales (Figure 6.7). Although there are no differences in material within the tire bale itself, the behavior of the bale along the interface was observed to be different than the behavior within the bale mass. The tire bale interface is defined as the tire material around the perimeter of the bale,

which can be characterized as an irregular and variable surface. The two interfaces of interest for this test are the horizontally loaded interface (where the shearing load is applied) and the sheared interface along which the bale displacement occurs. The tire bale mass is defined as any tire material confined within the baling wires.

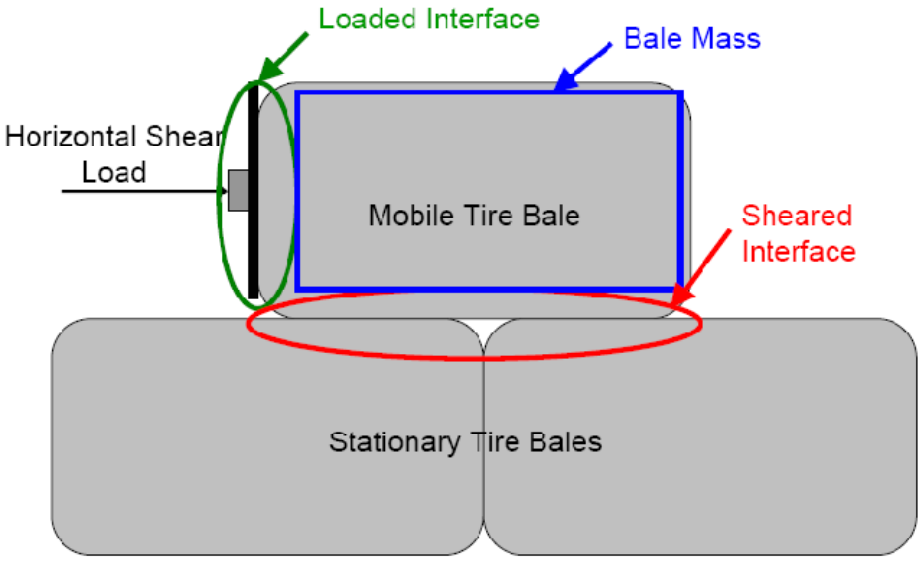

Figure 6.7: Illustration of the tire bale interface and tire bale mass

6.4 Phase One Test Results—Traditional Tire Bale-Tire Bale Interface Strength

The goal of the Phase One strength testing program was to characterize the interface strength of tire bale only interface, representing a tire bale structure with no soil infill (Cases A and B in Figure 6.1). The horizontal shearing load was applied in a direction parallel to the baling wires, and displacements at the front and rear of the mobile bale were measured during the testing. A dot matrix was also placed on the mobile bale (Figure 6.4) so that the compressions of the bale mass could be calculated using a digital photograph analysis and compared with compression data measured with the potentiometers.

Three different types of tire bale only interfaces were tested:

1. Dry Tire Interface—The mobile bale was placed and sheared under dry conditions, all excess dirt and moisture removed before testing.
2. Wetted After Placement Tire Interface (WAP)—The mobile tire bale was placed under dry conditions, but before application of shearing load the interface was saturated with water. The actual tire contact along the interface remained dry while all other areas were saturated (interface partially saturated), representing the strength of a tire bale mass when moisture is present after construction.
3. Wetted Before Placement Tire Interface (WBP)—The interfaces of the mobile and stationary tire bales were saturated before and after placement of the mobile bale (interface fully saturated). The test represented the impact of water on the tire bale structure strength during construction under wet conditions.

6.4.1 Results from the Traditional Direct Shear Testing of Tire Bale Interfaces

A series of stress-displacement curves were plotted for each of the interface tests to observe the development of shearing resistance along the interface as well as determine the failure stresses along the interface. The front displacement of the bale was used to plot the curves since it was maintained at a constant rate throughout the test and because the rear displacement also included compressions of the bale (Figure 6.12). An example of the stress-displacement curves plotted using both the front and rear displacement is shown in Figure 6.8 to illustrate the difference in curve shape when considering the displacements. Although the failure loads would be approximately the same, using the back displacement does not properly represent the total displacement of the bale required to mobilize the interface strength.

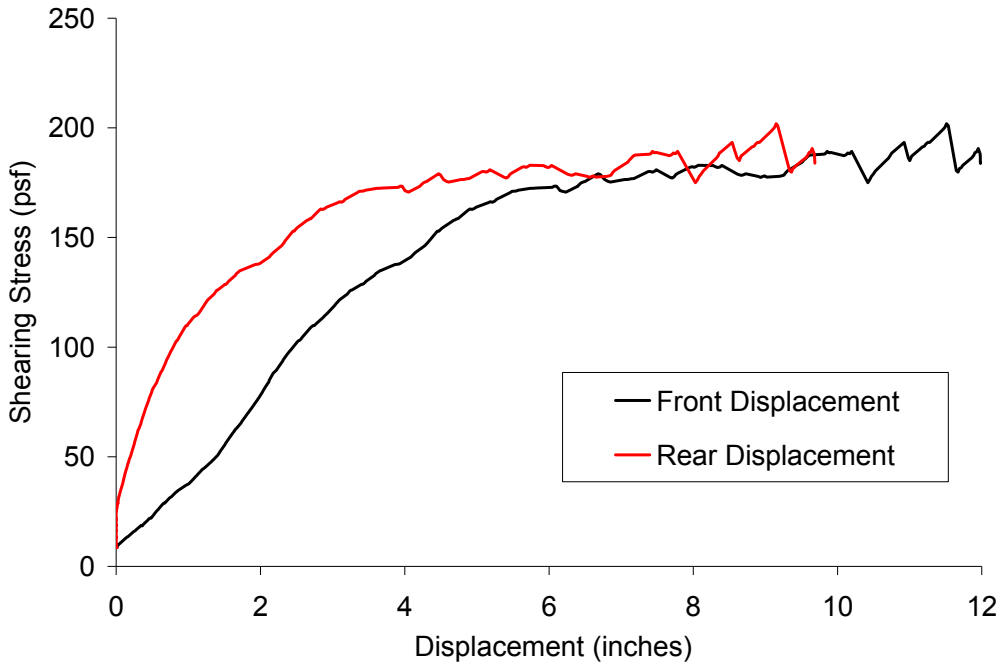

Figure 6.8: Interface Shearing Stress versus Tire Bale Displacement for the Dry Tire Bale Interface

Shearing stress versus bale displacement curves for the dry, WAP, and WBP direct shear tests are shown in Figures 6.9, 6.10 and 6.11, respectively. The shearing and normal (σ) stresses along the tire bale interface were defined as the applied load divided by the average footprint area of the tire bale (average length multiplied by the average width). The footprint area will be used throughout this report to define the interface stresses.

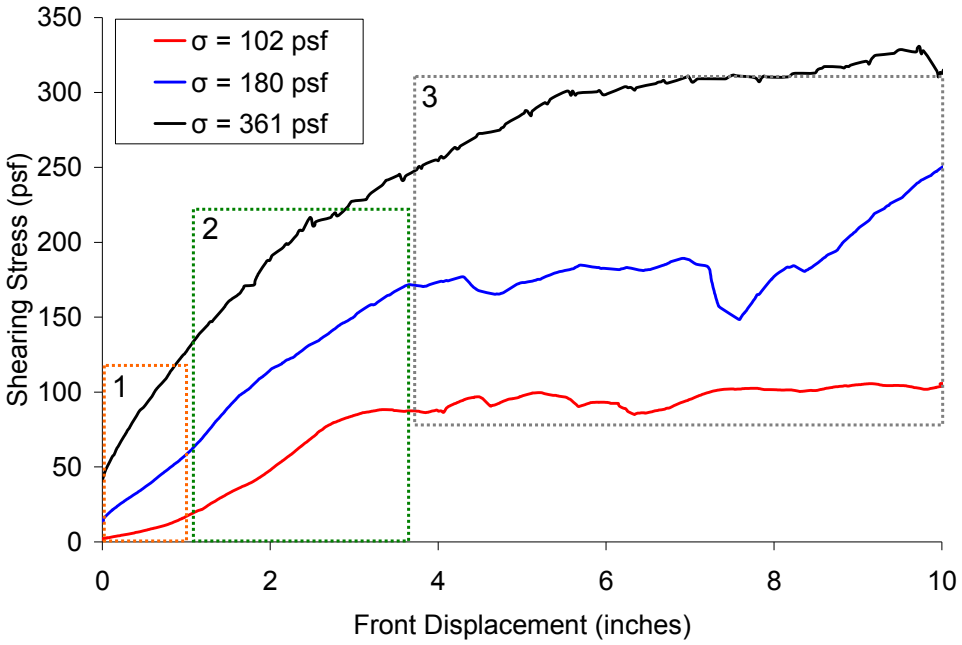

Figure 6.9: Stress-Displacement Curves for Direct Shear Testing of the Tire Bale Only Interface (Dry Interface)

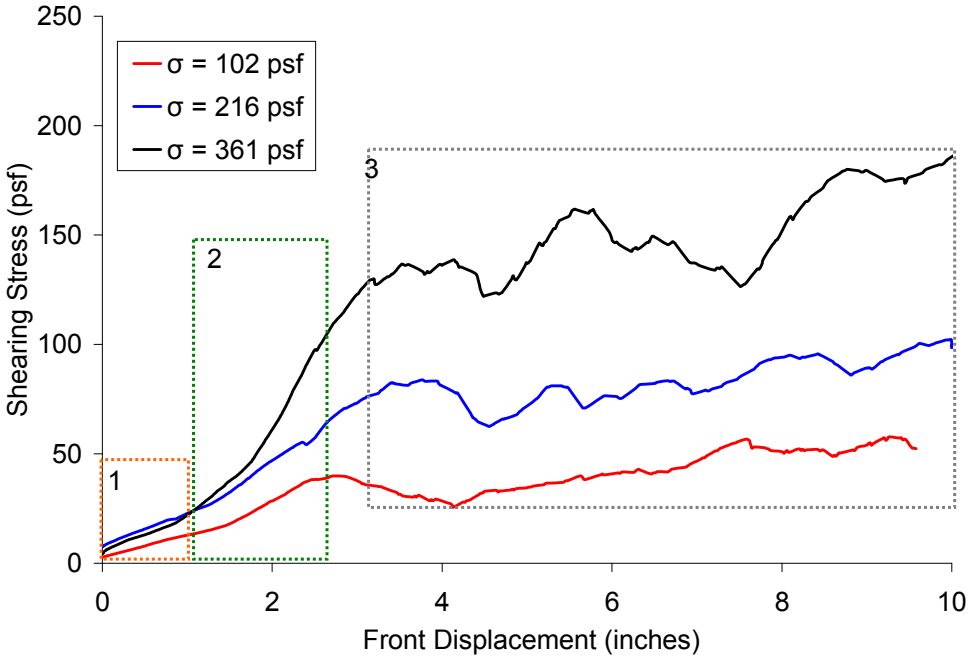

Figure 6.10: Stress-Displacement Curves for the Direct Shear Testing of the Tire Bale Only Interface (Interface Wetted After Placement)

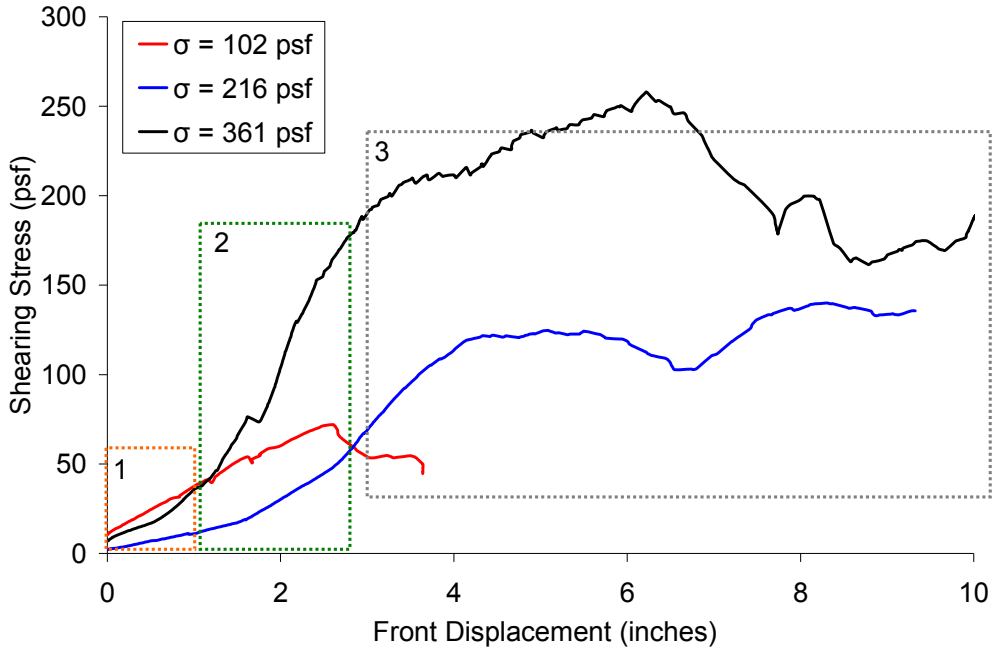

Figure 6.11: Stress-Displacement Curves for the Direct Shear Testing of the Tire Bale Only Interface (Interface Wetted Before Placement)

Three distinct sections can be observed along the stress-displacement curves (a general approximation is shown in the figures). The three sections are also apparent in the displacement measured at the front and rear of the bale, as shown in Figure 6.12. The three sections are:

- Section 1—displacement measured by the front potentiometers with only a small increase in the shearing resistance along the interface. The rear potentiometers measured little, or no, movement of the back of the mobile bale. (Section 1 in Figure 6.12).
- Section 2—increase in the interface shearing resistance with the frontal displacement. Displacement at the rear of the bale increases indicating rigid sliding along the interface. (Section 2 in Figure 6.12).
- Section 3—post peak shearing resistance, with no significant increase or decrease of the shearing resistance with displacement. Rate of displacement (with time) of the front and rear of the mobile bale are now the same. (Section 3 in Figure 6.12)

For some of the tests, Section 1 of the curve is not present due to horizontal seating loads applied to the bale before the test was conducted.

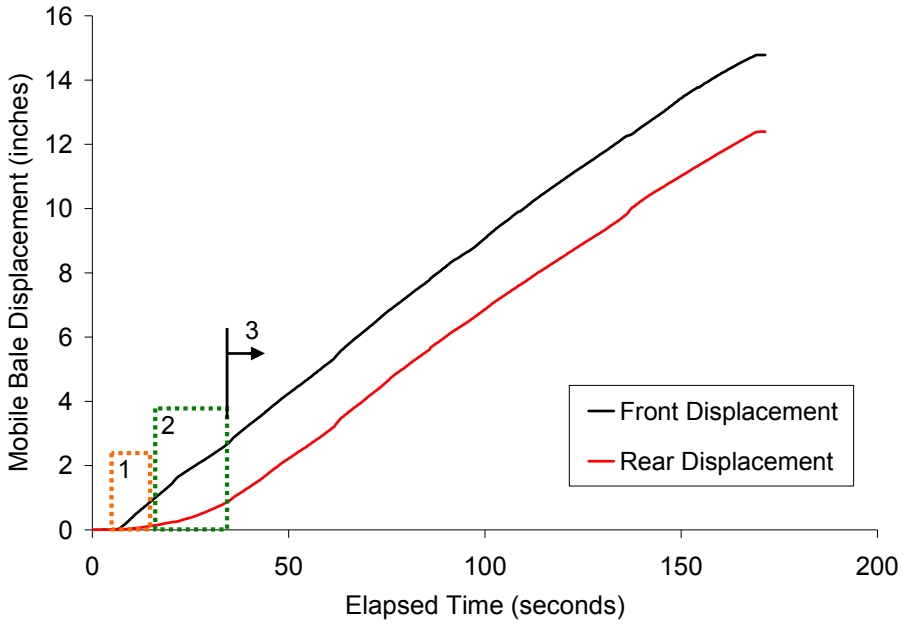

Figure 6.12: Typical Bale Displacement versus Elapsed Time Curve for a Dry Tire Interface

The behavior of the bale during shear is therefore directly related to the displacement and compression of the mobile bale due to the application of the shearing load. Upon the initiation of the shearing load ($0 < t < 50$ seconds), there is a significant compression of the bale—of almost 1.5 to 2 inches (Section 1)—without any displacement at the rear of the bale. After some time ($t > 90$ seconds), the compression of the bale has reached the maximum value, indicating pure sliding of the top bale and a post peak condition along the interface (Section 3 of the stress-displacement curves). Maximum values of the mobile tire bale compression ranged from 2 to 3.5 inches, similar to values reported by LaRocque (2005).

The different behavior between Sections 1 and 2 of the stress-displacement curve can be further differentiated using data from the digital photography analysis. Compressions of the tire bale mass (interfaces not included) measured from the digital photograph analysis are shown in Figure 6.13 for a dry interface test.

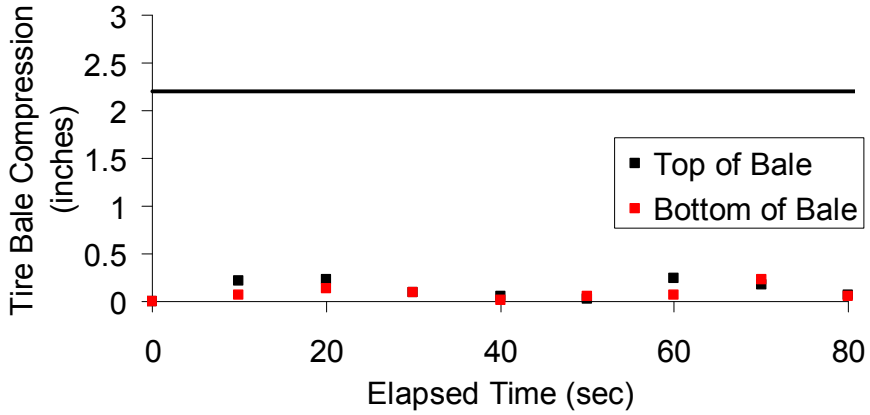

Figure 6.13: Bale Mass Compression Measured using Digital Photographs

The average compression measured using the potentiometers (Figure 6.12) were approximately 2.25 inches. However, analysis of the digital photographs indicates that the bale mass only compressed 0.5 inches during the direct shear test. Visual review of the digital photographs indicates that the total bale compression measured by the potentiometers is mostly due to the compression of the irregular loaded tire bale interface (Figure 6.14). Along with analysis of the digital photographs and video of the direct shear test, there is evidence that indicates Section 1 of the stress-displacement graph is mainly the compression of the loaded interface, and Section 2 is the development of strength along the interface due to rigid displacement of the bale along the sheared tire bale interface (and some small compression of the bale mass itself).

Figure 6.14: Irregular Loaded Bale Interface (Application of Shearing Load)

6.4.2 Shear Strength Parameters for the Tire Bale Interfaces

The failure shearing stress along the tire bale interface was determined using two different methods; the bi-linear method and the maximum compression method. For the bi-linear method, the stress-displacement curves were approximated as bi-linear curves to determine the peak shearing stress along the interface (approximately the intersection of Sections 2 and 3). The stress-displacement curve in Figure 6.15 illustrates the bi-linear approximation plotted with the actual data. Failure is defined as the intersection between the two lines that can be approximated for each bi-linear portion of the curve.

LaRocque (2005) defined failure as the initiation of pure sliding across the interface, which occurred at the maximum mobile bale compression. Failure was defined as the interface stress at the maximum bale compression. An example of the stress and compression versus time curves used for this method are shown in Figure 6.16. For the data presented in this document, failure was determined using only the bi-linear method, since it was found that there is some rigid displacement of the bale required to reach the peak interface strength. Determining the failure strength using the maximum compression method may therefore provide lower estimates of the tire bale interface strength.

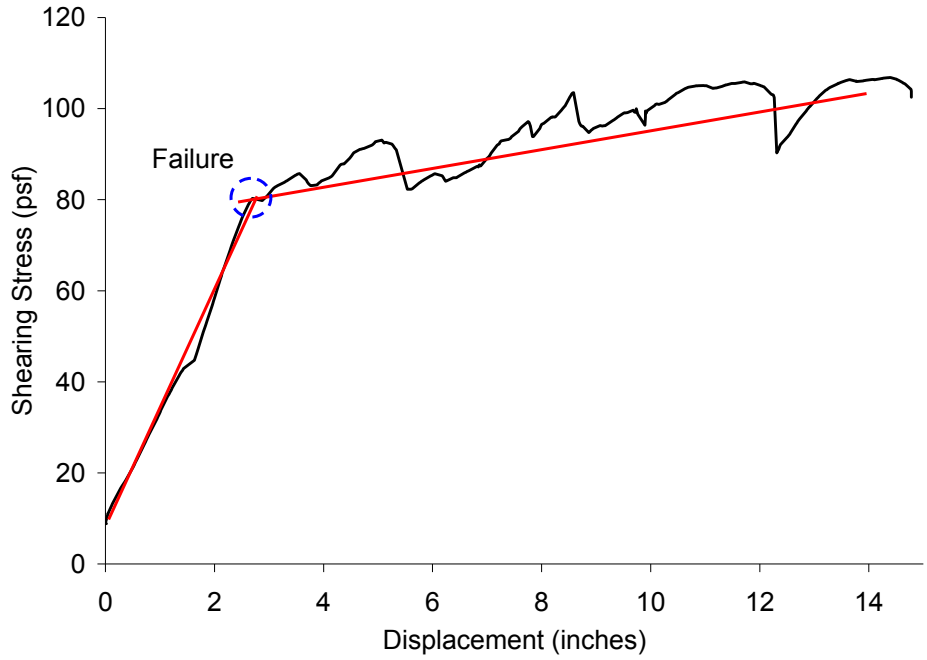

Figure 6.15: Illustration of the Bi-Linear Method to Determine Peak Interface Strength

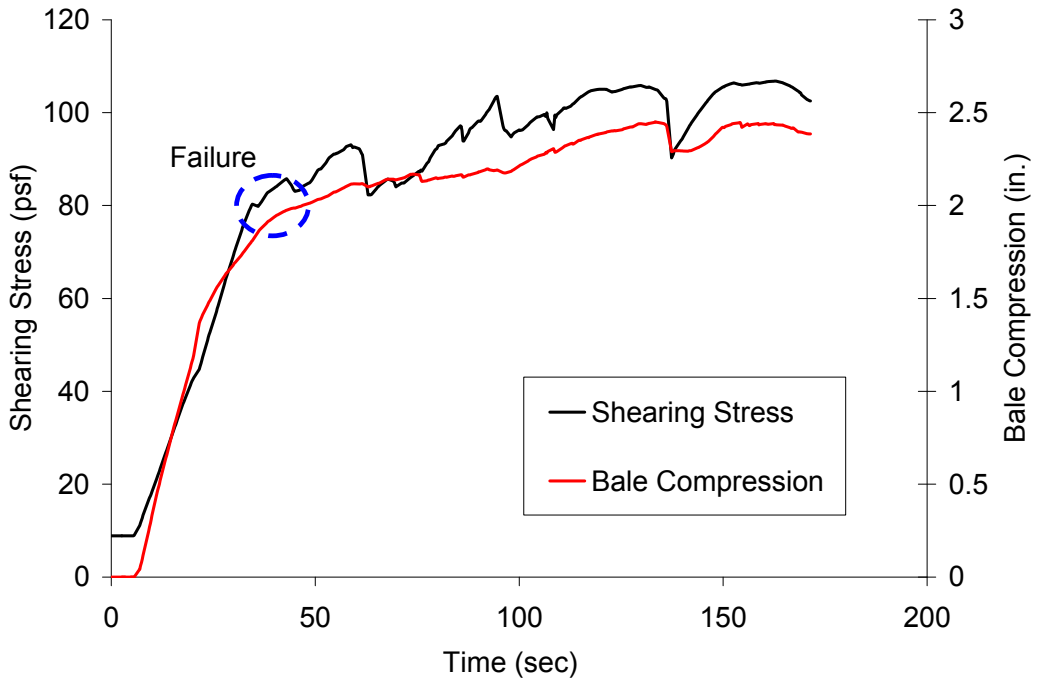

Figure 6.16: Maximum Bale Compression to Determine Peak Interface Strength

A comparison of the failure points reported by LaRocque (2005) (the red data points) and the failure points measured from this testing program (referred to as "This study" and represented by the black data points) are shown in Figure 6.17 for the dry tire bale interface. Due to the similarity in the peak interface strengths determined from both testing programs, the data was combined into a larger data set and can be modeled with a linear curve. The variability in the two data sets, due to differences in the bales, testing setup and test operators was almost indistinguishable, indicating a low variability of strength from bale to bale. There is, however, a significant amount of variability of the tire bale interface during the testing, resulting in a range of interface shear strengths determined for each applied normal load for the same tire bale interface. A linear trend line was used to represent a Mohr-Coulomb failure envelope passing through the points (as shown in Figure 6.17) with a cohesion intercept of 20 psf and a friction angle of 36°.

Failure envelopes for the three interfaces tested (dry, WAP, and WBP) are shown in Figure 6.18. The failure envelopes for all three cases were approximated with a linear Mohr-Coulomb envelope with a cohesion intercept and friction angle (Table 6.1). There is a significant decrease in both the friction angle and cohesion with increase in moisture along the interface due to the presence of water between the tire contacts. The difference between the WAP and WBP data may be attributed to the fact that the contacts for the WAP start out dry initially and require displacement to lubricate the tire contact areas with water. For the WBP interface, all the contacts are initially wet and therefore the strength reduction is present at the initiation of the test.

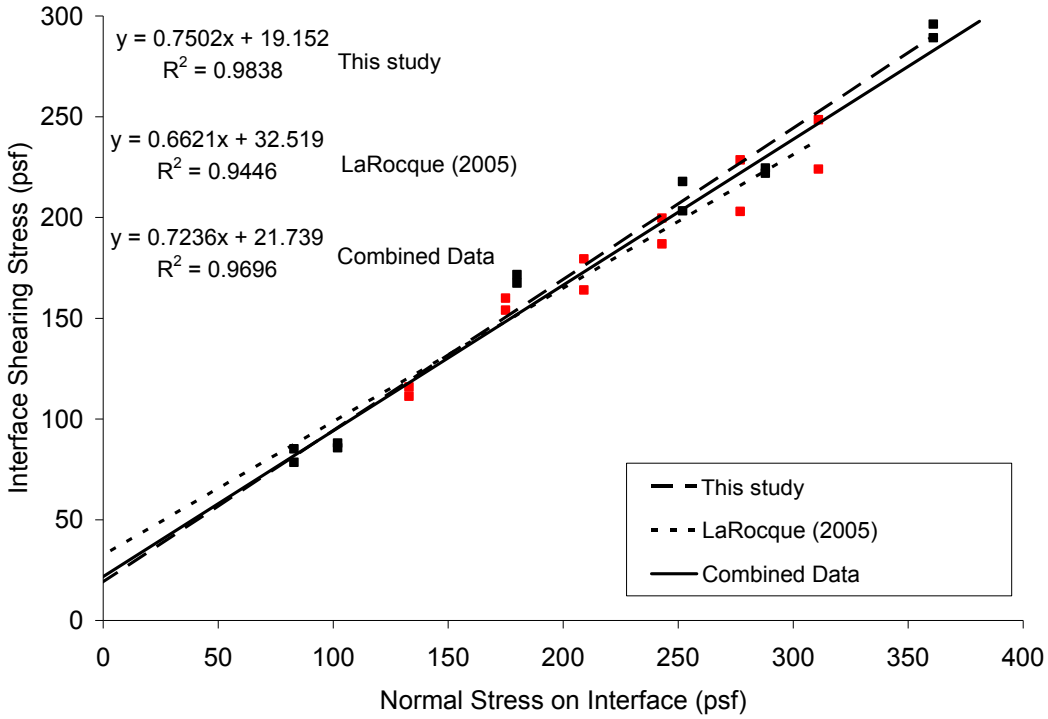

Figure 6.17: Failure Envelopes for the Dry Tire Bale Only Interface

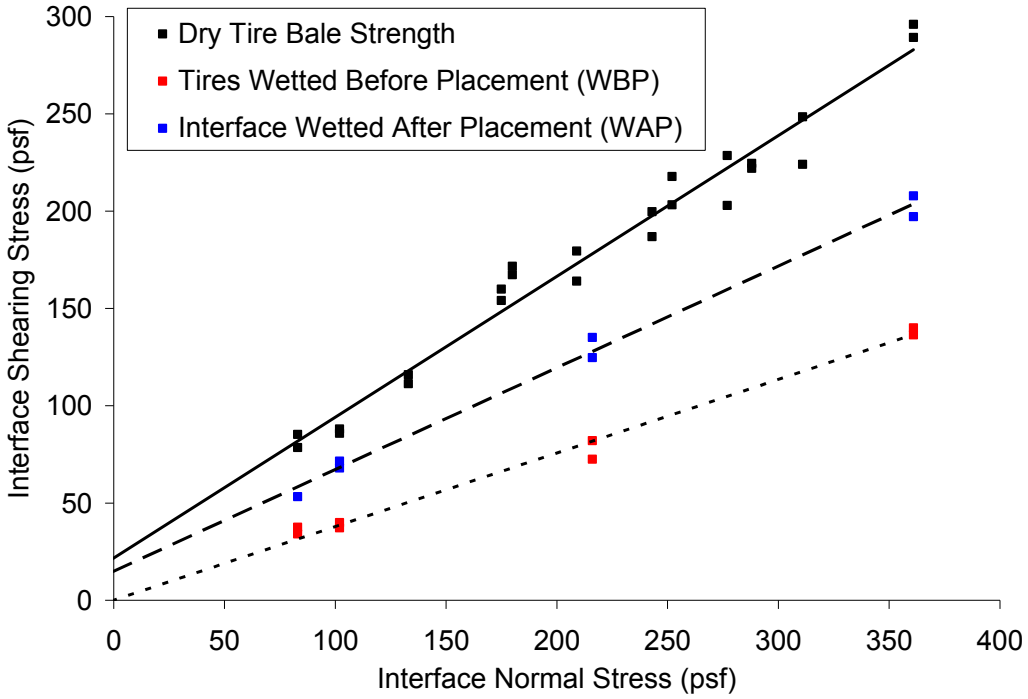

Figure 6.18: Failure Envelopes for the Dry and Wet Tire Bale Only Interfaces

Table 6.1: Mohr-Coulomb Strength Parameters for the Tire Bale Only Interface for Dry and Wet Conditions

Interface Condition	c' (psf)	ϕ' (degree)
Dry	20	36
Wetted After Placement (Partially Saturated)	13	27
Wetted Before Placement (Fully Saturated)	0	21

6.4.3 Appropriate Interface Strengths for Design of Tire Bale Structures

The loss in interface shearing strength due to the presence of moisture is an important aspect that must be taken into account for the design of any structure containing tire bales. Traditionally, only dry interface strengths have been obtained from lab testing and therefore were the only strength values used in designs. However, the critical conditions of many soil structures may include the presence of water within the soil mass, and therefore the presence of water should also be considered when designing with tire bales. Therefore, it may be a more conservative approach to use the wet interface tire bale strength parameters obtained from the wetted after placement (WAP or partially saturated) testing in design to take into account any movement of the bales that could occur during the life of the structure under wet conditions. The

shear strength parameters obtained from the wetted before placement (WBP or fully saturated) testing, although the most critical values of strength, would only exist for tire bales placed into a structure with wet interfaces, which is prohibited by specifications for tire bale embankments (Appendix A).

6.5 Phase One Test Results—Anisotropic Interface Shear Strength

An anisotropic testing program was also implemented with the Phase One testing (tire bale only interfaces) to determine the change in interface shearing stress with direction of loading. It has been assumed that the traditional direction of loading (shearing in the direction parallel to the baling wires) would provide the highest shearing resistance. However, in most bale structures there have been no specifications for the placement of bales, so many bales have been loaded both parallel and perpendicular to the baling wires. The goal of this testing phase is to determine if there is any significant loss in shearing resistance with change in loading direction, and the effect that this difference may have on future design. Both dry and wetted after placement (WAP) interfaces were tested under anisotropic conditions. The test setup for the anisotropic direct shear testing is shown in Figure 6.19.

6.5.1 Results from the Anisotropic Direct Shear Testing of Tire Bale Interfaces

Although the testing procedures for the traditional and anisotropic direct shear tests were the same, the behavior of the mobile bale during shear was significantly different. Compressions of the mobile bale increased from 2–3.5 inches (traditional testing) to 1.5 to 5 inches (difference in displacement curves in Figure 6.20) during shearing. Much of this compression was visually observed to occur at the rounded loaded interface (Figure 6.21).

Figure 6.19: Anisotropic Tire Bale Direct Shear Testing Setup

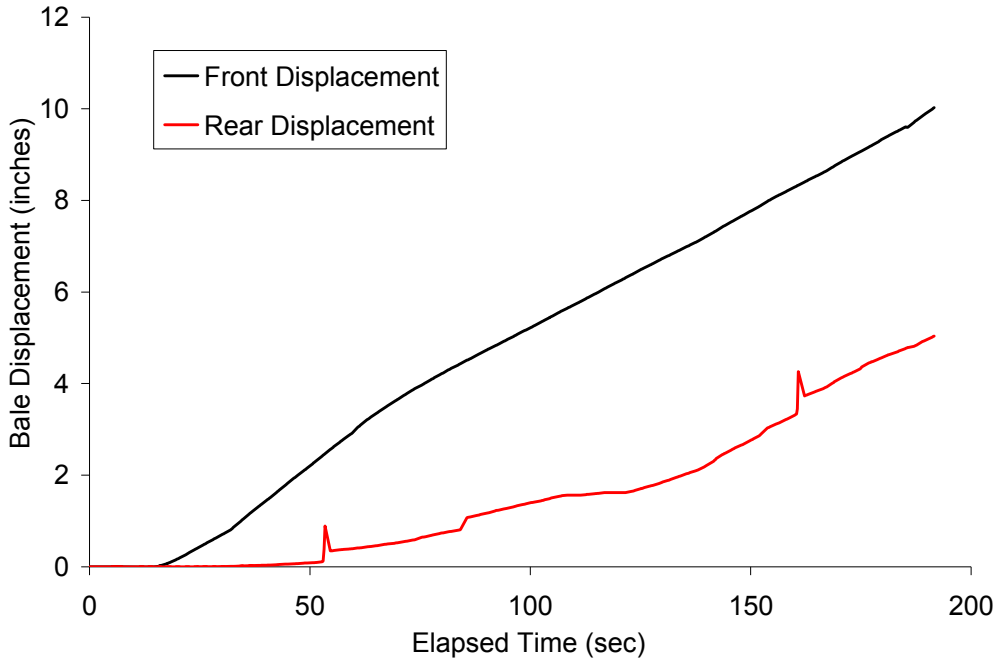

Figure 6.20: Displacements Measured at the Front and Rear of the Mobile Tire Bale During Anisotropic Direct Shear Testing

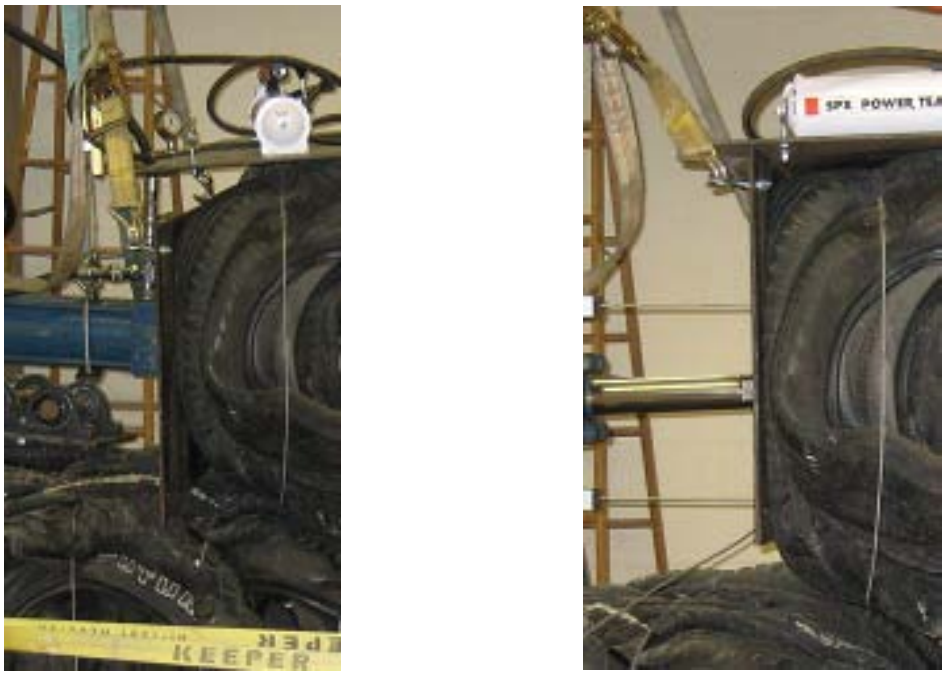

(a) Interface Before Loading. (b) Interface After Loading.

Figure 6.21: Loaded Interfaces from Anisotropic Direct Shear

Typical stress-displacement curves for the anisotropic testing are shown in Figure 6.22. The three sections of behavior (as described for the traditional testing) are present in the anisotropic testing (section 1 is missing from the 361 psf graph due to a seating load applied before shearing). An increase in displacement required to reach failure conditions, due mostly to the increase in compression of the loaded interface, was observed.

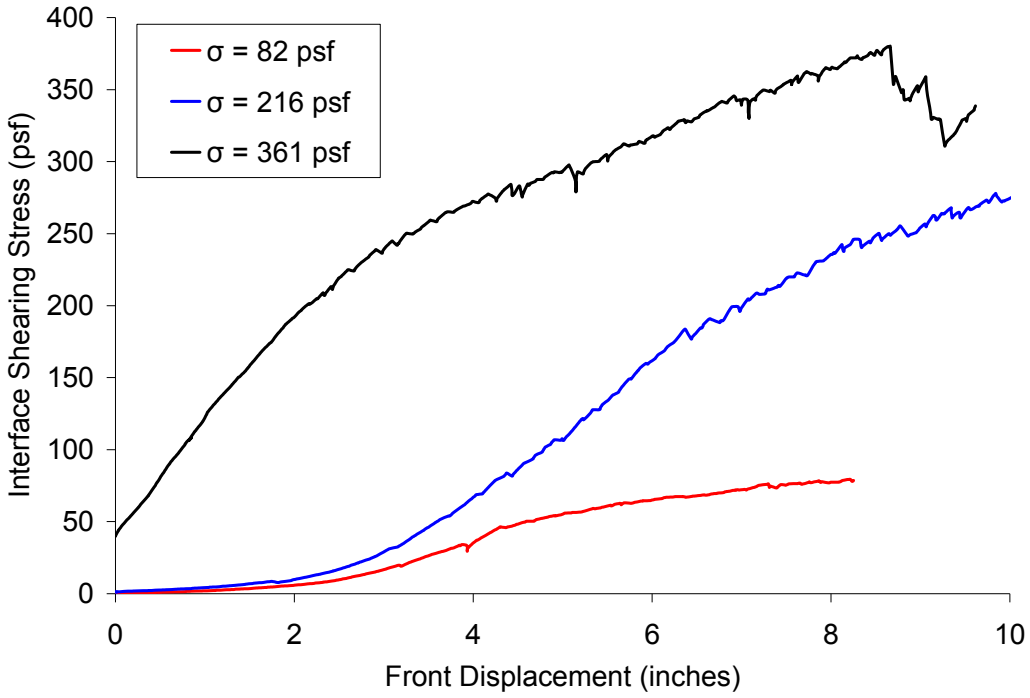

Figure 6.22: Interface Shearing Resistance versus Front Displacement of the Mobile Bale for Anisotropic Direct Shear Testing of Tire Bales (Dry Interface)

6.5.2 Shear Strength Parameters for the Anisotropic Tire Bale Interfaces

Failure, or peak, interface shearing stresses (Figure 6.23) were determined using both the bi-linear method and compression method described in Chapter 6.3.2. Linear failure envelopes were used to determine the cohesion and friction angle values for the dry and wet interfaces (Table 6.2). The traditional failure envelopes and strength parameters are also included with the anisotropic data for comparison.

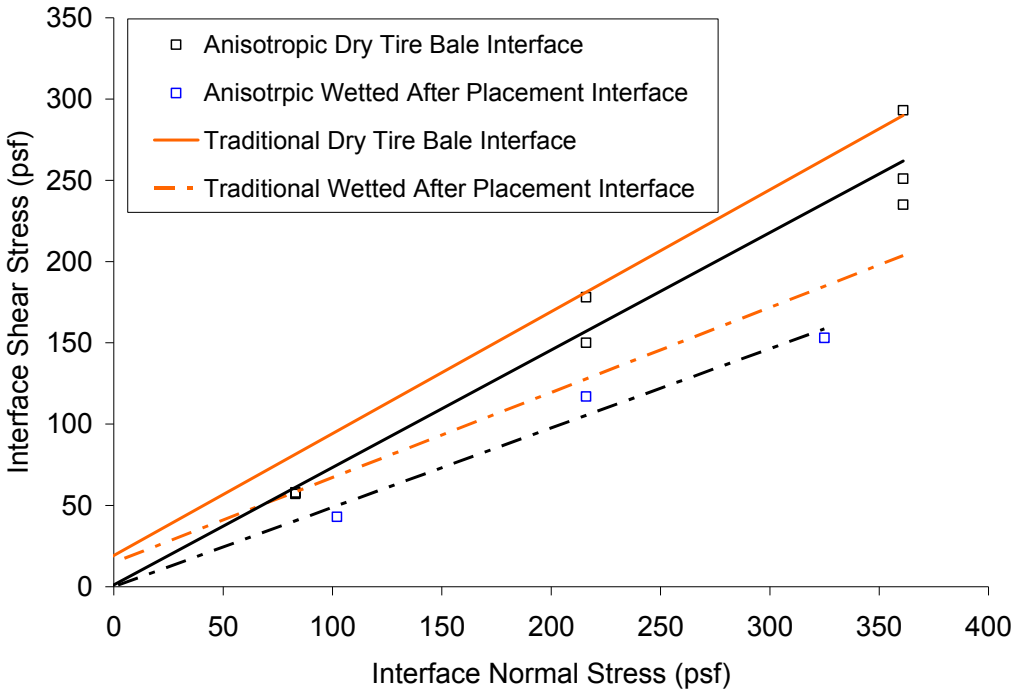

Figure 6.23: Failure Envelopes for the Dry and Wetted After Placement Tire Bale Interfaces for Traditional and Anisotropic Direct Shear Testing

Table 6.2: Mohr-Coulomb Strength Parameters for the Traditional and Anisotropic Tire Bale Only Interfaces for Dry and Wet Conditions

	Traditional Testing		Anisotropic Testing	
Interface Condition	**c' (psf)**	**ϕ' (degree)**	**c' (psf)**	**ϕ' (degree)**
Dry	20	36	4	36
Wetted After Placement (Partially Saturated)	13	27	0	26

6.5.3 Effect of Anisotropic Strength on Design of Tire Bale Structures

The only difference in the tire bale interface strength between the traditional and anisotropic testing is the reduction of the cohesion intercept for the anisotropic placement. This reduction in cohesion may be due to the change in how the bales are sliding past each other. In the anisotropic testing, the tire ridges along the mobile bale are no longer being sheared over the tire ridges from the stationary bales. Instead, the ridges are sliding parallel to each other, in which the friction between the tires is the same, but no significant cohesion is developed from the sliding of the ridges over each other. Even though there is a small change in cohesion, the strength of the bale interface with respect to the orientation of loading is not significantly reduced.

The main benefit of anisotropic placement of the bales is evident when considering the degradation of the tire baling wires. When tire bales are placed in the traditional manner (baling wires parallel to plane of maximum loading), any degradation of the baling wires would result in the tire bale expansion and subsequent pressures applied to the slope face (Figure 6.24). If the tire bales are placed in the anisotropic manner (baling wire perpendicular to the plane of maximum loading), then the expansion of the bale due to wire breakage will be confined by the surrounding tire bales. The placement of the bale in an anisotropic state may be more beneficial in the long term stability of the slope, when the baling wires have degraded and the bale expands. This topic is further discussed in Chapter 8.

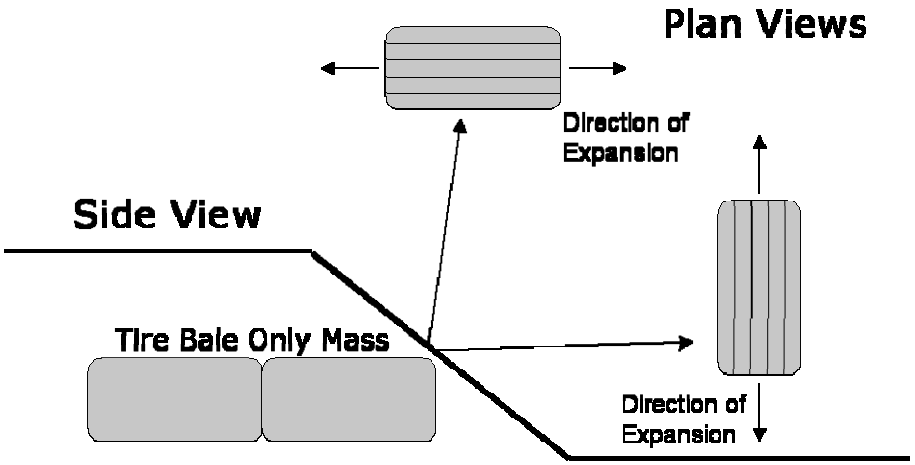

Figure 6.24: Illustration of Traditional and Anisotropic Tire Bale Placement in a Tire Bale Only Slope

6.6 Phase Two Test Results—Tire Bale on Soil Layer Interface Strength

In any tire bale structure, there is at least one interface in which the tire bales may potentially slide along a soil layer. In tire bale only structures, this interface is at the bottom of the tire bale mass, where the tires are placed on the foundation soils. The strength of this interface is usually increased by using a large stone rip-rap or gravel layer, in which the jagged stiff gravel particles resist the sliding of the irregular tire bale surface. When using tire bales as reinforcement elements within a soil slope (Illustration C in Figure 6.1) or for compacted soil covers along the tire bale mass, there needs to be an understanding of the behavior and strength of the tire bale-soil interface, especially for sand and clay soils.

6.6.1 The Tire Bale-Soil Layer Interface

Case histories presented two critical tire bale-soil interfaces: the tire bale-sand interface and the tire bale-clay interface. The main design concern with these tire bale-soil interfaces was the loss of soil into the voids of the tires bales, which is a prevalent problem with sandy soils. With clay soils, there is a concern of moisture storage within the bales causing the expansion (swelling) of clays and subsequent loss of strength. No research or field tests have been conducted to determine the strength of the tire bale-soil interface, which controls the stability of the structure. A series of tire bale-soil interface direct shear tests were therefore conducted to determine the strength of the interfaces.

Three different tire bale-soil interfaces were constructed for the testing program:

1. Thin Sand Fill: A sand fill was compacted around the bottom two stationary bales and placed up to a thickness of less than 0.5 inch on top of the bales. This thin sand layer filled in the tire ridges along the interface, but the top of the tire ridges from the bottom bales were still visible. This interface represents tire bale structures where a soil fill may be used around the bales, but no soil is compacted between the bales.
2. Thick Sand Interface: A 2 to 4 inch sand interface was compacted to a dry unit weight of 103 pcf on top of the stationary bales (Figure 6.25) to represent the tire bale-sand interface. The thickness of the sand layer was maintained to less than 4 inches to ensure that failure occurred along the interface and not within the sand mass.
3. Thick Clay Interface: A 2 to 4 inch compacted clay layer was placed between the stationary bales and mobile tire bale (Figure 6.26) to represent the tire bale-clay interface.

Figure 6.25: Photograph of the Thick Sand Interface

Figure 6.26: Photograph of the Thick Clay Interface after Testing

Compaction of the soil layers was accomplished with a vibratory hammer. Undrained shear strengths of both the sand and clay soils were determined from direct shear testing (Chapter 4). Soil properties for the sand and clay interface are presented in Chapter 4. The test procedure and setup for the tire bale-soil interface direct shear testing was the same as for the tire bale only interface. The applied shearing load, front and rear displacements, and vertical movements of the mobile bale were all measured (as illustrated in Figure 6.6). The tire bale interface was wetted after placement to simulate wet conditions within the structure.

6.6.2 Results from the Direct Shear Testing of Tire Bale-Soil Interfaces

Typical interface shearing stress versus displacement curves for the thin sand fill, thick sand interface and thick clay interfaces testing are shown in Figures 6.27, 6.28, and 6.29, respectively. The stress-displacement behavior of the soil interfaces is similar to that of the tire bale only interface; a compression of the loaded interface (Section 1), an increase in interface stress to the peak load due to rigid displacement (Section 2), and a post peak sliding of the mobile bale (Section 3). However, for the thick sand and clay layers, there is an increase of the displacement of the mobile bale before reaching the peak strength (increased from 2 to 3 inches for the tire bale only interface up to 3 to 5 inches for the tire bale-thick soil interfaces) when compared with the traditional tire bale only interface.

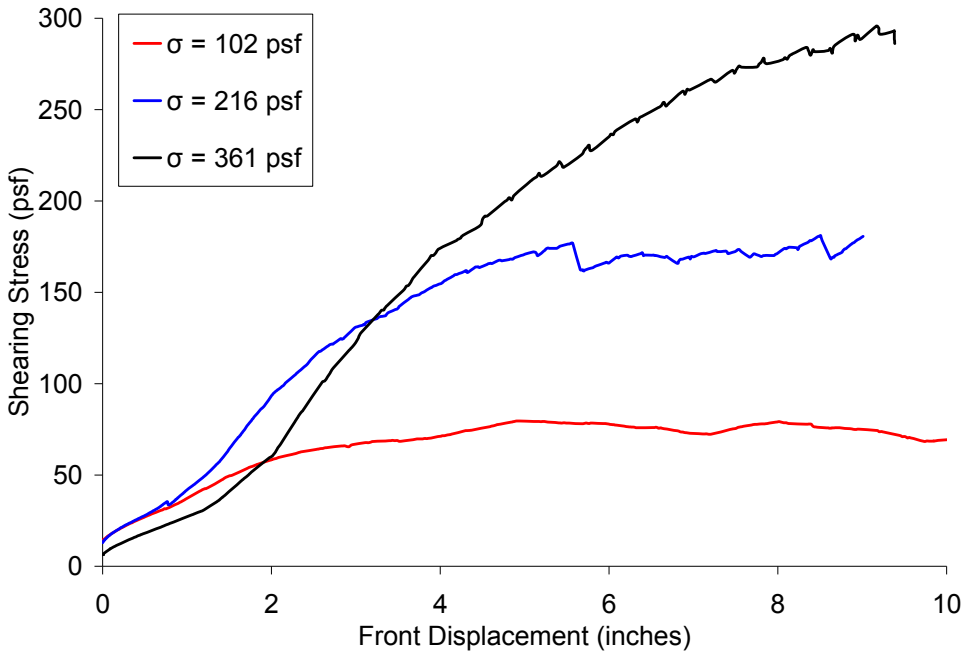

Figure 6.27: Interface Shearing Resistance versus Front Displacement of the Mobile Bale for the Thin Sand Layer Fill

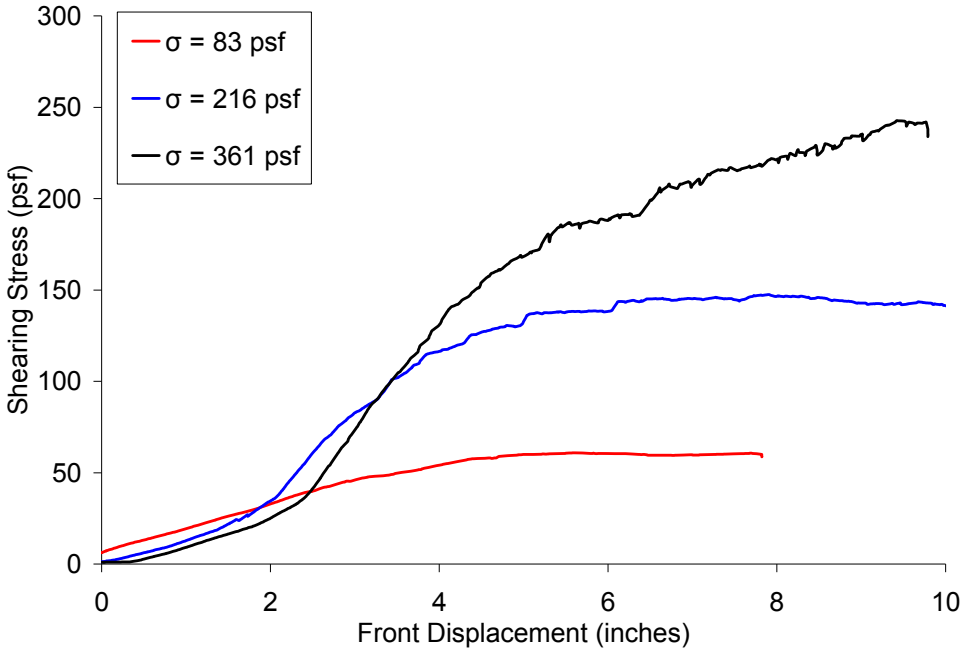

Figure 6.28: Interface Shearing Resistance versus Front Displacement of the Mobile Bale for the Thick Sand Interface

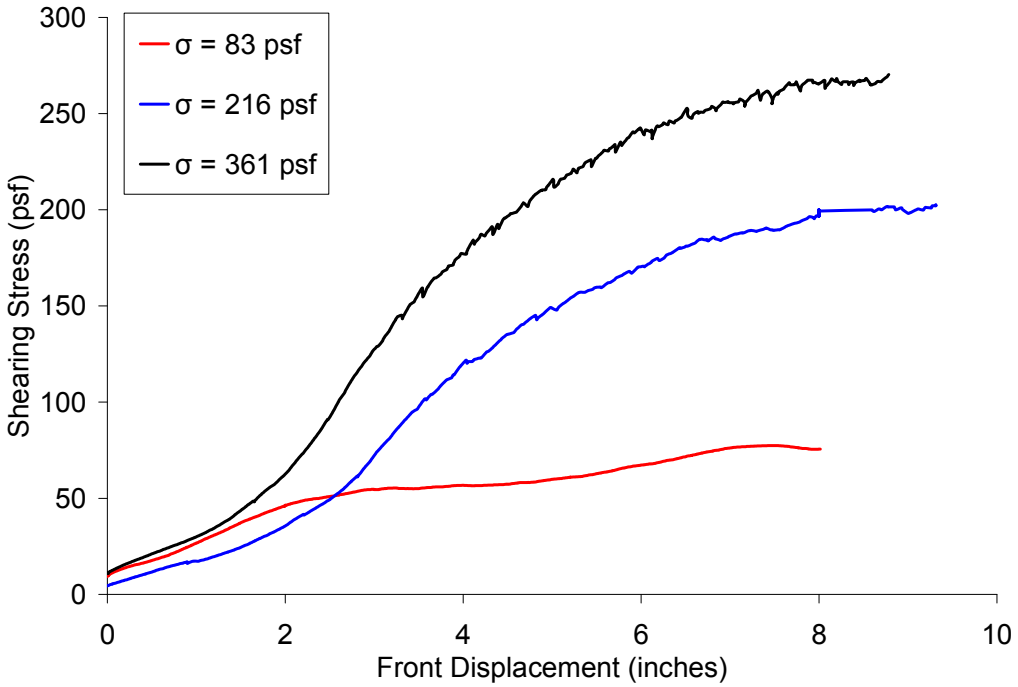

Figure 6.29: Interface Shearing Resistance versus Front Displacement of the Mobile Bale for the Thick Clay Interface

6.6.3 Shear Strength Parameters for the Tire Bale-Soil Interfaces

The failure shearing stresses were determined using the bi-linear method described in Chapter 6.3.2. The compression method was not used due to the large rigid displacements of the bale required to reach the failure condition (maximum compression of the bale occurred before the failure along the interface). The interface strength envelopes for the thin and thick sand interfaces are shown in Figure 6.30. Also included is the direct shear sand strength for the same unit weight and moisture content conditions.

The failure interface strength versus normal load along the interface for the thick clay interface is shown in Figure 6.31. A comparison between the tire bale-clay interface and the undrained clay strength (for the same unit weight and moisture conditions) determined from UU Direct Shear testing is shown in Figure 6.32.

The cohesion intercept values and friction angles from the tire bale-soil interfaces and from the soil testing is provided in Table 6.3. For the tire bale-sand interfaces, the friction angle for both the thin and thick sand interfaces are similar to the lower friction angle (for a unit weight of 93 pcf) measured for the sand for direct shear testing. The cohesion intercepts are a result of the interaction between the tire ridges and passive soil ridges created during shear causing the creation of a jagged, uneven failure surface. The higher value of the cohesion intercept for the thin sand layer, as compared to the thick sand layer, is due to contact of the mobile bale tire ridges to the stationary tire bale ridges still present along the interface. The lower friction angle of the thin sand fill (when compared to the tire only interface) is due to the reduced contact area between the tire ridges caused by the sand infill filling the voids.

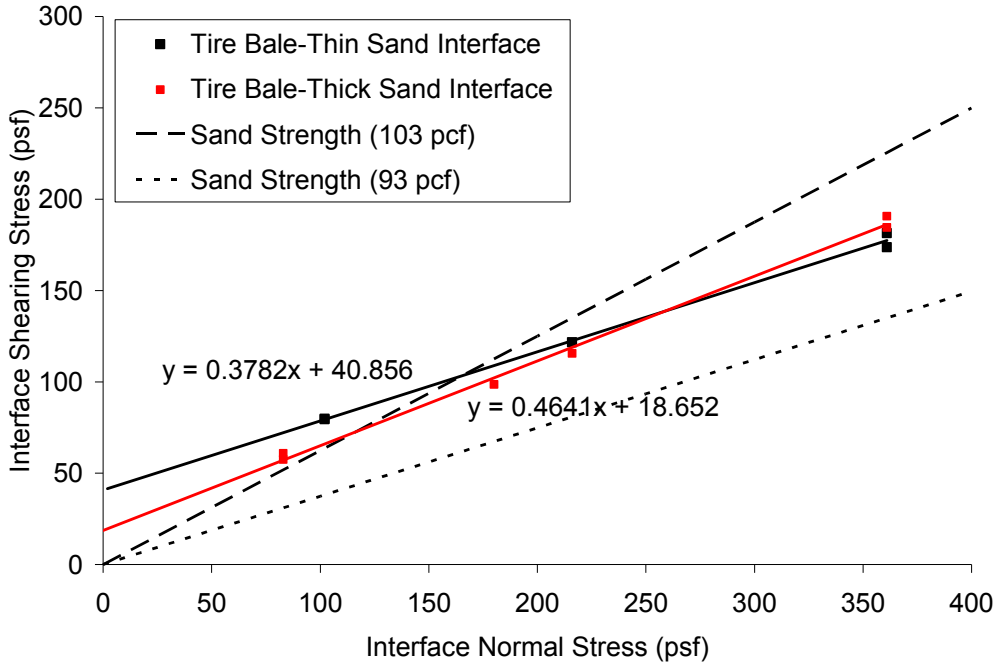

Figure 6.30: Failure Envelopes for the Thin Sand Fill and Thick Sand Interface Large Scale Direct Shear Tests and Sand Strength from Direct Shear Testing

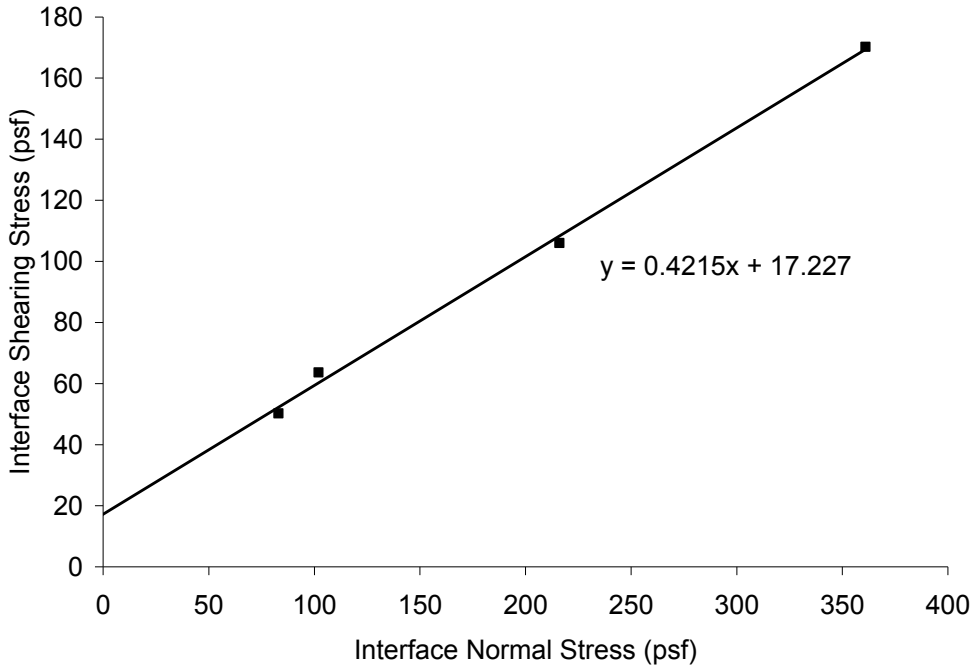

Figure 6.31: Failure Envelopes for the Tire Bale-Thick Clay Interface Direct Shear Tests

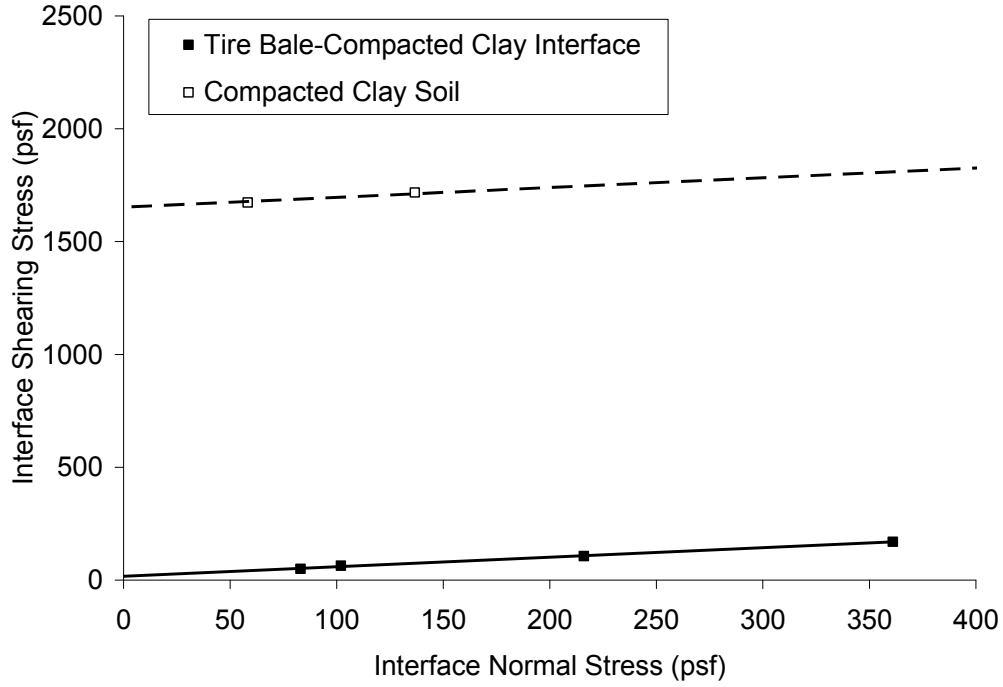

Figure 6.32: Comparison of the Clay Strength from Undrained Direct Shear and the Tire Bale-Clay Interface Testing

Table 6.3: Strength Parameters for the Tire Bale-Soil Interfaces and Direct Shear Testing of Soil Only Specimens

		Testing Procedure	
Soil Type		**Tire Bale Interface Testing (Large Direct Shear Testing)**	**Soil Only Testing (Traditional Direct Shear Testing)**
Thin Sand Fill	c'	38 psf	0 psf
	ϕ'	21^o	30^o (21^o)*
Thick Sand Interface	c'	18 psf	0 psf
	ϕ'	25^o	30^o (21^o)*
Compacted Clay Interface	c	17 psf	1653 psf
	ϕ	23^o	23^o

* Indicates Residual Strength Parameter

The tire bale-thick soil infill interface strengths and soil only strengths indicate that the frictional response along the tire bale interface cannot be directly predicted by the direct shear testing of the soil. The decrease in strength is due to the interface strength defined along the footprint area, which is significantly larger than the actual area (actual contact along the tire bale-clay interface). A more in depth discussion of the tire bale-thick soil interfaces is presented in Chapter 6.6.2.

6.6.4 Sand Loss into the Tire Bales

Observations of sand loss into the bales were made during the placement and construction of the thin sand fill and thick sand interface. In order to determine the potential for the loss of soil into the bale, dry sand was placed along the top of the bales and vibrated to cause inflow of the sand into the bales. It was estimated that over 0.17 cubic yards of dry sand was lost into the stationary bales during the compaction of the thin sand fill. Subsequent soil sink holes (Figure 6.33) were noticed during the direct shear testing of the thick sand interface. Sand was constantly replaced along the interface to maintain the thickness of the soil layer.

Figure 6.33: Sand Sink Holes Measured Along the Surface of the Thick Sand Interface

After the conclusion of the tire bale-soil interface testing, an attempt was made to weigh the tire bale with sand that had filled into the voids. Lifting the bale caused an instantaneous flow of sand from the bale before a measurement could be taken, but approximately 0.25 cubic yards of sand was removed from the bale (Figure 6.34). The significant loss of soil into the bales illustrates the need for proper design of tire bale structures to limit the loss of soil into the bales, whether this is accomplished by wrapping the bales in a geosynthetic or using large aggregate around the bale to limit the flow of soil.

Figure 6.34: Total Sand Outflow from the Tire Bale

6.7 Comments on the Tire Contact Area

In the previous sections, stresses along the tire bale interfaces were calculated by dividing the applied shearing and normal loads by the footprint area of the tire bale (average length times the average width). The footprint area was used in this testing program, as well as previous research programs, because it is easily measured and allows for the shear strength parameters and failure surface geometry to be directly plugged into a limit equilibrium analysis. However, no analysis was provided to take into account the actual irregular and complicated tire bale interface and the behavior of the interface during shear, which may be especially beneficial for understanding the tire bale-soil interfaces. The following section provides an analysis of the complicated tire bale interface to better explain the relationship between the assumed tire bale interface strength and actual material strength (due to tire friction or soil strength).

6.7.1 Measurement of the Actual Contact Area for the Tire Bale Only Interface

The value of the actual contact area was found using a tire "stamping" method that involved placing a piece of paper between the stationary and mobile layers of tires, painting the tire bale interfaces, and pressing the top tire bale down onto the interface (Figure 6.35). The result is a two dimensional representation of the actual contact area along the interface. The actual contact area was assumed to remain essentially constant during shearing, so that only the normal load had to be applied to the interface to measure to value. Application of a shearing

load, or horizontal displacement of the bale, would only cause a smearing effect and provide higher measurement of the area.

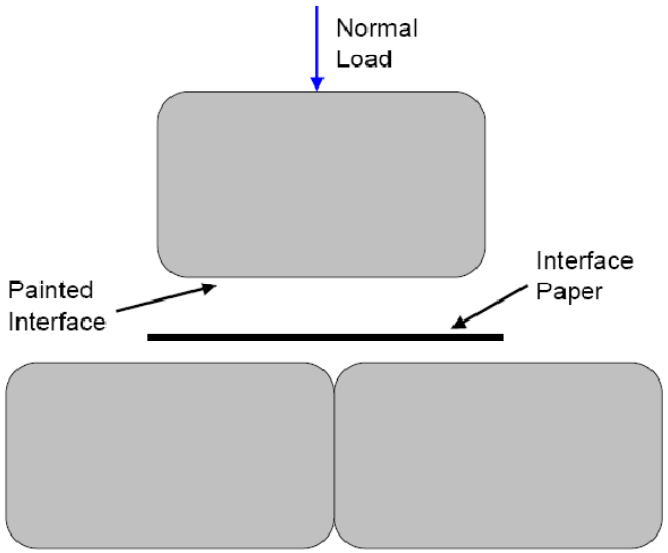

Figure 6.35: Illustration of the Tire Stamping Method to Measure the Actual Contact Area along the Tire Bale Interface

The result is two-dimensional area that represents the three-dimensional jagged interface contact area (Figure 6.36). Note that the piece of paper used for the tire stamping was exactly 22.5 ft^2 in area, exactly the same as the footprint area of the bale.

Figure 6.36: Photograph of a Tire Bale Interface Stamp

It can instantly be noticed that the actual contact area along the tire bale interface is much less then the assumed footprint area. The actual contact area was estimated for a range of normal loads to determine any effect of the applied loads to the contact area. Digital photographs of the tire stamps were taken and converted to black and white only images using Adobe Photoshop

CS2. The program was also used to count the number of black and white pixels, which was used to determine the ratio of actual contact area to the total stamp size. The ratio multiplied by the footprint area of the bale (area of the white paper) provides the actual contact area along the interface (Figure 6.37).

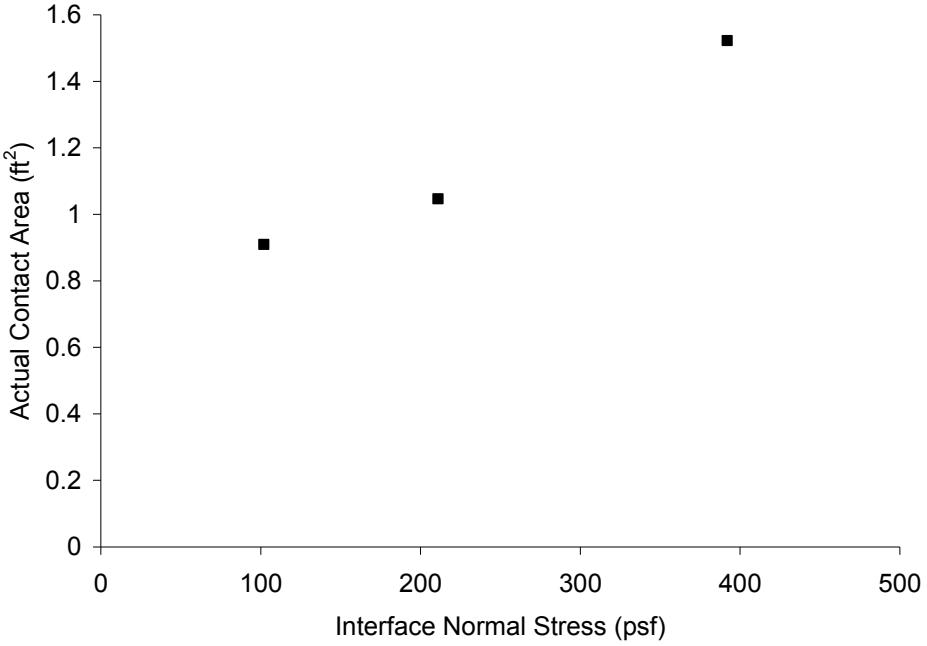

Figure 6.37: Actual Tire Bale Interface Contact Area with Applied Normal Load

It is immediately apparent from the tire stamp testing results that the actual contact area along the interface is only a small fraction of the assumed footprint area, resulting in higher stresses along the actual contacts by a magnitude of almost 20. For a predicted normal load of 211 psf along the footprint area, the normal stress along the actual contact areas is approximately 4500 psf.

6.7.2 Discussion of the Tire Bale-Soil Interface Strength

A comparison of the soil strength versus the tire bale-soil interface strength indicates only minor similarities between the two. A separate analysis is needed to better understand the behavior along the tire bale soil-interface and how to relate the soil strength to the interface strength. Unlike the tire bale only interface, consideration is needed to determine the effects of the actual contact area on the tire bale-soil interface strength. In this section, a brief analysis of the tire bale-soil interfaces is presented to better understand the behavior along the tire bale-soil interface.

The Tire Bale-Thick Sand Interface

The behavior of the tire bale-sand interface is controlled by the jagged, irregular tire bale surface sliding along the sand mass. After displacement across the interface, the tire bale remolds the top sand layers and creates a series of passive soil ridges (Figure 6.38) that resist the movement of the mobile bale. The failure surface under these sand ridges is most likely

controlled by the passive forces in the soil; however, shearing can only occur within the sand since the tire ridges cannot be sheared. Therefore the interface strength must be controlled by the sand strength (illustrated in Figure 6.39). Results from the direct shear testing have verified that the stress parameters defined along the interface (assuming the contact area is the footprint area of the bale) are different than those of the sand. The following section will provide visual observations and approximate measurements of the contact area along the interface to provide evidence that the stress parameters along the interface are different due to the assumption of the footprint contact area.

Estimated measurements and visual observations of the tire bale-sand interface during and after direct shear testing provided evidence that the area of the actual failure surface along the sand mass was less than that of the footprint area. For two tests, the sand surface was wetted so that the boundaries of the failure plane (areas of disturbed sand) could be photographed (Figure 6.40).

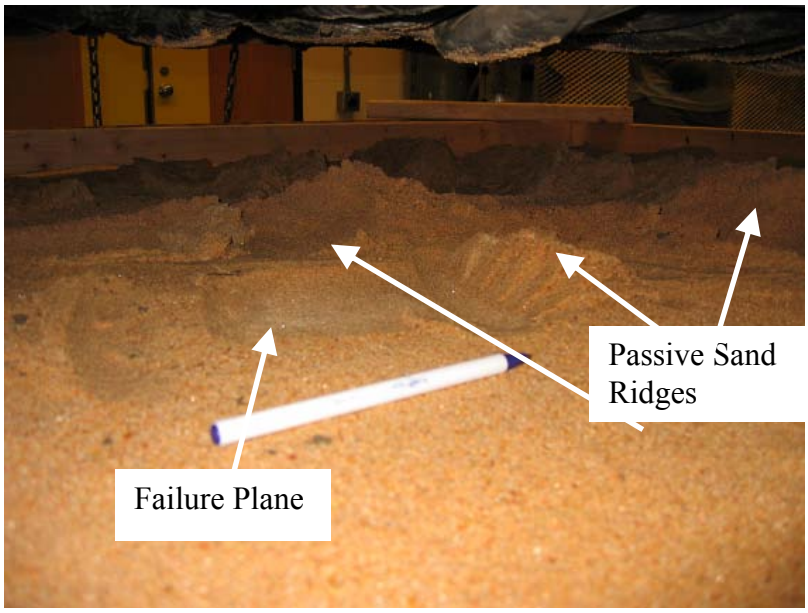

Figure 6.38: Photograph of a Failure Plane and Soil Ridge along the Interface

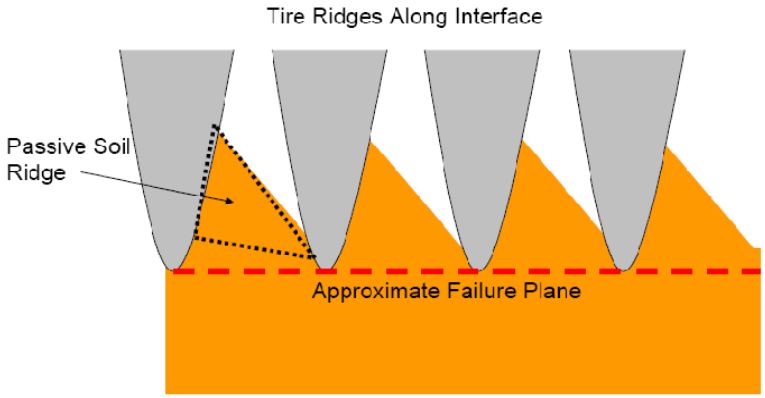

Figure 6.39: Illustration of the Tire Bale-Sand Interface at Failure

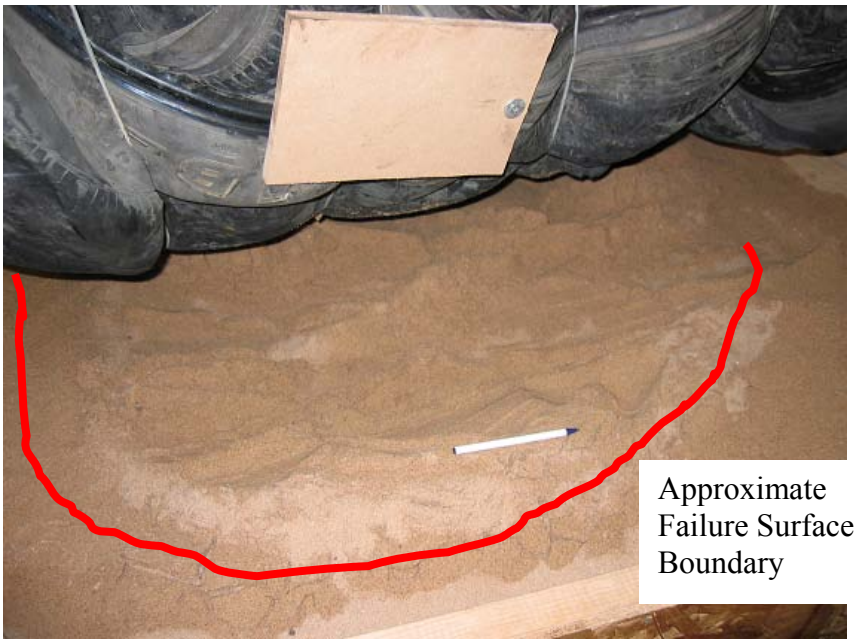

Figure 6.40: Approximate Failure Surface for the Tire Bale-Sand Interface for an Applied Normal Stress of 88 psf (Self Weight of Bale Only)

The actual contact area is less than the footprint area due to the rounded edges of the bale, (Figure 6.41). The footprint area assumes that the bale is perfectly rectangular, and that the cross sectional area at the middle of the bale is the same as the bottom and top of the bale. The rounded shape of the bale sides implies that the area at the base of the bale is less than that of the middle of the bale. The interface contact area is further reduced by areas along the interface in which the tire ridges do not contact the sand mass.

Figure 6.41: Photograph of the Rounded Bale Interface at the Tire Bale-Sand Interface Contact Area

Measurements along the interface indicate that the actual length and width of the contact area along the tire bale-sand interface are approximately 6 to 8 inches shorter than the footprint area of the bale, resulting in approximate contact areas of 17 to 18 square feet at lower normal loads. However, as the normal load increases, the size of the sand ridges increased (up to 6 inches in height), and the passive failure planes were observed to extend past the rear of the tire bale (Figure 6.42).

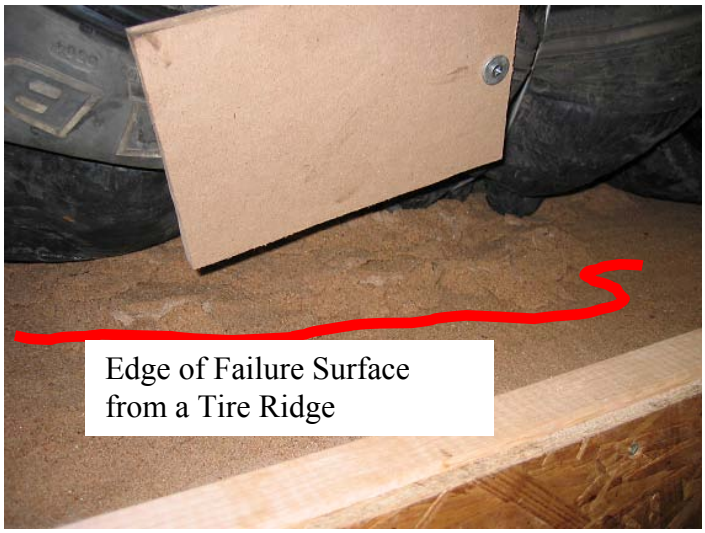

Figure 6.42: Photograph of the Failure Surface Extending Past the Rear of the Bale under a Sand Ridge

Some of the passive sand ridges allowed the failure surface to extend almost one (1) foot past the rear of the bale at higher normal loads, increasing the shearing area to approximately 24 ft^2, providing evidence that the approximate failure surface within the soil mass changes with normal load. This is the main discrepancy between the definition of the stress parameters for the interface and the soil, since the parameters for the interface are defined for a constant (footprint) area but the soil is actually sheared along changing area (Figure 6.43).

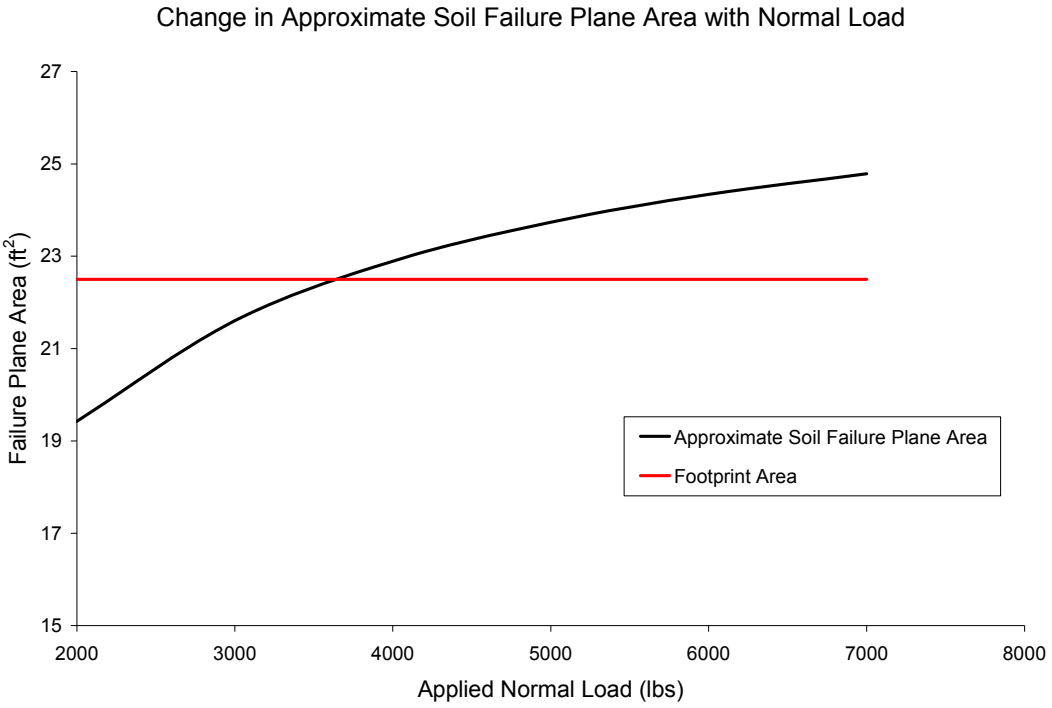

Figure 6.43: Change in the Sand Failure Plane Area with Applied Normal Load

The changing failure surface area and definition of the footprint shearing surface are the source of the decreased friction angle for the tire bale-sand interface as compared to the sand strength. For example, the normal stress along the failure surface is defined as the applied normal load divided by the contact area (Normal Load/Area), as shown in Figure 6.44. Three normal stresses are presented, the variable actual failure surface normal stress (takes into account the changing surface area), a constant actual failure area (19 ft^2 for this example), and the footprint normal stress of the tire bale.

The shear stresses along the different failure surface are defined as the normal stress multiplied by the tangent of the friction angle of the sand (Figure 6.45). Failure envelopes for the three contact areas are all plotted against the normal stress along the footprint area of the bale (area that was used to define the stress parameters and will be used in a limit equilibrium analysis). For the calculated envelopes, the friction angle of the footprint area and variable actual contact area are the same. The reduction in the variable actual contact area as compared to the constant actual contact area is due to the reduction in calculated stresses along the contact area due to the increase in area with normal load (as area increases the stress decreases). Notice that using the variable actual contact area produces the same friction angle as the footprint area, and using the constant actual contact area produces the same friction angle as the sand.

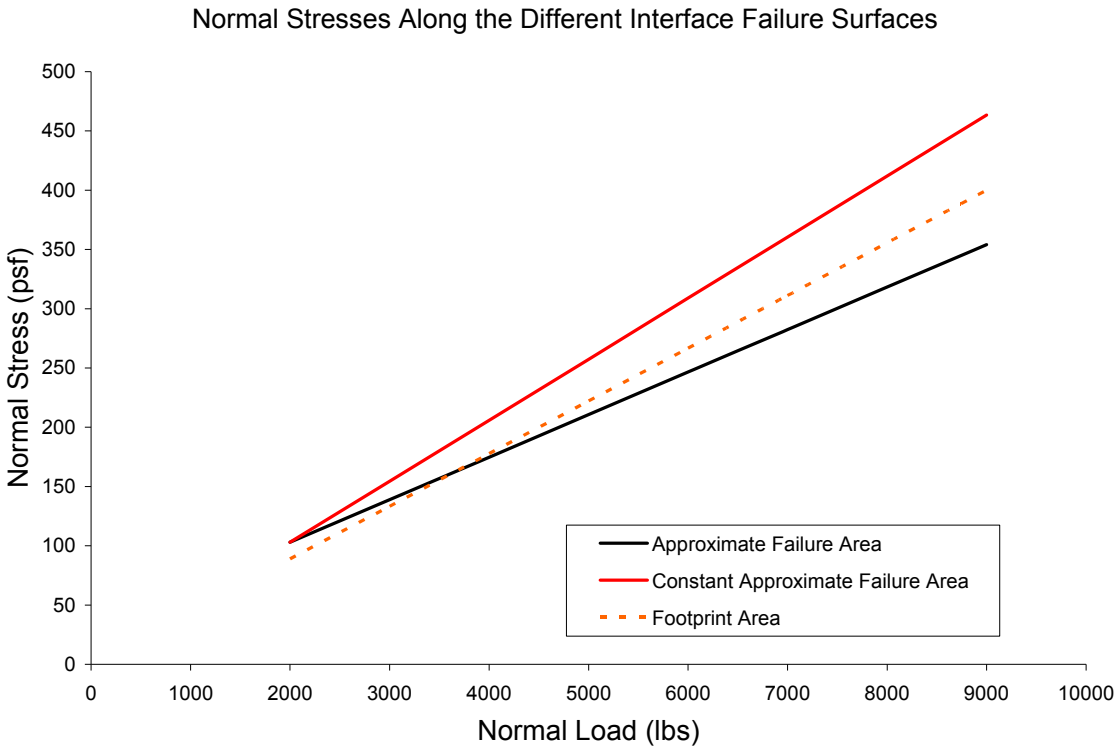

Figure 6.44: Different Normal Stresses Along the Interface for the Assumed Contact Areas

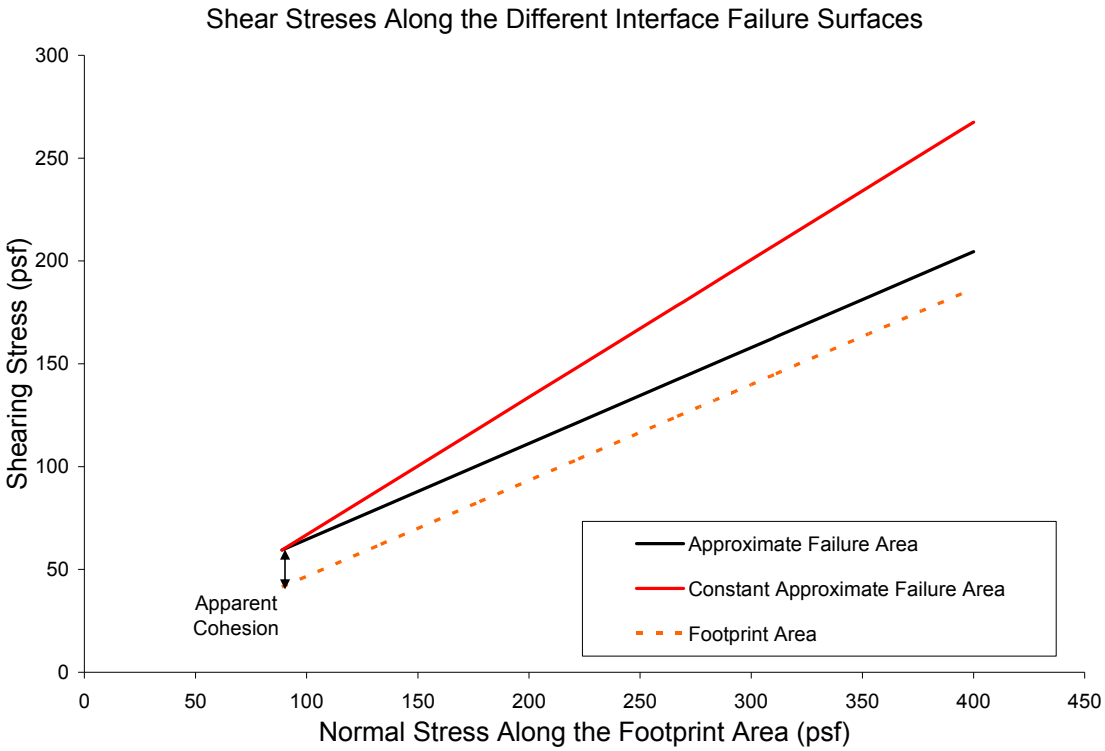

Figure 6.45: Failure Envelopes for the Different Interface Contact Areas

The results of this analysis indicate two main conclusions:

1. The reduction of the tire bale-soil interface friction angle (as compared to soil only strengths) and presence of the apparent cohesion is due to the definition of the shearing areas along the interface. In order to use simple c and ϕ stress parameters in a limit equilibrium analysis, the parameters must be defined over a flat constant footprint area of the bale, which was found to be different than the actual shearing surface within the soil. The effect of the variable, jagged actual failure surface on the stress parameters is a reduction in the tire bale-sand interface friction angle as compared to the sand only strength and the presence of a small cohesion. Results from this testing program indicate that the sand only peak friction angle must be reduced by 15%–20% to be used for the tire bale-sand interface, which is approximately the ratio of the actual contact area of the bale (18 ft^2) to the footprint area (22.5 ft^2). However, lower estimates of the interface strength have been used in design to remain conservative (for example, assuming the interface friction angle is $2/3\phi_{soil}$).
2. The loss of contact area along the tire bale-soil interface and reduced soil strengths along the interface provides evidence of a weaker plane that exists within the tire bale structure. Therefore, the interface of a tire bale and soil layer will always be the weakest plane due to reduced contact area, indicating that it would be more beneficial to either use an angular gravel material at the interface (which is expensive) or place tire bales in direct contact with each other. This reduction in tire

bale-soil interface strength is potentially worsened by the presence of excessive water (water stored in the bales) and the loss of soil into the bales over time.

The Tire Bale-Clay Interface

A similar method of analysis can also be used to illustrate the significant loss in strength of the tire bale-clay interface as compared to the undrained clay strength. Although the friction angles from both of the tests are approximately the same, there is a significant reduction in the cohesive portion of the shear strength. Visual observations indicate that this reduction is mostly due to the significant difference in the actual contact area along the interface as compared to the footprint area (Figure 6.46). Measurements of the actual clay contact area were unsuccessful, but can be considered approximately equal to the tire bale only contact area measurement described in Chapter 6.6.1 (Figure 6.37).

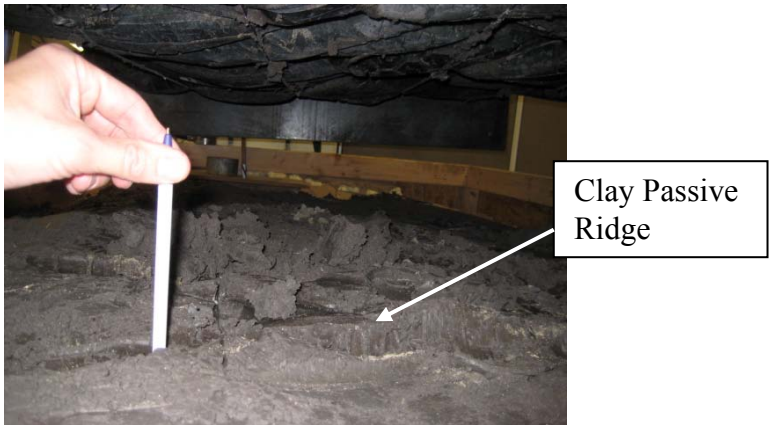

Figure 6.46: Photograph of the Clay Interface after Direct Shear Testing

The compacted clay, which was not as flexible and compressible as the sand interface, acted as a flat plate that the mobile tire bale was placed on, resulting in low contact areas. As the mobile bale was displaced along the interface, very small passive clay ridges were formed resulting in only a small area of soil resisting the bale motion and therefore the significant reduction in the tire bale-compacted clay interface as compared to the clay only strength (Figure 6.47).

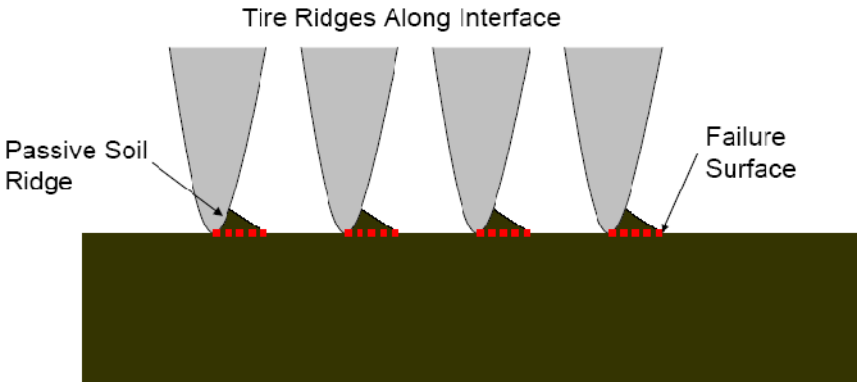

Figure 6.47: Illustration of the Tire Bale-Compacted Clay Interface at Failure

Summary

The following analysis provided a method to determine the proper reduction factors for the soil strength to be used along the tire bale-soil interface. The soil strengths are reduced because (1) the actual contact areas are less than that of the assumed footprint area (Figure 6.58), and (2) the geometry of the two areas is significantly different and changes with normal load. The reduction factor applied to the soil strengths is essential because the failure planes in limit equilibrium analyses are controlled by the footprint area (or geometry) of the tire bales and not the actual contact area, which changes with normal load. The previous analysis used the stresses along the footprint area to determine the corresponding area of the failure plane in the soil mass. By setting the stresses equal to each other, it is possible to essentially determine the area of soil needed in order to provide the same resistance over the footprint area. Results for both the clay and sand interface indicate an increase in the shearing area with normal load, most likely due to the increase in penetration of the tire ridges into the soil with increasing normal load increasing the size of the passive soil ridges. The change in the area is proportional to the reduction of the soil strengths that is needed for the soil strengths. These calculations were supplemented with observations and measurements from the tire bale testing that also provided evidence of the actual failure area and geometry. The result is a set of reduction factors for sand and clay soil fills that should properly represent the strength of the tire bale-soil interface.

6.8 Summary of Interface Shear Testing

The goal of the strength testing program presented in this chapter was to obtain the interface strength of the tire bale mass for different short term design considerations. Most importantly, the affects of moisture on the interface strength were determined for both the tire bale only and tire bale-soil interfaces. The conclusions from the testing program indicate that a more conservative value of the interface strength may be required to take into account moisture along the interface as well as tire bale orientation within the bale structure. In addition, the design of tire bale structures must also take into account the deformation behavior of the bales during shear. The compression of the bales (referred to as Section 1 in the stress-displacement curves), which ranged from 1.5 up to 6 inches, are half the value of those expected in the field since compression will be occurring on both faces of the bale. For some tire bale structure designs, it was required that bales placed into a structure are pushed together during placement to reduce voids and compressions along the loaded interfaces, with some projects even requiring the placement of sand between bales to further reduce any compressions.

Results from tire bale-soil testing also provide evidence of a significant decrease in the tire bale-soil interface as compared to the soil strength. An analysis of the tire bale-soil and tire bale only interface indicated that the difference in the soil and soil interface strength is due to the irregular tire bale interface and the variable interface contact area. However, the strength of the interface was defined along the constant and flat footprint area so that simple strength parameters can be determined and used in a conventional limit equilibrium analysis, which cannot take into account the actual complicated tire bale interface contact area.

Chapter 7. Material Characterization of Tire Bales—Compressibility

A series of compression tests were conducted to determine the behavior of tire bales when subjected to vertical normal loads, simulating surcharge pressures acting on the tire bale structure. Short term and long term loading conditions were both considered. The results of the compression testing on tire bales are presented in the following sections.

7.1 Large Scale Compression Testing Setup for Tire Bales

Early compression testing of tire bales consisted of placing a single tire bale between two rigid plates and loading the bale at a constant strain rate. Although nothing is fundamentally wrong with this testing setup, it neglects one of the most important aspects of the tire bale structure: the tire bale-tire bale interface. Loading the interface of the tire bale with a rigid plate changes the compression behavior of the bale structure as compared to the behavior of the tire bale-tire bale interface, as discussed later in the chapter. Two testing structures were implemented in this testing program to determine the compressibility of tire bale structures, both of which included the tire bale-tire bale interface. Illustrations of the test structures, the three bale structure (similar to that used in the direct shear testing) and the two bale structure, are shown in Figure 7.1. The three bale structure was considered the most critical (weakest) arrangement since the contact area along the interface was the smallest, resulting in higher stresses, and therefore was the focal test setup for compression testing. All long term testing presented at the end of this chapter was conducted with the three bale structure.

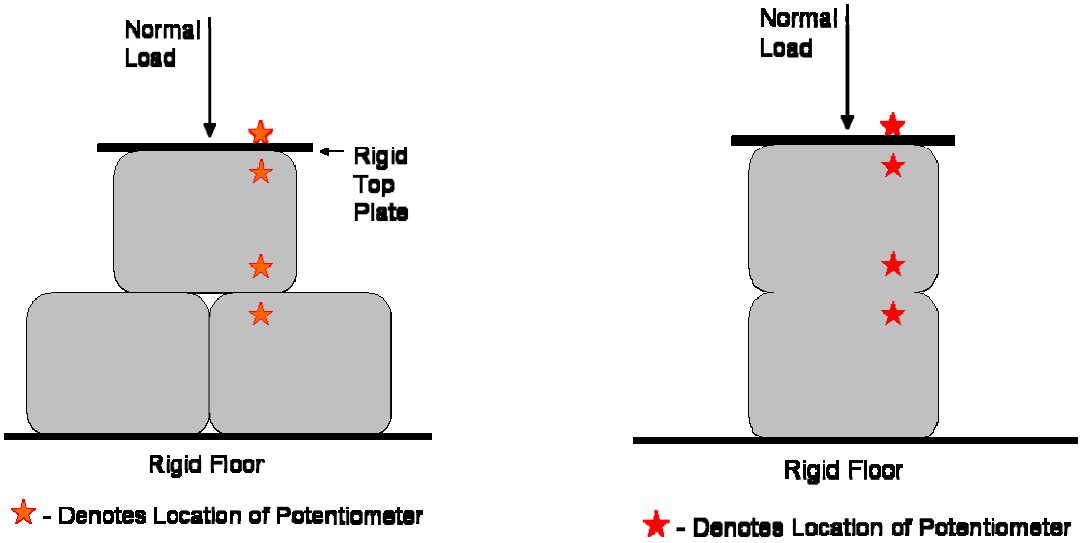

(a) Three Bale Structure. (b) Two Bale Structure.

Figure 7.1: Illustrations of the Compressions Testing Setup for Tire Bales

The application of the normal load was controlled by a hydraulic actuator (Figure 7.2). Vertical deformations of the bales were measured along the height of the bale structure at discrete points using potentiometers. Horizontal deformations were also measured with LVDTs

to determine the expansion of the bales due to vertical loading. All testing was conducted with tire bale only interfaces (soil infill was not considered).

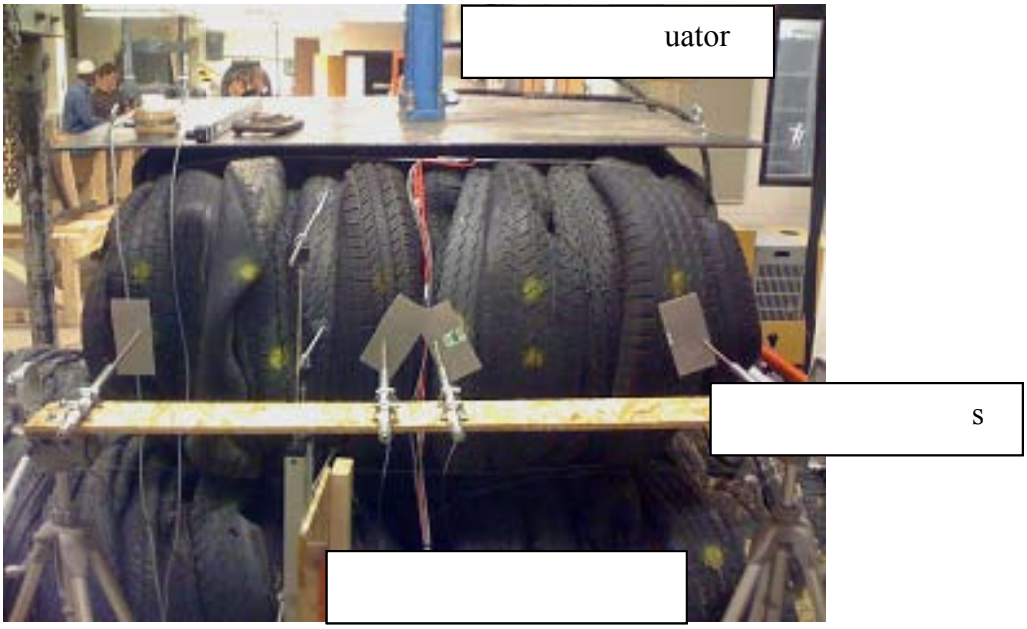

Figure 7.2: Placement of Potentiometers and LVDT's Along the Height of the Tire Bales to Measure Vertical and Horizontal Displacements

Two sets of compression tests were conducted for the three bale structure to observe the variability of the tire bale structure. An illustration of the two setups, in which the top bale was switched with a bottom bale to change the interface, is illustrated in Figure 7.3.

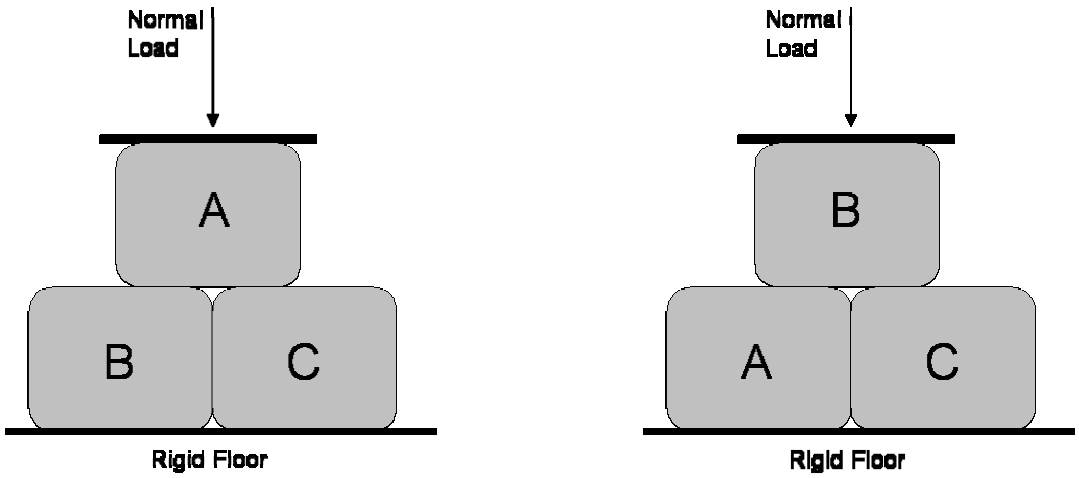

(a) Arrangement 1 (Initial Arrangement of Bales)

(b) Arrangement 2 (Bales A and B are Switched)

Figure 7.3: Different Bale Arrangements for the Three Tire Bale Compression Testing

7.2 Definition of the Tire Bale Sections

Four sections were defined along the height of the tire bale (Figure 7.4) to illustrate both the non-homogeneous behavior of the bale structure during compression and the importance of including a tire bale interface in the compression test. Vertical displacements were measured at the boundary between each of the sections (as shown in Figure 7.2) so that the total compression of each section could be calculated. Interface sections were defined as the contact between the tire bales, or the contact between the tire bale and a rigid boundary. The tire bale mass was defined as the tire material contained between the interfaces and bound by the baling wires. Dividing the tire bale structure up into sections allows for the isolation of the behavior of the top bale as well as the behavior of the tire bale interfaces. The four sections were defined as:

I. Top Bale Interface: Interface between the top tire bale and the rigid loading plate, with a thickness of 3 inches.

II. Top Tire Bale Mass: Represents the top tire bale. The thickness of the tire bale mass is approximately 24.5 inches.

III. Tire Bale Interface: Interface between the top and bottom layers of the tire bales, with an approximate thickness of 6 inches.

IV. Total Bale Structure: Represents the entire height of the tire bale structure from the top loading plate to the rigid floor.

The compressions of these bale sections will be presented in the following sections.

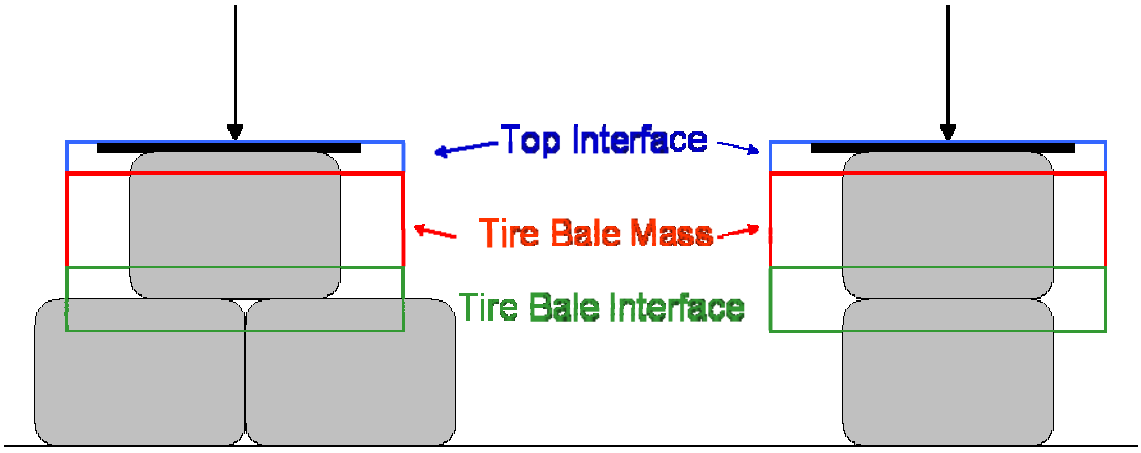

Figure 7.4: Illustration of the Defined Tire Bale Sections

The tire bale sections were also defined so that the compression of the equivalent tire bale mass could be determined. The compression of the equivalent tire bale mass is defined as the compression of the tire bale mass plus the compression of the tire bale interface as defined in Figure 7.4. The compressive behavior of the equivalent tire bale mass therefore neglects the compression of the tire bale interfaces in contact with the rigid boundaries, which behaves differently than the tire bale only interfaces. The rigid boundaries present in the testing setup are not present in the field, and therefore the effects of the rigid boundary on the compression should not be used to predict field behavior. The importance of the equivalent tire bale mass is

illustrated in Figure 7.5, in which the behavior expected in the field is compared with the behavior measured in the lab.

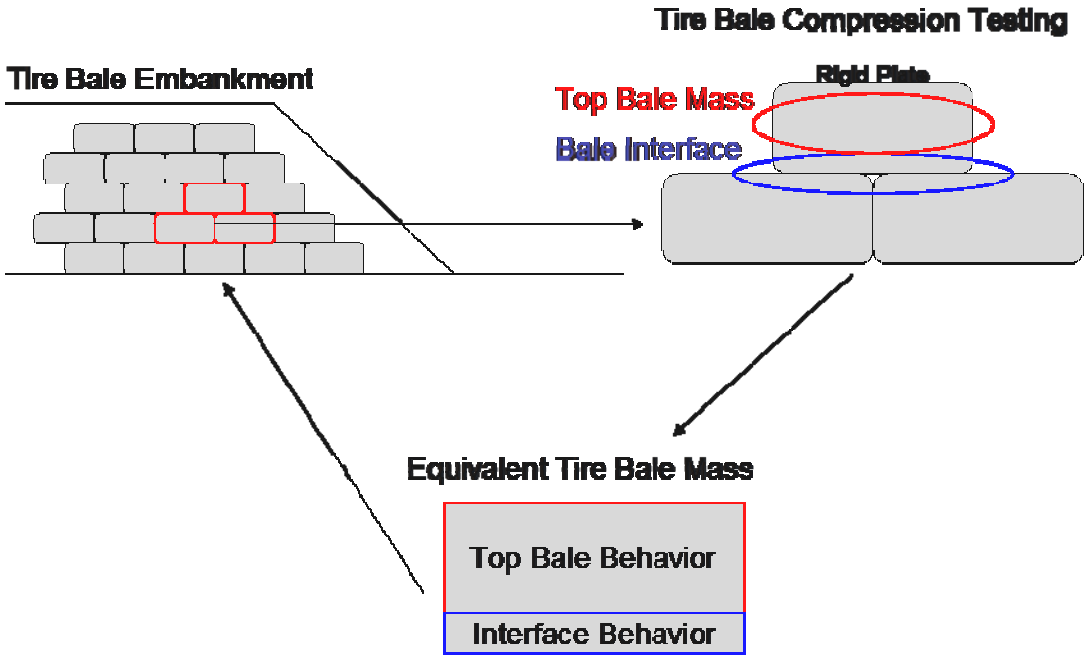

Figure 7.5: Illustration of the Tire Bale Sections in the Field and in the Compression Test Setup

7.3 Short Term Compression Testing of Tire Bales

Short term compression testing consisted of applying a vertical normal load to the bale structure while recording the vertical and horizontal displacements. The duration of a short term test was typically between 15 and 25 minutes. After each test, the interface was reset by lifting the top bale and replacing the bale in a new position. Results from the short term testing are presented in the following section.

7.3.1 Vertical Deformations of the Unconfined Three Tire Bale Structure

The vertical displacements versus applied normal stress curves for the three bale structure (Arrangement 1) are shown in Figure 7.6. There is a non-linear response of the tire bale structure to the application of the normal load as well as a hysteretic unloading curve. The hysteretic curvature implies that deformations remain in the tire bale structure even after the applied load is removed. This is evident by the apparent plastic deformation of the tire bale structure after unloading (orange circle in Figure 7.6), in which approximately 0.28 inches of deformation remain, most of which is fully recovered after letting the bale mass sit for 5 minutes to a value of 0.15 inches.

The compression of the individual tire bale sections was defined as the difference in the vertical displacements measured at the boundary of the sections. The tire bale section compressions versus the applied normal loads are shown in Figures 7.7 and 7.8 for Arrangements 1 and 2, respectively.

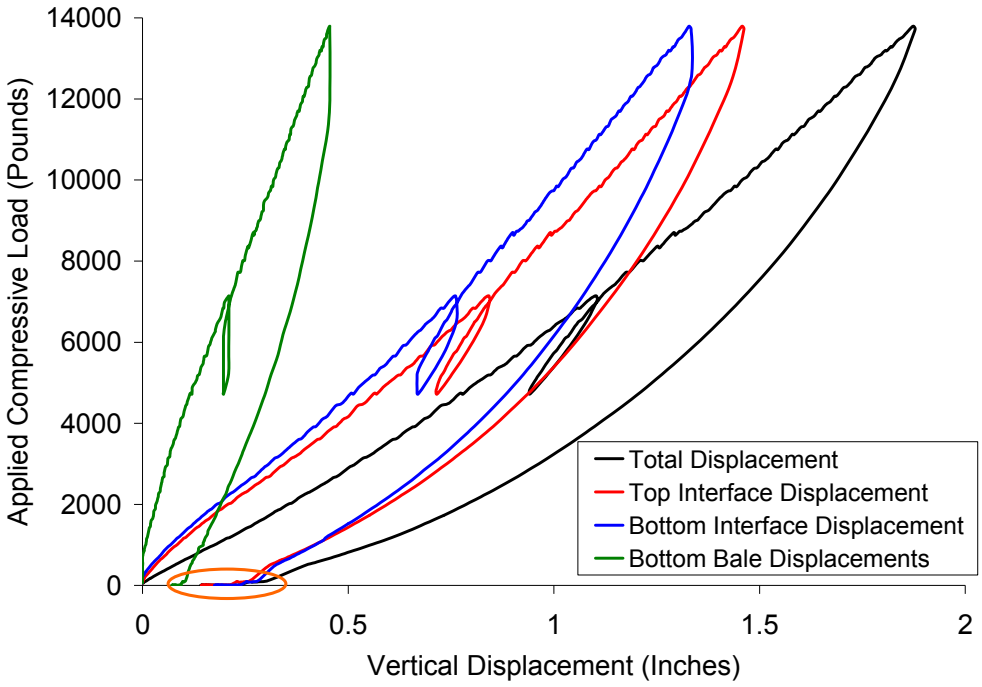

Figure 7.6: Vertical Displacement versus Applied Normal Load Along the Height of the Three Tire Bale Structure (Arrangement 1)

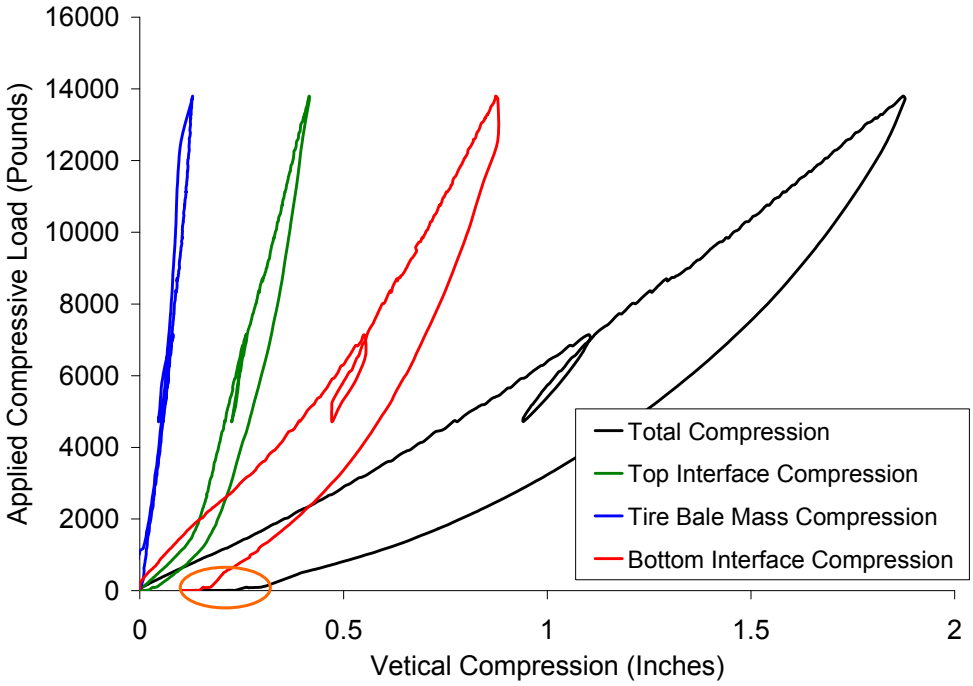

Figure 7.7: Compression of the Different Tire Bale Sections for Tire Bale Arrangement 1

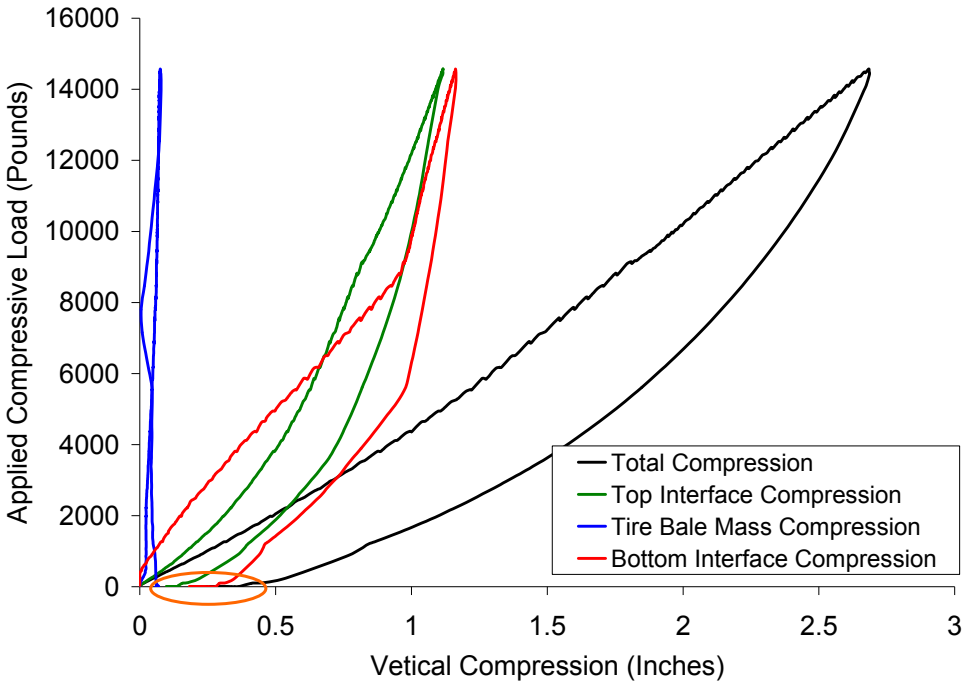

Figure 7.8: Compression of the Different Tire Bale Sections for Tire Bale Arrangement 2

Approximately half of the total vertical deformation of the tire bale structure (black curve) due to compressive loading occurred along the tire bale interface (red curve) for both arrangements. The stiffness of the interface also increased with the increasing compressive load, indicating strain hardening along the interface. The strain hardening can be related to the increase in actual contact area along the tire bale interface with increasing normal load, as discussed in Chapter 6.7.2. The compression of the tire bale mass increased linearly with normal load, with a much significantly higher stiffness than the interfaces. This higher stiffness of the tire bale mass can be attributed to the confinement already present in the bale mass due to the baling wires.

The difference in the total compression measured between the two arrangements, from 1.8 inches (Arrangement 1) to 2.6 inches (Arrangement 2), provides evidence of a significant variability of the tire bale compression from bale to bale, which may be attributed to both the variability of the tires used to make the bale as well as the variability of the tire bale interface. However, the increase in the total compression of Arrangement 2 was due to higher compressions of the top interface (green curve in Figure 7.8) caused by the contact between the rigid loading plate and the top bale (Figure 7.9). A comparison of the top interface compression and total compression (Figure 7.10) curves for the two arrangements illustrates that the difference in total compression of the two test arrangements is due primarily to the top interface compression (85% of the difference in the total compression is due to the increase in top interface compression for Arrangement 2). Therefore, the effects of this boundary must be isolated since it would not exist in the field and has a significant effect on the compression curve.

Figure 7.9: Photographs of the Contacts between the Rigid Top Plate and the Tire Bale for both Bale Arrangements

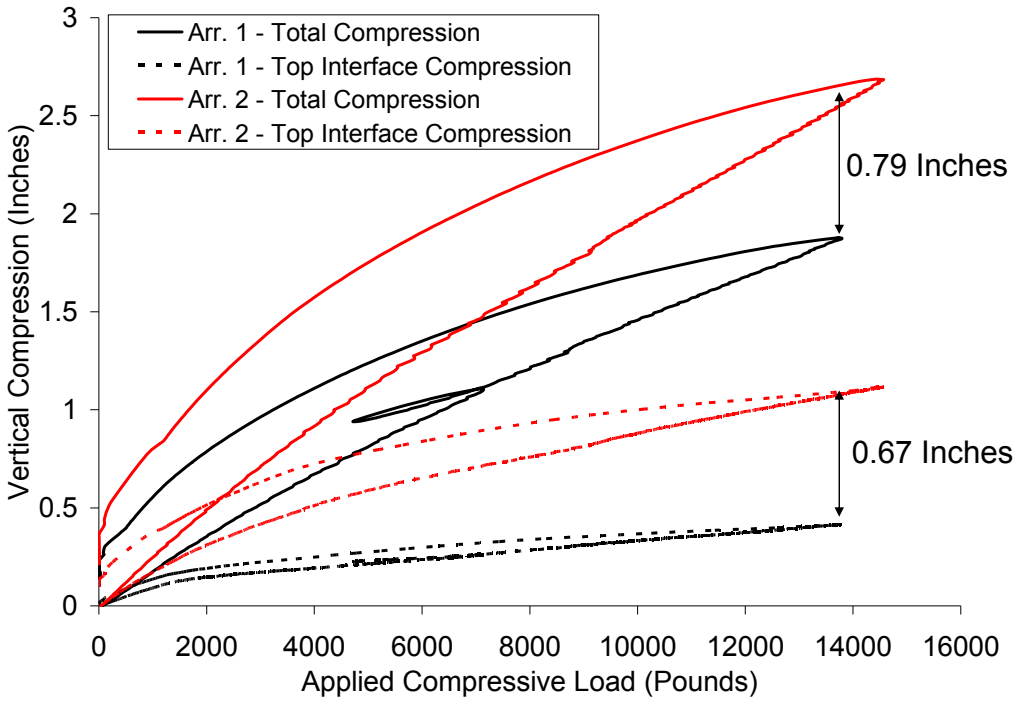

Figure 7.10: Total Compression and Top Interface Compression Curves for the Two Bale Arrangements for the Three Bale Structures

The compression results from this testing program (referred to as "This study") were compared with the results from Zornberg et al. (2005) and LaRocque (2005). The comparison of the three data sets provides evidence of the effects of tire bale structure and variability between bales. Zornberg et al. (2005) compressed a single bale between two rigid plates and LaRocque

(2005) used a similar three bale setup, but placed a layer of concrete along the top interface (top interface was a rigid section). The total strain (Equation 7.1), which is the common variable reported in the literature, was defined and used to compare the test results.

$$\text{Total Strain} = \varepsilon_T = \frac{\text{Total Tire Bale Stucture Compression}}{\text{Total Bale Structure Height}} = \frac{\text{Total Compression}}{5.1\,\text{ft}} \qquad (7.1)$$

The total strains versus the applied normal stress curves for the three testing programs are shown in Figure 7.11.

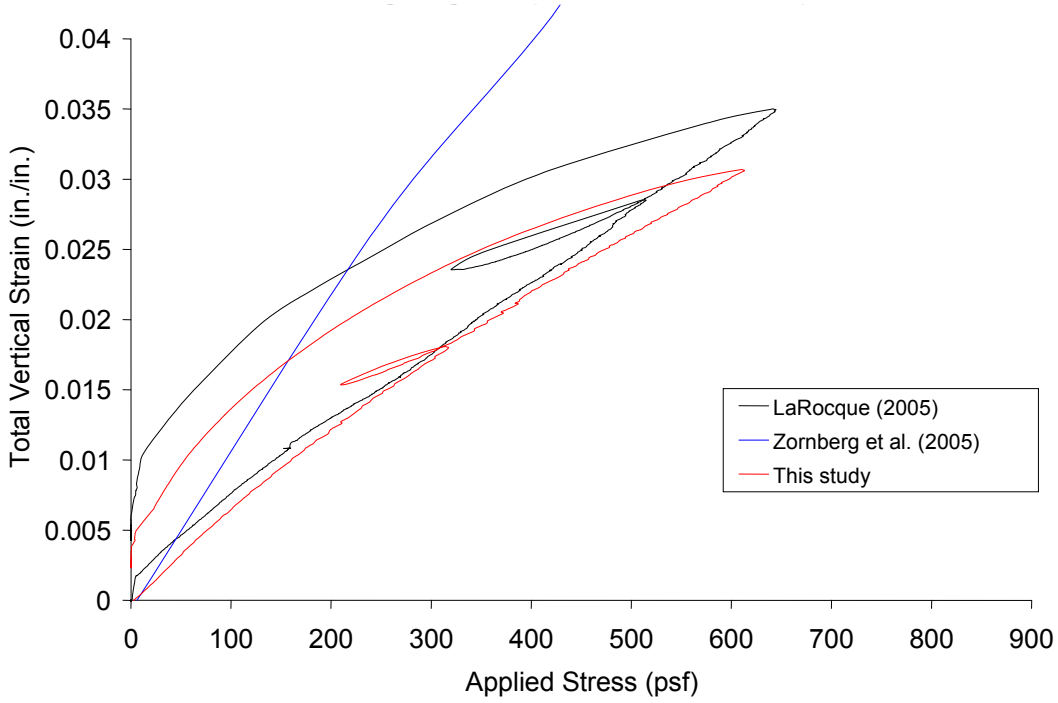

Figure 7.11: Total Strain versus Applied Normal Stress for Unconfined Compression Testing of Tire Bales

The effect of tire structure on the tire bale compressibility is significant, as illustrated by the difference in curves shown in Figure 7.11. The one bale structure compressed between two rigid plates (Zornberg et al. 2005) has a higher modulus (slope) than that of the three bale structures (LaRocque 2005) and results from this testing program. This is further evidence of the importance of including the tire bale interface with the compression testing structure. The difference in compression curves for the testing programs utilizing the three bale structures, most notably the semi-linear behavior reported by LaRocque (2005) not present in the data collected from this testing program, may be due to tire bale variability and the inclusion of a concrete loading surface at the surface of the tire bale structure, changing the top interface as compared with the data presented in this testing program.

7.3.2 Confined Stiffness and Poisson's Ratio

Tire bales used in the field will be placed so that they are surrounded by other tire bales or soil, and therefore the effects of the confinement on the stiffness of the tire bale structure needs to be determined. Two methodologies were employed to determine the effects of confinement, as follows:

I. Measurement of horizontal deformations of the bale during compression to calculate a Poisson's Ratio, which would also be applicable when determining the horizontal pressures applied by a tire bale section next to a rigid wall.

II. Measurement of the vertical deformations of the tire bale structure with simulated confinement around the bales.

Horizontal deformations of the top tire bale were measured along the tire bale mid-section (shown in Figure 7.2). Horizontal plates were attached at the measurement points (Figure 7.12) so that errors due to curvature of the tire bales were removed. Figure 7.13 shows horizontal displacements measured at four points along the bale during a typical compression test.

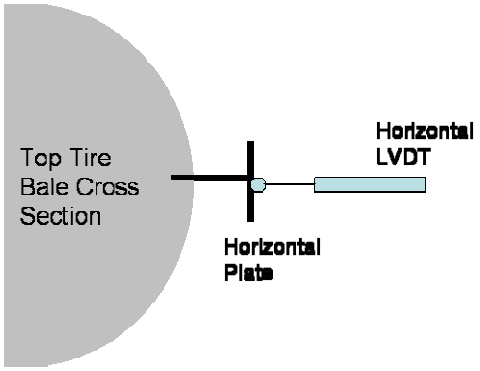

Figure 7.12: Illustration of the Horizontal Plates Placed Along the Top Tire Bale

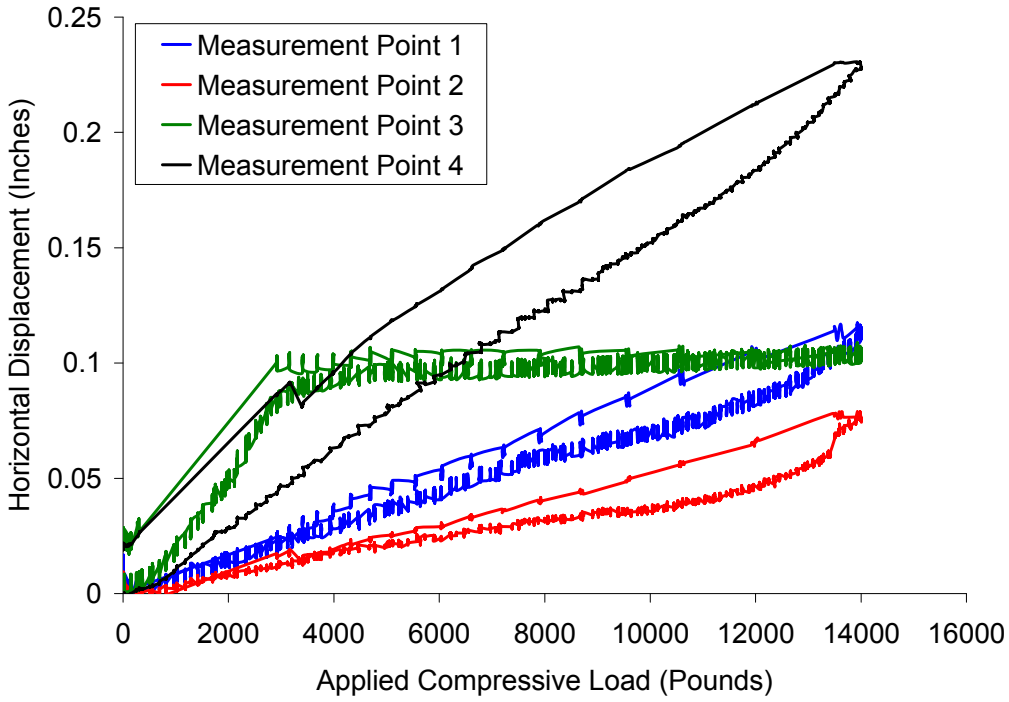

Figure 7.13: Horizontal Displacements of the Tire Bale Mid-Section

The horizontal deformations and corresponding total strain of the tire bale structure were used to define the Poisson's Ratio of the tire bale structure. The Poisson's Ratio was defined as the horizontal strain divided by the total vertical strain of the material. The horizontal strain was twice the measured horizontal deformation of the bale since deformations were only measured on one side, divided by the width of the tire bale (approximately 5 feet). The equation for the Poisson's Ratio is as follows:

$$\text{Poisson's Ratio} = \nu = \frac{\varepsilon_H}{\varepsilon_V} = \frac{\dfrac{2 \cdot \Delta_H \cdot \dfrac{1}{12}}{5}}{\dfrac{\Delta_V \cdot \dfrac{1}{12}}{5.08}} \qquad \text{Eq. 7.2}$$

where Δ_H is the horizontal deformation and Δ_V is the vertical deformation. Values ranged from 0.08 to 0.24 at a maximum stress of 650 psf. Values reported by Zornberg et al. (2005) ranged from 0.1 to 0.2 for stresses less than 1000 psf, and increased up to 0.3 - 0.4 at higher stresses.

Confinement of the tire bales was simulated by placing nylon cargo straps along the midsection of the top and bottom bales (Figure 7.14). Placement of the straps around the midsection of the bales represents a minimal confinement of the bales, or confinement due to the presence of tire bales surrounding the tire bale compression test. Results from the confined compression testing for both Arrangement 1 and Arrangement 2 are provided in Figure 7.15 and 7.16, respectively.

Figure 7.14: Placement of Nylon Cargo Straps Around the Mid-Section of the Tire Bales

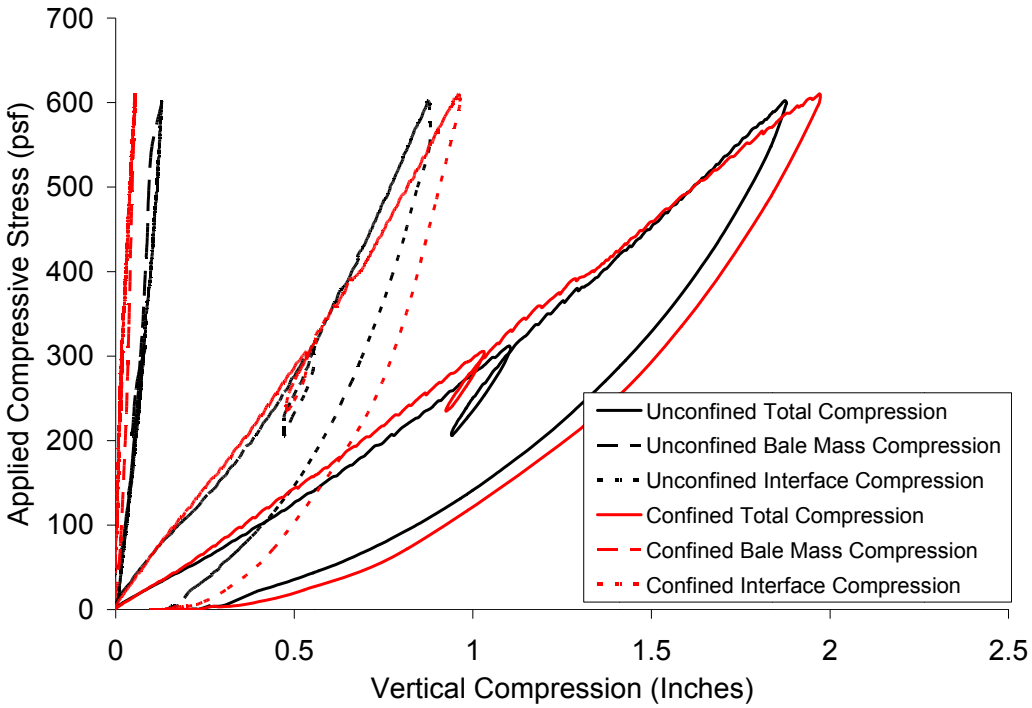

Figure 7.15: Confined and Unconfined Compression Test Results for Arrangement 1

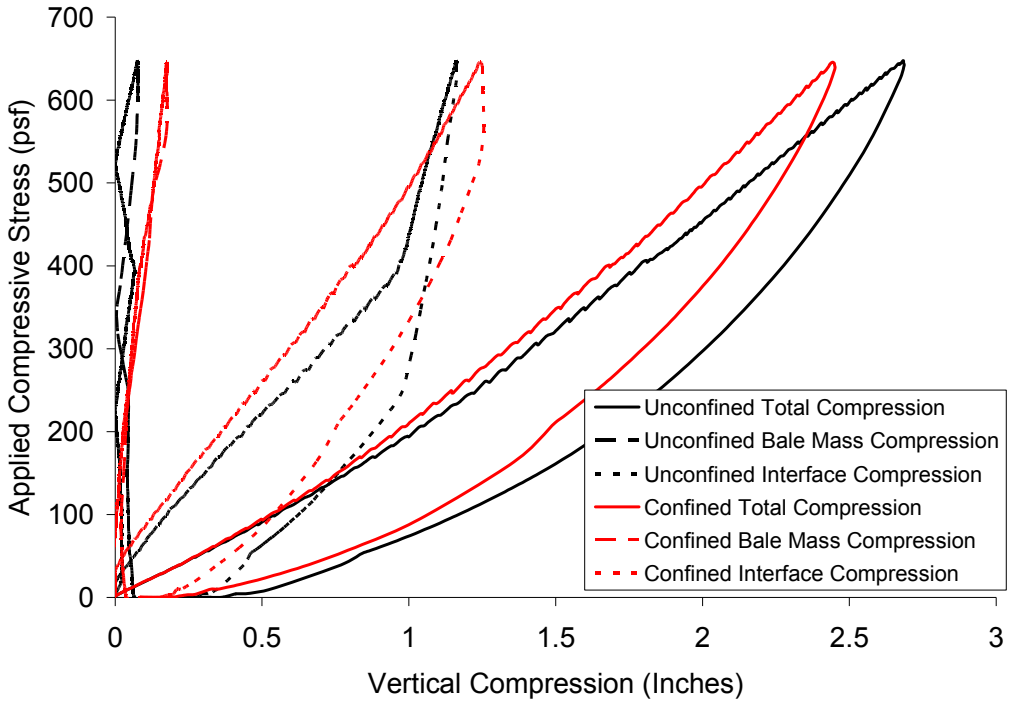

Figure 7.16: Confined and Unconfined Compression Test Results for Arrangement 2

The presence of minimal confinement on the tire bales increased the stiffness of the system, indicated by general reduction in the compression of the tire bales. Results from the two testing arrangements exhibit contradicting results, as follows:

- The stiffness of the tire bale mass increases with confinement for Arrangement 1, but decreases for Arrangement 2, implying that the presence of confinement around the bale increased the compression of the bale mass for the second setup. This was attributed to the variability of the test setup and the fact that no two tests, although using the same bales, were exactly the same.
- Although the total stiffness of both arrangements increases with the presence of confinement, at higher stresses the compression of Arrangement 1 is higher for confined conditions than for unconfined conditions (stiffness is lower at higher pressures with confinement). This is not present in the Arrangement 2 data, in which the compression is always lower for the confined condition. This is most likely due to differences in the behavior to the two testing setups due to changes in interface due to resetting the interface between tests.

The results illustrate the change in behavior of the interface with the presence of confinement. Since, in theory, the presence of confinement reduces the compression of the tire bale mass, the compression of the tire interfaces increases, as shown in Figure 7.15 (problems with the potentiometer for the unconfined case of Arrangement 2 distorted this). Therefore the presence of confinement, while increasing the stiffness of the total system, decreases the stiffness of the interface. Full confinement, such as that provided by a soil matrix around the bales, would further increase the stiffness more than minimal confinement since confinement is not present

along the entire perimeter of the bales. Results presented by Zornberg et al. (2005) indicated the stiffness increased up to 35% higher than the unconfined case with the presence of soil confinement.

7.3.3 Compressibility of Tire Bale Structures—The Equivalent Tire Bale Mass Behavior

The data presented in the previous sections cannot be directly applied to field conditions since two rigid boundaries are used to produce the compression. To more accurately imitate field conditions, the equivalent tire bale mass was defined, as discussed in Chapter 7.2. It is assumed that the compressibility behavior of a tire bale mass in the field is more accurately represented by the equivalent tire bale mass since the behavior of the rigid plate-tire bale interfaces have been removed. The equivalent tire bale mass compression versus applied load curves for unconfined and confined conditions is provided in Figure 7.17 for Arrangement 1.

The presence of the confinement straps produces a more linear response to compressive loading, allowing the compression of the tire bale mass to be predicted with a constant modulus. The compression versus applied load curves for the equivalent tire bale mass under confined conditions for Arrangement 1 and Arrangement 2 are provided in Figure 7.18. Differences in the slope of the loading curve provide additional evidence of the variability of the compressive behavior of the bales.

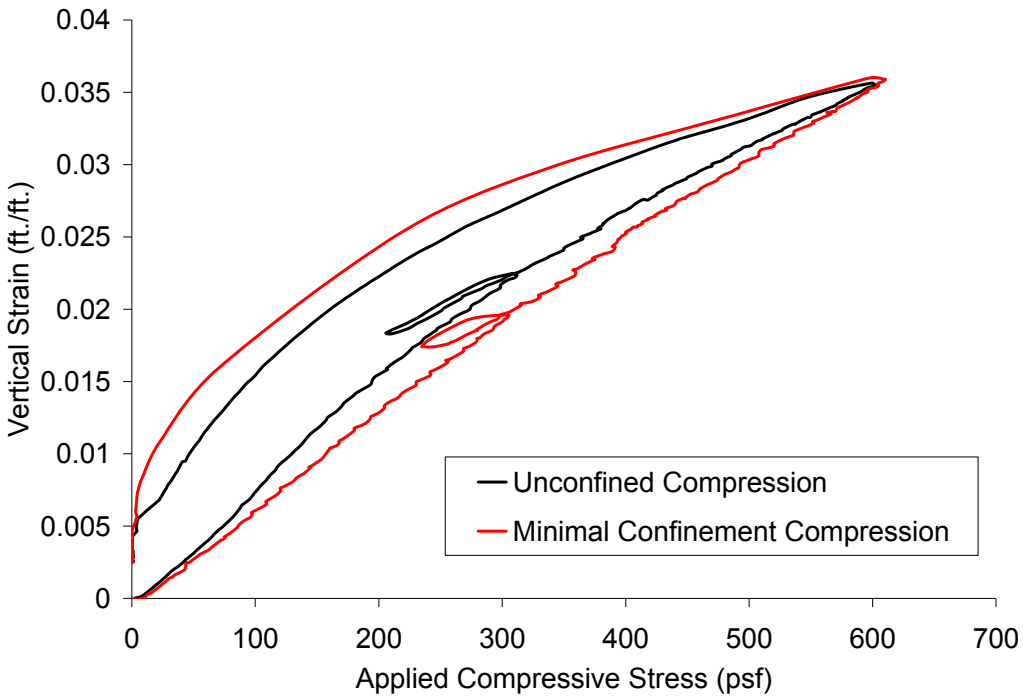

Figure 7.17: Comparison of the Unconfined and Minimally Confined Compression Curves for the Equivalent Tire Bale Mass

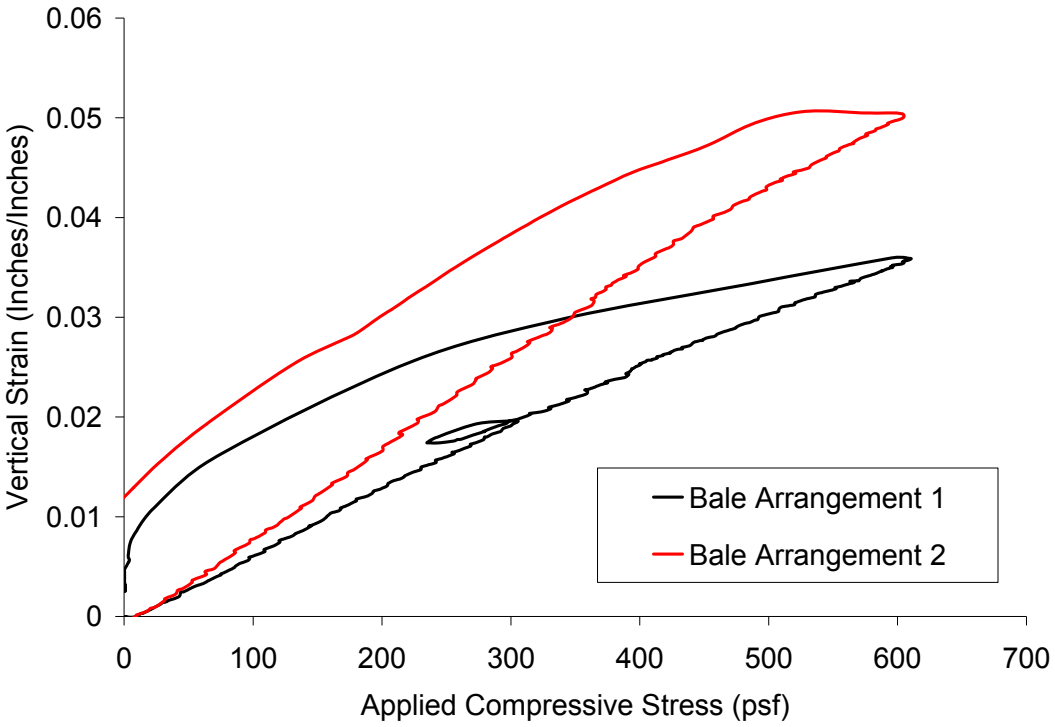

Figure 7.18: Compression Curves for the Equivalent Tire Bale Mass for Tire Bale Arrangements 1 and 2 (Confined Conditions)

It is evident from Figure 7.19 that the total strain due to loading of the equivalent tire bale mass is actually higher than the strain for the total tire bale mass, or that the equivalent tire bale mass is more compressible. This increase in compression may be due to stress distribution in the bottom two bales (loads are distributed over two bales rather than one, resulting in lower stresses and therefore lower deformations) resulting in decreased deformations in the bottom bales (Figure 7.20). By removing the stress distribution effects of the bottom bales, the compressibility of the equivalent tire bale mass is increased. The Young's Modulus (applied stress/strain) for the equivalent tire bale mass for minimally confined conditions (Figure 7.18) ranged from approximately 14000 psf to 17000 psf for the two bale arrangements. The approximate Young's Modulus for the total bale structure is approximately 17000 to 19000 psf, similar to the value of 19100 psf reported by LaRocque (2005) for a similar test setup. Therefore, by removing the effects of the loaded interfaces and the stress distributions within the test setup, the modulus (stiffness) of the tire bale is decreased.

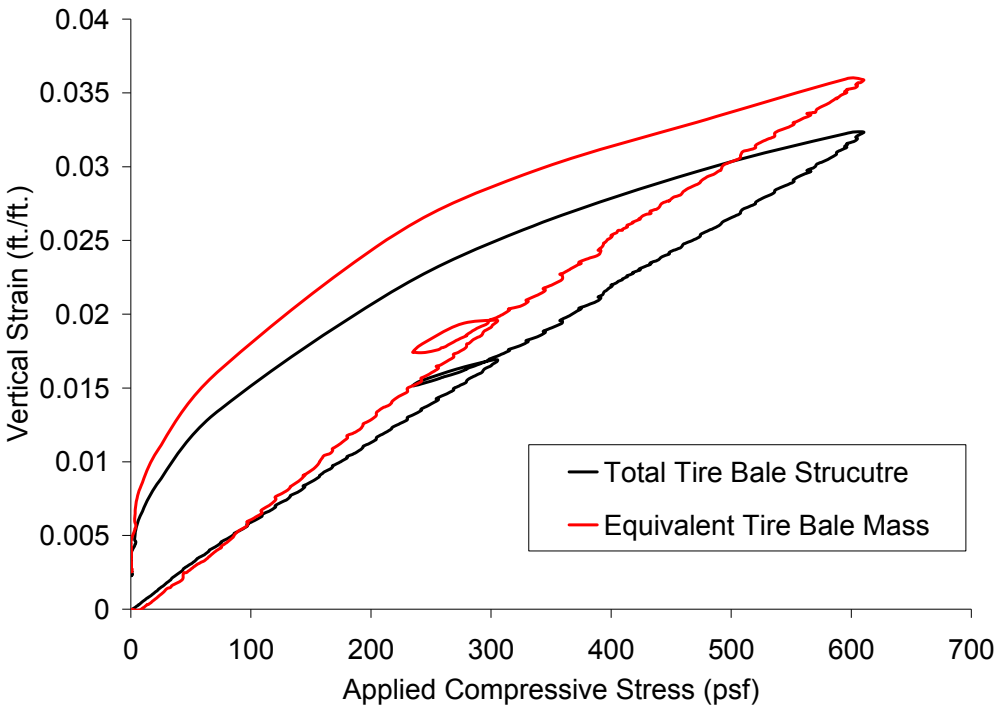

Figure 7.19: Compression Curves for the Total Bale Structure and the Equivalent Tire Bale Mass (Tire Bale Arrangement 1) for Confined Conditions

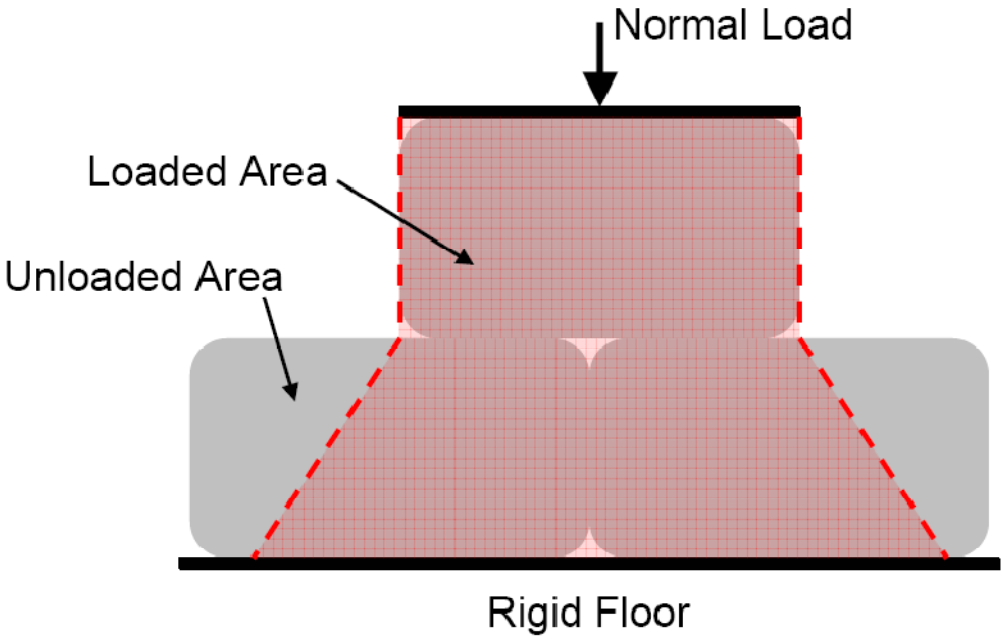

Figure 7.20: Estimated Stress Distribution within the Tire Bales for the Three Tire Bale Structure

7.3.4 Comparison of Results from Two and Three Bale Structures

It has been assumed throughout the section thus far that the three bale arrangement is the most critical placement of the bales, resulting in the largest deformations. This was based on the assumptions that:

1. The three bale structure has a lower contact area along the tire bale interface, increasing the compressions along the interface, and
2. The distribution of stresses in the bottom bales for the three bale structure that decrease the compression in the bottom layer of bales (refer to previous section).

To determine if this assumption was true, a series of compression tests were conducted on the two bale arrangement (Figure 7.1 b) for unconfined conditions to compare with the three bale compression results. Typical compression results from the two bale arrangement are provided in Figure 7.21. The deformation behavior of the two bale structure is similar to that of the three bale structure, in that the majority of the total compression occurs along the bale interfaces and the bale mass is significantly stiffer than the interface members. The two structures were compared using the total strain versus applied normal compressive stress curves, shown in Figure 7.22.

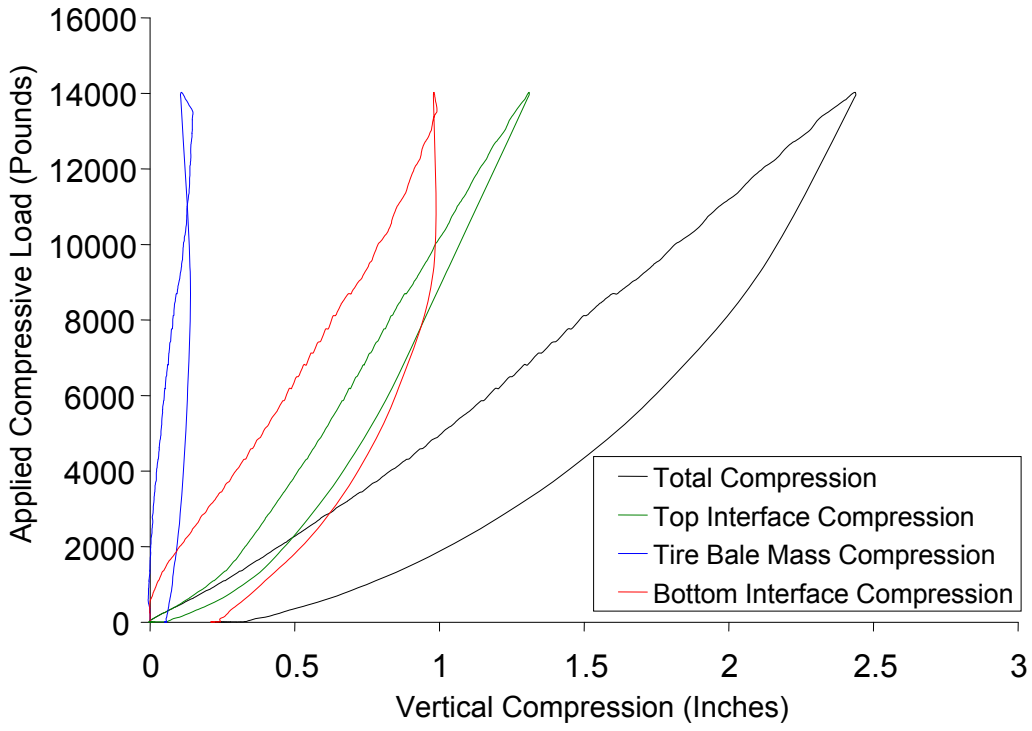

Figure 7.21: Tire Bale Section Compressions for the 2 Bale Arrangement

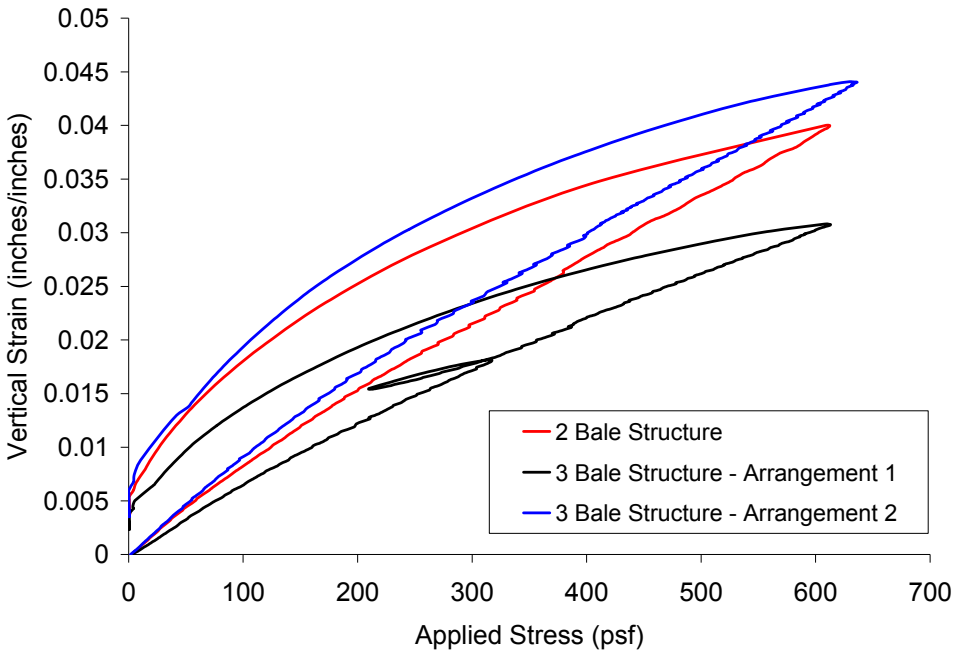

Figure 7.22: Comparison of the Stress-Strain Curves for the 2 and 3 Bale Arrangements

The stress-strain results indicate that the 2 bale structure was slightly stiffer than Arrangement 2 and more deformable than Arrangement 1 of the 3 bale structures, indicating that the effect of the tire bale structure on compressibility is minor when compared to the variability expected from rearranging the bale structure, or using different bales altogether. It should be noted though, that the 2 bale structure was accomplished by removing one of the bottom bales from Arrangement 2 (same top interface and bale mass). A comparison of the 2 bale structure and Arrangement 2 of the 3 bale structure does provide evidence of an increase in stiffness when using a 2 bale structure.

7.3.5 Discussion of Tire Bale Compressibility Results, Modeling the Compressibility of the Tire Bale Structure and the Application to Field Conditions

The testing program presented in the previous section was designed to determine the compressibility of a tire bale structure. Unconfined and minimally confined conditions were analyzed to determine the importance of including confinement in the test setup since tire bales will always be subjected to confinement in the field. Due to the irregular shape of the tire bale, a small Poisson's Ratio may still be associated with the confined bale since the cargo straps did not provide perfect confinement along the total perimeter of the bale. It is suggested to use the minimum value measured during testing of 0.08. The presence of the top interface and bottom bales, which was found to significantly influence the compression of the tire structure, was isolated by measuring compressions along the length of the tire bale structure and defining the equivalent tire bale mass.

The minimally confined equivalent tire bale mass behavior should be used for deformation analyses since it represents the lowest stiffness of an actual tire bale structure. The non-linear deformation of the confined tire bale structure can be represented by either an average linear modulus over the stress range of interest or a series of secant moduli with applied load, as

illustrated in Figure 7.23. The values of the average linear moduli for the compression curves of the equivalent tire bale mass presented in Figure 7.22 (both the three and two bale structure results were used) are presented in Table 7.1, including a predicted value of the tire bale stiffness with soil infill (modulus increased by 30% according to Zornberg et at. 2005). The secant moduli of the tire bale structure are presented in Figure 7.24 for the entire stress range.

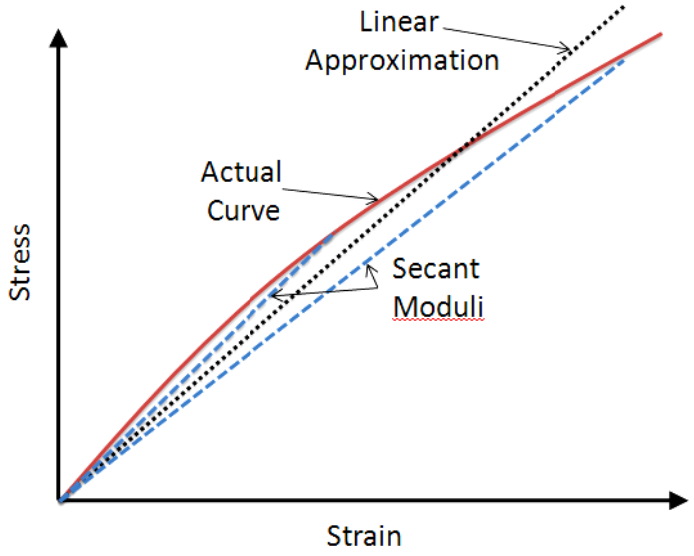

Figure 7.23: Illustration of the Modulus Representations for the Tire Bale Compression

Table 7.1: Values of Modulus and Poisson's Ratio for the Tire Bale Structures

	Modulus (psf)	Poisson's Ratio (%/%)
Unconfined	-	0.24
Minimal Confinement	16000	0.08
Soil Confinement*	22000	-

* Predicted Values of Modulus

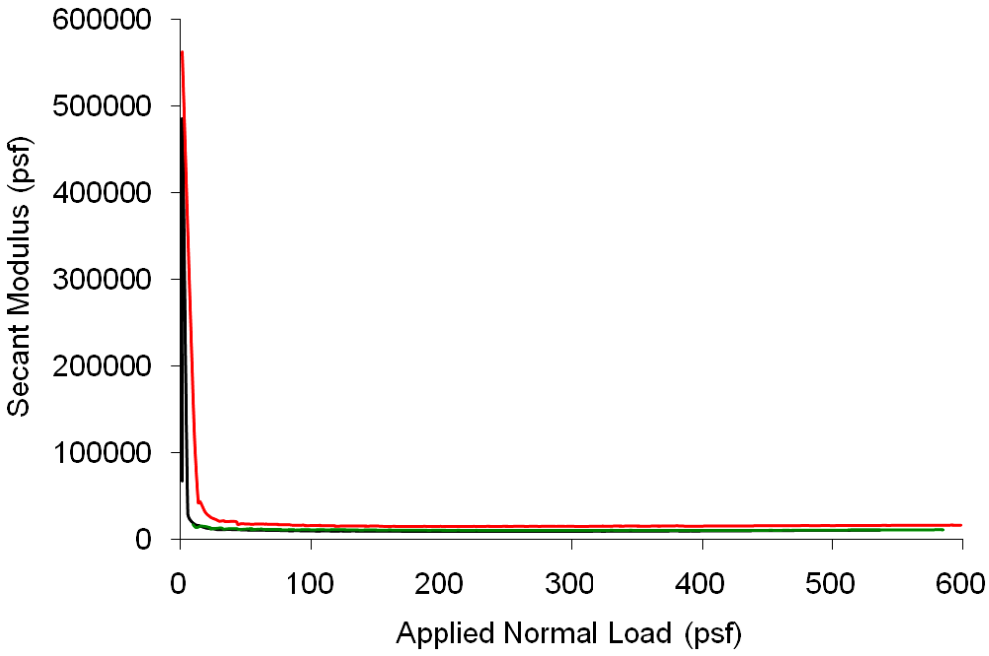

Figure 7.24: The Secant Moduli of the 2 and 3 Tire Bale Structure

The secant modulus curves presented in Figure 7.24 provide evidence of a significant decrease modulus with increasing stress for applied normal stresses of less than 30 psf. For very small applied loads on the tire bale surface, the stiffness of the tire bale is higher than for larger applied loads. For tire bale structures with surcharges over 88 psf (the stress applied by at least one layer of tire bales), the stiffness of the system reduces as shown in Figure 7.25. Although there is a change in secant modulus with increasing applied stresses (a stiffening of the tire bale structure), the representation of the tire bale stiffness with an average linear, or constant, modulus is an acceptable approximation for the stress range used during this testing program, considering the variability of the stiffness from each test conducted.

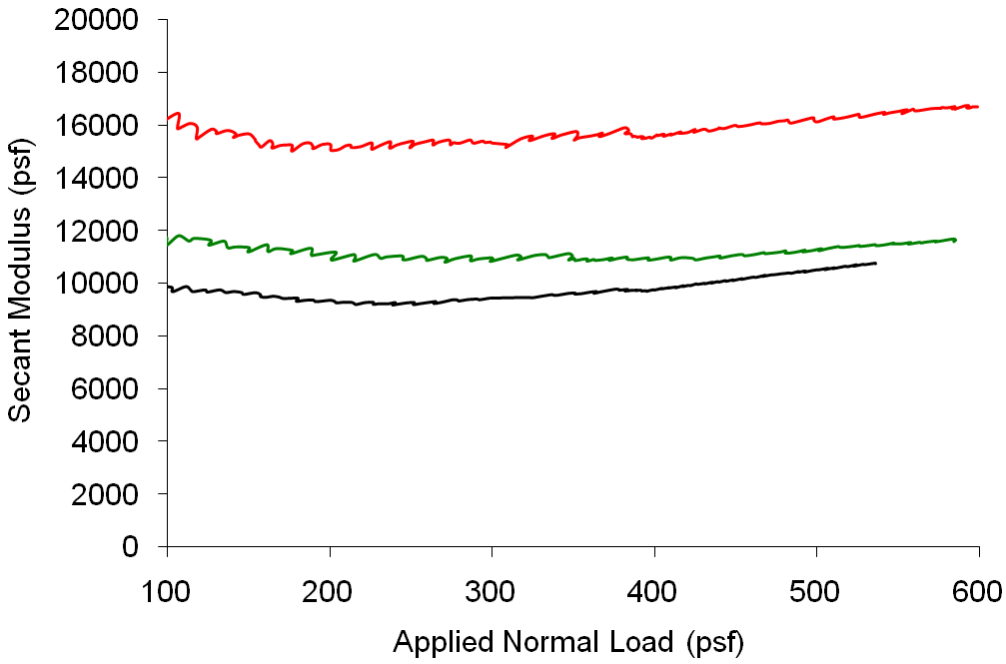

Figure 7.25: The Secant Modulus Curves for the 2 and 3 Bale Structure for Applied Stresses over 100 psf

7.4 Sustained Loading of the Tire Bale Structure (Long Term Compression)

The previous compression testing has been conducted to determine the short term loading characteristics of tire bales, yet the loading of the bales will be continuous for the life of the structure. A separate series of long term compression testing was conducted with the three bale testing setup to determine the creep deformations of the tire bales due to sustained loading. Loads were applied and maintained on the tire bale structure and compression measured for testing times ranging from 170 to 1000 hours. A typical stress-compression curve for the long term compression testing is illustrated in Figure 7.26. Compressions were measured at points along the height of the bales to determine the contribution of the creep from the bale mass and bale interface (Figure 7.27). Most of the creep compressions that were measured occurred along the interfaces (both the top and tire bale), and not within the bale mass, indicating the importance of including both the interfaces in the testing setup. Although the top interface data was removed from the short term compression data, it was included in the creep measurements so that the critical (highest) value of creep could be calculated.

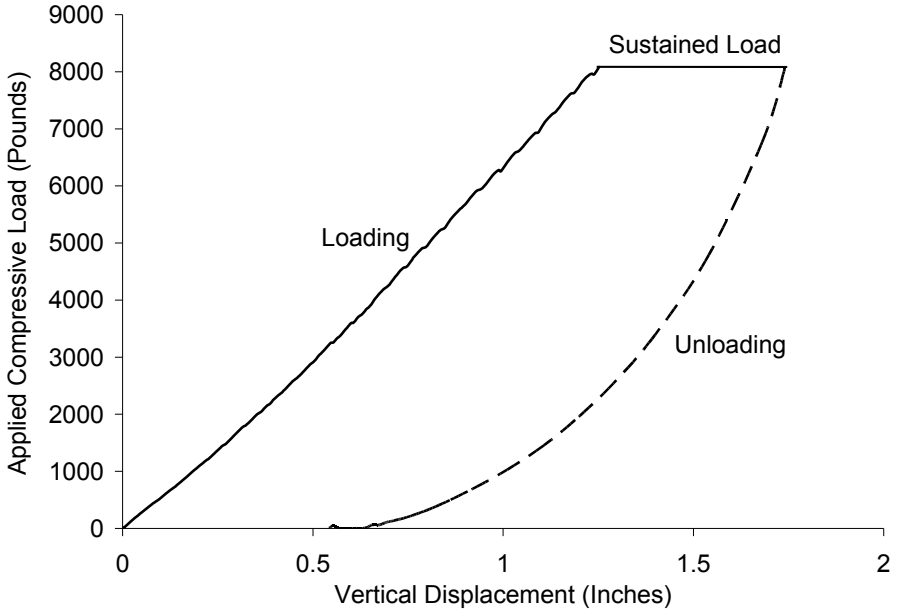

Figure 7.26: Stress-Compression Curve for a Long Term Compression Test of Tire Bales

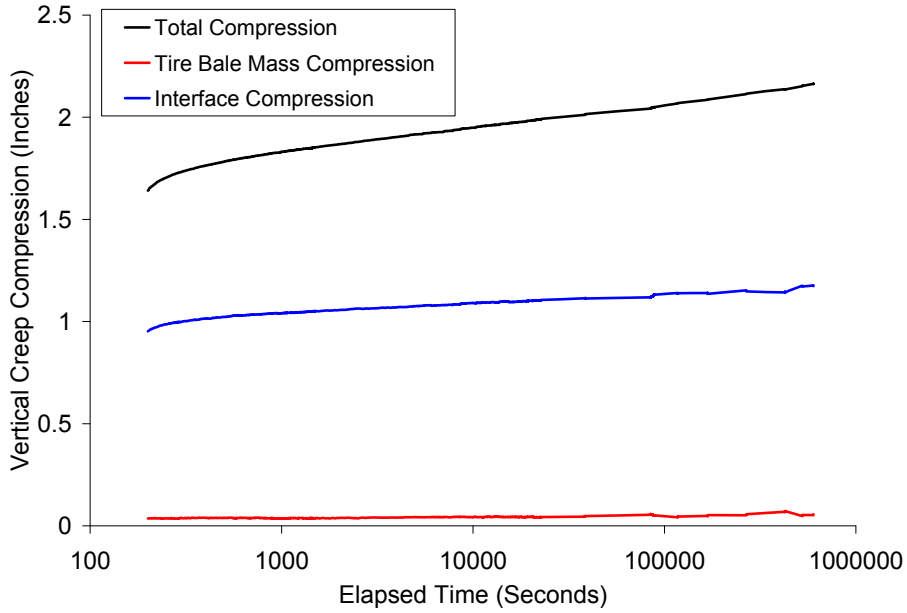

Figure 7.27: Creep Compressions for the Total Bale Structure and for the Tire Bale Sections

The total creep strains versus log elapsed time curves for the four sustained loading tests are shown in Figure 7.28. Tests 1 and 2 were conducted for Arrangement 1 and Tests 3 and 4 were conducted for Arrangement 2. All creep curves were approximately linear in semi-log space for testing times up to 1000 hours, indicating that creep tests did not need to be performed for more than a few days to properly characterize the behavior. There was no indication of an

increase in creep strains with time that is usually associated with the approaching failure of the material due to sustained loading.

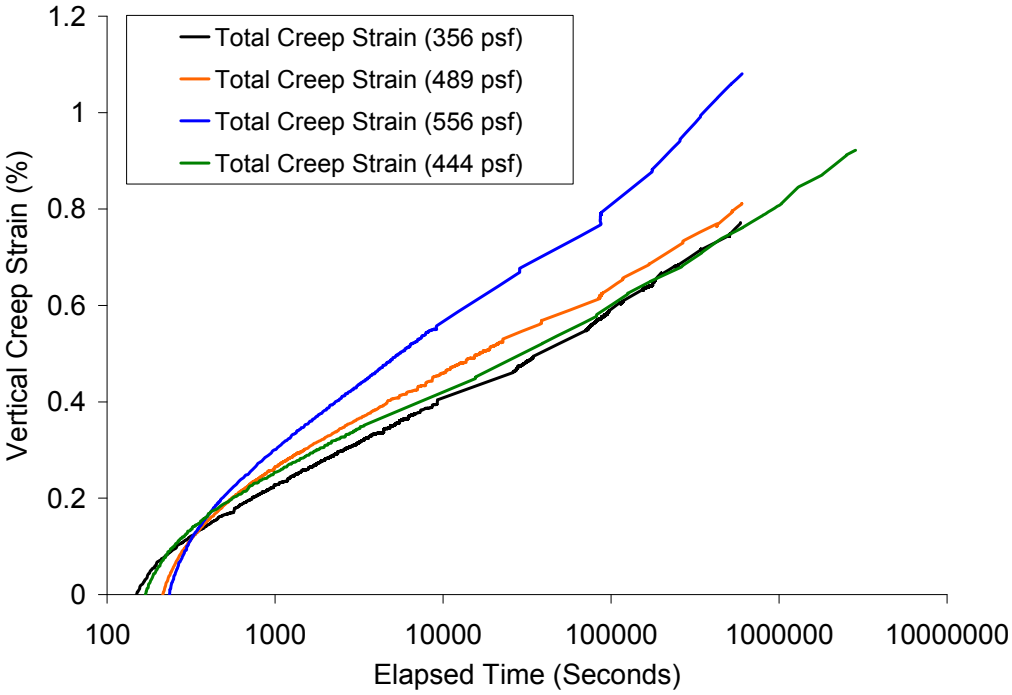

Figure 7.28: Creep Strains versus Log Elapsed Time for the Four Sustained Loading Tests

The creep strains of the tire bale structure were defined by the slope of the linear portion of the creep curve, as described by Zornberg, Byler, and Knudsen (2004). The creep strain is predicted using a dimensionless creep index, T_α, which is defined as the slope of the creep strain curve shown in Figure 7.25. This value is analogous to the C_α variable defined for secondary, or creep, compression of soils in a consolidation test. The total creep strain is predicted using Eq. 7.3.

$$\varepsilon_{CR} = T_\alpha \cdot \log\left(\frac{t}{t_o}\right) \tag{7.3}$$

where t is the time of interest (lifetime of the structure), t_0 is the time at the end of initial loading/beginning of sustained loading, and ε_{cr} is the total creep strain. The values of T_α calculated for the tire bales ranged from 0.18 to 0.28, much higher than the values of 0.017 reported by LaRocque (2005). The increase in T_α could be due to the removal of the concrete loading surface that was placed by LaRocque (2005), since it was observed that a significant amount of creep occurred along this top interface.

As a comparison to other construction materials, the creep index from the tire bale testing can be compared with values determined from soils and geosynthetics. Values of the T_α presented by Zornberg, Byler, and Knudsen (2004) ranged from 1.5 to 3.5 for geosynthetics loaded from 20 to 80 percent of the failure load. Values of C_α (the equivalent creep index for

soils) for soil can range from 0.016 to 0.6 for fined grained soils (Holtz and Kovacs, 1981), as measured in a consolidation test or back calculated from field measurements.

7.5 Summary

The results from the compression testing indicate that the stiffness of a tire bale structure can be modeled with a constant modulus and Poisson's Ratio for confined conditions over the stress range tested. An equivalent tire bale mass was also defined so that the effects of the loaded interfaces, which are not present in the field, and the stress distributions within the different bale structures could be removed. The tire bale structures and analysis of the results were different for this testing program as compared to previous programs, explaining the difference in modulus values reported. The modulus calculated from the minimal confinement testing was approximately 14000 to 17000 psf, less than the value of 19100 psf reported by LaRocque (2005). A small Poisson's Ratio (~0.8) is also suggested for the confined conditions to take into account additional deformation not present in the minimal confinement testing program due to the use of the cargo straps. Since no compression tests with soil confinement were conducted as part of this research program, it is suggested that a Modulus value of 23000 psf be used, predicted from data provided by Zornberg et al. (2005). Modulus values calculated from this testing program are less than that of soils (Table 7.2), providing evidence that the compression of tire bale structures will be higher than that of the corresponding soil structures (please refer to Chapter 8).

Table 7.2: Modulus Values Reported for Tire Bales and Soils

Material	Young's Modulus (psf)	ν
Stiff Clay	60890	0.33
Ganular Soils	62660	0.3
Compacted Clay	41770	0.35
Tire Bale Mass	15000*	0.15
	16000**	0.08
	22000***	0.08

* Unconfined Tire Bale Modulus and Poisson Ratio

** Minimal Confinement Tire Bale Modulus and Poisson's Ratio

*** Predicted Soil Confined Tire Bale Modulus and Poisson's Ratio

Creep deformations due to sustained loading were also measured to determine any substantial deformations over time. Results provide evidence that the creep of tire bale structures would be similar too, if not less then, soil structures. A significant portion of the creep deformations did occur along the interfaces, indicating the importance of including the interfaces in the test setup.

Chapter 8. Cost Benefit Evaluation and Analytical Study Considering Use of Tire Bales in Highway Structures

The choice of using tire bales as an alternative building material for highway construction is not only controlled by the mechanical benefits of using the bales, as discussed in previous chapters, but also by the costs associated with obtaining and implementing the bales. Numerous research programs have been conducted to quantify the mechanical properties of the tire bales, but not much has been reported on the financial aspects. The following chapter outlines the basic cost-benefit analysis conducted for the use of tire bales in highway applications as determined from data provided by the Texas Department of Transportation and the Texas Commission on Environmental Quality. In addition to the cost analysis, an analytical study will also be presented to indicate the mechanical benefits and limitations of using tire bales as a construction alternative.

The cost savings of using tire bales in highway structures can be illustrated using the three possible end-uses of scrap tires, as follows:

1. Do nothing with scrap tires.
2. Clean up scrap tires and properly dispose.
3. Beneficially reuse tires as bales in highway applications.

Analysis of each of the alternatives will use data collected throughout Texas. The benefit of using tire bales will be illustrated from a financial and mechanical perspective for a series of case histories presented in the literature (refer to Chapter 2).

8.1 Cost of Doing Nothing

The "doing nothing" alternative implies that nothing is done with the scrap tires, no matter their location. There is no cleanup of tires along the roadways, stockpiles of scrap tires are not properly stored, and the few tires that are properly disposed of end up in landfills. The cost of doing nothing is the cheapest alternative simply because the costs are zero ($0). No money is spent by the state to locate, clean, or store any scrap tires. The only costs for scrap tires would be the optional $2.00 charge per tire to properly dispose tires, which is paid for by the consumer disposing of the tires, assuming that the consumer properly disposes of them.

Although the actual cost to the State of doing nothing is zero, the social costs of doing nothing can be very high. Infestation of mosquitoes and rodents in scrap tire monofills can cause outbreaks of diseases such as Yellow Fever (Wappett 2004), as well as occupy large amounts of property. The major potential cost associated with doing nothing is the potential for scrap tire stockpiles to catch fire. There are multiple causes for the ignition of a tire fire, and can be as simple as arson, electrical ignition caused by faulty wiring, or lightning striking the tire stockpile. When burned, tires can break down into more than 2 gallons of oil (www.epa.gov/garbage/tires/fires), and therefore the ignition of tires can be very dangerous. Coupled with the large air voids present within the tire stockpile, tire fires are very difficult to extinguish (see Chapter 3 for a more detailed analysis of tire fires).

The costs of extinguishing a tire fire can be quite large due to both the difficulty of putting out the fire and the cost associated with cleaning up the pollutants from the fire. Some notable case histories of tire fires include:

- The Hagersville Tire Fire, Ontario, Canada (1990): This event consisted of a 12 to 14 million tire stockpile that required over 200 firefighters to extinguish and burned for 17 days. Over 4,000 people had to be evacuated. The costs of putting out the fire and the subsequent cleanup were estimated to be over $1 million.
- Tire Dump Fire, Westley, California (1999): A lightning strike ignited the fire that burned for more than 30 days. The tire dump contained millions of scrap tires located in a canyon. As a result of the fire, pyrolitic oil flowed into a nearby stream and which subsequently ignited. The cost to extinguish and clean up both fires was $3.5 million.
- Tire Monofill Site, Tracy, California (1998): A grass fire ignited the 7 million tires at the unlicensed S.F. Royster Tire Disposal Facility. It was extinguished after 26 months. No costs were listed for the cleanup, but a substantial amount of time and manpower was required to extinguish the fire.

The potential social costs of having large stockpiles of scrap tires results in the need for state funded programs aimed at cleanup and maintaining scrap tires. The task of maintaining the scrap tire stockpiles and illegally dumped tires falls under the jurisdiction of two State agencies.

8.2 Cost of Cleaning Up Scrap Tires and Proper Disposal

Scrap tires that are not recycled or burned for energy recovery are disposed in three ways:

1. Stockpiled in monofills or landfills;
2. Disposed in illegal stockpiles; or
3. Disposed randomly on public property.

To reduce the social costs and the potential costs of tire fires discussed in the previous section, the proper disposal and storage of scrap tires is required. Proper disposal implies that the State must pay to find and clean up illegal tire dumps and maintain scrap tire stockpiles or dispose of the tires (usually not in whole form) in landfills. There are two State agencies in Texas that have been in charge of the cleanup and proper disposal of illegally disposed scrap tires: the Texas Commission on Environmental Quality (TCEQ) and the Texas Department of Transportation (TxDOT).

TCEQ, charged with cleaning up and maintaining the scrap tire stockpiles around the state, was awarded $7.5 million during the 77th Legislature (2001) for the cleanup of scrap tire stockpiles around the state (TxDOT 2007). Some of the notable cleanups sponsored by TCEQ were the:

- Removal of 45 million scrap tire units (defined as 22.5 lbs of tire rubber material), or STU's, from both the Atlanta and Stamford sites,
- Cleanup of 850,000 scrap tires in San Antonio,
- Removal of 250,000 whole scrap tires from an El Paso site, and

- Removal of 750,000 scrap tires in Cleveland and Midlothian

Some of the funds were also used to retrofit cement kilns so that whole tires could be safely and efficiently burned for energy. In one report, it was estimated that a total of 3 million whole tires were reused as fuel in one cement kiln in 2006 (TxDOT 2007). However, even due to the significant cleanup efforts sponsored by TCEQ, it was still estimated that approximately 4.5 million whole tires still remained in illegal or unregistered stockpiles around the state as of September 1, 2006.

Unlike TCEQ, which is in charge of all scrap tire stockpiles around the state, TxDOT is only responsible for scrap tires produced by the Department or found along the roadways. The Department spent $1.25 to $3.50 for passenger tires and up to $40.00 for tractor or commercial truck tires (www2.cpa.state.tx.us) to handle the 34,200 whole scrap tires. They also spent approximately $0.06–0.09 per pound ($1.35 to $2.03 per STU) to remove tire scraps.

In addition to finding and cleanup of illegally disposed scrap tires, there is a significant cost of storing the tires in a registered site or disposing the tires in a landfill. On average (in 2003), taxpayers were charged $0.10 per pound (or $2.00 per tire) to throw away tire rubber material in a landfill. TCEQ also noted that it was required by the State that before any whole tires were placed in landfills, they needed to be shredded or cut into quarters to reduce the risk of tires damaging the landfill liners (www.tceq.state.tx.us/compliance/tires/#landfils), an additional process that further increases the cost of disposal. Not only is storing the scrap tires expensive, massive amounts of space are required, therefore causing the need for more landfill space that could be used for other purposes.

8.3 Cost of Reusing Scrap Tires as Tire Bales in Highway Applications

In order for tire bales to become a feasible alternative for use in highway construction, the bales must be easy to manufacture, cheap to implement, easy to use, and easy to find close to the site. The cost of using tire bales must be cheaper both from the field structure construction standpoint and from the production of the tire bales (cost of making the bales). The following chapter outlines a cost-benefit analysis for the use of tire bales in highway applications.

8.3.1 Considerations for the Use of Tire Bales in Highway Structures

The first consideration with using tire bales as a standard construction material is the availability of whole scrap tires. Projects that have used tire bales as a fill material have had the advantage of being one of only a few projects that have required the use of numerous whole scrap tires. Such projects have also been implemented as a way to remove tires from one stockpile and beneficially use them in an engineering project close by rather then throw the tires away. One proposed dam construction project in Arkansas required anywhere between 1 million to over 4.5 million tires, depending on the design, and used tire bales from a nearby stockpile. A gabion retaining wall in New Mexico required over 32,000 scrap tires (approximately 320 tire bales) to complete. It was evident from the review of tire bale case histories (Chapter 2) that a significant number of whole scrap tires can be required to complete just one structure, and therefore the number of projects that use scrap tire bales will be limited by the number of tires in an area.

The time to bale the tires may also become an important consideration. Two studies—Zornberg et al. (2004) and Winter et al. (2006)—have reported that a total of 4–6 bales can be produced per hour per baling machine with a two man crew. Placement of the bales in the

structure occurs at a faster rate, since bales only need to be placed with a forklift. In addition, many tire bale structures require significant amounts of tire bales to be completed. Winter et al. (2006) suggests that tires be baled as soon as they are received so that stockpiles of bales are readily available (Figure 8.1).

Figure 8.1: Stockpile of Tire Bales Ready to be Used in Construction

In Texas, there has been a significant push to reuse tires in civil engineering projects. In 2005, TxDOT reported that over 27.4 million tires (up from 23 million in 2001) were beneficially reused (only 24 million were produced) and approximately 1 million (down from 2.4 million in 2001) shredded, quartered or split tires were disposed of in landfills. Of the tires that were beneficially reused, over 60 percent were used as fuel, 24.8 percent were used in land reclamation projects (LRPUT), and less than 1 percent used in civil engineering applications, as illustrated in Figure 8.2. Winter et al. (2006) estimated that there were still potentially 69 million tires stored in stockpiles around the state.

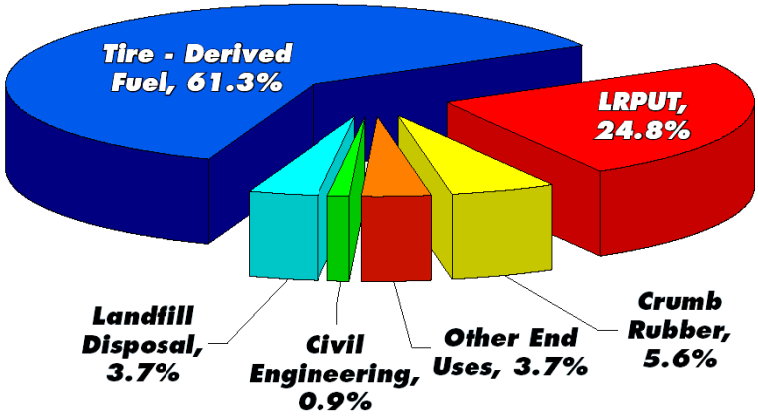

Figure 8.2: Beneficial Scrap Tire Usage (in Percent of Total Reused Tires) for 2005 in Texas (TxDOT 2007)

The main use of scrap tires in highway engineering projects was as tire shreds and crumb rubber (Figure 8.3), which is the by-product of shredding the scrap tires. Crumb rubber has been used as a lightweight fill in embankments, as a fill material in asphalt pavements, and a fill for

land reclamation projects (filling quarries). Over 15,000 tons of scrap tires were reused by the Department in 2006 (TxDOT 2007) just for roadway applications. The large amount of tire shreds used in highway construction indicates a significant amount of experience in beneficially reusing tires, but also a need to illustrate the benefits of using bales as compared to shreds in order to justifying switching from using shreds to bales.

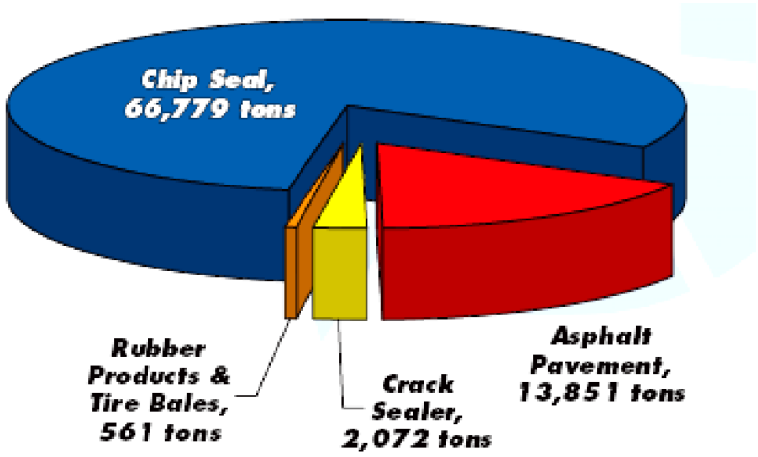

Figure 8.3: Total Amount of Scrap Tires Reused in Highway Applications from FY 2001 to FY 2006 (TxDOT 2007)

Only two highway projects in Texas thus far have beneficially reused tires in the form of tire bales, which are the slope remediation projects at IH 30 (see Prikryl et al. 2005 and LaRocque 2005). The two projects combined account for more than half of the 561 tons of rubber products and tire bales (whole tires) reported in Figure 8.3. Another tire bale project utilizing tire bales as a roadway subgrade is underway in Brownsville, Texas (Jones 2008). With the use of tire bales, there is an opportunity to increase the number of tires beneficially reused in highway applications and reduce the amount of effort required to manufacture the tire product.

8.3.2 Cost Comparison of Tire Bales and Shreds in Highway Applications

Two costs are associated with the reuse of scrap tires, (1) the cost to clean up and move the tires to registered facilities (as discussed in Chapter 8.2), and (2) the cost to process the tires and reuse them in a construction project. The main benefits to using tire bales, as compared to tire shreds or chips, are the energy and labor required to construct the bales and the transportation and storage cost reductions associated with baling the tires at the site. Therefore, there is a potential cost reduction of using bales both in regard to cleanup of the stockpiles, but also in reusing the tires in highway applications.

The typical tire baling machine is portable and can be moved from site to site, resulting in an instant processing of the tires which is typically not accomplished for tire shreds. In order to shred tires, the whole tires must be transported to the facilities, shredded, and then moved to storage. If it is assumed that the $1.25 per tire spent by TxDOT to clean up tires is volume based (this is the cost associated with the space required to move the bales), then baling the tires on site, resulting in an instant decrease in the volume of the tires and reduced by the number of trips required to remove a stockpile, would decrease the costs associated with disposing the tires. Although the volume reduction of baling tires is approximately 10 (1 bale is 10 times smaller

than the associated 100 whole tires), truck volume and load limits reduce the actual transportation reduction to approximately 3 (Raine 2008). This volume reduction is derived from the MEC volume, which indicates that the bales required 25% more space than the average volume, and a load limitation of the trucks of 20 tons. The cost of moving a scrap tire in baled form therefore reduces to $0.42 per tire ($1.25/3), which is a cost reduction of $0.83 per tire baled. This cost reduction would therefore decrease the $814,000 spent by the State to move whole tires from one stockpile to another.

There is a further cost benefit to using tire bales when considering the construction process to make the bales as compared to shreds. Winter et al. (2006) estimated that it required 125 kW per tire to shred a tire, while only 7.5 kW per tire is required to bale it. This is reflected in the total cost to shred tires, which can range from $19–110 per ton depending on size of the final shred (TxDOT spends on average $0.64 per tire), and requires that over 20 tons of tires be shredded an hour to be profitable (Raine 2008). Tire bales cost approximately $25 per ton ($0.013 per tire) to manufacture and only require that enough tires be available to compress. Placement of the tire products into the structure also affects the cost, with shreds requiring both mixing and compaction while bales only require placement, which will be further discussed in Chapter 8.3.3.

Another significant benefit to using tire bales as opposed to other lightweight fills (including tire shreds) are the cost of the materials and the ease of construction. A list of the costs associated with lightweight material alternatives is provided in Table 8.3. Although not the cheapest alternative, tire products provide drainage within the structure and can easily be constructed and placed (like building blocks) within the structure. With the other non-tire alternatives, drainage must be provided by other means if it is required.

Table 8.1: Cost of Soil Replacement Alternatives (Zornberg et al. 2005)

Material	Cost ($/yd^3)
Scrap Tire Bales	2.80 - 9.70
EPS Blocks	25.10 - 50.00
Foamed Concrete	50.00 - 73.00
Fly Ash and Slag	2.30 - 16.00
Tire Shreds	19.00 - 110.00

8.3.3 Cost Benefit Analysis and Analytical Study of Tire Bale Case Histories

The cost-benefit and mechanical advantages of using tire bales, as opposed to other alternatives, can be illustrated using the different scrap tire bale case histories. The main uses that are of concern to the highway construction industry are tires bales used in embankments and bridge overpasses, tire bales as a retaining wall material, and tire bales used as a roadway subgrade material. An overview of the cost benefit and analytical studies are provided in the following sections.

Case History 1: Tire Bales in Embankment Construction and Remediation

The TxDOT IH 30 slope remediation project is an example of the use of tire bales as a light weight fill in highway embankment remediation and construction. The project consisted of

an initial embankment remediation and then a subsequent Phase Two remediation at an adjacent slope. Tire bales were used in the Phase One remediation as reinforcement layers placed along the height of the slope (Figure 8.4 a).

(a) Tire Bales as Reinforcement Layers (b) Tire Bale Slope

Figure 8.4: Tire Bale Embankment Illustrations for the IH 30 Slope Remediation Projects

Water storage in the permeable tire bale layers increased the seepage into the adjacent slope, initiating a second slope failure. The Phase Two slope remediation consisted of rebuilding the slope entirely with tire bales (Figure 8.4 b) with the additional of a drainage blanket at the base to prevent water storage within the bale mass.

General

The cost estimates and stability analyses were conducted using a general slope geometry and soil properties provided in Prikryl et al. (2005), as shown in Figure 8.5. The conditions at failure for the IH 30 embankment were determined so that similar conditions could be analyzed for the tire bale embankment stability analyses. The approximated failure surface and excavation limits (determined from photographs of the failure) as well as the general slope geometry are shown in Figure 8.6. The failure was considered typical of cut slopes consisting of clayey soils. Clay soils lose strength with time due to weathering (shrink/swell cycles), and additional loading caused by rain events, causing the water table to be elevated into the permeable weathered limestone layer, initiated the failure (Prikryl et al. 2005). Two boreholes were drilled in the failed soil area and indicated slickenside surfaces in the lower clay layers, in which a significant portion of the failure surface existed.

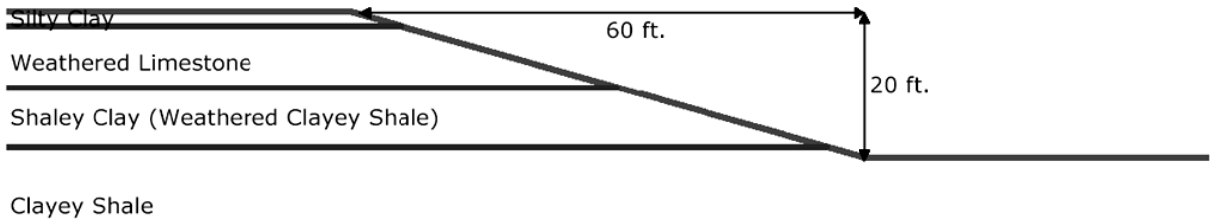

	Peak Strengths		Residual Strengths	
Soil	c' (psf)	φ' (deg.)	c' (psf)	φ' (deg.)
Silty Clay	100	12	100	12
Weathered Limestone	150	20	150	20
Shaley Clay	290	19	100	15.5
Clayey Shale	100	32	100	15

Figure 8.5: General Slope Geometry for IH 30 Slope Remediation Project

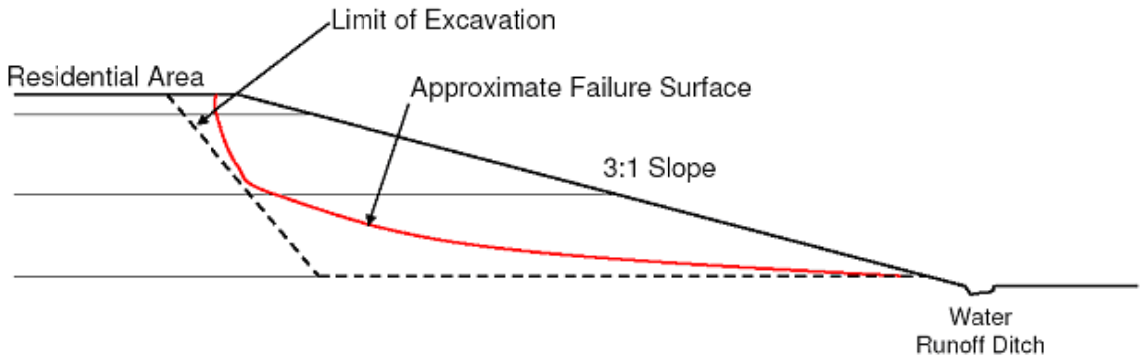

Figure 8.6: Embankment Geometry and Failure Surface Location for IH 30 Slide

The UTEXAS4 slope stability program, developed by Dr. Stephen G. Wright at the University of Texas at Austin (Wright 2007), was used to determine the soil strength conditions necessary to produce failure for a groundwater table at the top of the limestone layer. The analysis indicated that strengths in the shaley clay layer (layer with the slickenside surfaces) needed to be reduced approximately 10% from the peak values to result in a factor of safety of 1. Similar groundwater table elevations will be used in the analytical study of the slope remediation alternatives to represent the worst case scenario of the slope.

Cost Benefit Analysis

Five different slope remediation alternatives were considered in the analysis of the highway embankment, as follows:

1. Re-compaction of the Failed Material (with and without drainage blanket)
2. Re-compaction of the Slope with Tire Bale Reinforcement Layers
3. Removal and Replacement of Failed Material with Tire Bale Mass
4. Re-compaction of Failed Material with Tire Shred Fill

5. Re-compaction of Failed Material Around a Pile Reinforced Retaining Wall.

The general construction costs, as determined from the TxDOT average low unit bid prices for 2007 (www.txdot.gov/business/avgd.htm), is provided in Table 8.2. The units for each of the actions or materials are cubic yard (cy), square yard (sy), linear yard (ly), linear foot (lf), ton of material (ton), and average day use (day*). The following section outlines the cost analysis of the different remediation alternatives.

Table 8.2: Cost Estimates for General Re-Compaction of Failed Slope Material Based on Low Bid Unit Prices

Description of Action or Material	Construction Unit	Cost, $
Excavation	cy	6.33 - 14.86
Embankment Compaction (Type D)	cy	22.32
Coarse Aggregate (Drainage Blanket)	cy	1.53 - 51.56
Stone Riprap (8")	cy	75 - 115
Embankment Compaction (Type B)	cy	20.07
Geogrid Base Reinforcement	sy	1.60 - 4.10
Geotextile Reinforcement/Drainage Layer	sy	0.63 - 3.04
Scrap Tire Bale (Standard Dimension)	cy	2.80 - 9.60
Forklift	day*	215.00 - 233.00
Tractor Loader (Front End Loader)	day*	193.80 - 305.00
Clamshell Bucket	day*	29.00 - 68.20
PVC Pipe (4" Inner Diameter)	lf	1.59 - 2.50
Concrete Flume	cy	350
Tire Shreds	ton	19 - 116
Tire Shred-Soil Mixing (Rotary Tiller)	cy	1.87
Drilled Shafts (18" to 36" Dia.) Includes Concrete	ly	177.69 - 894.3
Wide Flange Steel I Beams (8x4, 10 lb/ft to 12x12, 120 lb/ft)	ly	21.30 - 271.80**
Metal Guardrail Fence	ly	0.00 (Roadway damaged) 7.33 (Used)*** 19.56 (New)***

* May be assumed zero if equipment is already present.

** Price provided by Saginaw Pipe Company, INC.

*** Price provided by American Timber and Steel Corp, INC.

The cross sectional area of the excavation limit (as illustrated in Figure 8.6) is approximately 77.8 square yards (700 square feet). The cost of excavation, which is required for all of the remediation alternatives, is $1,156 per linear yard of embankment ($14.86/yd^3), a cost that is associated with all of the remediation alternatives. The cost of simply re-compacting the failed soil back into the original shape of the slope is $1,734 per linear yard of the embankment. Therefore, re-compacting the slope would cost approximately $2,890 per linear yard. Addition of a one foot thick drainage blanket constructed around the perimeter of the excavation, consisting of a coarse grained material ranging from filter sand to stone rip-rap, would change the total embankment cost to $2,890 to $3,900 per linear yard of embankment. The addition of geosynthetic reinforcements along the height of the slope (assuming 8 equally spaced layers along the height) would increase the total cost to $2,890 to $3,150 per linear yard. A summary of the re-compaction costs are provided in Table 8.3.

Table 8.3: Summary of Estimated Embankment Re-Compaction Costs for IH 30 Embankment Failure

Remediation Method	Cost (per linear yard)
Recompaction	$2,890.00
Recompaction with Drainage Blanket	$2,910.00 - $3,900.00
Recompaction with Geosynthetics	$2,930.00 - $3,150.00

The generic slope remediation with four planar layers of tire bale added as reinforcement/drainage layers is illustrated in Figure 8.7. Although only three tire bale reinforcement layers were placed in the Phase One IH 30 embankment, the following example (Figure 8.7) considers a slope with four tire bale layers to illustrate the maximum use of scrap tires within the structure. An eight (8) inch thick soil layer was compacted between each tire bale reinforcement layer. It should be noted that for the Phase One slope remediation of the IH 30 slope, a compacted soil cover was placed on the slope surface and no flow was allowed out of the tire bales. This analysis, however, will assume that drainage is provided out of the slope. Drainage is provided by a series of PVC pipes placed between the tire bale layers to a concrete flume drain at the surface of the slope at every twenty (20) feet.

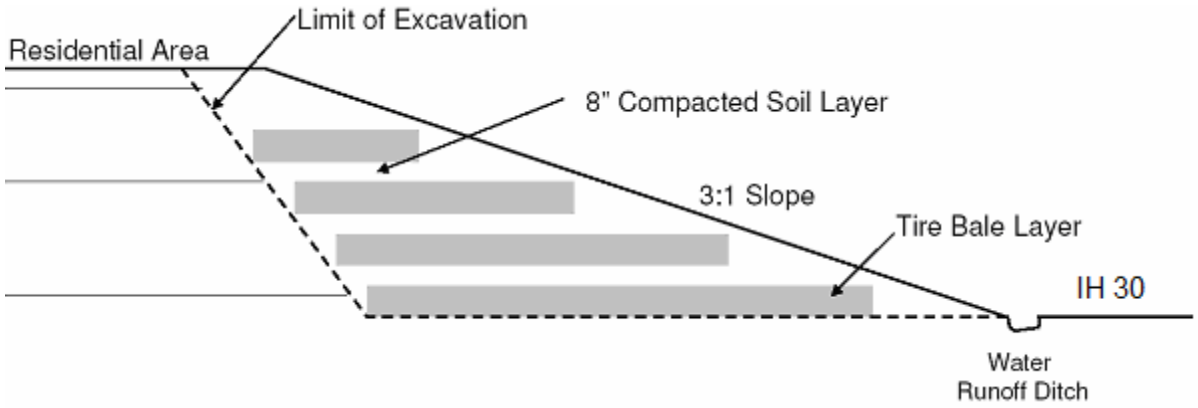

Figure 8.7: Tire Bale Reinforced Embankment Geometry

The approximate number of scrap tire bales needed to complete the four layers of reinforcement is 25 bales. The cost of the bales is the product of the cross sectional area of the bale (1.25yd^2), the price of the tire bales ($9.60/yd^3) and the number of bales needed, which results in a cost of $300.00 per linear yard of embankment. Placement of the bales can be neglected since some form of forklift or front end loader is already present at the site for excavation or for removal of the bale from the baling machine or truck. The compaction of the 8" intermediate soil layers and soil cover would cost approximately $1,040.00 per linear yard of embankment, which is less than the cost to recompact the entire embankment ($1,734) since the tire bales have replaced soil within the structure. Placement of a PVC pipe drain at each tire bale layer and construction of a concrete flume drain every 20 feet along the embankment would cost approximately $197.00. As shown in Table 8.4, the total cost of the tire bale reinforced embankment without drainage would therefore cost $2,496.00 per linear yard and with drainage would cost $2,693.00.

Table 8.4: Summary of Embankment Re-Construction Costs with Tire Bale Layers for IH 30 Embankment Failure

Remediation Method	Cost (per linear yard)
Tire Bale Reinforced Embankment	$2,496.00
Tire Bale Reinforced Embankment with Drainage	$2,693.00

An alternative use of tire bales in slope remediation is the use of the bales as a fill material within the slope, such as done for the Phase Two remediation of the IH 30 slope. A general cross section of the tire bale fill embankment is shown in Figure 8.8. The soil cover is typically included to limit the degradation of tires due to UV radiation, limit water and air into the slope (reduce any exothermic reactions), provide a soil layer for vegetation to grow, and to provide an aesthetically pleasing appearance. At the base of the tire bale mass, a stone rip-rap layer was placed to act as a drainage layer, and a pipe was placed perpendicular to the slope to drain the water at the base of the tire bale mass to the water runoff ditch along the highway. A geotextile was also placed around the sides and top of the tire bale mass to prevent any soil flow into the tire bale mass.

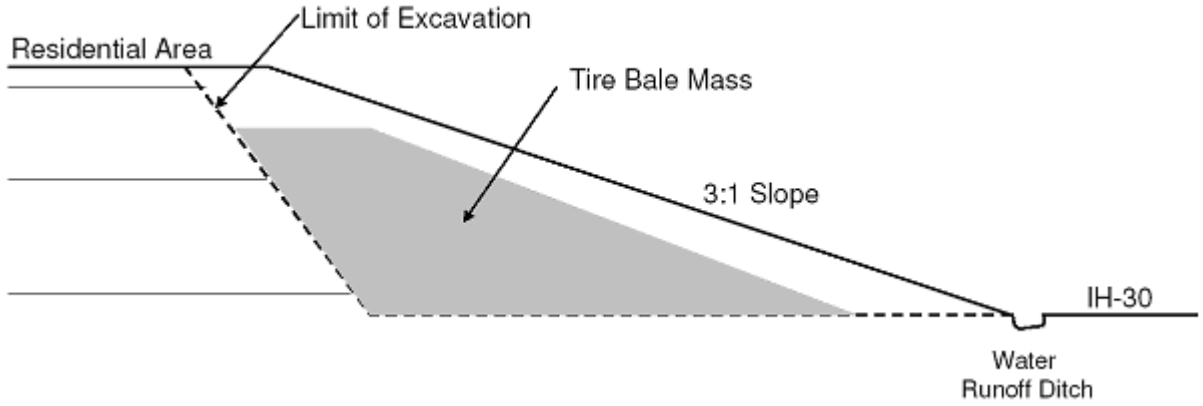

Figure 8.8: Tire Bale Only Embankment Geometry for IH 30 Site

The approximate number of tire bales needed for a five layer high embankment, considering that a three foot soil cover is compacted on top, is 36 bales per 5 feet of embankment. The cost of the bales, per linear yard of the embankment, is approximately $450.00. The cost of compacting the 3 foot soil cover and top 12 feet of the embankment (32.8 yards squared cross section) costs approximately $732.10. The placement of the 8 in. thick drainage layer at the base of the tire bale mass costs approximately $400–427 per linear yard of embankment, depending on the coarse grained material used. The placement of a PVC drain at every 20 feet of embankment would cost $1.13 per linear yard. The geotextile covering of the tire bale mass, which requires an approximate length of material of 42.6 yards, ranges in cost from $26.84 to 129.50 per linear yard. As shown in Table 8.5, in total, the cost of construction for a tire bale embankment, including drainage and geotextile covering, would cost approximately $2767.00–$2896.00 per yard of embankment

Table 8.5: Summary of Embankment Re-Construction Costs with Tire Bale Mass for IH 30 Embankment Failure

Remediation Method	Cost (per linear yard)
Tire Bale Embankment with Drainage Layer	$2,767.00 - $2,896.00

An alternative re-use of scrap tires in embankment construction is the use of tire shreds as reinforcement elements and/or a fill material with the soil mass. Assuming that tire shreds are mixed in with the soil material at a ratio of 30% tire shreds by dry weight of soil, the cost of the tier shreds required is approximately $719 per yard of embankment ($19/ton). The cost of mixing the soil and shreds would be approximately $150 per yard and compaction would cost $1,734 per yard of embankment. The total cost of a tire shred reinforced embankment would therefore cost approximately $3,795 per yard of embankment (Table 8.6).

Table 8.6: Summary of Tire Shred Reinforced Embankment

Remediation Method	Cost (per linear yard)
Tire Shred Reinforced Embankment	$3,759.00

The final alternative analyzed for this case history is the re-use of highway materials to build a retaining wall within the embankment. In general, the retaining wall consists of concrete drilled shafts with steel beam placed in it to some height and metal guardrails welded between the beams (Figure 8.9). The failed soil material is then compacted around the retaining wall which acts as a reinforcement structure within the embankment. Most of the materials used are leftovers or scrap parts from previous highway construction or remediation projects or rail damaged by the traveling public, so that the materials essentially cost nothing. However, prices of the new and used materials are included in the analysis to illustrate the cost to the State if materials are required for the project.

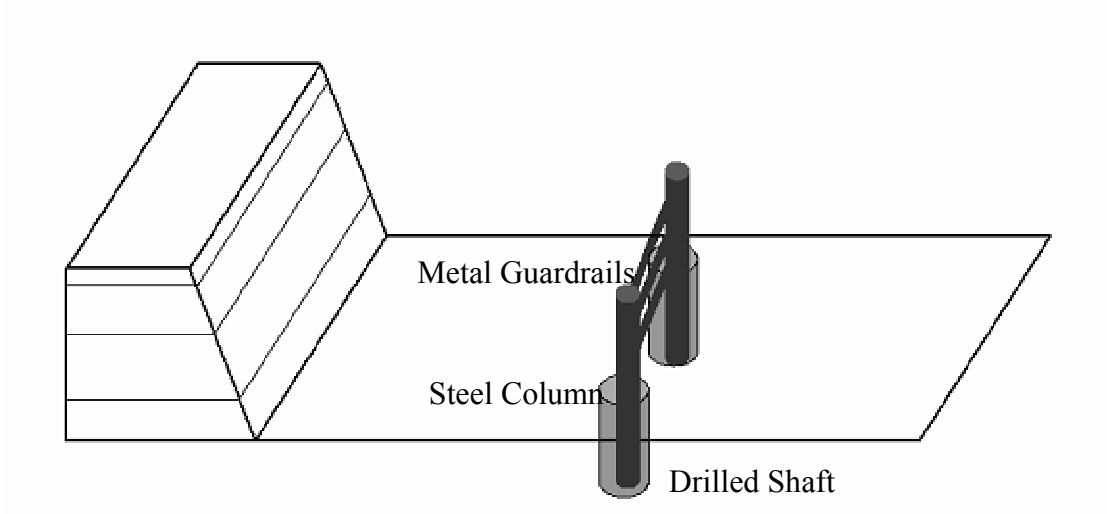

Figure 8.9: Illustration of the Pile Retaining Wall Reinforced Embankment Before Placement of Soil Mass

For the IH 30 case history, it is assumed that the retaining wall will be placed at the center of the excavation, so the height (and subsequent depth) of the pile wall is approximately 9 feet (one foot thick soil layers compacted on top of wall), resulting in a 18 foot long piece of steel needed for the beams. The cost of 18 foot long Wide Flange Steel I Beams (ranging from 8x4 and 10 lb/ft to 12x12 and 120 lb/ft) is approximately $30.34–$1,014.48 per yard of embankment for pile spacing of 5–10 feet. The cost of drilled shafts, ranging in diameters from 12 to 48 inches and at spacing of 5–10 feet, is approximately $159.92–$1,609.74 per linear yard. For three layers of metal guardrails placed along the height of the piles, the cost ranges from $0 (re-use of guardrails) to $21.99 per yard for used guardrail. Compaction of the excavated soil around the retaining wall would cost $1,734 per yard of embankment. The cost of the pile reinforced embankment for pile spacing of 5 and 10 feet is provided in Table 8.7.

Table 8.7: Summary of the Costs of the Pile Reinforced Soil Embankment

Remediation Method	Cost (per linear yard)
Pile Wall Reinforced Embankment (5 Foot Spacing)	$3,286.52 - $5,533.78
Pile Wall Reinforced Embankment (10 Foot Spacing)	$3,088.26 - $4,221.67

Analytical Study

The analytical study of the embankment remediation alternatives provides a method to numerically illustrate the mechanical benefits of using tire bales as a construction material that can be combined with the cost benefit analysis. The UTEXAS4 slope stability program (Wright 2007) was used to perform limit equilibrium analyses of the remediation alternatives. Spencer's method of stability analysis, which satisfies all equilibrium equations and can be used

for circular and non-circular failure surface geometries, was used to determine the factor of safety (resisting strength/driving forces) of the embankment. The following section outlines the results from the analytical study.

The analysis of the re-compacted slope without drainage indicates the factor of safety reduces to 1.1 for groundwater conditions similar to those causing the initial failure (as shown in Figure 8.10). The strength of the re-compacted slope was assumed to be similar to that of the peak shaley clay material (as illustrated in Figure 8.5). The inclusion of the drainage layers at the base of the excavation, or reduction of the elevation of the piezometric line, increases the factor of safety to 1.68 (Figure 8.11).

The use of tire bales as reinforcement layers within the embankment provides two improvements to the stability of the slope: a layer of strong material that intercepts the failure surface and a drainage layer to provide a path for water out of the slope. Analysis of the tire bale reinforced slope (with drainage) indicates that even for high groundwater tables in the soil retained behind the embankment, the lowest factor of safety is 1.7 (Figure 8.12). The strength of the tire bale interface was set equal to the tire bale-clay interface strengths reported in Chapter 6. The unit weight of the tire bale mass was altered to take into account the soil fill around the bales (Chapter 5), increasing unit weight from 36.5 pcf (the value typically assumed) to approximately 69 pcf. The inclusion of the tire layers allows drainage along the height of the embankment and therefore a reduction in the elevation of the piezometric line down to the base of the tire bale reinforcement layers. Although the strength of the tire bale-clay interface is lower than that of the clay only, the presence of the tire bales forces the failure surface to extend underneath the tire bale layers.

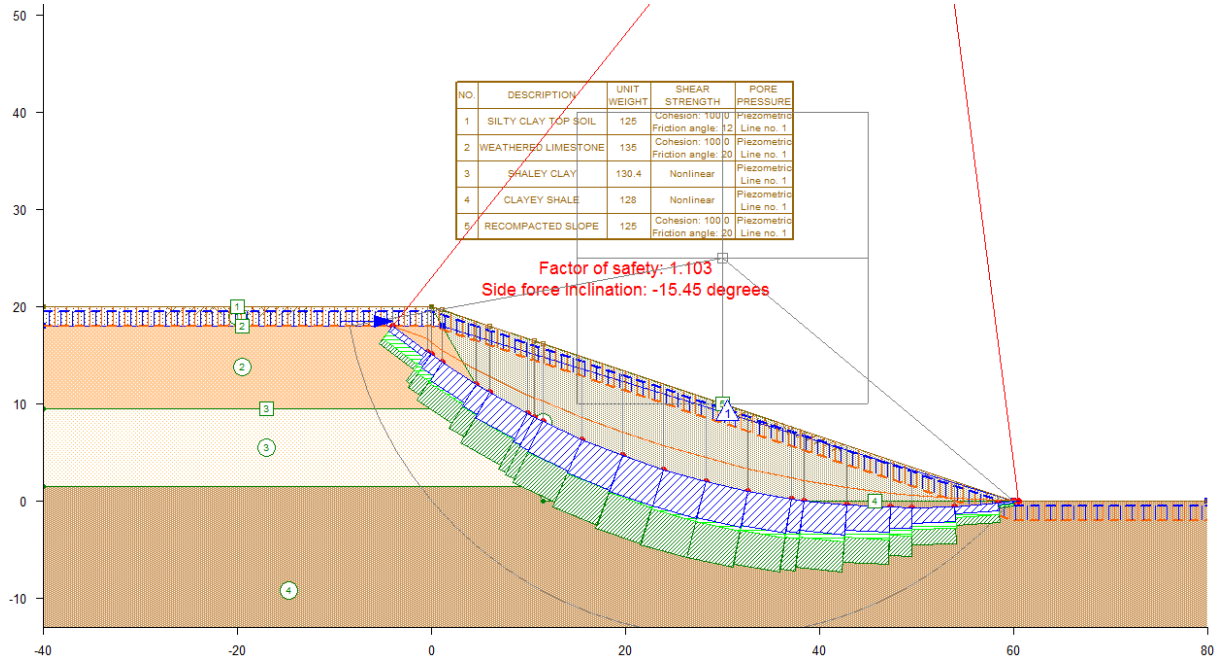

Figure 8.10: Limit Equilibrium Analysis of Re-Compacted Soil Slope without Drainage

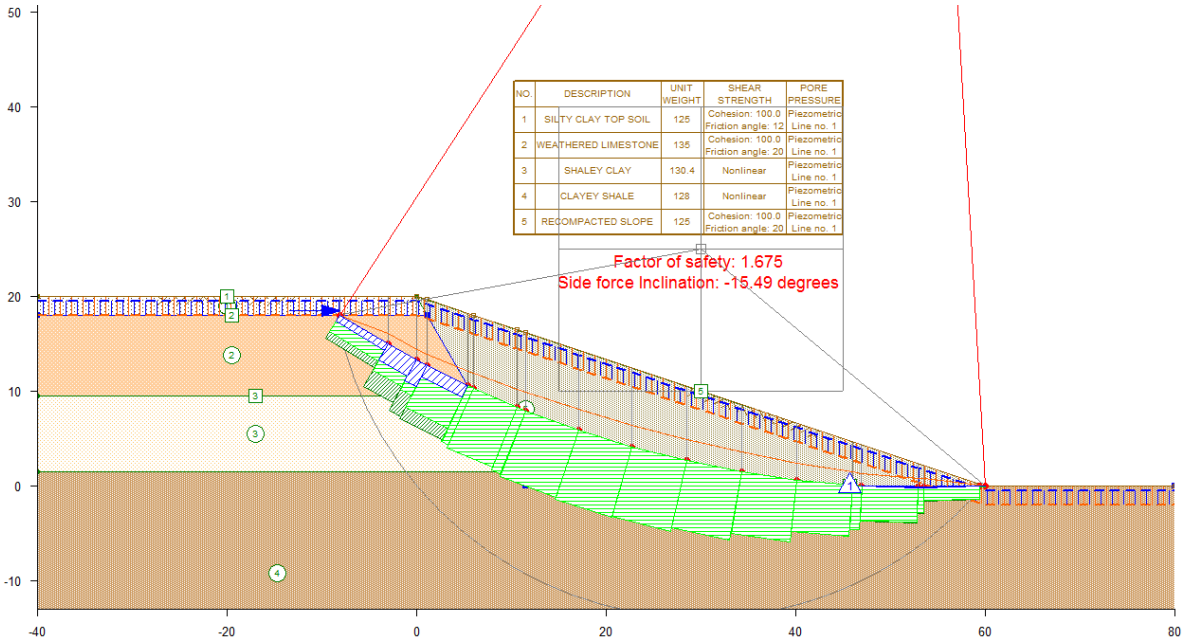

Figure 8.11: Limit Equilibrium Analysis of Re-Compacted Soil Slope with Drainage Layer

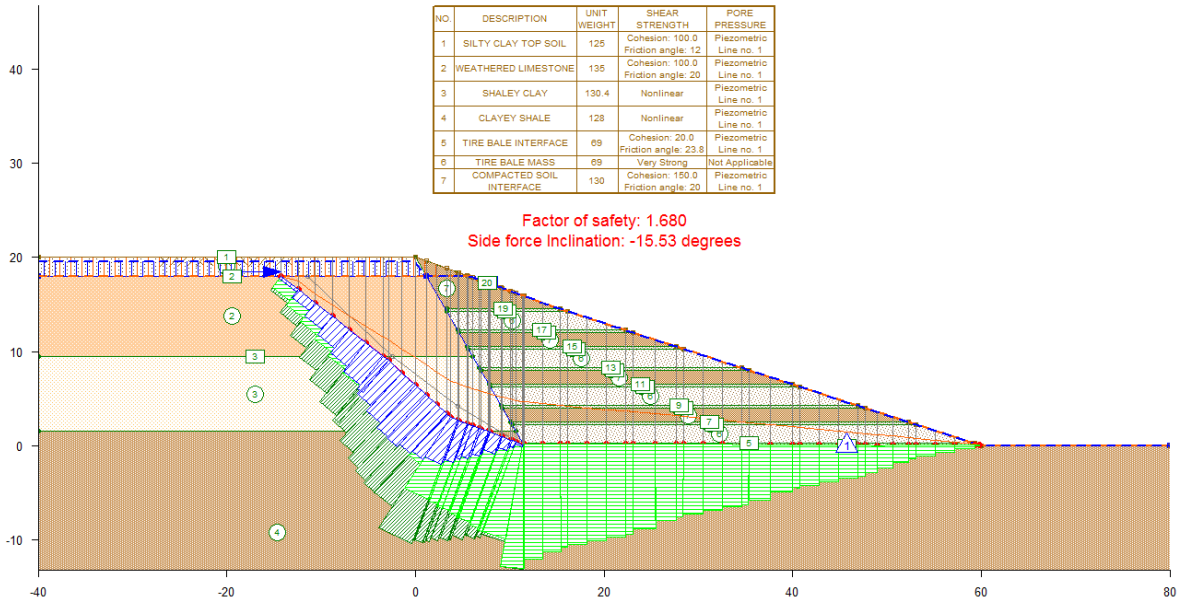

Figure 8.12: Limit Equilibrium Analysis of the Tire Bale Reinforced Soil Slope with Drainage

The analysis of the tire bale mass embankment can be used to illustrate three important scenarios of the tire bale embankment stability; the stability for drained conditions, the effects of submergence on stability, and the surficial stability of a soil cover. The strengths of the analyses were assumed to be the tire bale interface strength for wet conditions (Chapter 6). For the tire bale embankment with drainage and a high groundwater table within the limestone layers behind

the embankment, the critical failure surface exists at the base of the tire bale mass with a factor of safety of 1.6 (Figure 8.13).

When drainage is not allowed from the slope and the piezometric line elevation increases to the top of the limestone layer and slope face, the factor of safety reduces to 0.9, indicating failure of the slope (Figure 8.14). The low unit weight of the tire bale mass is the main cause of the significant reduction in stability of the submerged slope. The saturated unit weight of the tire bale mass, as discussed in Chapter 5.4.2, is approximately 66 pcf. The submerged, or effective unit weight, is therefore approximately 3.6 pcf, indicating that the effective normal stresses within the tire able mass decrease by a factor of almost ten from dry (~40 pcf) to submerged (~4 pcf) conditions.

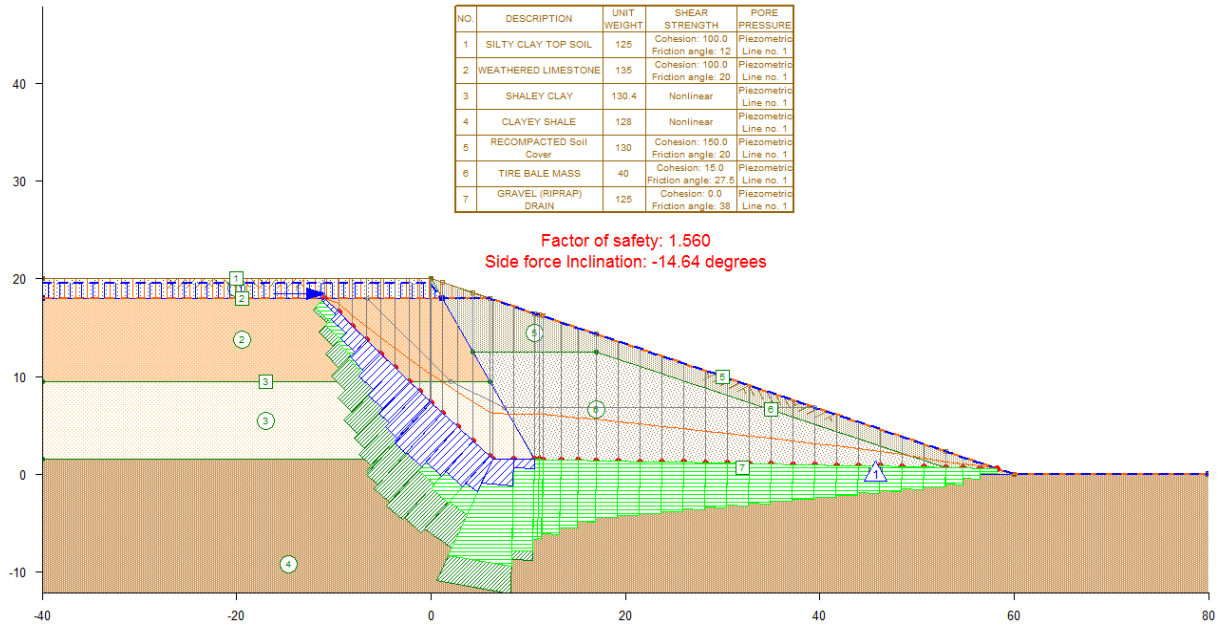

Figure 8.13: Limit Equilibrium Analysis of the Tire Bale Fill Soil Slope with Drainage

The placement of a soil cover on the tire bale mass is a precaution to limit degradations of the tires due to UV radiation and to prevent free access of water and air, which may increase any exothermic reactions occurring within the tire bale mass. When compacted clay covers are used as the soil cover, there are no indications of surficial stability problems or the formations of a shallow slope failure (Figure 8.15) for short term conditions. However, for sandy soils or clays subjected to wet/dry cycles (decrease in cohesion), the purely frictional strength of the soil leads to the formations of a shallow slip surface within the soil cover (Figure 8.16).

Remediation of the shallow slope failure could potentially include grouting the soil, using geosynthetics along the embankment height, or increasing the dimensions of the tire bale slope. Another alternative, that again beneficially re-uses tires, is to mix the soil cover with tire shreds to act as discrete reinforcement fibers within the soil mass. Zornberg et al. (2004) presented triaxial testing results for a sand mixed with tire shreds that provided evidence of an increase in the apparent cohesion of the soil-tire mixture at a ratio of approximately 30% tires by dry weight of soil. The apparent cohesion was found to increase by almost 400 psf for dosages of tire shreds between 30 and 40 percent. However, for the IH 30 case with sand cover, and increase in the apparent cohesion of the soil of only 25 psf increases the factor of safety against surficial failure

to over 1.5 (Figure 8.17). This is also coupled with a reduction in weight of the surficial soils with the inclusion of the lighter tire shreds, which decreases the saturated unit weight from 125 pcf to approximately 100 pcf.

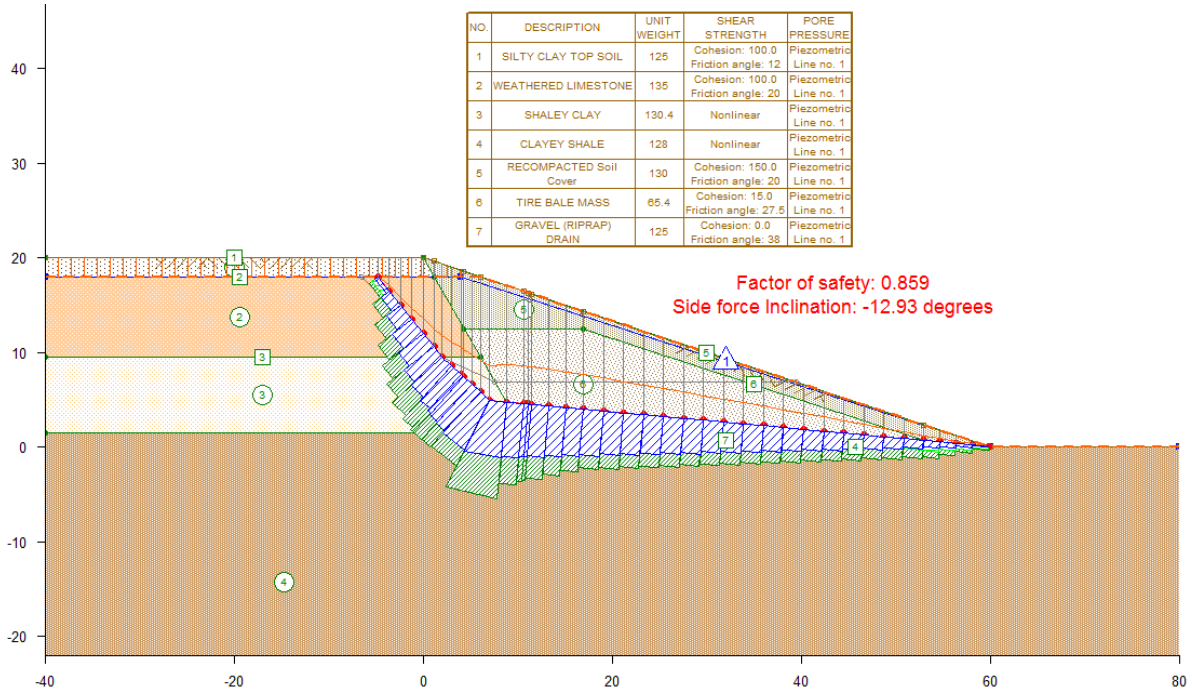

Figure 8.14: Limit Equilibrium Analysis of the Tire Bale Fill Soil Slope without Drainage (Piezometric Line at the Top of the Limestone Layer)

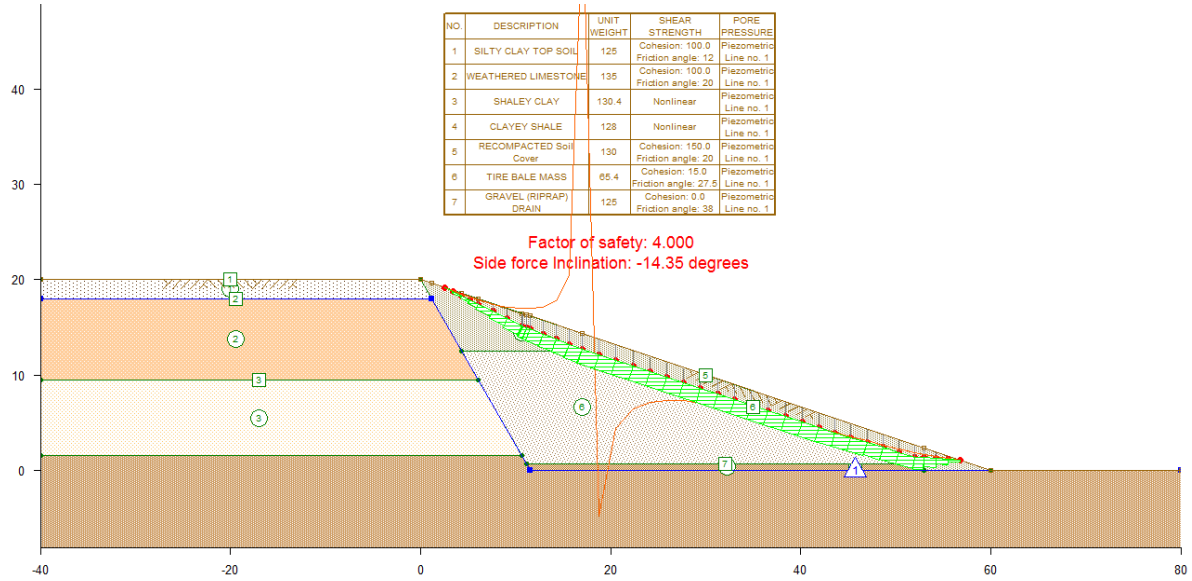

Figure 8.15: Limit Equilibrium Analysis of the Surficial Stability of a Compacted Clay Cover on the Tire Bale Fill Soil Slope with Drainage

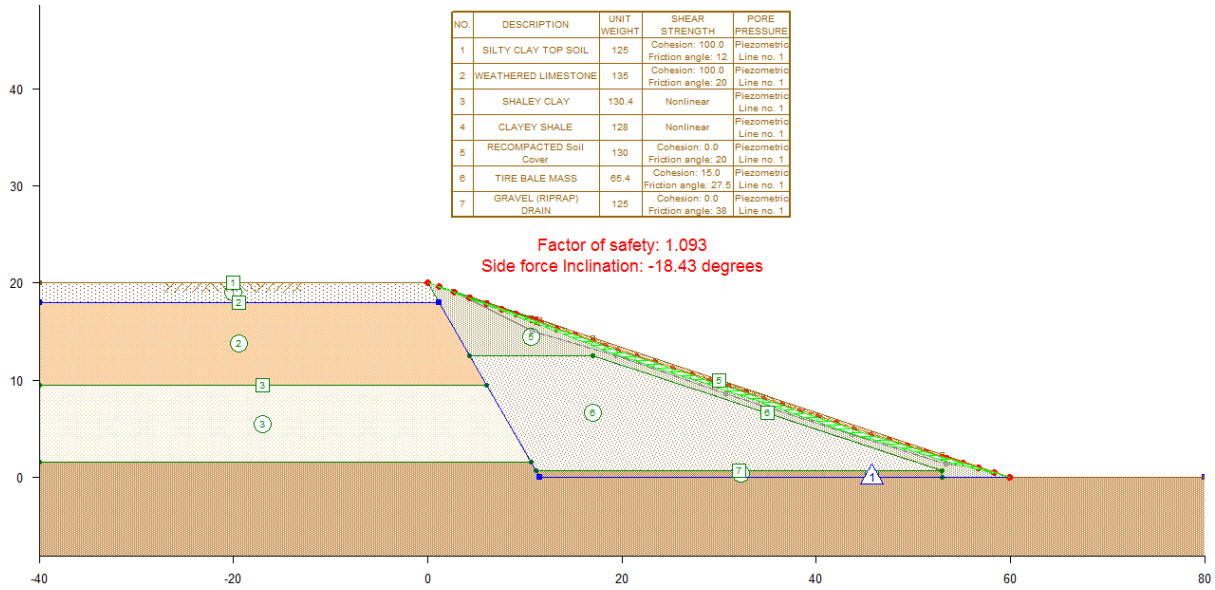

Figure 8.16: Limit Equilibrium Analysis of the Surficial Stability of a Sand Cover on the Tire Bale Fill Soil Slope with Drainage

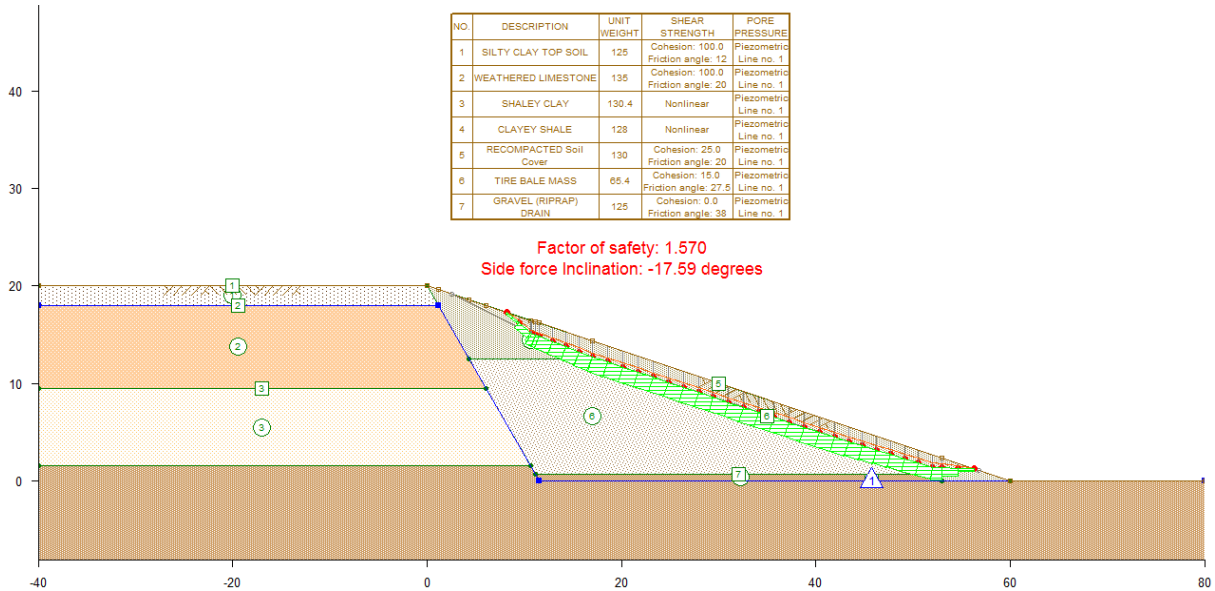

Figure 8.17: Limit Equilibrium Analysis of the Surficial Stability of a Tire Shred Reinforced Sand Cover on the Tire Bale Fill Soil Slope with Drainage

The same soil parameters presented for the tire shred reinforced soil cover can also be used to determine the stability of the re-compacted soil embankment with tire shred reinforcement. The saturated unit weight of the tire shred reinforced soil, with a ratio of 30% tires by dry weight of soil, decreases to approximately 100 pcf. The strength of the tire shred-soil

mixture was set constant to that of the pure soil embankment to illustrate the effect of just decreasing the weight of the structure on the stability. The result of the limit equilibrium analysis is shown in Figure 8.18 for undrained conditions (no drainage blanket) and a piezometric line at the surface of the limestone layer. The factor of safety against failure, approximately 1.2, indicates that the reduction in weight provided by the tires in not enough to increase the stability; drainage from the slope is still the critical factor in the stability of the structure.

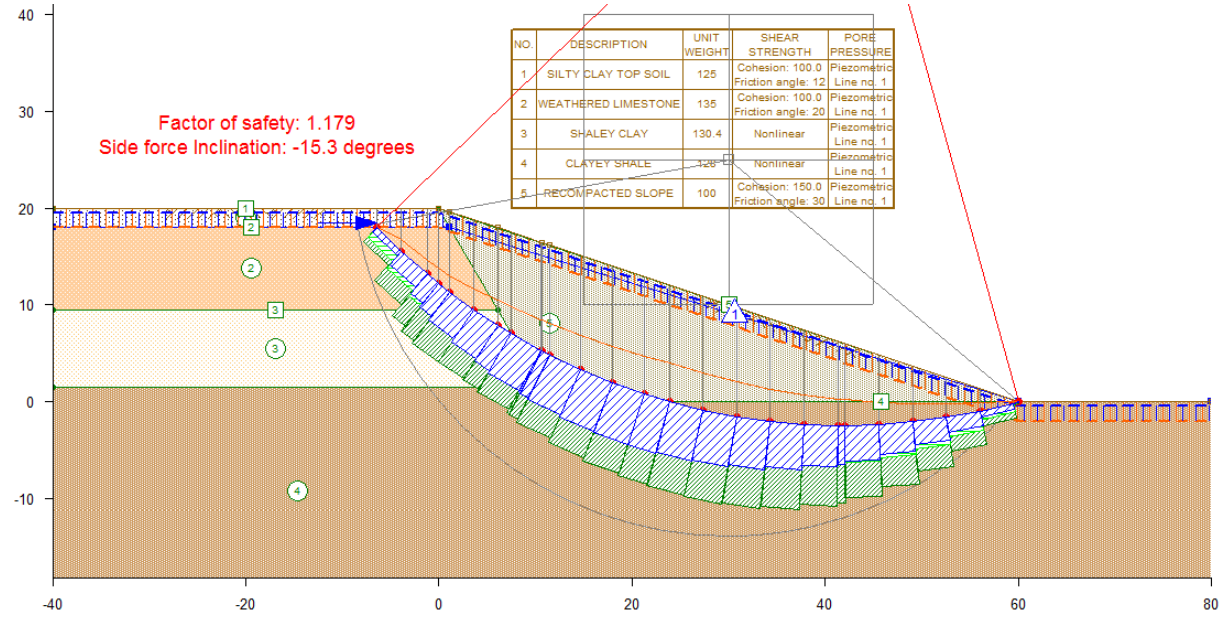

Figure 8.18: Limit Equilibrium Analysis of the Tire Shred Reinforced Re-Compacted Soil Embankment

Summary

A summary of the costs and associated factors of safety for the different IH 30 slope remediation alternatives is provided in Table 8.8. The inclusion of tires bales into the embankment for all embankment designs costs less than the re-compaction of the slope and provided adequate factors of safety against failure even for the worst case groundwater conditions. The benefits of using tire bales in embankment construction are the ease of construction, which is the cause of the lower costs, and the increase in stability of the structure due to the strength and high permeability of the tire bale mass. For the IH 30 case history, the main advantage of using tire bales was the drainage provided by the bale mass from the permeable limestone layer within the existing geology. The other remediation alternatives were only effective in increasing the stability of the slope if drainage layers were included, which in most cases significantly increased the cost of the structures.

Table 8.8: Cost and Factor of Safety Calculated for Each IH 30 Embankment Remediation Alternative

Remediation Method	Cost (per linear yard)	Factor of Safety
Recompaction	$2,890.00	1.1
Recompaction with Drainage Blanket	$2,910.00 - $3,900.00	1.7
Recompaction with Geosynthetics	$2,930.00 - $3,150.00	-
Tire Bale Reinforced Embankment	$2,496.00	
Tire Bale Reinforced Embankment with Drainage	$2,693.00	1.5
Tire Bale Mass Embankment with Drainage	$2,767.00 - $2,896.00	1.6
Tire Shred Embankment without Drainage	$3,501.70	1.2
Pile Wall Reinforced Embankment	$3,088.26 - $5,533.78	No Reported Failures

The previous analysis does not include the cost savings to the state by baling tires at the site, which may decrease the cost of hauling tires by approximately $1.20 per tire. The actual cost to the state of a tire bale structure is the construction costs presented in this section minus the savings per tire times the number of tires used (Table 8.9). For the tire bale reinforced slope, approximately 2,500 tires are re-used as bales per five feet of embankment, resulting in a savings of $1,800 per yard of embankment if the tires are baled before transportation, resulting in a net cost of the embankment of only $893 per yard of embankment. For the tire shred embankment, there is no savings and therefore no cost reduction for using shreds, indicating another benefit of using tire bales over tire shreds for embankment construction.

Table 8.9: Costs of the IH 30 Slope Remediation Alternatives with Savings Due to Tire Baling Included

Remediation Method	Cost (per yard)	Cost Savings (per yard)	"Total" Cost to TxDOT
Recompaction	$2,890.00	0	$2,890.00
Recompaction with Drainage Blanket	$2,910.00 - $3,900.00	0	$2,910.00 - $3,900.00
Recompaction with Geosynthetics	$2,930.00 - $3,150.00	0	$2,930.00 - $3,150.00
Tire Bale Reinforced Embankment	$2,496.00	$1,245.00	$1,251.00
Tire Bale Reinforced Embankment with Drainage	$2,693.00	$1,245.00	$1,448.00
Tire Bale Mass Embankment with Drainage	$2,767.00 - $2,896.00	$1,792.80	$974.20 - $1,103.2
Tire Shred Embankment without Drainage	$3,501.70	0	$3,501.70
Pile Wall Reinforced Embankment	$3,088.26 - $5,533.78	0	$3,088.26 - $5,533.78

The actual cost presented in Table 8.11 includes the savings to the state of baling the tires at the site, and is not the final cost of the structure since no transportation costs were included in the analysis. The cost of transporting the bales to the site would still need to be included in the analysis to get the final cost of the structure.

Case History 2: Proposed Tire Bale Highway Overpass

The cost benefit of using tire bales as a lightweight fill for highway overpasses over soft soil is similar to that of the highway embankment, but the analytical study requires a more in-depth analysis of deformation which cannot be found using limit equilibrium. Plans for a proposed highway overpass were provided by Richard Williammee from the Fort Worth District of TxDOT (Figure 8.19). Two alternatives can be considered for the overpass: a soil only overpass and a tire bale reinforced overpass with 12 inch thick compacted soil layers between layers of tire bales. Both alternatives will have the same final dimensions and traffic loadings.

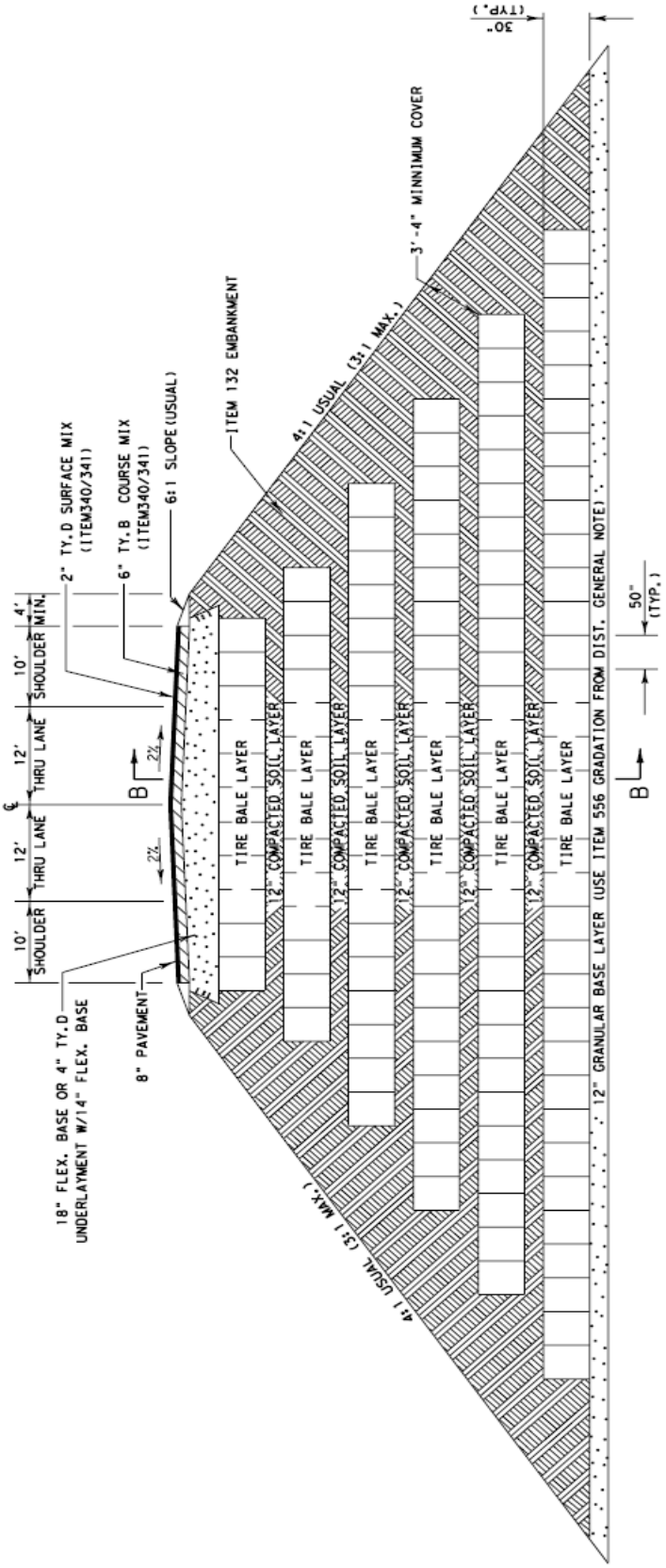

Figure 8.19: General Cross Section of the Proposed Highway Overpass Provided by TxDOT

Cost Benefit Analysis

The costs associated with the overpass construction, as determined by the unit price list from the Fort Worth and Austin Districts of TxDOT for 2006 are listed in Table 8.10 (available at www.txdot.gov/business/avgd.htm).

Table 8.10: Costs Associated with Materials for the Proposed Highway Overpass

Description of Action or Material	Construction Unit	Cost ($)
Embankment Fill (Type D)	cy	6.33 - 14.86
Embankment Compaction (Type D)	cy	22.32
Coarse Aggregate (Upper and Lower Layers)	cy	1.53 - 51.56
Embankment Compaction (Type B)	cy	20.07
Scrap Tire Bale (Standard Dimension)	cy	2.80 - 9.60
Forklift	day*	215.00 - 233.00
Tractor Loader (Front End Loader)	day*	193.80 - 305.00
Clamshell Bucket	day*	29.00 - 68.20
Geotextile Reinforcement/Separation Layer	sy	0.63 - 3.04
PVC Pipe (4" Inner Diameter)	lf	1.59 - 2.50
Concrete Flume	cy	350

* May be assumed zero if equipment is already present.

The total cost per yard of length of overpass was calculated for both alternatives considering the overpass geometry shown in Figure 8.19. The cost of the soil assumes that an excavation is made near the site (Type D soil) and that transportation costs are negligible. For the soil only overpass, approximately 350 cubic yards of soil need to be excavated and compacted at a total cost of $13,087.36 per yard of embankment. Addition of the tire bale layers replaces 180 cubic yards of soil and costs $1,728.00. The total number of bales needed (per five feet of overpass) is approximately 75 bales, which requires that 5,000 to over 7,500 whole scrap tires are needed per five feet of overpass. The major cost benefit between the soil and tire bale embankments is the reduction in labor/compaction of the tire bale overpass, a reduction in cost of $7,856.64 per yard for the tire bale reinforced overpass.

The total costs of the two alternatives are provided in Table 8.11, including the cost of the gravel sub-base, stone rip-rap and the foundation, and geotextile coverings and drainage in the tire bale sections. The roadway construction costs were not considered and would be equal for both cases, so is not crucial to the analysis. The values in parenthesis are the cost of the overpass without considering the cost of obtaining the soil, indicating that a third of the cost of the soil overpass is due just to excavating the soil.

Table 8.11: Summary of Costs of Highway Overpasses for Proposed Alternatives

Construction Method	Cost (per linear yard)
Soil Only Embankment	$15,580.48 ($10,349.76)
Tire Bale Reinforced Embaknement	$10,914.43 ($8,324.95)

Analytical Study

The analytical study of the highway overpass was concerned with the deformation of the overpass due to loads imposed on the embankment. The finite element program Plaxis v.8 was used to predict the deformations within the highway overpass for the two different alternatives. Due to symmetry of the overpass, only one half of the structure was modeled, as shown in Figures 8.20 and 8.21 for the soil only and tire bale reinforced overpasses, respectively.

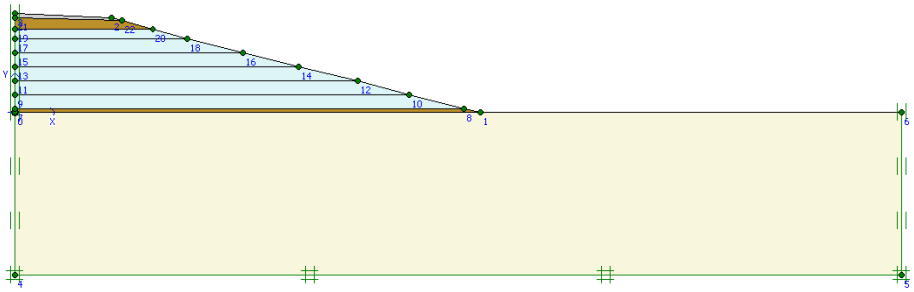

Figure 8.20: Finite Element Model for the Soil Only Overpass

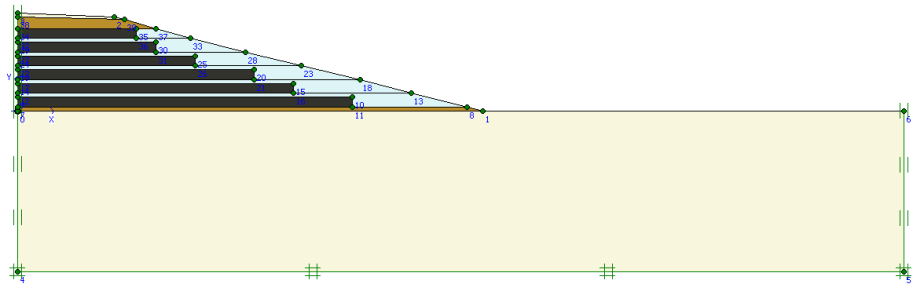

Figure 8.21: Finite Element Model for the Tire Bale Reinforced Overpass

The analysis was simplified by using a linear, constant modulus of the tire bale structure as determined in Chapter 7. Typical soil linear elastic properties used in the analysis, as provided by Plaxis, are provided in Table 8.12. The tire bale elastic properties used in the analysis were obtained from compression testing conducted in the testing program and from results presented by Zornberg et al (2004), as defined in Chapter 7. A stiff clay foundation was used in this analysis so that the compressions of the overpass embankment could be isolated from the compressions of the foundation layer.

Table 8.12: Linear-Elastic Properties of the Overpass Materials

	Material Properties				
Material	Young's Modulus (psf)	ν	c (psf)	ϕ (deg)	γ_{dry} (pcf)
Stiff Clay Foundation	60890	0.33	41	24	103
Upper and Lower Ganular Soils	62660	0.3	20	30	101
Compacted Clay Slope	41770	0.35	10	24	105
Tire Bale Mass	15000*	0.15	20	28	61.3
	16000**	0.08			
	22000***	0.08			
Concrete Roadway	31458	0.2	50	40	145

* Unconfined Bale Modulus and Poisson Ratio
** Minimal Confinement Tire Bale Modulus and Poisson's Ratio
*** Predicted Soil Confined Bale Modulus and Poisson's Ratio

The moduli values listed in Table 8.12 illustrate the stiffness of the tire bales as compared to the typical soil materials used for the highway overpass. In general, it can be concluded that the stiffness of the soil confined tire bale layer is almost half of the stiffness of a compacted clay, indicating that the compressions of a tire bale structure will be higher than that for a soil only slope. The results from finite element analysis were used to determine the stresses, quantify the overpass deformations, and determine the critical failure planes within the overpass sections. Both a compacted clay overpass and tire bale reinforced overpass were considered in the analysis. The deformed mesh of the soil only and tire bale reinforced alternatives are shown in Figures 8.22 and 8.23, respectively.

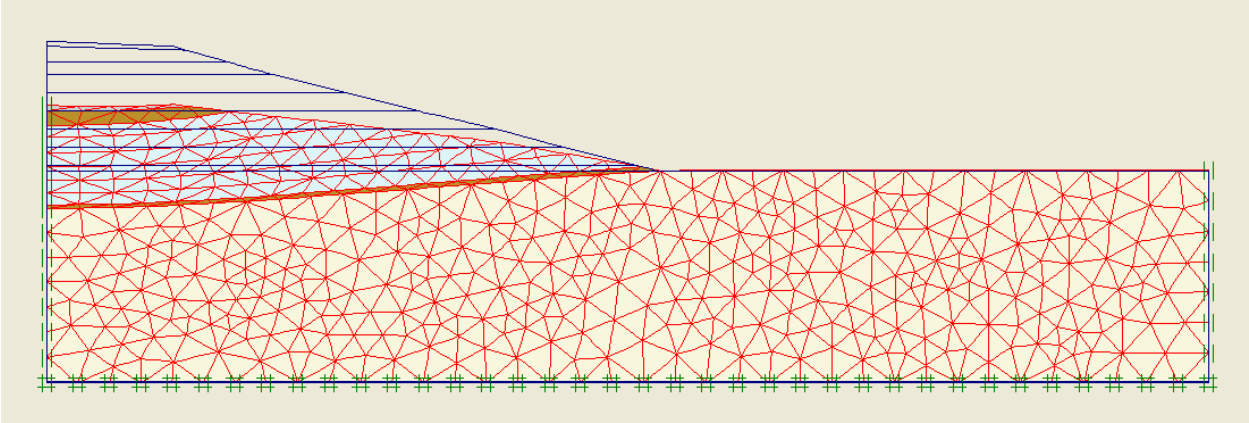

Figure 8.22: Deformed Finite Element Mesh for the Soil Only Overpass

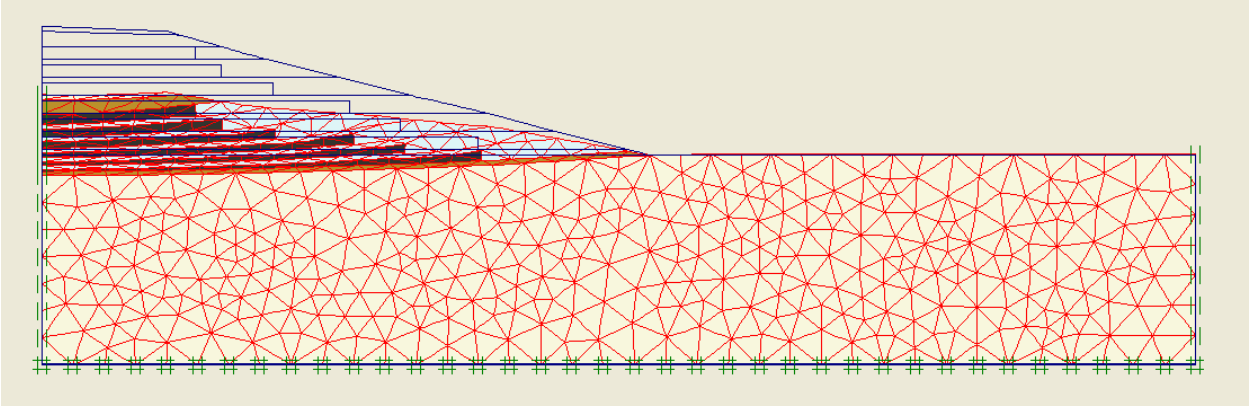

Figure 8.23: Deformed Finite Element Mesh for the Tire Bale Reinforced Overpass

The benefit of using the tire bales within the overpass structure are that the weight of the structure is reduced and a drainage layer is included within the soil mass. However, the deformation of the tire bale structure will be higher due to the reduced stiffness of the tire bale layers, as shown in Figures 8.24 and 8.25 for the tire bale reinforced and soil only overpasses, respectively. The reduced stiffness results in larger predicted vertical compressions at the midpoint of the structure by as much as 5–6 inches for the tire bale reinforced overpass. However, the compression of the foundation is less for the tire bale reinforced slope by up to 4 inches due to the lighter bales (a reduction in the applied surcharge pressure of 400–800 psf at the base of the embankment). The analysis provides evidence that the total vertical movement of the roadway at the midpoint of the tire bale overpass is only 1–3 inches more than the soil only, yet the deformation of the tire bale overpass itself is significantly higher due to the reduced stiffness of the tire bale mass.

The shearing strains calculated for the soil only and tire bale reinforced overpass finite element models, which indicate the distribution of shear stress within the structure mass, are shown in Figures 8.26 and 8.27, respectively. The predicted shear strains within the tire bale layers are approximately 3 times higher than those in the soil only model, indicating a larger displacement to mobilize shearing stresses. The results also indicate that the shear stresses are

dissipated mainly within the tire bale layers, indicating that the tire bale layers act as reinforcement layers within the soil mass.

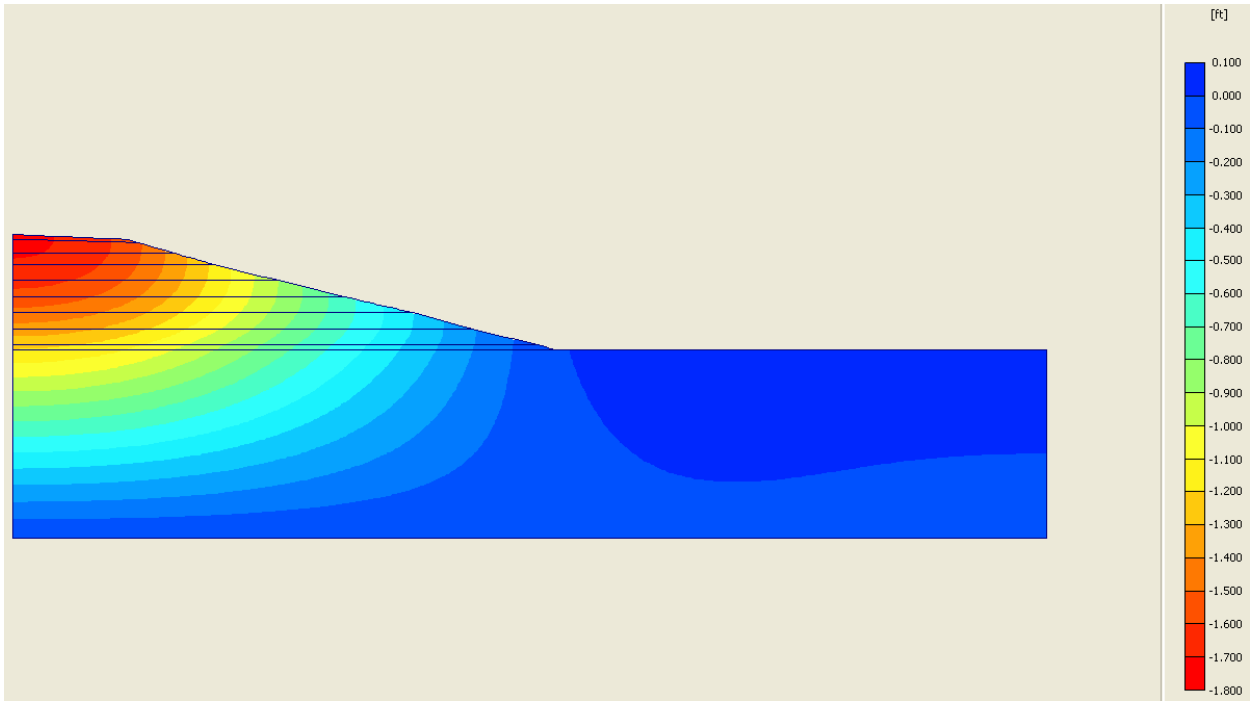

Figure 8.24: Vertical Compression of the Soil Only Overpass (Stiff Clay Foundation)

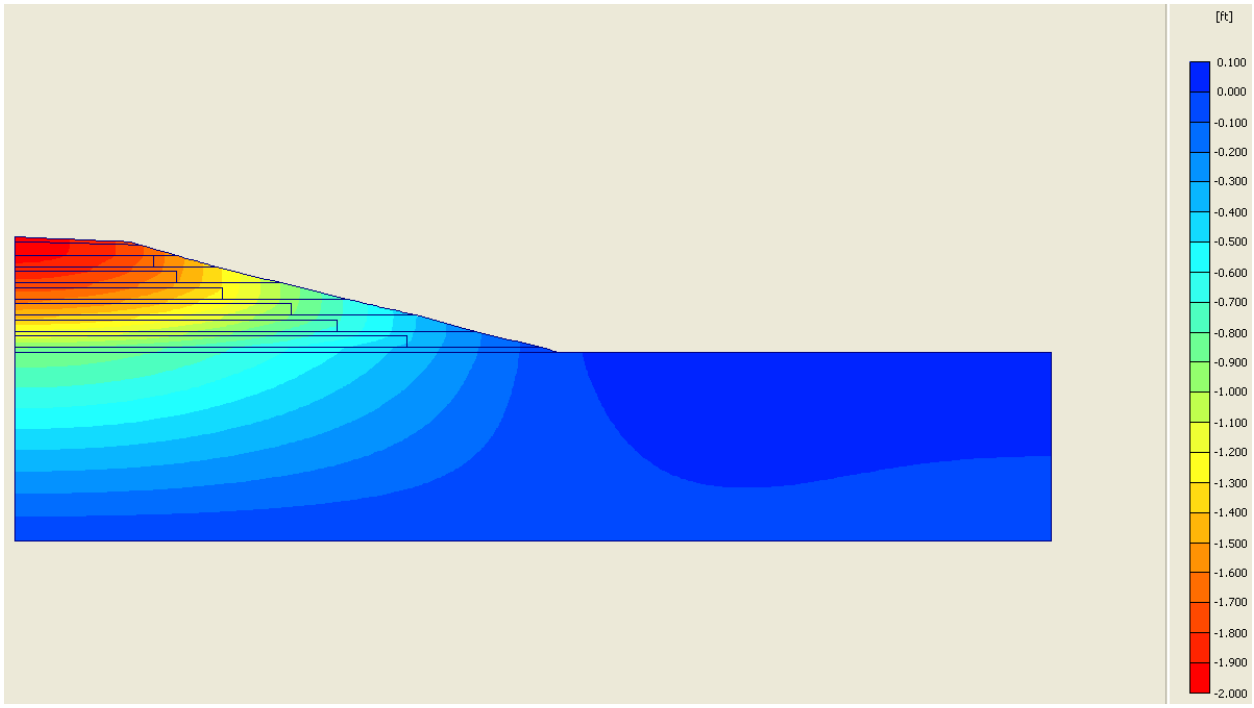

Figure 8.25: Vertical Compression of the Tire Bale Reinforced Overpass (Stiff Clay Foundation)

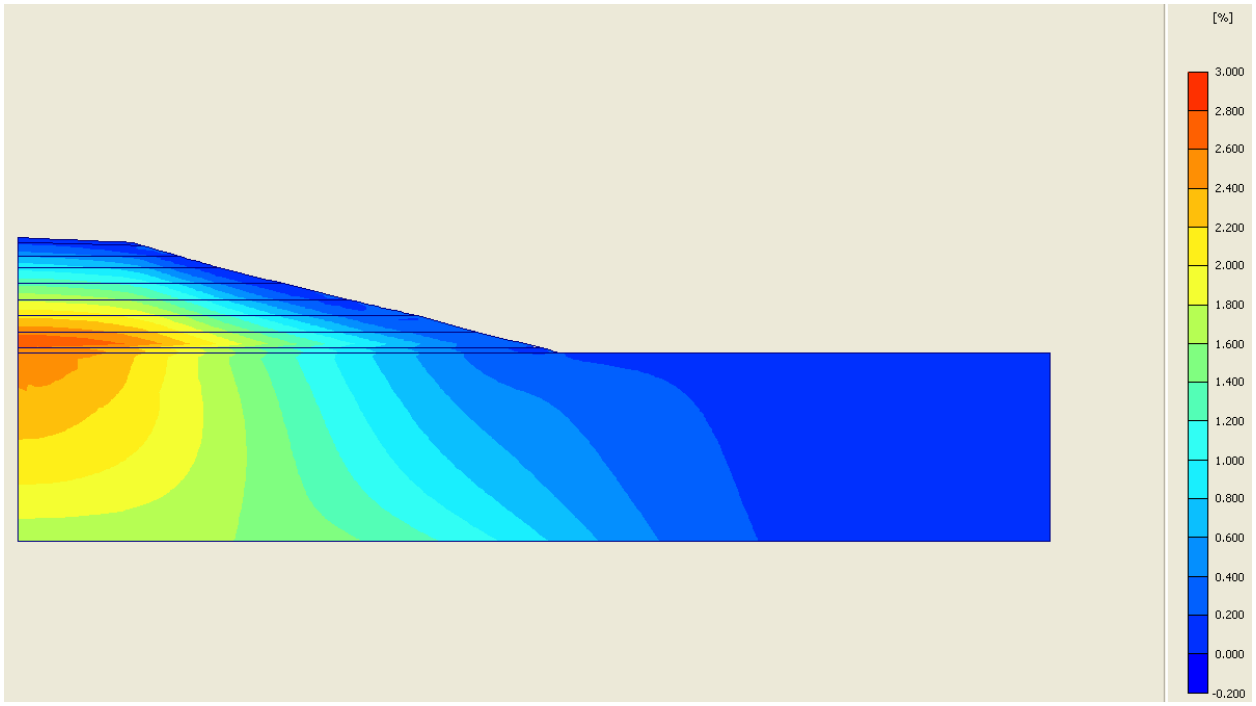

Figure 8.26: Shear Strains within the Soil Only Overpass

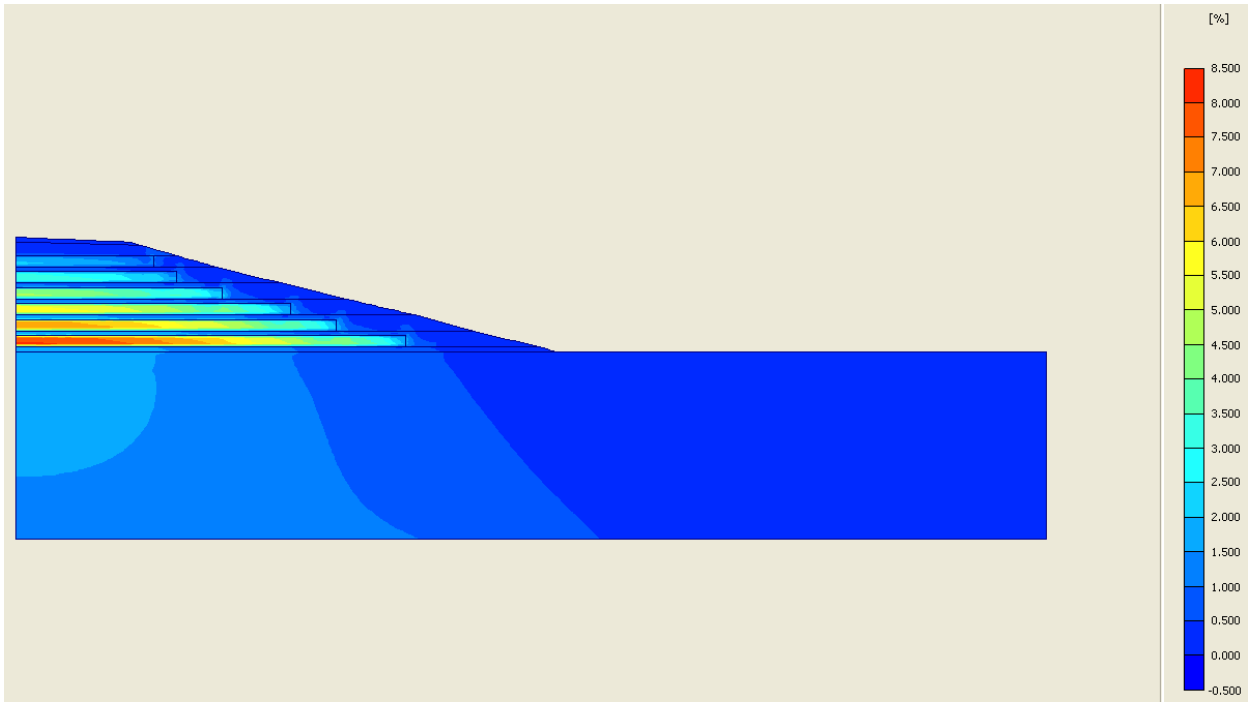

Figure 8.27: Shear Strains within the Tire Bale Reinforced Overpass

Plaxis was also used to predict a failure surface and calculate a factor of safety for the overpasses that could be used to compare with results from the UTEXAS4 program to indicate similarities in the results from the two programs. Predicted failure planes for the soil only

overpass from Plaxis and UTEXAS4 are shown in Figure 8.28 and 8.29, respectively. Both programs indicate the same factor of safety (approximately 2.1) and similar failure planes. Results from the finite element and limit equilibrium analyses for the tire bale reinforced overpass are also similar, as shown in Figures 8.30 and 8.31.

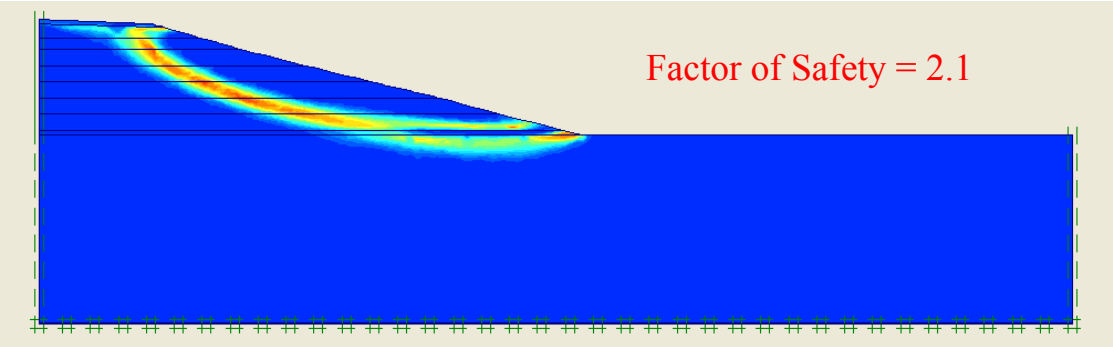

Figure 8.28: Predicted Failure Plane and Factor of Safety from Finite Element Analysis (Plaxis) for Soil Only Overpass

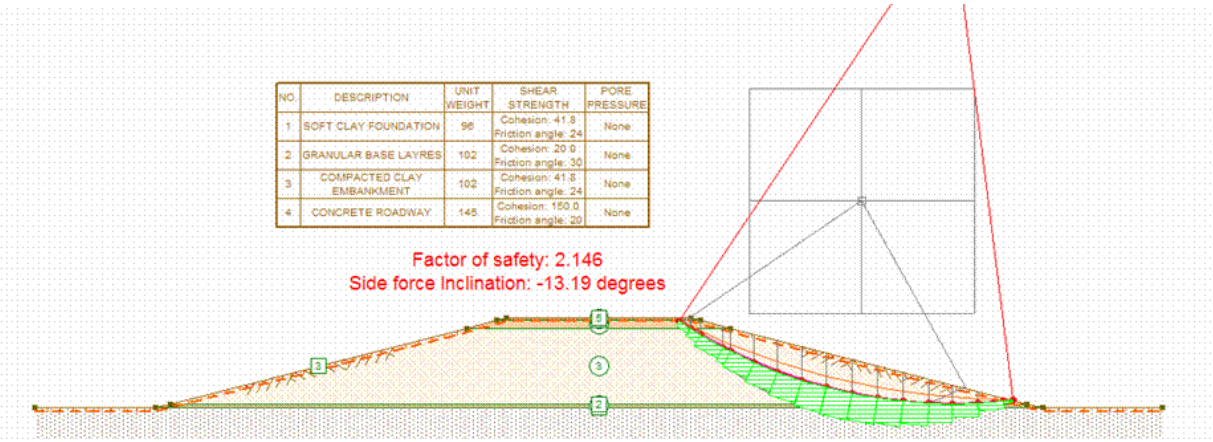

Figure 8.29: Predicted Failure Plane and Factor of Safety from Limit Equilibrium Analysis (UTEXAS4) for Soil Only Overpass

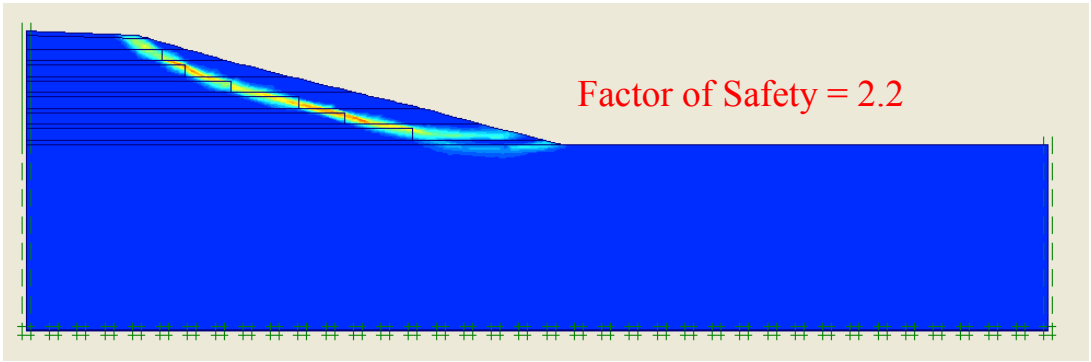

Figure 8.30: Predicted Failure Plane and Factor of Safety from Finite Element Analysis (Plaxis) for Tire Bale Reinforced Overpass

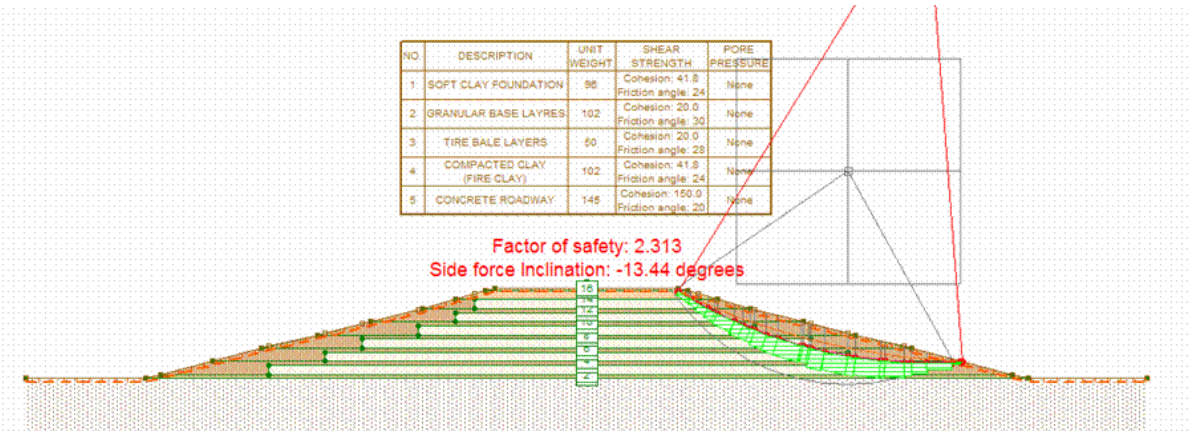

Figure 8.31: Predicted Failure Plane and Factor of Safety from Limit Equilibrium Analysis (UTEXAS4) for Tire Bale Reinforced Overpass

Summary

The cost benefit analysis and analytical study of the tire bale overpass highlight a few important aspects of the use of tire bales within highways embankments. The most important aspect is that although tire bales may be a stronger and lighter material than the surrounding soil, the tire bales are much more deformable than the soil (Table 8.13). So for higher factors of safety against failure there will be more deformation in the tire bale section, which may aesthetically or structurally cause problems.

Table 8.13: Summary of Tire Bale and Soil Overpass Cost Benefit and Analytical Studies

			Deformations	
Construction Method	**Cost (per yard)**	**Cost Savings (per yard)**	**Embankment**	**Total**
Soil Only Embankment	$15,580.48 ($10,349.76)	$0.00	7"	21.6"
Tire Bale Reinforced Embankment	$10,914.43 ($8,324.95)	$50,820.00	12"	24"

The cost savings of transporting tire bales as opposed to whole tires is also included in Table 8.13. The tire bale reinforced highway overpass can potentially use more than 70,000 whole tires per five feet of the structure, resulting in a cost savings of more than $50,000 per yard of the overpass. The cost savings is more than five times the actual cost of the overpass, indicating a significant savings just by transporting the bales.

Case History 3: Tire Bales as Roadway Subgrade (Cost Benefit Only)

One of the main benefits of replacing roadway sub-grade with tire bales is the reduction in weight of the total roadway. This is especially attractive in areas with very soft soils in which removal or surcharging would be required to prepare the foundation, both of which can be very time consuming and labor intensive, and therefore expensive. Successful applications of tire bales as a roadway sub-grade in New York and the UK have been outlined in reports by Zornberg et al. (2004) and Winter et al. (2006).

Two types of tire bale roadway construction have been outlined by Winter (2006), as follows:

1. Floating construction: tire bales are placed directly on the ground surface and a coarse grained soil embankment constructed on both sides to cover the bales.
2. Buried construction: an excavation is made so that the tire bales can be placed below the ground surface and the roadway can be placed level with the surrounding ground.

Both methods require that a coarse grained soil infill, such as sand or small gravel be vibrated between the tire bales and that bales are placed so that the baling wires are parallel to the roadway. A geotextile separator is also placed around the bales to prevent any soil loss into the bales over time, resulting in settlements of the pavement at discrete locations. An illustrative comparison of the typical roadway cross-section and the tire bale sub-grade cross-section are shown in Figure 8.32.

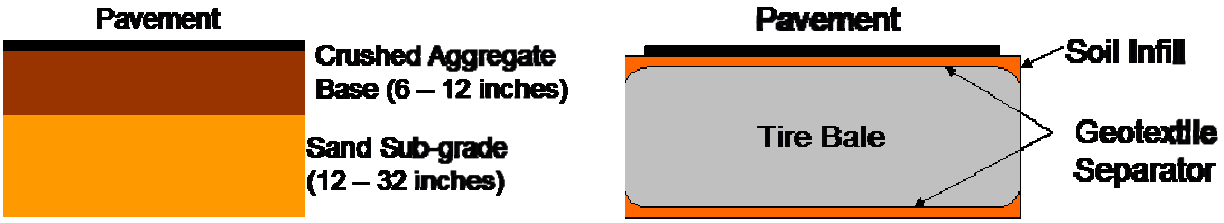

(a) Typical Roadway Section (b) Tire Bale Sub-grade Section

Figure 8.32: Illustrations of the Typical Roadway Cross Section and the Tire Bale Subgrade Cross Section

Zornberg et al. (2004) estimated that for the Chautauqua County, New York tire bale roadway, an average taxpayer savings of $1.60 per tire resulted from using the tires instead of throwing them away, or it cost the State that much less to re-use the tire in the roadway then have them disposed of. In total, it was estimated that the tire bale roadway cost $3,050.00 less than a traditional roadway per 1000 feet of road constructed ($9.15 per linear yard of road).

Typical TxDOT material and construction costs associated with an asphalt roadway are shown in Table 8.14. The materials cost of using tire bales as a subgrade material (including a sand infill), is approximately $8.90 per square yard. The material costs for a typical aggregate sub-grade can range from $5.97 to $12.27 per square yard, depending on the thickness of the material. The compaction of the typical aggregate subgrade would cost $10.01 to $24.46 per square yard, while the compaction of the soil infill between the bales (assuming that 0.28 cubic yards is required per bale) would cost only $11.71 per cubic yard. It is evident that the cost benefit of using bales is not due to the material costs, but the reduction in construction costs, which can be a savings of up to $12.75 per square yard of the roadway.

Table 8.14: Costs Associated with Materials and Construction of Roadways

Description of Action or Material	Construction Unit	Cost
Roadway Excavation	cy	3.31
Asphalt Pavement	sy	1.41 - 1.71
Subgrade Aggregate	cy	32.73 - 69.22
Sand Infill	cy	1.53 - 2.50
Embankment Compaction (Type B)	cy	20.07
Scrap Tire Bale (Standard Dimension)	cy	2.80 - 9.60
Forklift	day*	215.00 - 233.00
Tractor Loader (Front End Loader)	day*	193.80 - 305.00
Clamshell Bucket	day*	29.00 - 68.20
Geotextile Reinforcement/Separation Layer	sy	0.63 - 3.04

* Assumed zero if equipment is already present.

Case History 4: Tire Bales as Fill in Gabion Retaining Walls

There are a number of case histories reported by the New Mexico Department of Transportation in which tire bales have been used as the fill material for gabion retaining walls. A retaining wall project along the US 550 highway was analyzed due to the significant amount of design data provided by the DOT (Duggan 2007, Hudson 2008). The design drawing of the tire bale gabion retaining wall is provided in Figure 8.33. The design called for tire bales to be placed behind gabion cages filled with gravel and fastened with steel cables, which would provide a compressive force binding the series of tire bales into a large wall mass.

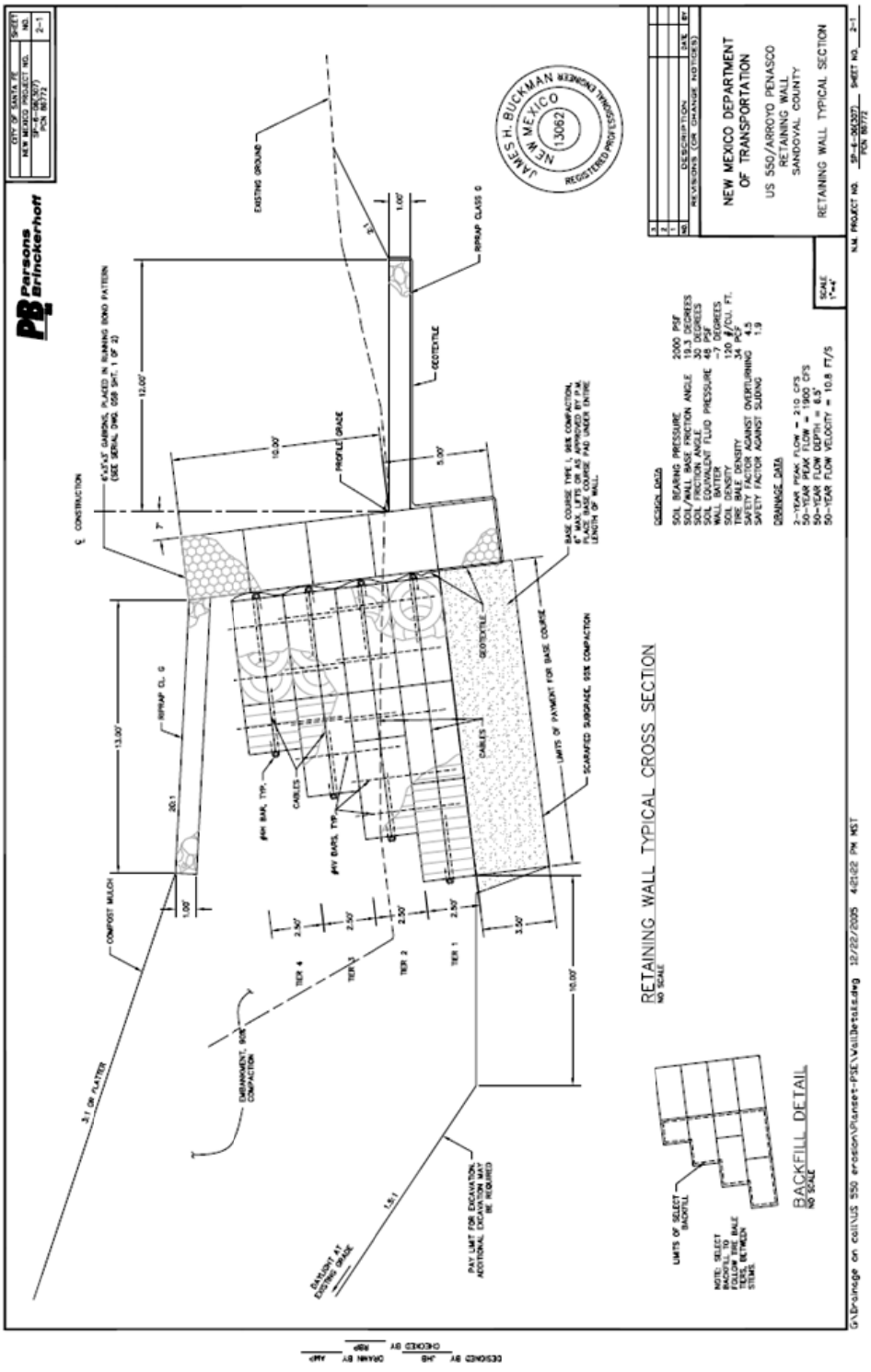

Figure 8.33: Design Plan for the US 550/Arroyo Penasco Retaining Wall in Sandoval County, New Mexico (Provided by Toni Duggan, 2007)

Cost Benefit

The costs associated with a typical gravel gabion and tire bale gabion retaining walls, in terms of average low bid unit prices reported by TxDOT (www.txdot.gov/business/avgd.htm), are provided in Table 8.15. The total cross sectional area of the gabion wall is approximately 18 square yards.

Table 8.15: Costs Associated with Materials and Construction of Gabion Retaining Walls

Description of Action or Material	Construction Unit	Cost
Gabions (Galvanized Steel Cage)	cy	175.11
Scrap Tire Bale (Standard Dimension)	cy	2.80 - 9.60
Forklift	day*	215.00 - 233.00
Tractor Loader (Front End Loader)	day*	193.80 - 305.00
Clamshell Bucket	day*	29.00 - 68.20
Geotextile Reinforcement/Separation Layer	sy	0.63 - 3.04

For a traditional gabion wall, filled with a typical gravel soil, the cost of the wall would be approximately $3,143.22 per yard of wall. A gabion wall of the same geometry, using tire bales as the main component and a 3 foot thick traditional gabion wall along the surface would cost approximately $496.92 per yard of wall. The cost of both walls is provided in Table 8.16. The reduction in costs is related to the difference in costs of the materials, but more importantly the reduction in labor required to build the wall.

Table 8.16: Summary of Costs of Gabion Retaining Walls

Construction Method	Cost (per linear yard)
Tradtional Gabion Wall	$3,143.22
Tire Bale Filled Gabion Wall	$496.92

Analytical Study

The strength of the traditional gravel gabion wall and tire bale gabion wall are similar in that both materials (tire bales as gravel) can be approximated by a friction angle of approximately 28 degrees under wet conditions and are held together by similar steel cages. However the unit weight of the two materials significantly alters the stability of the structure, since tire bales (γ_{dry} = 36 pcf) can be more than 1/3 the unit weight of the gravel (γ_{dry} = 125 pcf). A model of the gabion retaining wall was analyzed using the UTEXAS4 program (Figure 8.34) to determine how the reduction in weight altered the global factor of safety for the system.

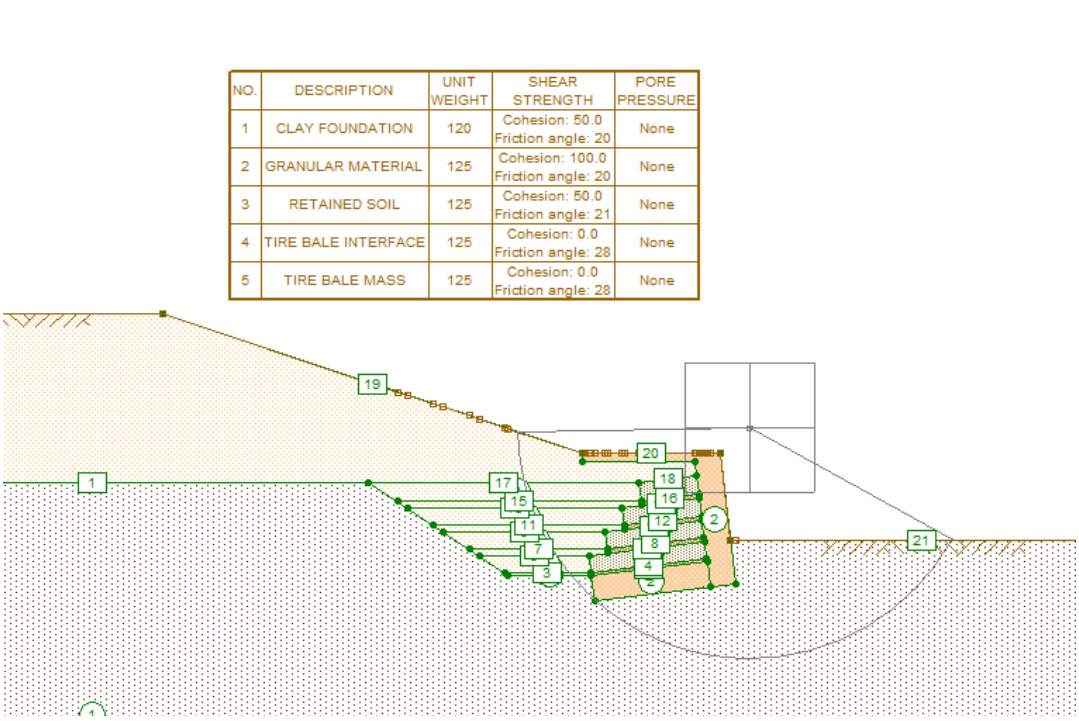

Figure 8.34: Gabion Wall Geometry used in UTEXAS4 for the Global Stability Analysis

Three different stability analyses were performed for the retaining walls; a global stability analysis, sliding stability analysis, and overturning moment stability analysis. The factor of safety against global failure (under dry conditions) was determined for a circular failure surface as illustrated in Figure 8.34. The factor of safety for the traditional gabion wall was 1.52 (see Figure 8.35), which reduced to 1.45 for the tire bale retaining wall (Figure 8.36).

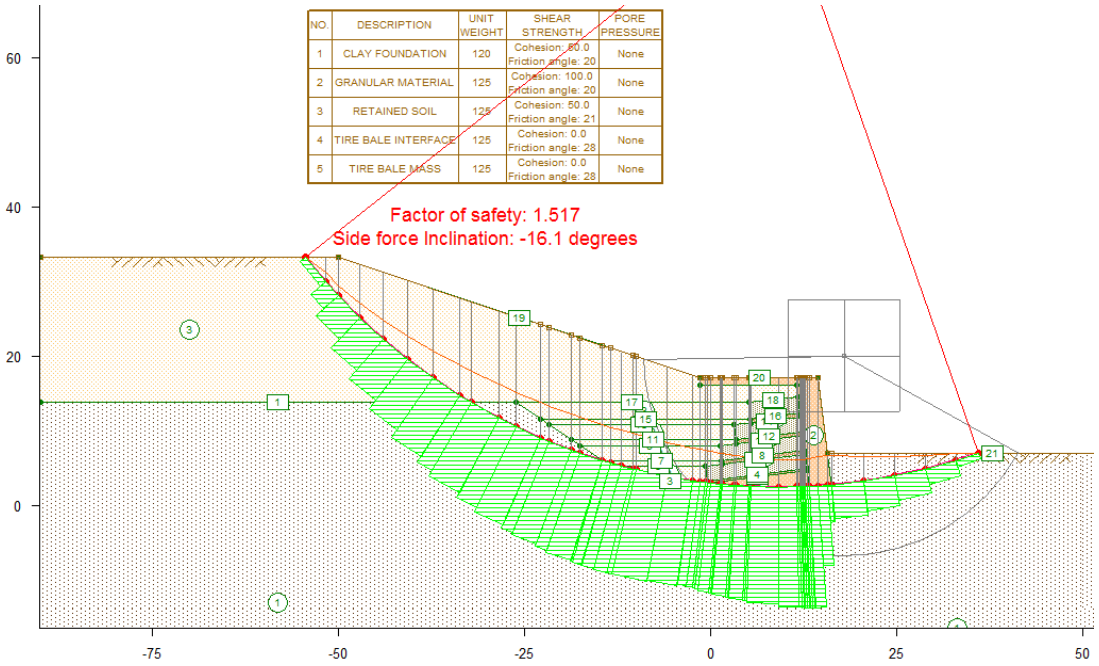

Figure 8.35: Global Stability Analysis for the Traditional Gravel Gabion Retaining Wall for Dry Conditions

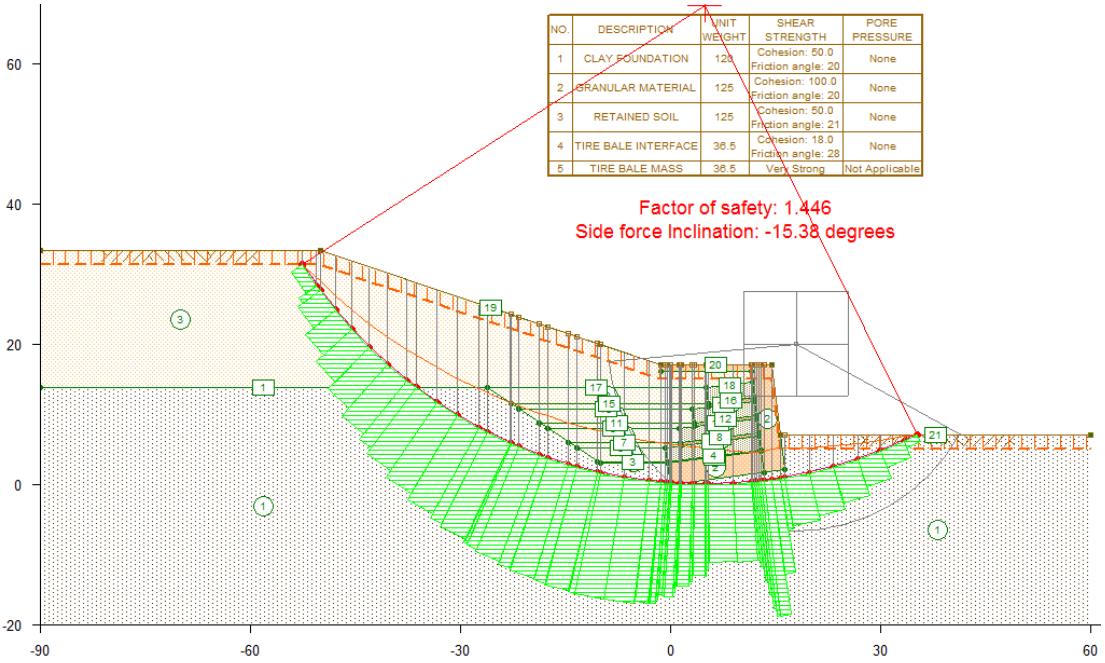

Figure 8.36: Global Stability Analysis for the Tire Bale Gabion Retaining Wall for Dry Conditions

The factor of safety against sliding failure was determined by placing a non-circular failure surface at the base of the retaining wall. The decrease in the weight of the wall decreased the factor of safety from 1.5 for the traditional gabion wall (Figure 8.37) to 1.4 for the tire bale

wall (Figure 8.38). The sliding stability of the wall was increased by tilting the tire bale wall by approximately 7°, which increased the stability above the minimum factor of safety of 1.3.

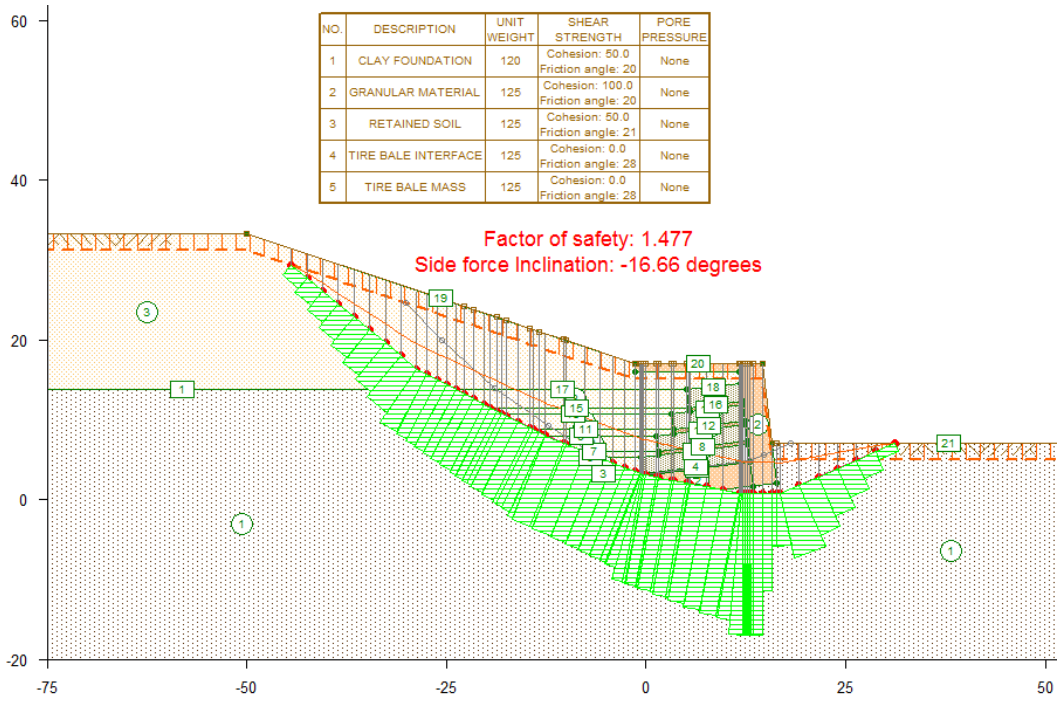

Figure 8.37: Sliding Stability Analysis for the Traditional Gravel Gabion Retaining Wall for Dry Conditions

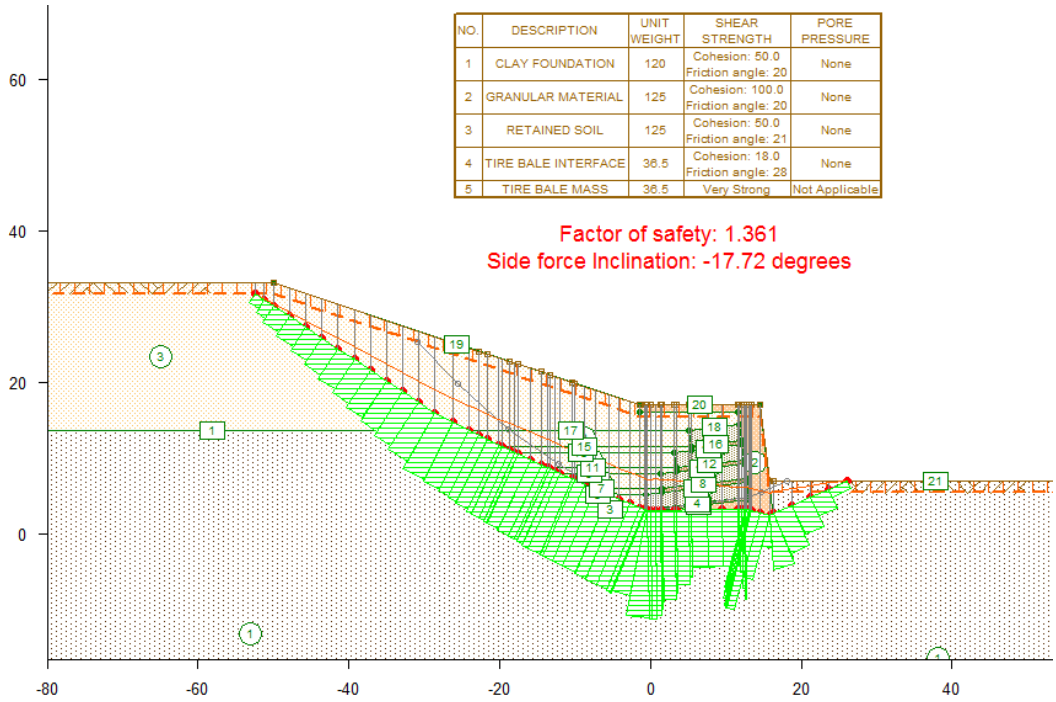

Figure 8.38: Sliding Stability Analysis for the Tire Bale Gabion Retaining Wall for Dry Conditions

A separate analysis of the overturning moment of the gabion wall was also conducted by taking moments about the bottom front corner of the wall (Figure 8.39). The factor of safety against overturning is defined as the summation of the moments due to the weight of the wall divided by the moments due to the pressure applied by the retained soil:

$$\text{Factor of Safety} = \frac{\Sigma \text{Resisting Moments}}{\Sigma \text{Overturning Moments}} \tag{8.1}$$

Pressures applied by the retained soil were predicted using Rankine Active Earth Pressures:

$$\text{Rankine Active Earth Pressure Coefficient} = K_A = \cos\alpha \frac{\cos\alpha - \sqrt{\cos^2\alpha - \cos^2\phi}}{\cos\alpha + \sqrt{\cos^2\alpha - \cos^2\phi}}$$

$$\text{Active Force} = P_A = \frac{1}{2}\gamma H^2 K_A - 2cH\sqrt{K_A} \tag{8.2}$$

Decreasing the weight of the structure by using tire bales also decreases the factor of safety against overturning of the structure from 3.7 (for typical rock fill) to 2.9 (for the tire bales). Although there is a significant loss in the factor of safety, the stability of the tire bale structures is still acceptable.

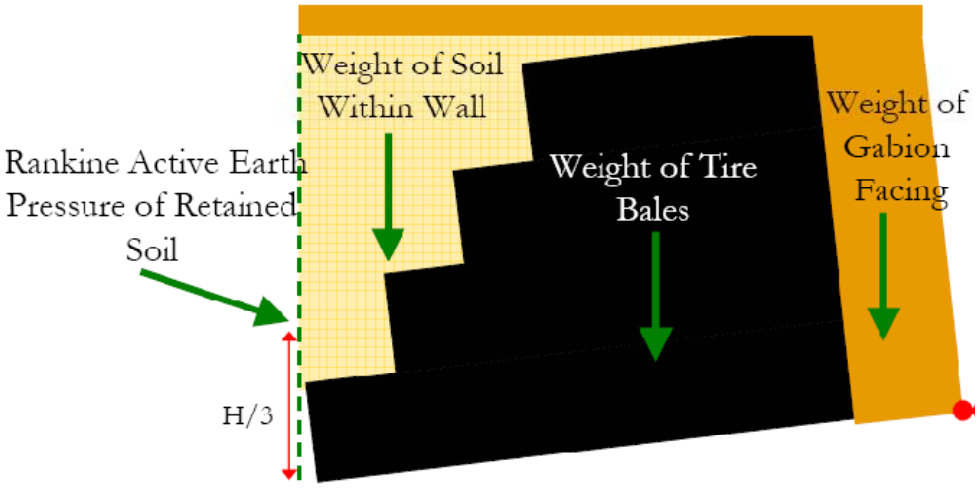

Figure 8.39: Illustration of Overturning Moments for the Tire Bale Gabion Retaining Wall

Summary

The cost and analytical analyses of the tire bale gabion wall provided evidence that tire bales can be used as retaining wall fill. However, the design of the wall must take into account the significant loss in weight of the wall due to removal of the heavy gravel material and replacement with the much lighter tires. The NMDOT has successfully designed, constructed and maintained a number of tire bale retaining walls around the state that have performed satisfactory during both dry and wet conditions. For the case history analyzed in this chapter, there was only

a slight loss in stability, yet a significant decrease in the actual cost of the retaining wall due to the replacement of the expensive gravel fill and reduction in labor (Table 8.17).

Table 8.17: Summary of Tire Bale and Gravel Gabion Retaining Wall Cost Benefit and Analytical Studies

Construction Method	Cost (per linear yard)	Factor of Safety		
		Global	Sliding	Overturning
Tradtional Gabion Wall	$3,143.22	1.5	1.47	3.5
Tire Bale Filled Gabion Wall	$496.92	1.46	1.36	2.7

The savings associated with transporting and storing tire bales is taken into account in the total cost in Table 8.18. In this case, the savings of baling tires at the site is higher than the total cost of materials and construction of the retaining wall. Therefore, the use of tire bales saves more money than is actually spent.

Table 8.18: Costs of the Tire Bale and Gravel Gabion Retaining Walls Considering the Savings Due to Tire Baling

Construction Method	Cost (per yard)	Cost Savings (per yard)	"Total" Cost to TxDOT
Tradtional Gabion Wall	$3,143.22	0	$3,143.22
Tire Bale Filled Gabion Wall	$496.92	$653.40	-$156.48

It should again be noted that the costs presented in Table 8.20 do not include the actual transportation, which would need to be determined based on the location of the tire bales relative to the construction site.

Case History 5: Tire Bale Storage and Use as Random Fill

In the previous case history analyses, the use of tire bales in specific highway construction projects has been discussed using both the cost and mechanical benefits. However, in many cases the use of tire bales may be beneficial just due to the volume reduction of baling at the site and the subsequent ease of storage and transportation of the bales. An example of the benefits of tire baling would be the “production” of scrap tires by the TxDOT Districts. In general, any TxDOT facility can only store a maximum of five hundred (500) whole tires at any time. Figure 8.40 shows an example of the tire storage at the Austin District TxDOT facility.

Figure 8.40: Photograph of the Tire Storage Area at the Austin District TxDOT Facilities

Baling the tires reduces the volume of the stockpile by a factor of approximately 7.4. Four hundred (400) tires, in bale form, are shown in Figure 8.41. The volume reduction and ease of transportation can instantly be observed. The cost of handling the tires significantly reduces when baled; instead of a crew of workers taking the time to remove the whole tires, only a forklift is required.

Figure 8.41: Photograph of Four Tire Bales at the TxDOT Facilities

8.4 Summary

The cost benefit analysis and analytical study presented in this chapter provides evidence that tire bales can be effectively implemented in numerous highway structures. The mechanical benefits to using tire bales include:

- Reduction in weight of the structures, beneficial when constructing on a soft soil but may require additional design considerations for gravity retaining walls with tire bales,
- Provides and increases drainage from the structure,

- Increases in the stability of the structure by adding a reinforcement layer, or stronger material layer in the form of discrete building blocks, and
- Increase in the stability of the structure by adding layers of material that force the failure plane to take certain geometries that result in higher factors of safety.

However, it was also demonstrated that the presence of tire bale reinforcement layers increased the compression and flexibility of the structure, indicating that the use of bales be limited to structures that can withstand these displacements without reaching a critical state, or failure. In addition, the submergence of tire bales was also found to be a critical aspect, indicating that drainage of the bales should always be provided.

The cost benefits to using tire bales, as opposed to soil or tire shred reinforced soil, are:

- The cost to construct and transport tire bales is significantly less than that of whole tires, tire scraps, and tire shreds. Baling the tires at the site results in an instant cost saving of $0.83 per tire as compared to moving whole tires.
- Tire bales do not require any form of compaction or special equipment to be placed into the structure. A fork lift, front end loader, or clamshell bucket can be used to properly place the tire bales into the structures. This reduces the cost of the structure by at least approximately $22.00 per cubic yard.
- Soil structures require moisture conditioning, density control, mixing, blading, or other methods required to prepare the soil embankment; tire bales just require that they are dry before placement.
- Soil structures must accommodate for shrink/swell of the soils.
- Drainage from the soil must be constructed into the slope, increasing the cost of the structure; drainage from tire bales only requires that a pipe is placed so that water can be removed.

The time to make the tire bales, location of the bales relative to the structure, and the number of tire bales available are the main limitations of using tire bales in soil structures. In many cases, a significant number of bales must be present or pre-constructed near the site so that they can be placed within the structure in a timely, and therefore cost effective, manner. Transporting the tire bales, although approximately ten times cheaper than moving whole tires, can cancel out the cost benefit of using tire bales in a structure located away from the bales. It must be decided on a case-by-case basis whether or not tire bales would be a feasible alternative based on the location and number of bales relative to the site. Tire bales may be more suitable for smaller remediation projects rather than larger projects requiring a large amount of material. A review of the case histories indicates that the use of tire bales in highway structures has been controlled thus far by the presence of tires near the site and the need to quickly dispose of them. Baling of the tires usually occurs before the construction of the structure and not during construction, so that the bales just need to be transported to the site and placed into the structure.

Chapter 9. Field Monitoring of IH 30 Tire Bale Embankments

A field data collection program has been ongoing for a tire bale embankment constructed along IH 30 in Ft. Worth, Texas. The slope, which is located along IH 30, near mile marker 18, in Ft. Worth, TX, experienced recurring slope failures, which were attributed to heavy precipitation at the site. The Texas Department of Transportation (TxDOT) used a non-traditional method to remediate the failed slope in the form of tire bales as reinforcement layers and as a replacement fill material (Prikryl et al. 2005).

9.1 Description of the IH 30 Tire Bale Embankments

The initial (Phase One) slope remediation consisted of three single layers of tire bales used as reinforcement layers with six to eight inches of soil fill placed between the bale layers. The fill soil was also placed over the entire surface of the slope to allow for vegetation and UV protection for the bales. The slope was completed in 2002. However, a drainage layer was not installed during construction and infiltration of water into the tire bale layers eventually led to a failure in the adjacent slope (LaRocque 2005). Water from the tire bales drained from the bale layers and downhill into the adjacent slope, causing another slope failure.

To repair the second slope failure (Phase Two), TxDOT constructed a second tire bale slope adjacent to the previously constructed tire bale reinforced slope. Construction was completed in August 2005. Since infiltration was a major problem with the first slope, a drainage layer, consisting of a gravel layer underlain by a geotextile, was placed beneath the tire bale layers in the new slope (Figure 9.1). A drain outlet was installed between the two tire bale slope sections perpendicular to the slope to allow drainage out of the slopes. The tire bales were placed in direct contact with each other instead of covering each tire bale layer with a layer of soil (Figure 9.2). The construction of the Phase Two slope included placement of two inclinometer tubes to measure movements within the slope (Figures 9.3 and 9.4). In addition, survey stakes were placed along the face of the slope for surveying purposes to observe movements in the embankment surface (Figure 9.5).

Figure 9.1: Gravel Drainage Layer and Pipe Drain for the Phase Two Remediation

Figure 9.2: Tire Bale Mass for Phase Two Remediation (No Soil Infill between Layers)

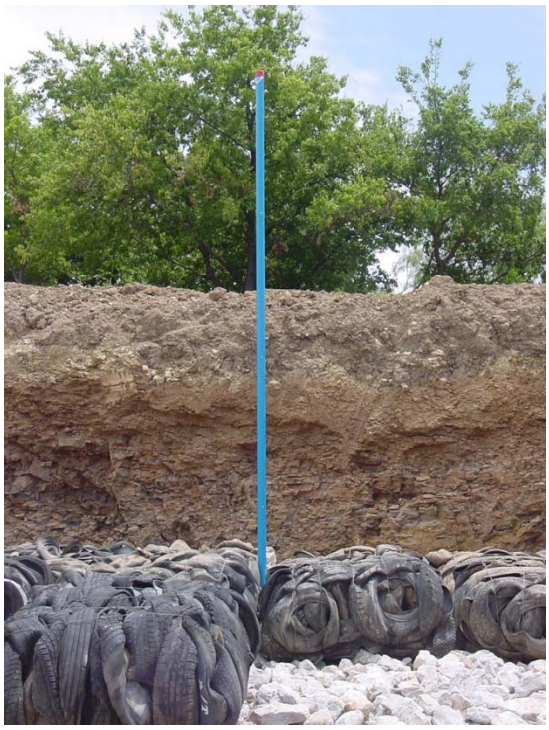

Figure 9.3: Inclinometer Tube Installed at the Base of the Phase Two Tire Bale Slope

Figure 9.4: Tire Bale Components, Including the Two Inclinometers, for Phase Two Remediation

Figure 9.5: Location of Stakes Placed Along Slope Surface for Surveying

9.2 Slope Data Collection Program

The Center for Transportation Research (CTR) conducted inclinometer readings for the period of December 2005 to January 2008 (Figure 9.6). Readings were taken once a month, or after significant rain events, to determine if movement of the slope had occurred. Analysis of surveying measurements was conducted by CTR as supplement to the lab characterization of the tire bales. CTR also assessed the flow of water from the drain outlet at the site. The surveying was performed by TxDOT personnel and provided to CTR. Overall, eleven (11) site visits were made since the beginning of the project.

Inclinometer readings were taken at four different orientations within the inclinometer tubes. Initial readings were taken at the location labeled A_0, assumed to be movements perpendicular to the slope face. The inclinometer was then rotated 90° and the B_0 reading was taken. Again, the inclinometer was rotated 90° and the A_{180} was recorded and similarly, the B_{180} reading was taken.

Figure 9.6: Taking Inclinometer Readings

9.3 Weather Records

The recorded precipitation for the Ft. Worth, TX area, which was used to compare with movements of the embankment, is provided in Figure 9.7. The weather records were obtained from the Meacham Airport weather station in Ft. Worth, the closest station to the tire-bale slope site. During the time period from December 2005 to August 2006, the largest recorded rainfall in Ft. Worth was 3.06 inches on March 19, 2006. The average precipitation for the Ft. Worth area is about 36 inches. From August 2005, when construction of embankment was completed, to August 2006, recorded precipitation for the area was about 20 inches, well below average values.

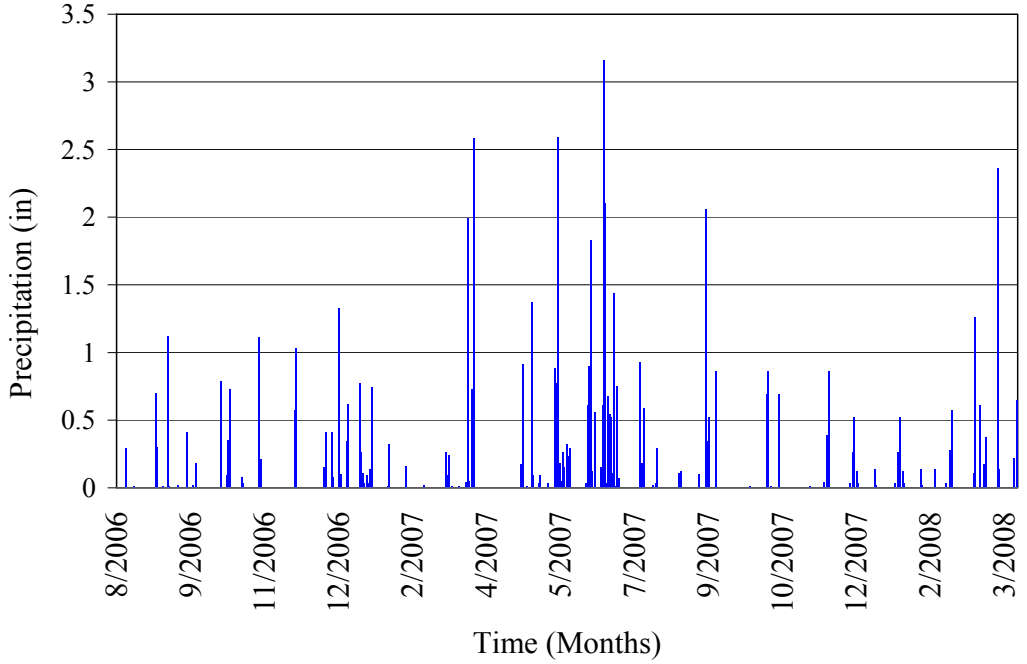

Figure 9.7: Precipitation Measured for Ft. Worth, TX Beginning December 1, 2005

9.4 Inclinometer Readings

The first set of inclinometer readings were taken in late December 2005. There were no significant rain events between completion of construction in August 2005 and December 2005, when the first inclinometer readings were taken by CTR. For the purposes of the evaluation presented in this report, the December measurements were used as the initial values to which all future measurements were compared. Inclinometer readings were taken after each significant rainfall, with two exceptions. Significant rainfall occurred in late February and a trip was made to the site to take readings but the inclinometer cable was damaged and could not be repaired on-site. However, a survey team recorded measurements at the site to capture any surface movements after the rain event a few days later. A new inclinometer cable was purchased, but did not arrive until early April. An inclinometer was borrowed from UT-Arlington to take readings on March 21. Heavy rainfall was recorded on June 17; however, a site visit did not occur until mid-July due to the need to conduct administrative arrangements.

Typically, inclinometer data is presented for the direction perpendicular to the slope, which is typically reported as the "A" readings. Positive values of displacement imply down slope movement, while negative values imply upslope movements. Inclinometers were also used to measure cross slope movements, or movements parallel to the slope face reported as the "B" readings. Positive values imply displacements to the left. Inclinometer tubes are typically installed so that the A grooves, and therefore the A measurements, are oriented perpendicular to the slope face, such as for the West Hole illustrated in Figure 8 b (north is the direction of down slope movements). However, for the East Hole, the inclinometer was installed to where the grooves are rotated about 45° from a typical installation (Figure 9.8 a). To get a clear understanding of the behavior of the slope at the East location, both A and B data were used to calculate the approximately down slope movement, as shown in Equation 9.1. The A and B inclinometer measurements for the East and West stations along the tire-bale slope are shown in Figures 9.9 and 9.10, respectively.

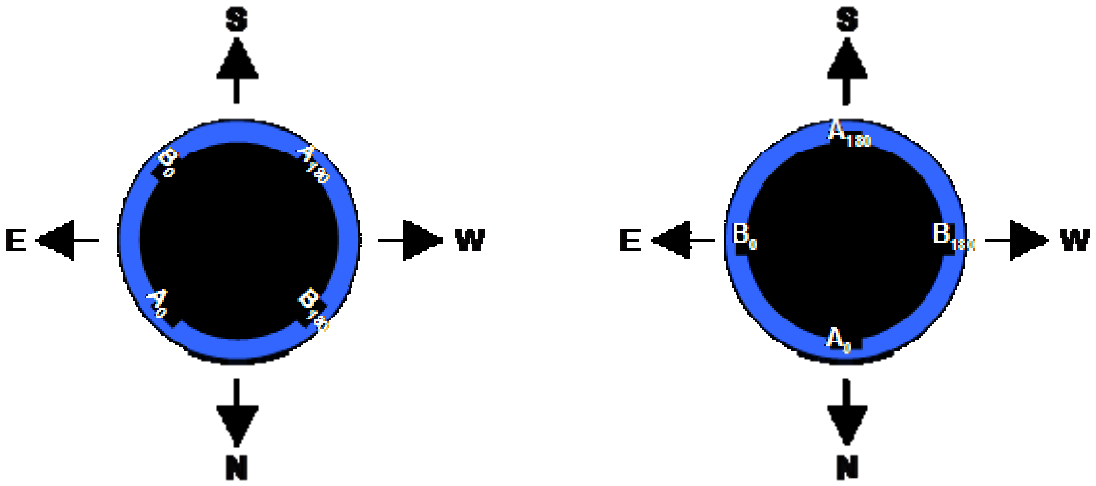

Figure 9.8: Orientation of the Inclinometer Tubes, a) East Hole and b) West Hole

$$\text{Down Slope Movements for East Hole} = A_{\text{Displacement}} \cdot \cos 45^{o} - B_{\text{Displacement}} \cos 45^{o} \quad (9.1)$$

The measured and calculated slope displacements, for the West and East holes respectively, were superimposed on a cross-section of the tire-bale slope to help illustrate the movements that occurred within the surficial soil layers and those within the tire bale mass (Figure 9.11). These figures will be used throughout the following discussions.

Very little movement along the slope was recorded until after a rainstorm on March 19, 2007, when the top of the East inclinometer tube moved down slope 8.7 mm and the West inclinometer down slope 16.75 mm (illustrated by the Mar 2007 readings shown in Figure 9.11). After the March readings, the measurements at the West tube indicated a progressive down slope (northeast) movement of the top 2 m of the inclinometer tube (the top 1 meter being above ground) until the final readings in January 2008. Readings at the East tube indicated a slight upslope movement of the slope during the same time period, maybe indicating some form of circular slope movement. The largest down slope displacement recorded for the East hole was 11.07 mm, which was measured in April 2007. The largest down slope displacement recorded for the West hole was 50.82 mm, measured in June 2007.

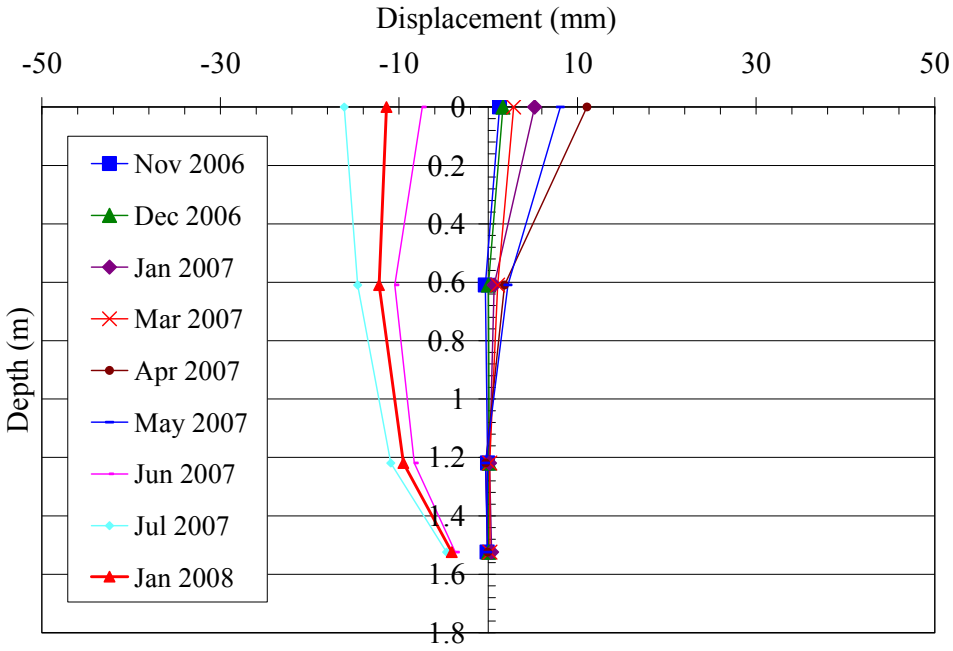

(a) "A" Direction Measurements

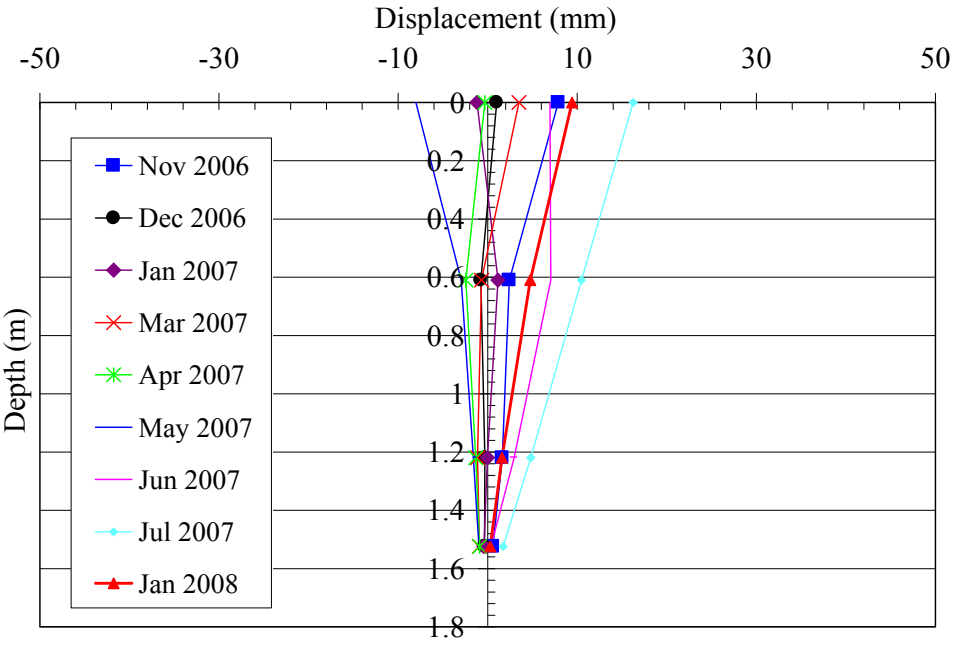

(b) "B" Direction Measurements

Figure 9.9: Inclinometer Readings for the East Hole; a) A readings and b) B readings

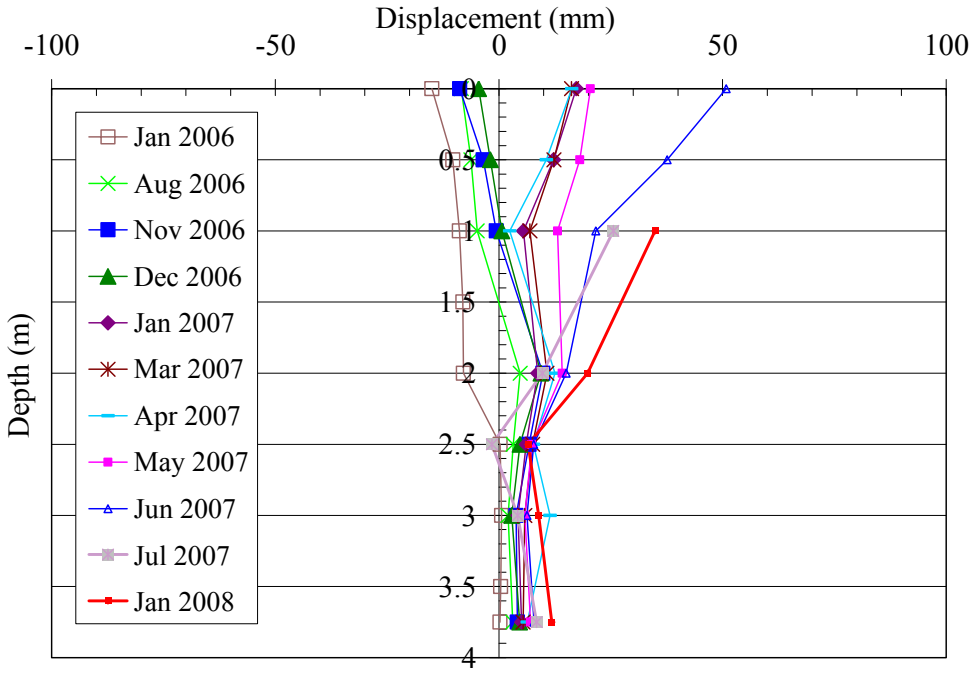

(a) A Measurements (Down Slope Movements)

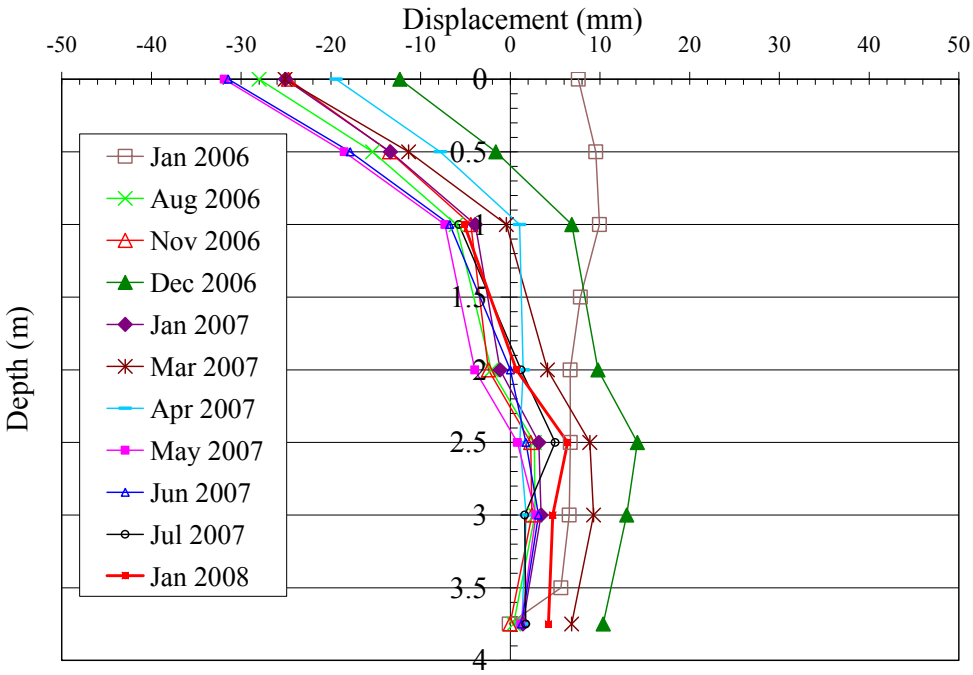

(b) B Measurements (Cross Slope Movements)

Figure 9.10: Inclinometer Readings for the West Hole; a) A readings and b) B readings

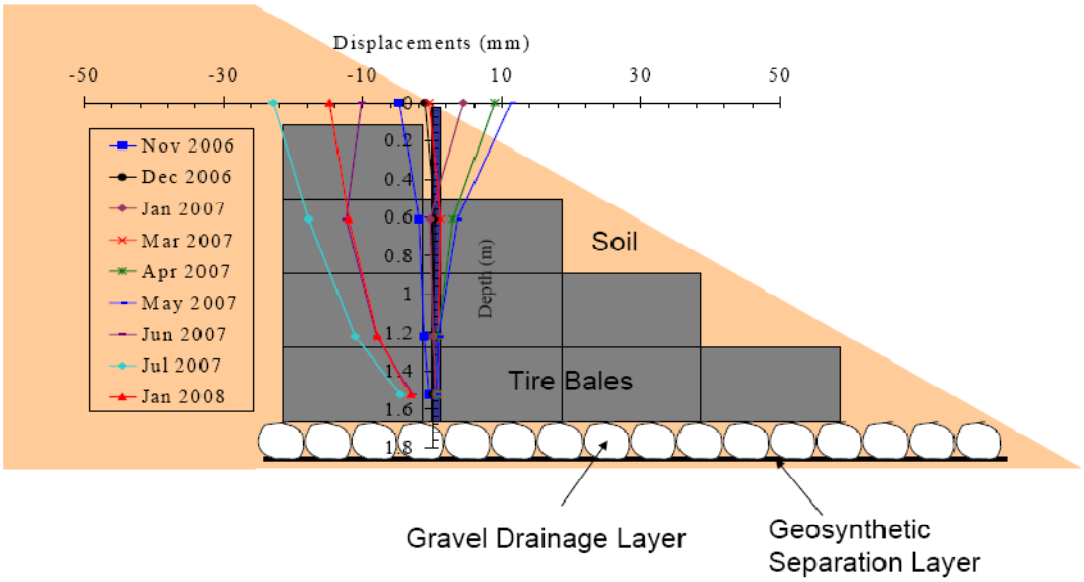

(a) Slope Movements Calculated for the East Hole

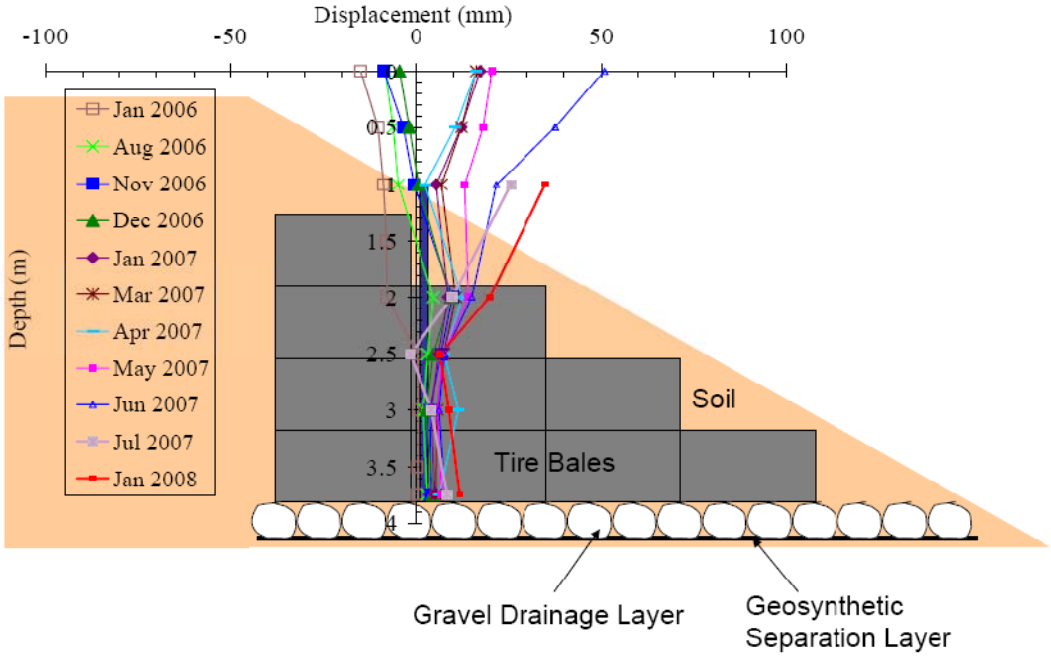

(b) Slope Movements Measured for the West Hole

Figure 9.11: Inclinometer A-readings from August 29, 2006 for a) East Hole and b) West Hole

The large upslope movements of the East hole, which were first observed in June 2007, correspond to a soil slump developing at the top of the tire bale slope (Figure 9.12). The depth of the soil slump was approximately 1.5 to 2 feet during the last visit to the site. Soil loss around the tire bale mass, dragging the inclinometer tube to the south (or upslope), may be the cause of the apparent up slope movements.

Figure 9.12: Soil Slump Observed at the Upper East Corner of the Tire Bale Slope

There is also evidence of oscillation in the inclinometer tube readings, and was further observed that the slope movements typically correspond with wet and dry periods. It was observed from the data in Figure 9.9 that the largest movement upslope corresponds with dry periods, but after significant precipitation, down slope movements were observed. The precipitation data plotted with the maximum inclinometer readings for the East Hole is shown in Figure 9.13, which provides evidence that down slope displacement increases after heavy rainfall and decreases, or even reverses, after drought periods.

Figure 9.14 shows the inclinometer data for the West Hole with the precipitation data. For the A readings (Figure 9.14 a), displacements increased in the upslope direction after large rain events, the opposite of the trend measured for the East hole. For the B readings (shown in Figure 9.14 b), there is a similar correlation between rainfall and movement parallel to the slope, indicating larger movements to the left after rain events.

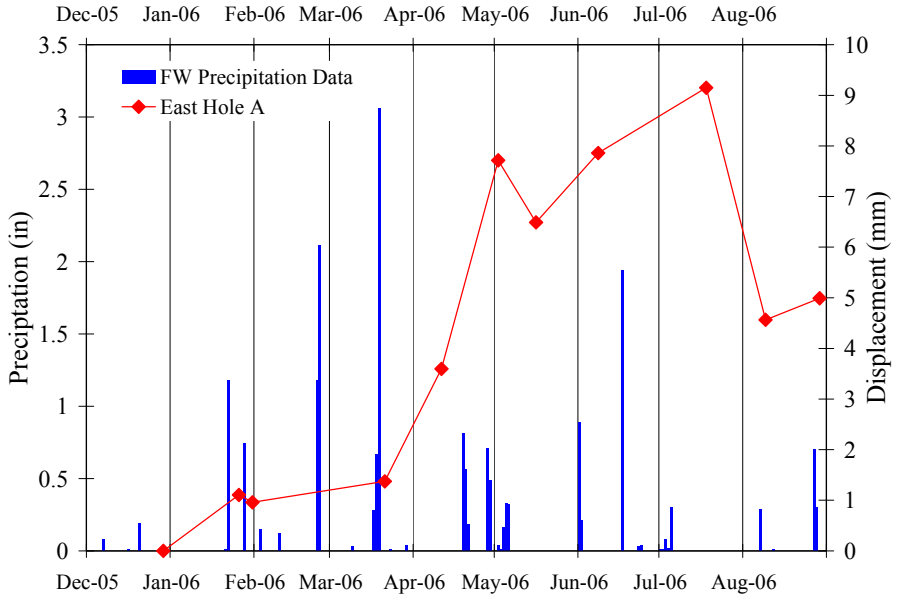

(a)

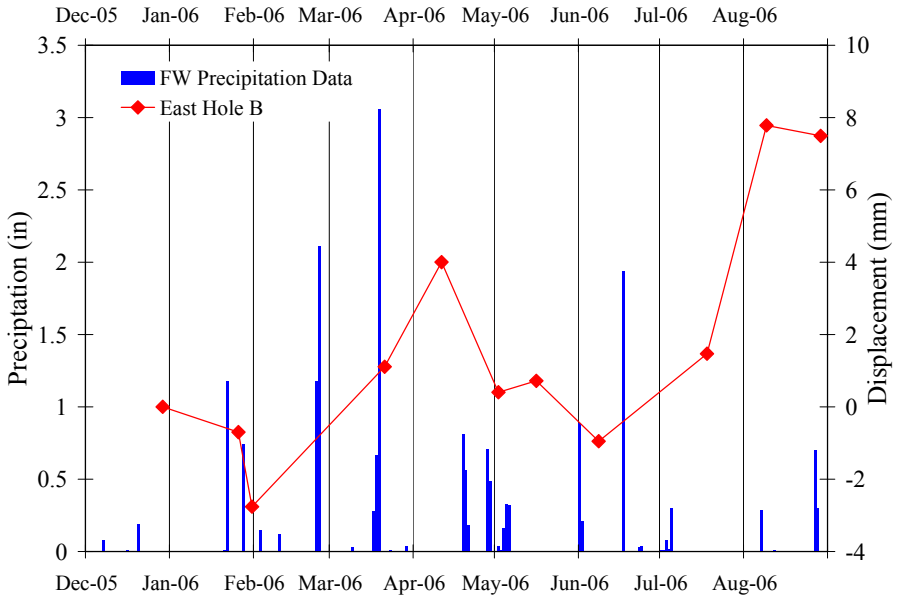

(b)

Figure 9.13: Precipitation Data and Inclinometer Readings for the East Hole: a) A Readings and b) B Readings

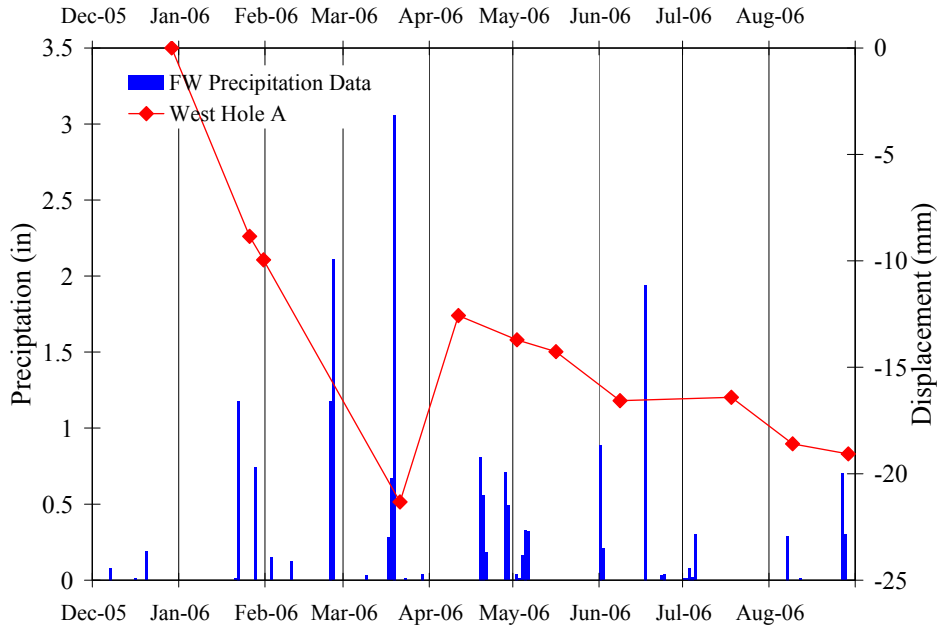

(a)

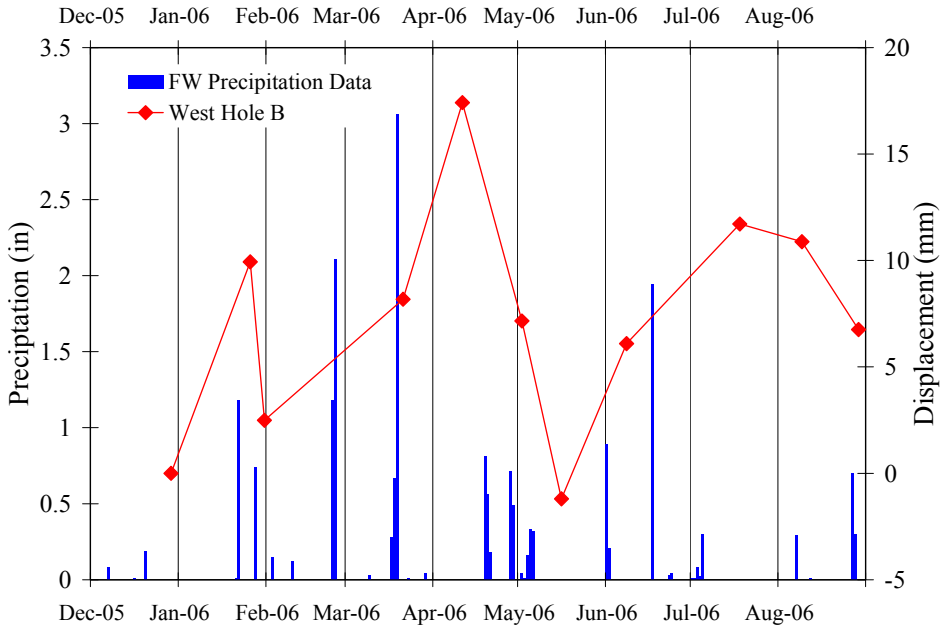

(b)

Figure 9.14: Precipitation Data and Inclinometer Readings for the West Hole a) A Readings and b) B Readings

The movement of the slope in relation to rainfall is shown in Figure 9.15 for the East hole. Three inclinometer measurements are plotted to illustrate the slope movements after a heavy rainfall. January 26 measurement was the first measurement taken after the initial readings; significant rainfall had not occurred at the site since installation in August 2005. Even

so, slight displacements were observed at this time. Readings on March 21 were taken two days after a heavy rainfall event. There was a relatively large movement of the slope in the northeast direction, or down slope. No significant rainfall events occurred between March 21 and the readings taken on August 9, indicating up slope movements during dry periods.

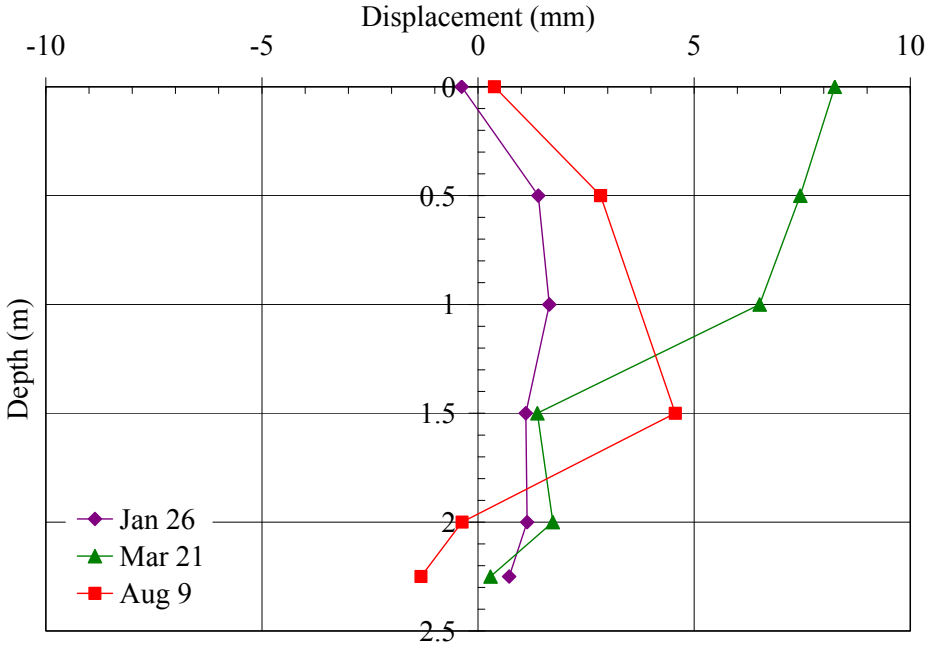

Figure 9.15: Inclinometer Readings for the East Hole "A" Direction for a Dry-Wet-Dry Cycle

Figure 9.16 shows similar measurements for the West Hole for the same time periods. There is movement of the inclinometer tube upslope after the heavy rainfall event but as the slope dries out, the base of the tube is beginning to slide down slope. This pattern is typical of slopes undergoing a rotational failure. However, it should be noted that the displacements are relatively small and the inclinometer tubes were not grouted during installation so this movement might be due to the tube being able to move around in the tire-bale reinforcement.

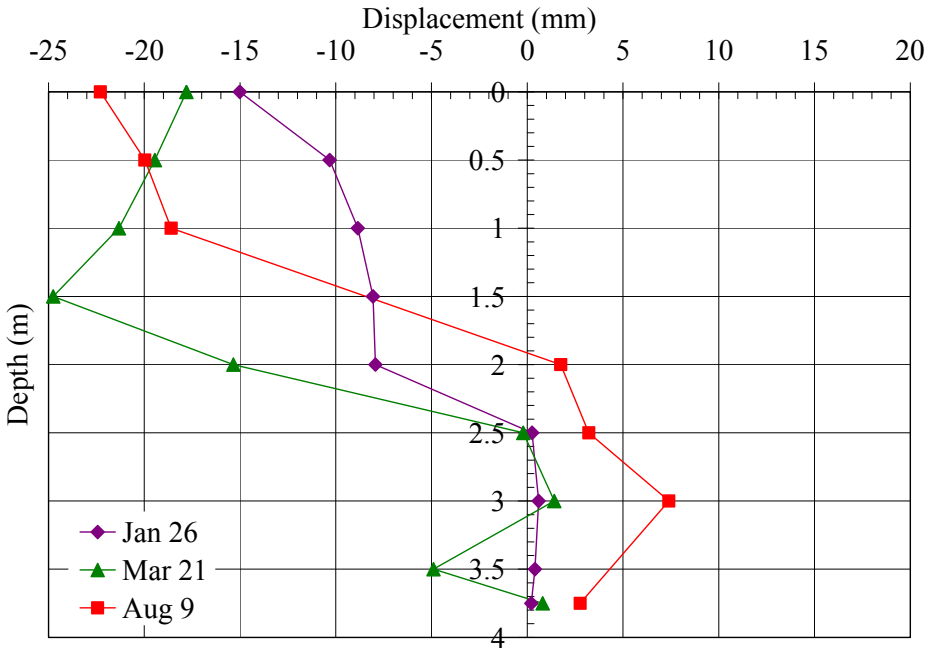

Figure 9.16: Inclinometer Readings for the West Hole "A" Direction for a Dry-Wet-Dry Cycle

9.5 Survey Measurements

Survey measurements were taken by TxDOT on six occasions to help measure any form of surficial slope failure along the soil-tire bale interface. A three-dimensional surface plot of the initial and final slope survey measurements are shown in Figure 9.17. The first survey measurements were taken in August 2005 and the final set of readings taken in May 2006. There were no significant surficial movements measured that would indicate a surficial slope failure. Measurements indicate a settlement of the surficial soils at the top of the slope, but no significant displacements at the base. Additional observations of the slope face did provide evidence of some soil loss at the top of the slope behind the East hole (Figure 9.12), but no observations of a global slope failure were found.

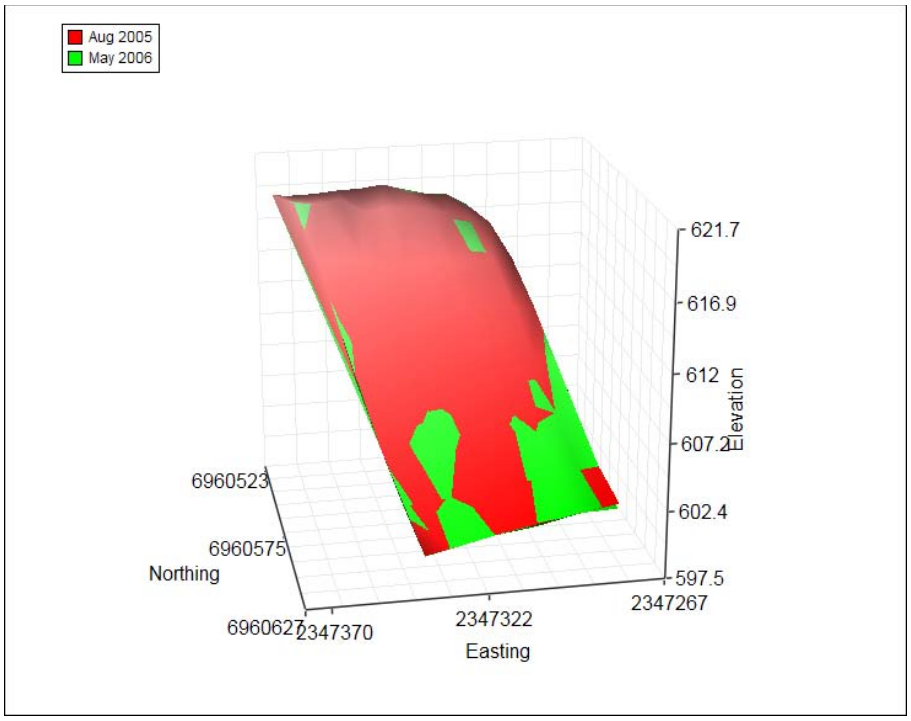

(a)

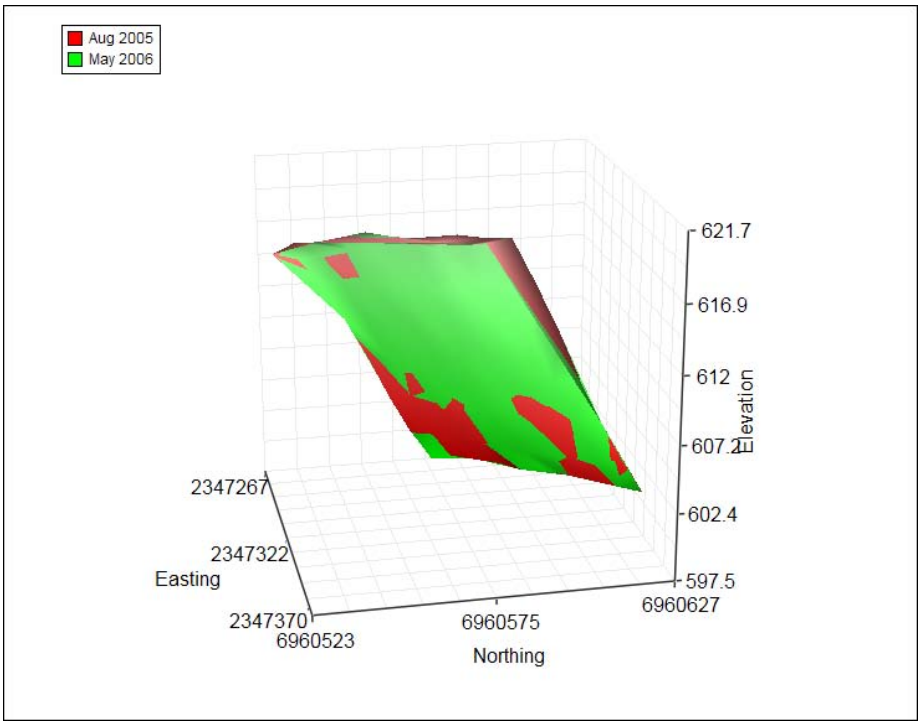

(b)

Figure 9.17: Survey Measurements as 3D Surface Plot: a) View in Front of Slope, and b) View behind Slope

9.6 Assessment of Flow

Water was not flowing from the drain during the first four site visits. The ground was moist near the drain but actual flow was not observed. During the March 21 site visit, which was after the significant rain event on March 19, water was flowing out of the drain so flow measurements were taken. The water flow rate was determined to be 60 mL/s ($6x10^{-5}$ m^3/s). Water flow has not been observed at the site since March 21. During the August 9 site visit, the soil near the drain appeared dry but grass was growing out of the drain. During the August 29 visit, there was about an inch of standing water in the drain but no flow was observed; it had rained an inch over the previous two days. It is recommended that the drain and the area around the drain be kept as clean as possible to facilitate drainage.

9.7 Summary

The survey measurements do not indicate substantial slope surface movement up to May 2006. The installed drainage system works well after heavy rain. However, the drain outlet should be properly maintained to ensure complete drainage. The largest recorded displacement in either inclinometer was no more than 50.82 mm. This indicates that the displacements occurring in the tire-bale reinforced slope one year after installation are not significant. However, it is recommended that monitoring of the slope should be continued for several reasons: 1) heavy rainfall can induce large movement within the slope, 2) there are possible indications of a potential slope failure, and 3) this is a new method of slope reinforcement and should be studied in the long term to validate this method as a feasible solution to the prevention of slope failures.

Chapter 10. Conclusions

The testing program presented throughout the document illustrates both the mechanical properties and financial aspects of using tire bales for highway projects. The conclusions from each chapter are applicable to both the administrative decision to use tire bales, as well as the design and construction of the structures themselves. Brief outlines of the conclusions stated throughout the document are presented in this chapter.

- The dry weight of the tire bales was found to range from 1880 to 2030 lbs. Submergence of the bales reduced the weights to about 230 lbs, a reduction in weight of a factor of approximately 10. Although the weight of the tire bales was considered acceptable and within the range reported in the literature, the number of tires in each of the bales was less than the specified 100 tires, averaging around 83 tires per bale.
- Three values of the volume were defined and measured: the average volume (59.2 ft^3), the maximum enclosing cuboid (76.8 ft^3) and the actual tire bale volume (45 ft^3). The unit weight defined using the average volume was found to be slight higher than values reported in the literature (57 ft^3), but within the variability (±5 ft^3) reported from the research programs.
- In contrast to previous research programs, the unit weight of the tire bale mass was redefined using the actual tire bale volume (instead of the average volume) and coupled with an equation presented by Winter et al. (2006) to determine the equivalent unit weight of the tire bale structure. This method allows for the designer to take into account soil fill, submergence, and numerous other design considerations when determining the weight of the structure.
- The permeability of the tire bale mass was found to range from 0.5 to 2.0 cm/sec. It must be noted that for tire bale only structures, the permeability is further increased by the void network within the bale mass.
- A large scale direct shear testing program, utilizing a three bale pyramid structure, was adapted from LaRocque (2005) to determine the interface strength of a tire bale mass for dry, wet, anisotropic and soil infill interfaces.
- The results from the dry tire bale only interface testing matched values provided by LaRocque (2005), indicating limited variability between different bales and from different testing setups. Both data sets were combined and modeled with a linear failure envelope with cohesion of 20 psf and friction angle of 36^o.
- The presence of water along the interface decreased the shearing resistance of the tire bale structure. The strength parameters of the partially saturated interface (wetted after initial placement of the bales) decreased to a cohesion of 13 psf and a friction angle of 27^o, an approximate strength reduction of 25%. The strength parameters of the totally saturated interface (wetted before placement of the bales) reduced to a cohesion of 0 psf and a friction angle of 21^o.
- A series of anisotropic tire bale only interfaces was also conducted to determine the influence of bale orientation on strength. The friction angle parameters for the dry and partially wetted interfaces were similar to those of the traditional orientation (friction

angles of 36° and 27°, respectively), however the cohesion values for both anisotropic interfaces reduced to 0 psf.

- The large scale direct shear testing setup was further altered so that a tire bale-soil interface could be constructed and tested. The results from the tire bale testing was compared with soil strength determined from UU direct shear testing of the soil, and provided evidence that the tire bale-soil interface strength is weaker then the soil only strength. This reduction in strength was found to be caused by the assumption of the stresses acting along the tire bale footprint area, and that the actual contact area between the tire bale and soil was less than the assumed footprint area and changed with applied normal load. The results from this testing program indicate that for sands, the friction angle of the tire bale-sand interface can be estimated with a small cohesion (15 psf) and a friction angle of 80% of the sand strength. For the tire bale-clay interface, the strength can be estimated with a significantly reduced friction angle (20 psf) and the friction angle of the clay determined from UU direct shear testing.
- Results from the large scale direct shear testing setup provided evidence that the tire bale interfaces (tire bale only, anisotropic and soil infill) do not exhibit a post peak strength loss during deformation.
- A compression testing setup, similar to that used for the direct shear tests, was also developed and used to measure the deformations of a tire bale structure due to normal compressive loading. Results from both this testing program, Zornberg et al. (2005), and LaRocque (2005) provide evidence of a significant influence of using one tire bale or a tire bale structure to determine the stiffness of the tire bale mass. For the testing programs in which a three tire bale pyramid structure was used, the stiffness due to compressive loading was much less than that of a single bale under compressive loading.
- The equivalent tire bale mass was defined so that the effects of the laboratory test setup could be removed from the compression of the tire bale structure. The non-linearity of the tire bale stiffness was taken into account by defining a series of secant moludi of over the range of applied normal loads. However, the minimally confined modulus of the equivalent tire bale mass was also approximated with a average constant value, ranging from 14,000 to 17,000 psf, less than the value reported by LaRocque (2005) of 19,100 psf for the total tire bale structure.
- Long term conditions of the bales without wire breakage were also considered during the compression testing. Creep deformations due to sustained normal compressive loads were measured for up to one month of loading. A significant portion of the creep deformation occurred along the interfaces. The total creep deformation was modeled with a linear line when plotted against log-time. The slope of the curves, referred to as the creep index, ranged from 0.18 to 0.28, much higher than the values measured by LaRocque (2005).
- Before considering the effects of wire breakage on the bale behavior, a series of tests were conducted to non-destructively measure the tension in the baling wires. Tensions measured in the wires for the three bales used for the laboratory testing (Bales 6 through 8) provide evidence that the outer wires hold less tension than the three inner

wires. In addition, the breakage of one wire re-distributes the tensions into the surrounding wires.

- A series of rapid expansion tests conducted on Bales 1 through 3 indicate that there is not violent horizontal deformation of the bale after wire breakage. In fact, the bales did not exhibit any large deformation until the last two wires were cut. Total expansion of the bales ranged from 39 to 42 inches for the three bales and did not increase more than 6 inches a couple of hours after cutting. Limited data now exists that the expansion deformation of the bales does decrease with time after bale construction.
- A horizontal expansion pressure test setup was also developed and conducted to measure the expansion pressure of the bales and tensions in the baling wires during wire breakage. An expansion pressure of approximately 200 psf may be expected for a bale when all baling wires are cut. In addition, tensions measured from strain gauges placed on the baling wires indicate that there is a redistribution of tensions within the baling wires due to breakage of surrounding wires. The results from the strain gauges were also used to back calculate the initial tensions in the wires, which in general were similar to those measured with the tension meter except for a few exceptions, in which the tensions in the wires were higher than the range of the tension meter.
- An in-depth cost benefit analysis and analytical study was presented for the use of tire bales in highway structures. The most notable cost savings associated with using bales is the reduction in cost of transporting and storing tire bales due to the instant volume reduction of the tires that can be accomplished at the site of the scrap tire dump. The cost of transporting tires in whole form is approximately $1.25, while transporting a whole tire in bale form only costs $0.42. Other cost benefits to using tire bales in highway structures includes the reduction in cost to make bales ($0.013) as compared to producing tire shreds ($0.64), and the ease of using tire bales in construction as compared to the methods required to place tire shreds.
- The cost benefits of using tire bales in highway structures are illustrated using a series of case histories and construction alternatives commonly used for highway construction. In addition, each cost benefit analysis is coupled with an analytical study of the structure to illustrate the mechanical benefits of using tire bales. Both a limit equilibrium analysis and finite element code were used in the study. In general, the use of tire bales as drainage layers and reinforcement elements increased the stability of the structure. However, the low stiffness of the bales did increase the flexibility and deformations of the structures.
- Constant field monitoring of the IH 30 Phase Two slope remediation project has indicated a satisfactory performance of the tire bale reinforced and tire bale fill embankments during dry and wet periods. Deformations of the slope have been limited (less than 2 inches) and have occurred mainly in the compacted soil cover during wet/dry periods in the weather. Additional information has been provided by the New Mexico Department of Transportation that provides evidence of the satisfactory performance of tire bale retaining walls during dry and wet weather periods.

References

American Society of Testing and Materials. (2004). "Standard Test Method for Direct Shear of Soils Under Consolidated Drained Conditions," *ASTM D3080-04.* West Conshohocken, Pennsylvania.

American Society of Testing and Materials. (2005). "Standard Test Methods for Liquid Limit, Plastic Limit, and Plasticity Index of Soils," *ASTM D4318.* West Conshohocken, Pennsylvania.

American Society of Testing and Materials. (2006). "Standard Practice for Classification of Soils for Engineering Purposes (Unified Soil Classification System)," *ASTM D2487.* West Conshohocken, Pennsylvania.

American Society of Testing and Materials. (2007). "Standard Test Methods for Laboratory Compaction Characteristics of Soil Using Standard Effort," *ASTM D698*. West Conshohocken, Pennsylvania.

American Society of Testing and Materials. (2007). "Standard Test Method for Particle-Size Analysis of Soils," *ASTM D422-63.* West Conshohocken, Pennsylvania.

Baxley, L. (2006) Personal communication to the Authors

Chen, L. (1996), *Laboratory Measurement of Thermal Conductivity of Tire Chips,* Masters Thesis, Department of Civil Engineering, University of Maine.

Collins, K. C., Jensen, A. C., and Matthews, M. C. (1995), "A Review of Waste Tyre Utilization in the Marine Environment," *Chemistry and Ecology,* Vol. 10, pp 205–216.

Collins, K. C., Jensen, A. C., Mallinson, J. J., Roenelle, V., and Smith, I. P. (2002), "Environmental Impact Assessment of a Scrap Tyre Artificial Reef," *ICES Journal of Marine Science,* Vol. 59.

Duggan, T. (2007) Personal communication to the Authors.

Eagle Equipment, LLC (2008), "Earthen Dam Project, Mountain Home, Arkansas." www.eagle-equipment.com/enviroblock.html

Fitzgerald, T. (2003), *Investigation of the Thermal Response of Tire Shred Fills,* Masters Thesis, Department of Civil Engineering, University of Colorado, Boulder.

Holtz, R. D., and Kovacs, W. D. (1981), *An Introduction to Geotechnical Engineering.* Prentice Hall, New Jersey.

Hudson, D. (2008) Personal communication to the Authors.

Humphrey, D.N. (1996), "Investigation of Exothermic Reaction in Tire Shred Fill Located on SR 100 in Ilwaco, Washington," Prepared for: Federal Highway Administration.

Humphrey, D. N. (2004), "Effectiveness of Design Guidelines for Use of Tire Derived Aggregate as Lightweight Embankment Fill," *Geotechnical Special Publication,* No. 127 pp 61–74.

Humphrey, D.N., Chen, L., and Eaton, R. (1997 a), "Laboratory and Field Measurement of the Thermal Conductivity of Tire Chips for Use as Subgrade Insulation," Prepared for the Transportation Research Board 76th Annual Meeting, Washington, D.C.

Humphrey, D.N. and Katz, L.E. (2001), "Field Study of Water Quality Effects of Tire Shreds Placed Below the Water Table," *Transportation Research Record,* No. 1714, pp. 18-24.

Humphrey, D. N., Katz, L. E. and Blumenthal, M. (1997 b), "Water Quality Effects of Tire Chip Fills Placed Above the Groundwater Table," *Testing Soil Mixed with Waste or Recycled Materials, ASTM STP 1275*, Mark A. Wasemiller, Keith B. Hoddinott, Eds, American Society for Testing and Materials.

Humphrey, D. N., and Manion, W. P. (1992), "Properties of Tire Chips for Lightweight Fill," *Geotechnical Special Publication,* Vol. 2, No. 30, pp 1344–1355.

Hylands, K. N. and Shulman, V. (2003), "Civil Engineering Applications of Tyres," *Viridis Report VR5*. Crowthorne: TRL Limited.

Jones, L. D. (2005), "Building with Tire Bales – Addressing Some Engineering Concerns." www.buildwithearth.com/tirebale4c.pdf.

Jones, K. (2008) Personal communication to the Authors.

LaRocque, C. J. (2005), *Mechanical Properties of Tire Bales*, Masters Thesis, Department of Civil, Architectural and Environmental Engineering, The University of Texas at Austin.

Moo-Young, H., Sellasie, K., Zeroka, D., and Sabnis, G. (2003), "Physical and Chemical Properties of Recycled Tire Shreds for Use in Construction," *Journal of Environmental Engineering,* Vol. 129, No. 10, pp 921 – 929.

Najjar, S. S., and Rauch, A. F. (2003), "Standard Laboratory Test Soils," *Geotechnical Engineering Laboratories Data Report,* The University of Texas at Austin.

Nightingale, D. E. and Green, W. P. (1997), "Unresolved Riddle: Tire Chips, Two Roadbeds and Spontaneous Reactions." *Testing Soil Mixed with Waste or Recycled Materials, ASTM STP 1275,* American Society of Testing and Materials.

Prikryl, W., Williammee, R. and Winter, M. G. (2005), "Slope Failure Repair Using Tyre Bales at Interstate Highway 20, Tarrant County, Texas, USA," *Quarterly Journal of Engineering Geology and Hydrogeology,* Vol. 38, pp. 377-386.

Raine, W. (2008) Personal communication to the Authors.

Rooke, L. (2001), "Building Dams from Baled Scrap Tires," *Biocycle,* Vol. 42, No. 9, September 2001, p 74.

Shalaby, A. and Khan, R. A. (2002), "Temperature Monitoring and Compressibility Measurement of a Tire Shred Embankment," *Transportation Research Record,* No. 1808.

Simm, J. D., Wallis, M. J. and Collins, K. (2004), "Sustainable Re-Use of Tyres in Port, Coastal, and River Engineering: Guidance for Planning, Implementation, and Maintenance," *HRW Report SR 669,* Wallingford: HR Wallingford.

Tandon, V., Velazco, D. A., Nazarian, S., and Picornell, M. (2007), "Performance Monitoring of Embankments Containing Tire Chips: Case Study," *Journal of Performance of Constructed Facilities,* Vol. 21, No. 3, pp. 207-214.

Texas Department of Transportation (2007), "Using Scrap Tire and Crump Rubber: 2007 Progress Report on Using Scrap Tires and Crumb Rubber in Texas Highway Construction Projects," *TCEQ Publication SFR-069/07.*

Wappet, H. L. (2004), *Investigation of the Thermal Response of a Tire Shred-Soil Embankment,* Masters Thesis, Department of Civil, Architectural and Environmental Engineering, The University of Texas at Austin.

Washington State Department of Transportation (2003), "Evaluation of the Use of Scrap Tires Transportation Related Applications in the State of Washington," *Report to the Legislature as Required by SHB 2308,* Olympia, Washington.

Winter, M., Watts, G.R., and Johnson, P.E. (2006), "Tyre Bales in Construction." *Published Project Report PPR080,* TRL Limited.

Wright, S. G. (2007), "UTEXAS4 A Computer Program for Slope Stability Calculations." Shinoak Software, Austin, Texas.

Zornberg, J. G., Cabral, A. R., and Viratjandr, C. (2004), "Behavior of Tire Shred-Sand Mixtures," *Canadian Geotechnical Journal,* Vol. 41, pp. 227-241.

Zornberg, J. G., Byler, B. R., and Knudsen, J. W. (2004), "Creep of Geotextiles Using Time-Temperature Superposition Methods," *Journal of Geotechnical and Geoenvironmental Engineering,* Vol. 130, No. 11, pp. 1158-1168.

Zornberg, J. G., Christopher, B. R., and LaRocque, C. J. (2004), "Application of Tire Bales in Transportation Projects," *Geotechnical Special Publication, n 127, Proc. of Sessions of the ASCE Civil Engineering Conference and Exposition,* Baltimore, MD, pp. 42 – 60.

Zornberg, J. G., Christopher, B. R., and Oosterbaan, M. D. (2005), *Tire Bales in Highway Applications: Feasibility and Properties Evaluation.* Colorado Department of Transportation, Report No. CDOT-DTD-R-2005-2, Denver, Colorado.

Appendix A: Development of Specifications for the Design and Construction of Tire Bale Embankments

Proper scrap tire disposal has been one of the most pressing issues faced by the waste management industry over the past few decades. Research efforts and industry initiatives have resulted in resourceful re-use applications for waste tires to mitigate the disposal of tires in landfills. These applications include the use of scrap tires as a fuel source in industrial plants, crumb rubber as an additive in asphalt products, and numerous other promising applications. However, current re-use levels are not sufficient to solve the scrap tire disposal problem completely. Presently, over 1 million tires are still disposed in landfills around Texas (TxDOT 2007). The highway construction industry, which uses significant volumes of construction materials, has been at the forefront for finding inventive ways to use scrap tires. Two new inventive uses of scrap tires in highway applications are as tire bales, constructed using whole scrap tires, and as tire chips and shreds.

In one 12 month period (2005), TxDOT constructed approximately 29 million cubic yards of embankment under Item 132. If one percent of the embankment material used was replaced with scrap tires, over 150,215 bales could potentially be used, which translates to over 15 million tires.

The following specifications are intended to promote the re-use of scrap tires, in the form of tire bales or as tire chips or shreds, in applications where their use has been proven beneficial. Tire bales may be used as embankment fill, retaining wall backfill, and in gabion baskets as a replacement for course gravel material. Scrap tire bales have also been successfully used as a fill material for stream bank erosion control. The following specifications generally address all of the above mentioned applications.

Special Provision to
Item 132

Embankment

132.1. Description. Furnish, place and compact materials for construction of roadways, embankments, levees, dikes, or any designated section of the roadway where additional material is required.

132.2. Material. Furnish approved material capable of forming a stable embankment from required excavation in the areas shown on the plans or from sources outside the right of way. Provide 1 or more of the following types as shown on the plans:

Type A. Granular material that is free from vegetation or other objectionable material and meets the requirements of Table 1.

Table A.1: Testing Requirements

Property	Test Method	Specification Limit
Liquid Limit	Tex-104-E	≤ 45
Plasticity Index (PI)	Tex-106-E	≤ 15
Bar Linear Shrinkage	Tex-107-E	≥ 2

The Linear Shrinkage test only needs to be performed as indicated in Tex-104-E.

Type B. Materials such as rock, loam, clay, or other approved materials.

Type C. Material meeting the specification requirements shown on the plans.

Type D. Material from required excavation areas shown on the plans.

Type E. Tire bales consisting of approximately 70 to 105 whole, scrap, passenger and light truck vehicle tires compressed into approximately a 4.5 ft. long by 5 ft. wide by 2.5 ft. high block. Use commercial tires when approved or as directed.

Provide scrap tires for the tire bales that are:

- free from dirt, vegetation, and organic material,
- free of contaminants such as oil, grease, gasoline, or diesel fuel,
- have not been part of or exposed to a fire,
- have no significant exposed reinforcing steel, and
- have no significant portions of the tire missing, such as tire halves, quarters, or shreds.

Additional requirements may be specified as shown on the plans or as directed. Properly dispose any scrap tires that do not meet the requirements for use in tire bales.

Place five (5), 7-gauge galvanized steel or stainless steel wires evenly around the width of the compressed tire bale as shown on the plans or as directed. Use other material as approved. Place additional synthetic straps around the bales if corrosive conditions of the surrounding materials do not meet Item 423.2.C.5 Electrochemical.

Provide equipment to properly lift and move tire bales without using the baling wires. Properly discard of bales that have been altered from their original manufactured condition.

Provide tire bales manufactured from a supplier that is authorized to process waste tires by the Texas Commission on Environmental Quality (TCEQ). Provide a written statement of compliance from the tire bale manufacturer.

Construct tire bales on the project site or transport bales from other sites. Each manufacturing site must be properly authorized by the TCEQ. Do not construct any tire bales under wet conditions. Keep all tire bale faces dry before and during placement into the embankment. Inspect each manufactured or delivered bale to ensure proper shape prior to placement. Properly discard bales that have been altered from their original manufactured condition.

Type F. Material consisting of 100 percent scrap tire chips/shreds obtained by chipping/shredding scrap passenger and commercial tires or a blend of scrap tire chips/shreds and conventional embankment fill material as described in Item 132.2.A or B. Inspect tire chips/shreds to ensure that they:

- are free of containments such as soil, grease, gasoline, diesel fuel, etc.,
- have not been subjected to a fire, and
- are free of organic matter such as wood, wood chips, and other fibrous organic matter.

Type F fills are divided into three classes:

Class I Fills. Embankment constructed using a blend of scrap tire chips/shreds and more than 30% (by weight of the blend) of a Type A or Type B material.

Class II Fills. Embankment constructed using a blend of tire chips/shreds with less than 30% (by weight of the blend) of a Type A or Type B material. Furnish tire chips/ shreds with a maximum of 50% of the tire chips passing the 1-1/2 inch sieve and a maximum of 5% passing the #4 sieve.

Class III Fills. Embankments constructed using 100% tire chips/shreds. Furnish tire chips/shreds that have less than 1% (by weight) of metal fragments which are not at least partially encased in rubber. Furnish tire chips/shreds with a maximum of 25% (by weight) passing the 1-1/2 inch sieve and a maximum of 1% (by weight) passing the #4 sieve.

Retaining wall backfill material must meet the requirements of the pertinent retaining wall Items.

132.3. Construction Methods. Meet the requirements of Item 7, "Legal Relations and Responsibilities to the Public," when off right of way sources are used. To allow for required testing, notify the Engineer before opening a material source. Complete preparation of the right of way, in accordance with Item 100, "Preparing Right of Way," for areas to receive embankment.

Backfill tree-stump holes or other minor excavations with approved material and tamp. Restore the ground surface, including any material disked loose or washed out, to its original slope.

Compact the ground surface by sprinkling in accordance with Item 204, "Sprinkling," and by rolling using equipment complying with Item 210, "Rolling," when directed.

Scarify and loosen the unpaved surface areas, except rock or surfaces receiving tire bales, to a depth of at least 6 in., unless otherwise shown on the plans. Bench slopes before placing material. Begin placement of material at the toe of slopes. Do not place trees, stumps, roots, vegetation, or other objectionable material in the embankment. Simultaneously recompact scarified material with the placed embankment material. Do not exceed the layer depth specified in Section 132.3.F, "Compaction Methods."

Construct embankments to the grade and sections shown on the plans. Construct the embankment in layers approximately parallel to the finished grade for the full width of the individual roadway cross sections, unless otherwise shown on the plans. Ensure that each section of the embankment conforms to the detailed sections or slopes. Maintain the finished section, density, and grade until the project is accepted.

A. Earth Embankments. Earth embankment is mainly composed of material other than rock. Construct embankments in successive layers, evenly distributing materials in lengths suited for sprinkling and rolling.

Obtain approval to incorporate rock and broken concrete produced by the construction project in the lower layers of the embankment. When the size of approved rock or broken concrete exceeds the layer thickness requirements in Section 132.3.F, "Compaction Methods," place the rock and concrete outside the limits of the completed roadbed. Cut and remove all exposed reinforcing steel from the broken concrete.

Move the material dumped in piles or windrows by blading or by similar methods and incorporate it into uniform layers. Featheredge or mix abutting layers of dissimilar material for at least 100 ft. to ensure there are no abrupt changes in the material. Break down clods or lumps of material and mix embankment until a uniform material is attained.

Apply water free of industrial wastes and other objectionable matter to achieve the uniform moisture content specified for compaction.

When ordinary compaction is specified, roll and sprinkle each embankment layer in accordance with Section 132.3.F.1, "Ordinary Compaction." When density control is specified, compact the layer to the required density in accordance with Section 132.3.F.2, "Density Control."

B. Rock Embankments. Rock embankment is mainly composed of rock. Construct rock embankments in successive layers for the full width of the roadway cross-section with a depth of 18 in. or less. Increase the layer depth for large rock sizes as approved. Do not exceed a depth of 2-1/2 ft. in any case. Fill voids created by the large stone matrix with smaller stones during the placement and filling operations.

Ensure the depth of the embankment layer is greater than the maximum dimension of any rock. Do not place rock greater than 2 ft. in its maximum dimension, unless otherwise approved. Construct the final layer with graded material so that the density and uniformity is in accordance with Section 132.3.F, "Compaction Methods." Break up exposed oversized material as approved.

When ordinary compaction is specified, roll and sprinkle each embankment layer in accordance with Section 132.3.F.1, "Ordinary Compaction." When density control is specified, compact each layer to the required density in accordance with Section 132.3.F.2, "Density Control." When directed, proof-roll each rock layer where density testing is not possible, in accordance with Item 216, "Proof Rolling," to ensure proper compaction.

C. Tire Bale Embankments. Tire bale embankment is composed entirely of scrap tires bales or of a combination of tires bales and soil. Limit the maximum height of any tire bale layer to twenty (20) feet unless otherwise shown on the plans or directed. Place tire bales to insure placement of a 24 inch soil, or other approved material, cover. Limit access of water and organic materials to each tire bale layer. Cover tire bales during storage and in the embankment to reduce exposure to water.

Place tire bales in horizontal layers parallel to the finished roadway surface, unless otherwise shown on the plans or as directed. Place tire bales so that the baling wires are parallel to the slope face, unless otherwise shown on the plans or as directed. Construct tire bale embankments to the grade and sections shown on the plans. Provide proper drainage from the base of the tire bale mass both during and after the completion of construction.

When compaction of soil is required between layers of tire bales, or around tire bales within each layer, test the soil using the color test for organic impurities in accordance with Test Method Tex-408-A. The results should show a color that is not darker than standard. Use a cohesionless, non-plastic, dry material (such as sand or manufactured stone) such that it is easily packed or vibrated between the bales when soil fill is required around individual bales within each layer. Use a similar material, or local material with PI less than 35, with a thickness of at least 12 inches, when soil layers are rewired between tire bale layers.

Wrap an approved geotextile covering that meets the Department Material Specifications, DMS-6320, around the entire tire bale structure to provide a separation between tire bales and the surrounding materials. Also place the same approved geotextile at all interfaces between each tire bale and soil layer when a soil infill around the bales in each layer is not used. The Engineer may exclude the use of the geotextile for such situations as tire bale and rock or gravel interfaces, tire bales used as reinforcement in a shallow fill, the tire bale-foundation interface, or others specified on the plans or as directed.

Compact at least a 24 inch thick soil, gravel, rock, or appropriate covering along the top surface of all exposed tire bale embankment faces unless otherwise shown on the plans or as directed. Use a soil cover with PI between 20 and 35.

D. Tire Chip/Shred Embankments. Tire chip/shred embankment is composed entirely or partially with tire chips/shreds. Protect the tire chips/shreds from leakage of hydrocarbon material from the construction equipment onto the tire chips/shreds. The soil to be used in blending with the tire chips/shreds must meet the requirements of the color test for organic impurities in accordance with Test Method Tex-408-A, with results not showing a color darker than standard. Provide approved equipment to accomplish mixing. Place tire chip/shred embankment in 12 in. loose and 10 in. compacted layers. Compact the tire chip/shred material with rollers in accordance with Item 210, "Rolling." Limit Class II fills to a maximum thickness after compaction of ten (10) feet. Limit Class III fills to a maximum compacted thickness of three (3) to ten (10) feet, as shown on the plans or directed.

Do not place the tire chip/shred embankment fill within thirty (30) feet of open or underground drains. Remove organic material coming into contact with the tire chip/shred embankment.

When required, wrap an approved geotextile meeting Department Material Specifications (DMS-6320) completely around any Class II or Class III fills.

E. Embankments Adjacent to Culverts and Bridges. Compact embankments adjacent to culverts and bridges in accordance with Item 400, "Excavation and Backfill for Structures."

F. Compaction Methods. Begin rolling longitudinally at the sides and proceed toward the center, overlapping on successive trips by at least 1/2 the width of the roller. On super elevated curves, begin rolling at the lower side and progress toward the high side. Alternate roller trips to attain slightly different lengths. Compact embankments in accordance with one of the following methods as shown on the plans:

1. **Ordinary Compaction.** Use approved rolling equipment complying with Item 210, "Rolling," to compact each layer. The plans or Engineer may require specific equipment. Do not allow the loose depth of any layer to exceed 8 in., unless otherwise approved. Before and during rolling operations, bring each layer to the moisture content directed. Compact each layer until there is no evidence of further consolidation. Maintain a level layer to ensure uniform compaction. If the required stability or finish is lost for any reason, recompact and refinish the subgrade at no additional expense to the Department.

2. **Density Control.** Compact each layer to the required density using equipment complying with Item 210, "Rolling." Determine the maximum lift thickness based on the ability of the compacting operation and equipment to meet the required density. Do not exceed layer thickness of 16 in. loose or 12 in. compacted material, unless otherwise approved. Maintain a level layer to ensure uniform compaction.

   The Engineer will use Tex-114-E to determine the maximum dry density (D_a) and optimum water content (W_{opt}). Meet the requirements for field density and moisture content in Table 2, unless otherwise shown on the plans.

Table A.2: Field Density Control Requirements

Description	Density	Moisture Content
	Tex-115-E	
PI ≤ 15	≥ 98% D_a	
15 < PI ≤ 35	≥ 98% D_a and ≤ 102% D_a	≥ W_{opt}
PI > 35	≥ 95% D_a and ≤ 100% D_a	≥ W_{opt}
Soils within Tire Bale Embankments PI ≤ 35	≥ 98% D_a	≥ W_{opt} (All tire bale interfaces must be dry before placement)
Blended Tire Chip Embankments	≥ 98% D_a	≥ W_{opt}

Each layer is subject to testing by the Engineer for density and moisture content. During compaction, the moisture content of the soil should not exceed the value shown on the moisture-density curve, above optimum, required to achieve:

- 98% dry density for soils with a PI greater than 15 but less than or equal to 35 or
- 95% dry density for soils with PI greater than 35.

When required, remove small areas of the layer to allow for density tests. Replace the removed material and recompact at no additional expense to the Department. Proof-roll in accordance with Item 216, "Proof Rolling," when shown on the plans or as directed. Correct soft spots as directed.

G. Maintenance of Moisture and Reworking. Maintain the density and moisture content once all requirements in Table 2 are met. For soils with a PI greater than 15, maintain the moisture content no lower than 4 percentage points below optimum. Rework the material to obtain the specified compaction when the material loses the required stability, density, moisture, or finish. Alter the compaction methods and procedures on subsequent work to obtain specified density as directed.

H. Acceptance Criteria.

1. Grade Tolerances.

a. Staged Construction. Grade to within 0.1 ft. in the cross-section and 0.1 ft. in 16 ft. measured longitudinally.

b. Turnkey Construction. Grade to within 1/2 in. in the cross-section and 1/2 in. in 16 ft. measured longitudinally.

2. **Gradation Tolerances.** When gradation requirements are shown on the plans, material is acceptable when not more than 1 of the most 5 recent gradation tests is outside the specified limits on any individual sieve by more than 5 percentage points.

3. **Density Tolerances.** Compaction work is acceptable when not more than 1 of the 5 most recent density tests is outside the specified density limits, and no test is outside the limits by more than 3 lb. per cubic foot.

4. **Plasticity Tolerances.** Material is acceptable when not more than 1 of the 5 most recent PI tests is outside the specified limit by no more than 2 points.

5. **Tire Bale Dimension Tolerances.** Tire bales with tire extrusions extending from any side more than 6 inches must be cut off from the bale or bale must be rejected if unable to be removed.

6. **Tire Bale Construction Tolerances.** Tire bales are acceptable when one (1) tire bale out of every fifty (50) constructed or delivered weighs more than 1800 lbs.

132.4. Measurement. Embankments will be measured by the cubic yard. Measurement will be further defined for payment as follows:

A. Final. The cubic yard will be measured in its final position using the average end area method. The volume is computed between the original ground surface or the surface upon which the embankment is to be constructed and the lines, grades, and slopes of the embankment. In areas of salvaged topsoil, payment for embankment will be made in accordance with Item 160, "Topsoil." Shrinkage or swell factors will not be considered in determining the calculated quantities.

B. Original. The cubic yard will be measured in its original and natural position using the average end area method.

C. Vehicle. The cubic yard will be measured in vehicles at the point of delivery.

When measured by the cubic yard in its final position, this is a plans quantity measurement Item. The quantity to be paid is the quantity shown in the proposal, unless modified by Article 9.2, "Plans Quantity Measurement." Additional measurements or calculations will be made if adjustments of quantities are required.

Shrinkage or swell factors are the Contractor's responsibility. When shown on the plans, factors are for informational purposes only.

Measurement of retaining wall backfill in embankment areas is paid for as embankment, unless otherwise shown on the plans. Limits of measurement for embankment in retaining wall areas are shown on the plans.

132.5. Payment. The work performed and materials furnished in accordance with this Item and measured as provided under "Measurement" will be paid for at the unit price bid for "Embankment (Final)," "Embankment (Original)," or "Embankment (Vehicle)," of the compaction method and type specified. This price is full compensation for furnishing embankment; tire bales; tire chips/shreds; hauling; placing, compacting, finishing, and reworking; disposal of waste material; and equipment, labor, tools, and incidentals.

When proof rolling is directed, it will be paid for in accordance with Item 216, "Proof Rolling."

All sprinkling and rolling, except proof rolling, will not be paid for directly, but will be considered subsidiary to this Item, unless otherwise shown on the plans.

When subgrade is constructed under this contract, correction of soft spots in the subgrade will be at the Contractor's expense. Where subgrade is not constructed under this contract, correction of soft spots in the subgrade will be paid in accordance with Article 9.4, "Payment for Extra Work."

Appendix B: Fabrication of Scrap Tire Bales

The following appendix provides a draft guideline for the construction of the tire bales used as part of this research program. The guidelines are based on lessons learned while constructing the tire bales, specifications already in place for tire shred structures, and previously published draft construction guidelines (Winter et al. 2006). The guidelines have been written in the TxDOT specification style guide so that the style is easily understood and can be incorporated into construction specifications already in place by TxDOT. The construction of the tire bales is based on using the standard tire baling machine (Figure B.1) manufactured by Encore Systems (www.tirebaler.com) and used for the construction of the bales used during this testing program.

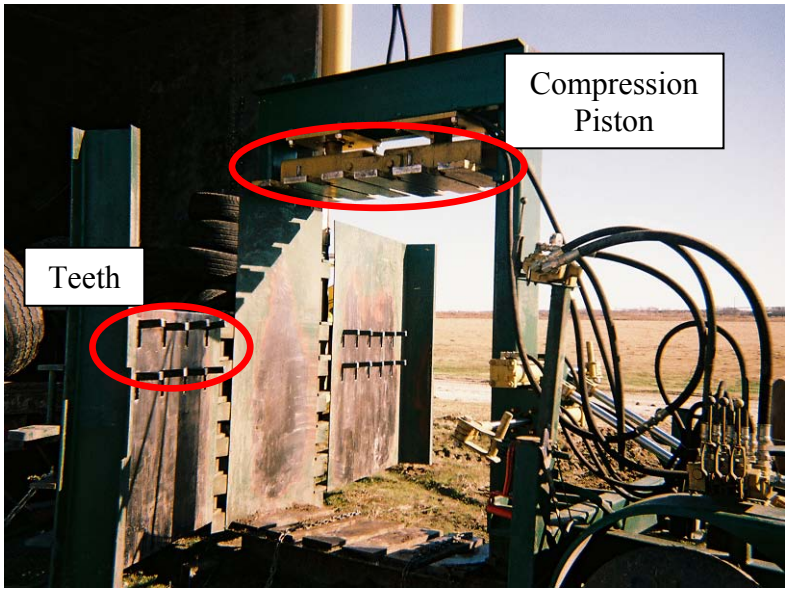

Figure B.1: The Encore Systems Tire Baler used to Construct the Tire Bales

Fabrication of Standard and Reduced Volume Scrap Tire Bales

B.1 Description. Furnish, or construct, scrap tire bales for the use in embankments, roadways, or other soil structures according to this Item.

B.2. Material. Furnish approved scrap tires and baling equipment as directed, or shown on the plans, to construct the tire bales. Tire bales must be constructed to one of the following types:

Standard Scrap Tire Bale. The standard scrap tire bale is defined as:

- containing approximately 70 to 105 whole tires,
- having a density of no less than 32 lb/ft^3,
- having average dimensions of 4.5 feet in length (parallel to wires), 5 feet in width (perpendicular to wires), and 2.5 feet in height (Figure B.2), and
- having at least 5 baling wires placed along the length of the bale.

Additional requirements may be specified as shown on the plans or as directed.

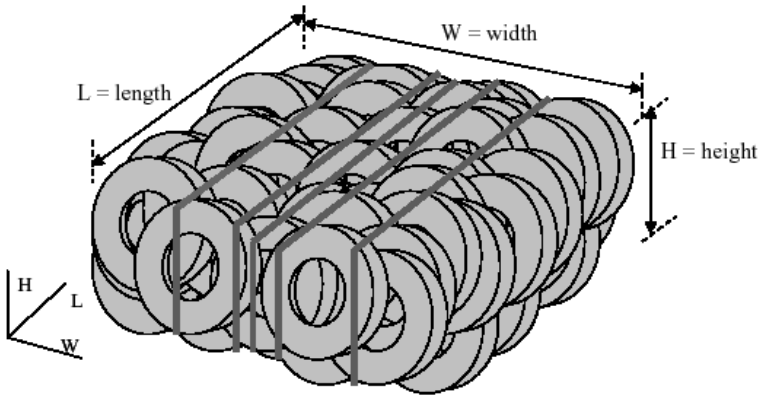

Figure B.2: Illustration of Standard Tire Bale Dimensions (LaRocque 2005)

Reduced Volume Tire Bale. Construct reduced volume bales to the same width and height as the standard bale; the length shall be reduced as shown on the plans or as directed. The number of whole tires placed in the reduced volume bale, as defined by Winter et al. (2006), shall be defined as:

$$N_{NST} = \frac{N_{st} \cdot L_{nst}}{L_{st}} \quad \text{(B.1)}$$

Where: N_{NST} is the number of tires in the non-standard bale
N_{st} is the number of tires in the standard bale = 100 tires
L_{nst} is the length of the non-standard bale
L_{st} is the length of the standard bale = 4.5 feet

a. Scrap Tires. Provide, or ensure, that scrap tires placed in the bales are:

- free from dirt, vegetation, and organic material,
- free of contaminants such as oil, grease, gasoline, or diesel fuel,
- have not been part of or exposed to a fire,

- have no significant exposed reinforcing steel, and
- have no significant portions of the tire missing, such as tire halves, quarters, or shreds.

Additional requirements may be specified as shown on the plans or as directed. Shred or dispose any tires not meeting the requirements for use in the baling process.

b. Tire Bale Wires. Five 7-gauge galvanized steel or stainless steel wires must be spaced evenly along the width of the bale. Place additional wires or geosynthetic straps as directed, or shown on the plans, around the bales if corrosive environments are expected (refer to Item 432.2).

c. Movement and Storage of Bales. Provide equipment able to properly lift and move tire bales without loading the baling wires. Place bales flat on the ground during storage or stacked in a pyramid fashion. Cover all bales during storage to prevent degradation prevent water from entering the bales.

d. Eligibility of Baling Contractor. Tire bales may only be constructed or furnished by a supplier authorized to process waste tires by the Texas Commission on Environmental Quality (TCEQ). Provide a written statement of compliance from the tire bale manufacturer.

B.3 Construction. Construct scrap tire bales as described in this Item, unless otherwise specified on the plans or directed.

1. Open and inspect baler walls to ensure that teeth are intact and machine parts are not damaged.
2. Thread the baling wires through the grooves located along the bottom base plate. Place the first three tires, with the first (or bottom) tire covering the middle three wires, and the two remaining tires placed in a reverse pyramid fashion on top.
3. Close and secure the walls of the baling machine. Place the first layer of tires, typically about 20 tires, in a “zigzag” fashion.
4. Apply a compressive load sufficient enough compress the tire layer past the bottom layer of teeth. Inspect the compressed tires and machine teeth and make sure that the tires did not get caught on the teeth.
5. Remove the compressive load slowly and inspect the compressed tires to make sure that all the tires are retained by the teeth. Place a second layer of tires on top of the compressed tires, and repeat the tire compression process. Compress each section so that all tires are compressed past the top layer of teeth. The compression process is completed once 100 tires have been used, or the tires can no longer be compressed past the dog teeth.
6. Compress the piston onto the bale and open the steel box.
7. Thread and attach the baling wires around the bale, making sure that the wires are placed through the appropriate groves in the baler.

8. Attach the removal chains to the loading piston. Remove the bale from the baling machine by lifting up on the piston and rolling the bale out of the baler onto a forklift and inspect for proper shape.

Appendix C: Testing Data from Field Determination of Tire Bale Index Properties

The following appendix provides a detailed outline of the testing results obtained for the field determination of the tire bale index properties. Refer to Chapter 5 for an analysis of the data provided in this appendix.

The measured tire bale dimensions and weights, as well as the calculated unit weights, void ratios and specific gravities, for Tire Bales 1 through 5 are provided in Table C.1.

Table C.1: Results from the Field Index Testing of Tire Bales 1 through 5

	Tire Bale				
	1	2	3	4	5
Length	4.67	4.66	4.7	4.62	4.73
Width	5.01	5.1	4.98	5.19	5.1
Height	2.38	2.57	2.49	2.51	2.51
MEC_L	5.21	5.48	5.23	5.13	5.33
MEC_W	5.27	5.4	5.38	5.63	5.73
MEC_H	2.5	2.708	2.73	2.77	2.56
Dry Weight	2034	1972	1884	1902	1932
Sub Weight	240	232	245	215	235
Average Volume	55.68	61.08	58.28	60.18	60.55
Maximum Enclosing Cuboid	68.64	80.14	76.82	80.00	78.18
Percent Difference	23.27	31.20	31.80	32.93	29.13
Average Dry Unit Weight	36.53	32.29	32.33	31.60	31.91
Average Sub Unit Weight	4.31	3.80	4.20	3.57	3.88
MEC Dry Unit Weight	29.63	24.61	24.53	23.77	24.71
MEC Sub Unit Weight	3.50	2.90	3.19	2.69	3.01
Volume of Solids	28.75	27.88	26.27	27.04	27.20
Volume of Voids (avg V)	26.93	33.19	32.01	33.15	33.35
Volume of Voids (MEC V)	39.89	52.25	50.55	52.97	50.99
Void Ratio (avg vol)	0.94	1.19	1.22	1.23	1.23
Void Ratio (MEC vol)	1.39	1.87	1.92	1.96	1.87
Specific Gravity	1.13	1.13	1.15	1.13	1.14

The change in weight of the tire bales with time after removal from the water bath for the five bales is shown in Figure C.1. The permeability of the tire bales, calculated from the data provided in Figure C.1, is shown in Figure C.2.

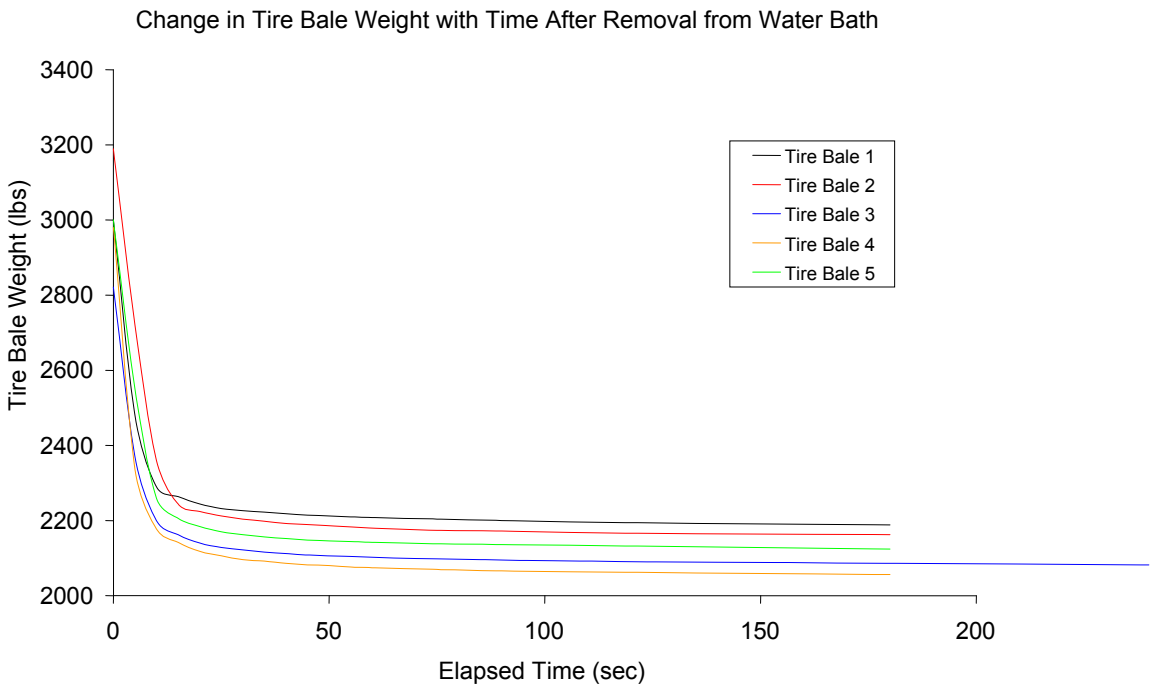

Figure C.1: Change in Tire Bale Weight with Time after Removal from the Water Bath (Bales 1 through 5)

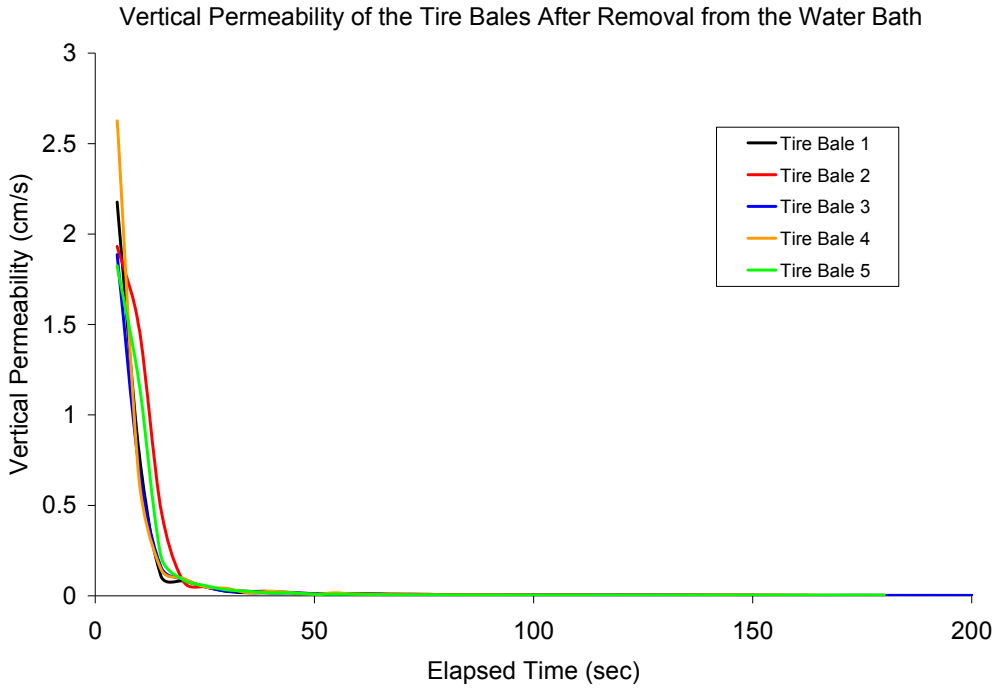

Figure C.2: Back-Calculated Vertical Permeability for Tire Bales 1 through 5

Appendix D: Testing Data from the Large Scale Direct Shear Testing of the Dry and Wet Tire Bale Only Interface

The following appendix section provides the data obtained for each of the large scale direct shear tests conducted for the dry and wet tire bale only interfaces that was not specifically reported in Chapter 6. A detailed analysis of the data is provided in Chapter 6.3.

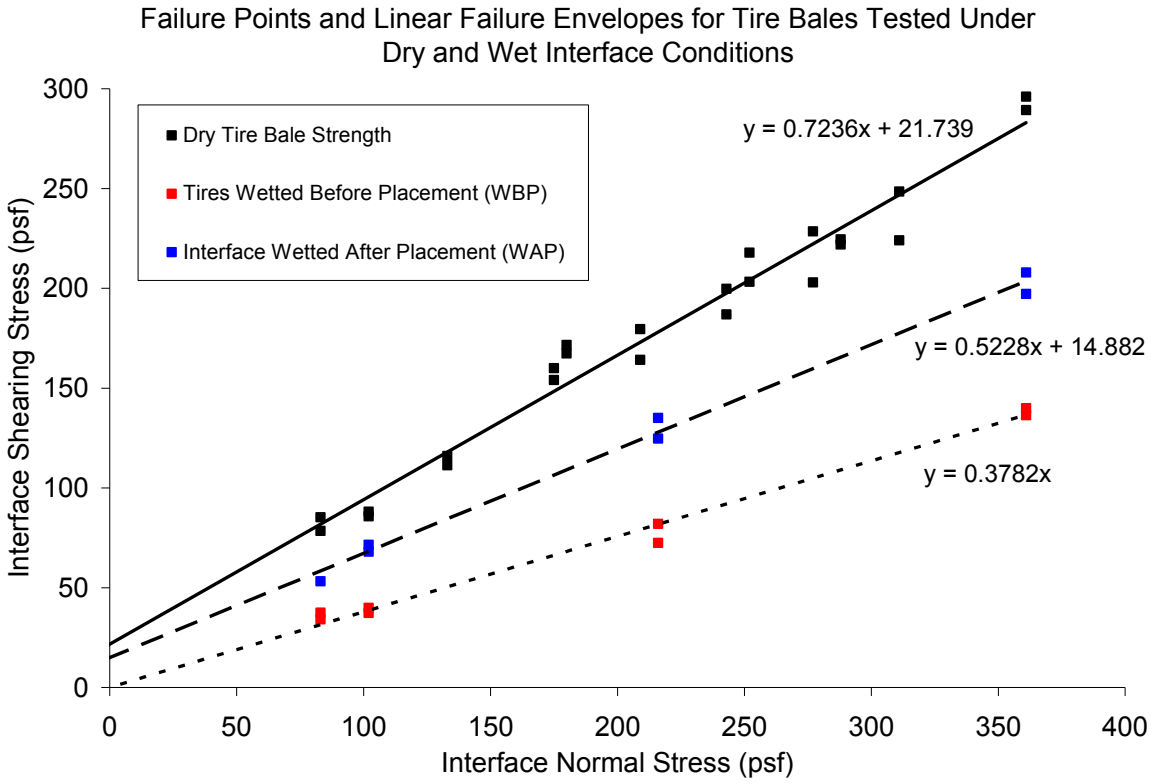

Figure D.1: Shear Strength Envelopes for the Dry and Wet Tire Bale Only Interfaces

Results for Dry Tire Bale Interface Test #1: Normal Stress = 83 psf

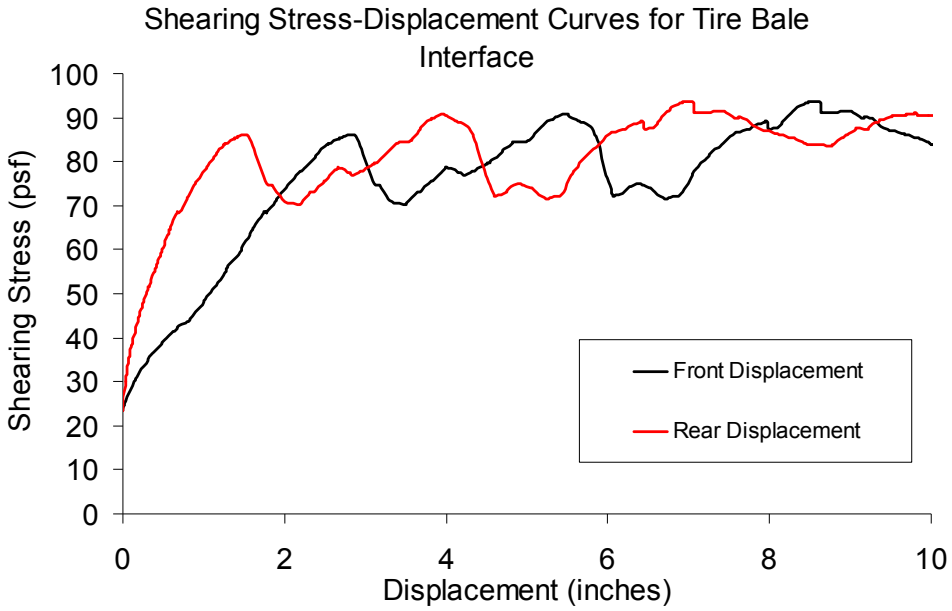

Figure D.2: Interface Shearing Resistance versus Displacement for the Dry Tire Bale Only Interface (Normal Stress = 83 psf)

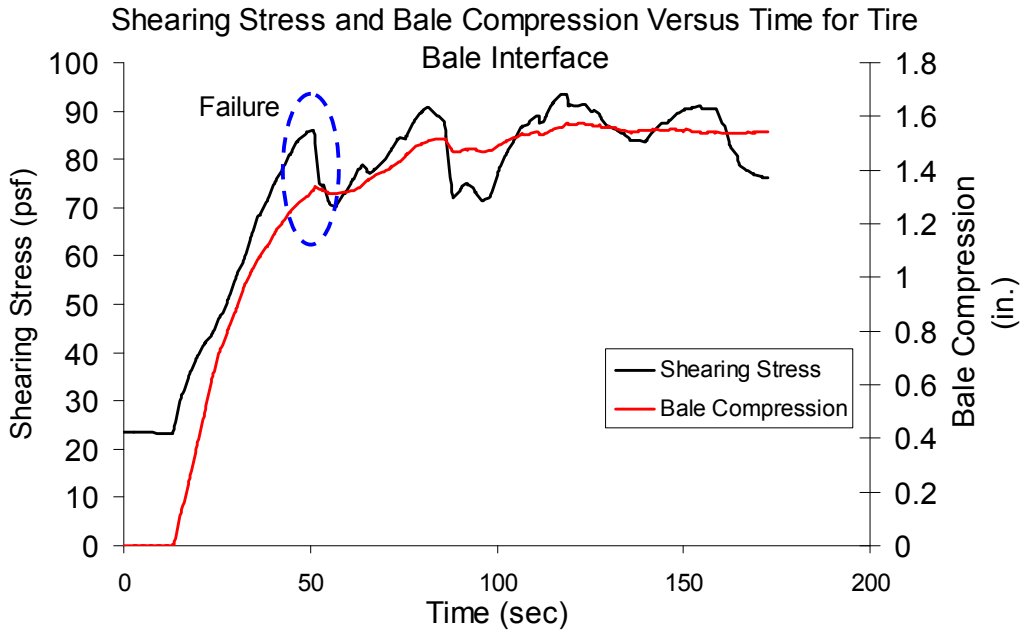

Figure D.3: Interface Shearing Resistance and Tire Bale Compression versus Elapsed Testing Time for the Dry Tire Bale Only Interface (Normal Stress = 83 psf)

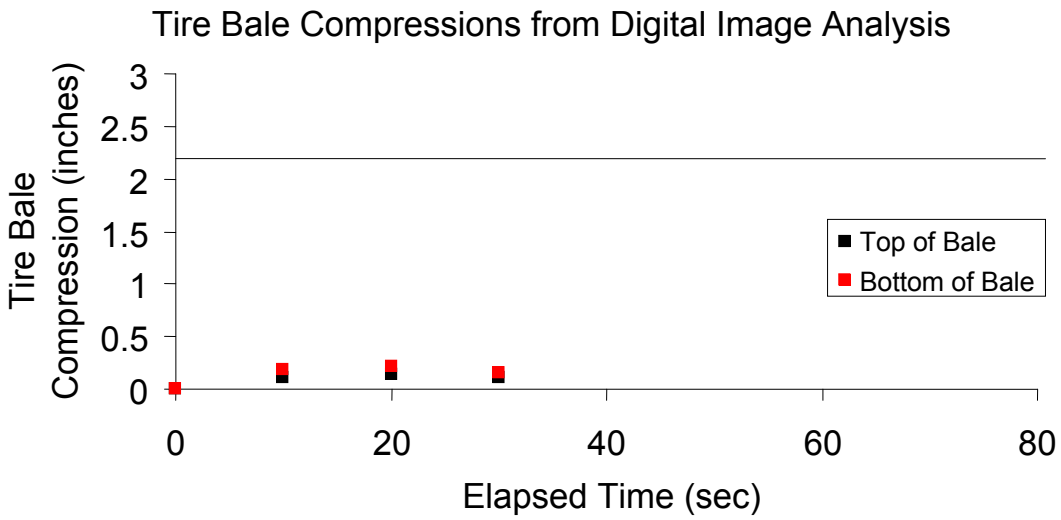

Figure D.4: Compressions of the Mobile Tire Bale Measured with Digital Image Analysis for the Dry Tire Bale Only Interface (Normal Stress = 83 psf)

Results for Dry Tire Bale Interface Test #2: Normal Stress = 83 psf

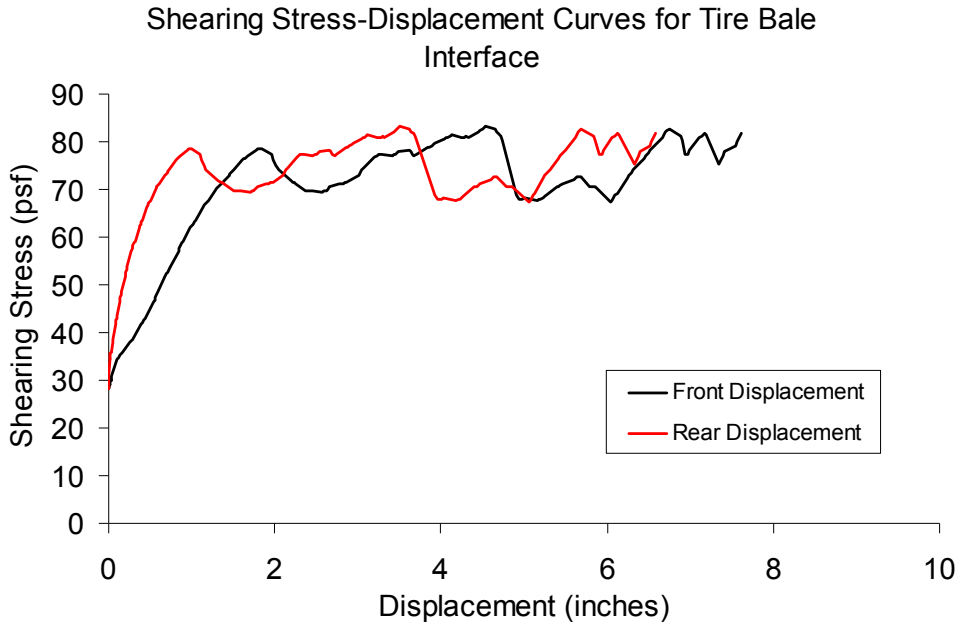

Figure D.5: Interface Shearing Resistance versus Displacement for the Dry Tire Bale Only Interface (Normal Stress = 83 psf)

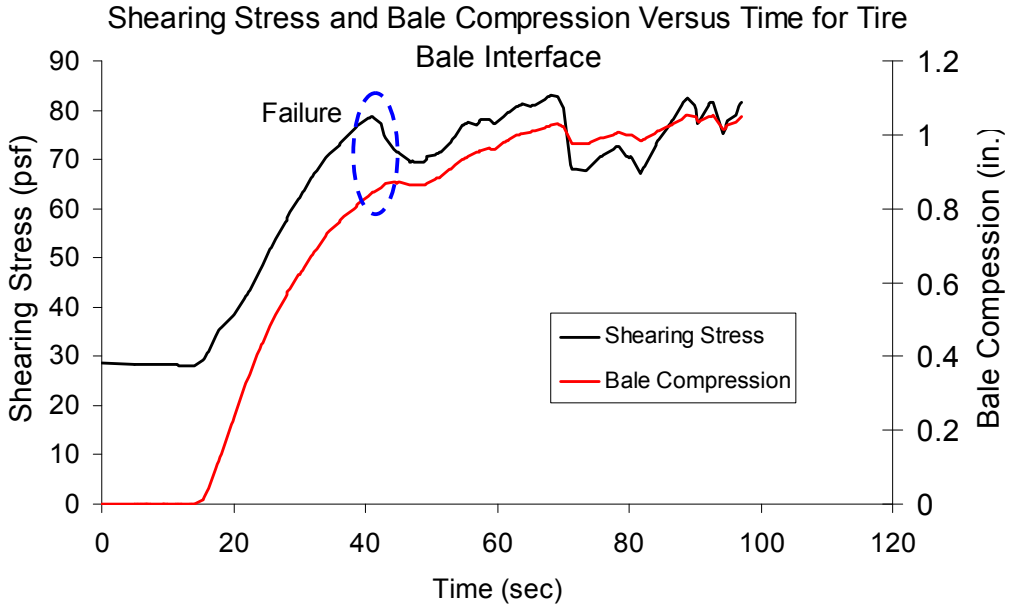

Figure D.6: Interface Shearing Resistance and Tire Bale Compression versus Elapsed Testing Time for the Dry Tire Bale Only Interface (Normal Stress = 83 psf)

Results for Partially Saturated (WAP) Tire Bale Interface Test #1: Normal Stress = 83 psf

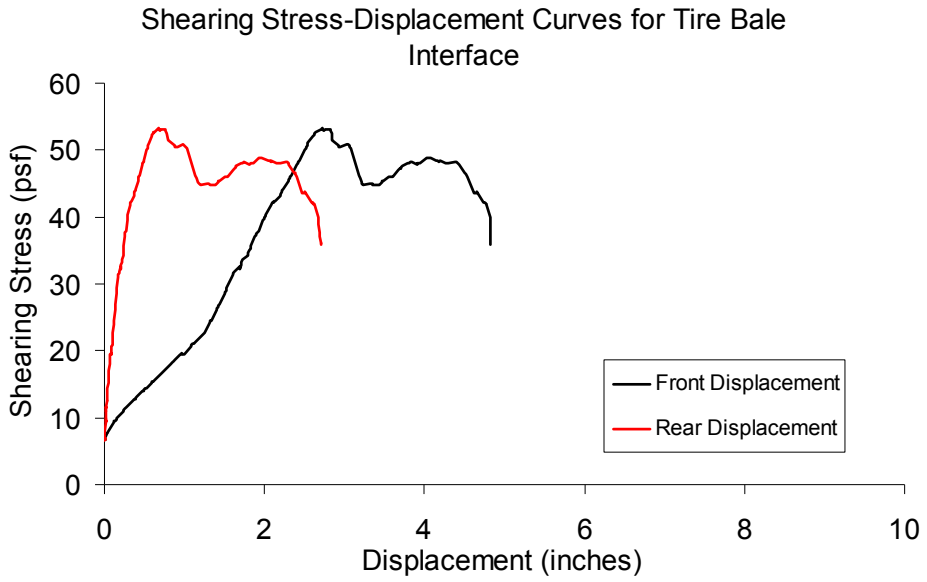

Figure D.7: Interface Shearing Resistance versus Displacement for the Partially Saturated (WAP) Tire Bale Only Interface (Normal Stress = 83 psf)

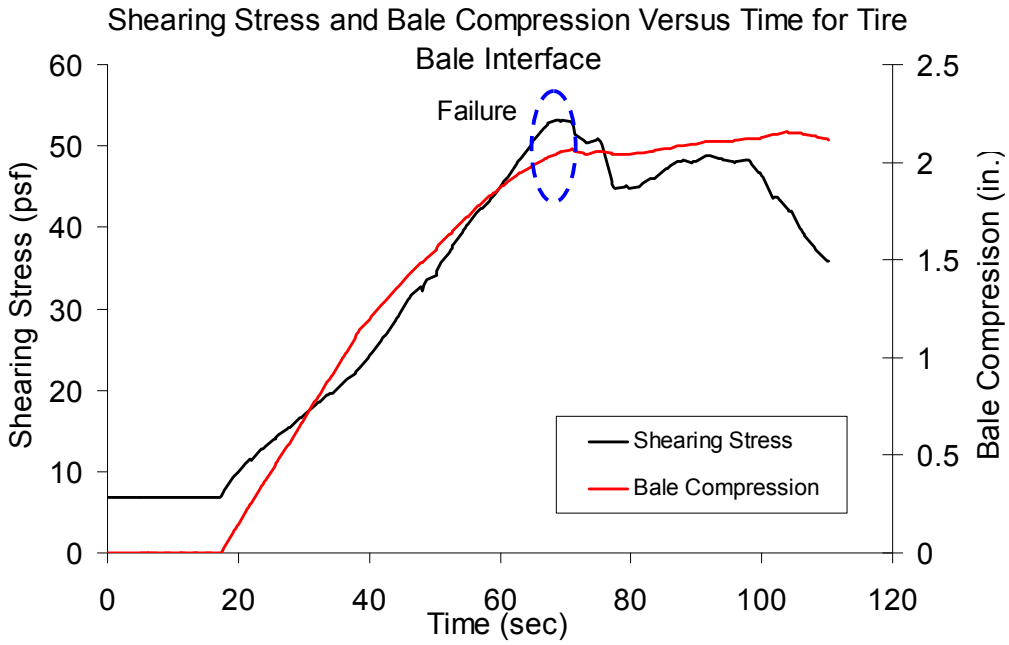

Figure D.8: Interface Shearing Resistance and Tire Bale Compression versus Elapsed Testing Time for the Partially Saturated (WAP) Tire Bale Only Interface (Normal Stress = 83 psf)

Results for Fully Saturated (WBP) Tire Bale Interface Test #1: Normal Stress = 83 psf

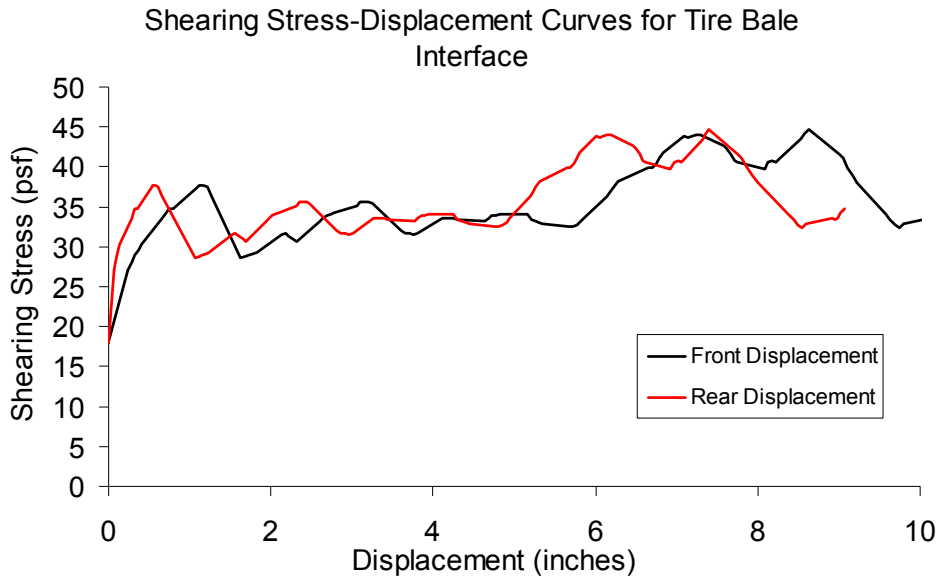

Figure D.9: Interface Shearing Resistance versus Displacement for the Fully Saturated (WBP) Tire Bale Only Interface (Normal Stress = 83 psf)

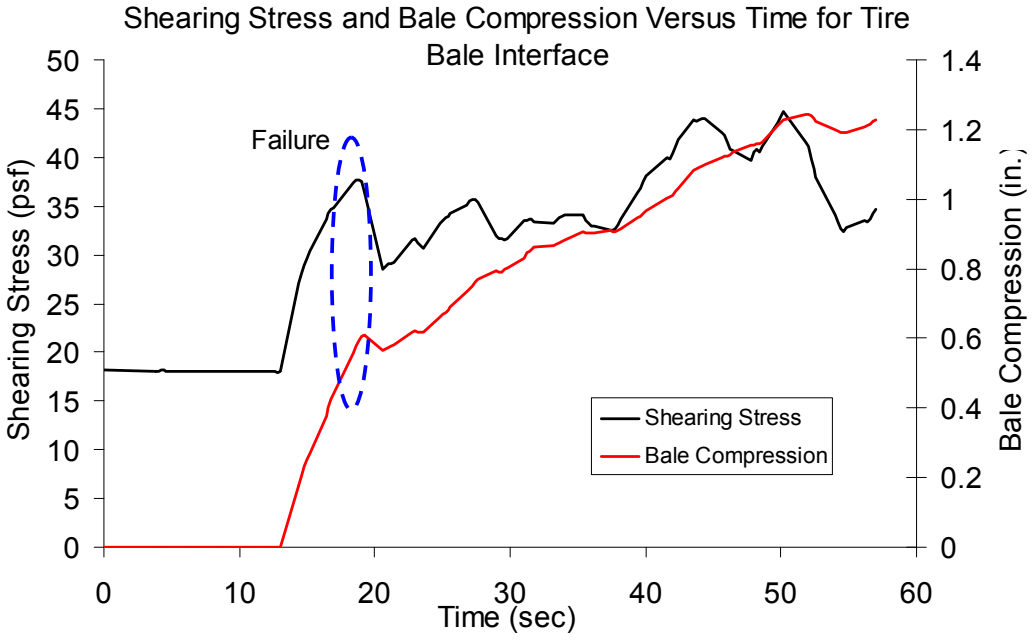

Figure D.10: Interface Shearing Resistance and Tire Bale Compression versus Elapsed Testing Time for the Fully Saturated (WBP) Tire Bale Only Interface (Normal Stress = 83 psf)

Results for Fully Saturated (WBP) Tire Bale Interface Test #2: Normal Stress = 83 psf

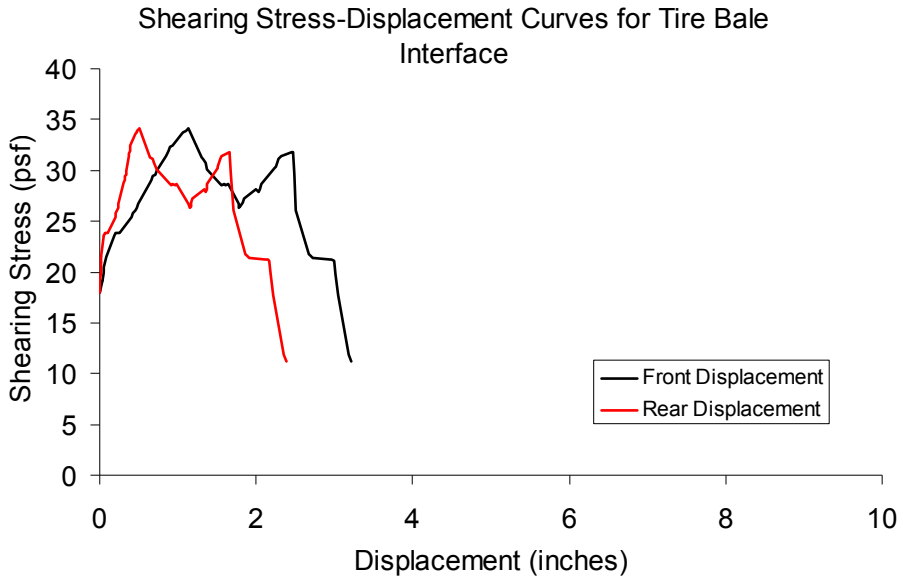

Figure D.11: Interface Shearing Resistance versus Displacement for the Fully Saturated (WBP) Tire Bale Only Interface (Normal Stress = 83 psf)

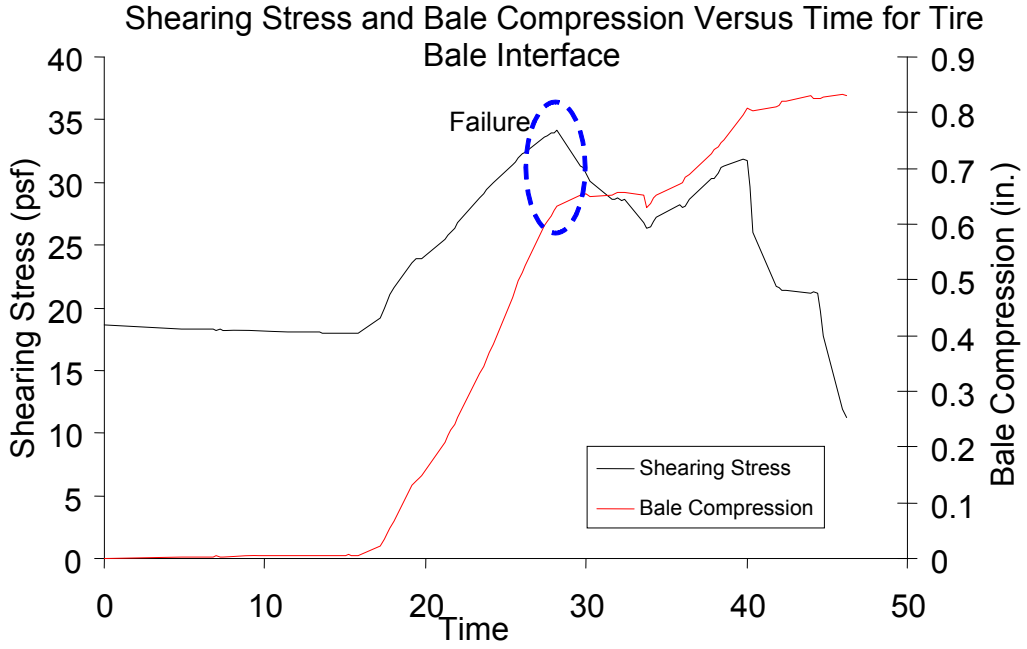

Figure D.12: Interface Shearing Resistance and Tire Bale Compression versus Elapsed Testing Time for the Fully Saturated (WBP) Tire Bale Only Interface (Normal Stress = 83 psf)

Results for Dry Tire Bale Interface Test #3: Normal Stress = 102 psf

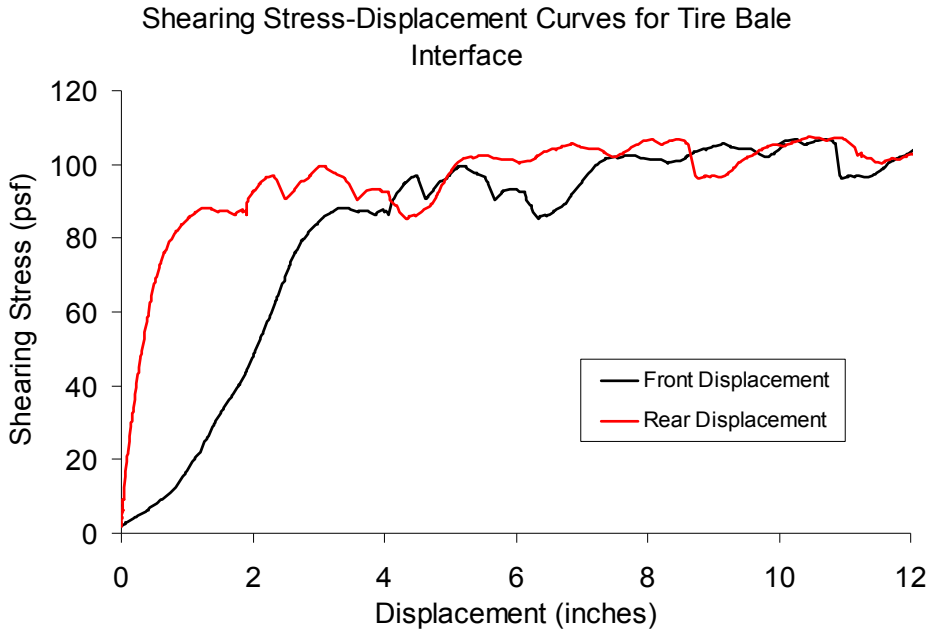

Figure D.13: Interface Shearing Resistance versus Displacement for the Dry Tire Bale Only Interface (Normal Stress = 102 psf)

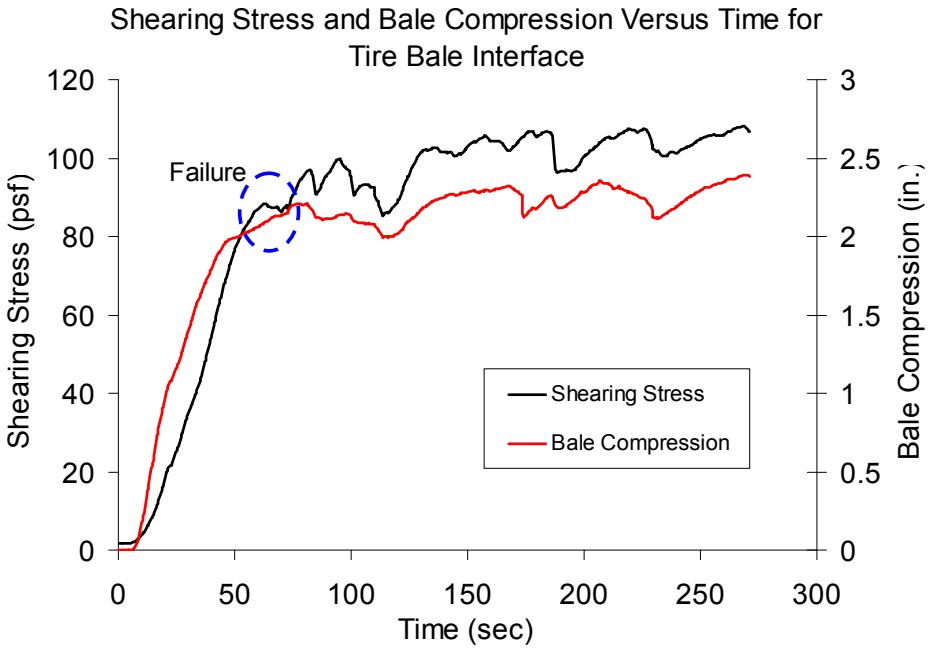

Figure D.14: Interface Shearing Resistance and Tire Bale Compression versus Elapsed Testing Time for the Dry Tire Bale Only Interface (Normal Stress = 102 psf)

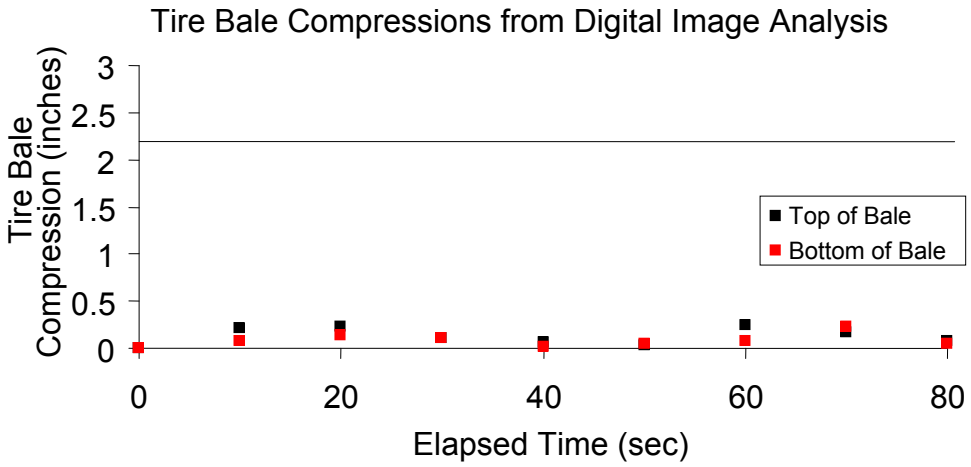

Figure D.15: Compressions of the Mobile Tire Bale Measured with Digital Image Analysis for the Dry Tire Bale Only Interface (Normal Stress = 102 psf)

Results for Dry Tire Bale Interface Test #4: Normal Stress = 102 psf

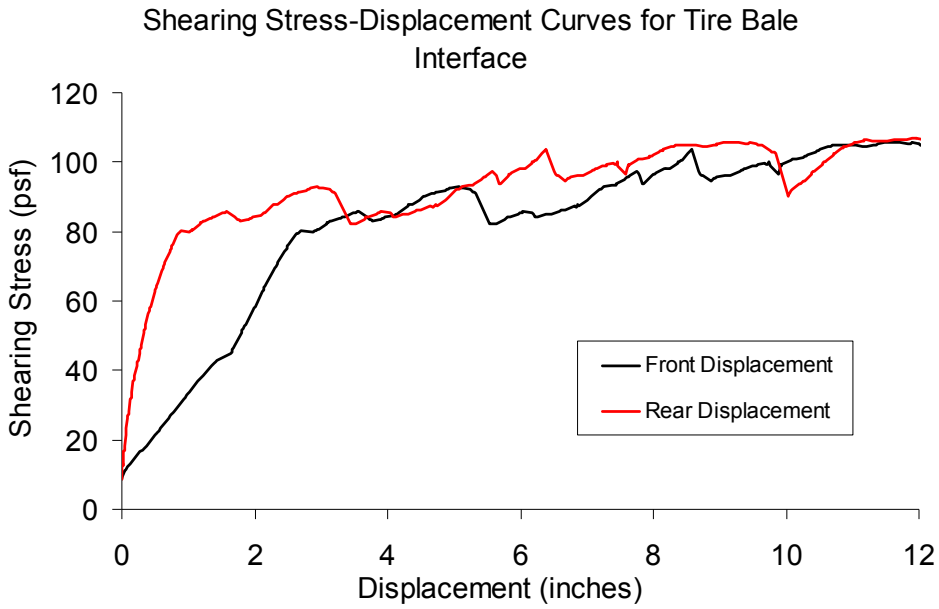

Figure D.16: Interface Shearing Resistance versus Displacement for the Dry Tire Bale Only Interface (Normal Stress = 102 psf)

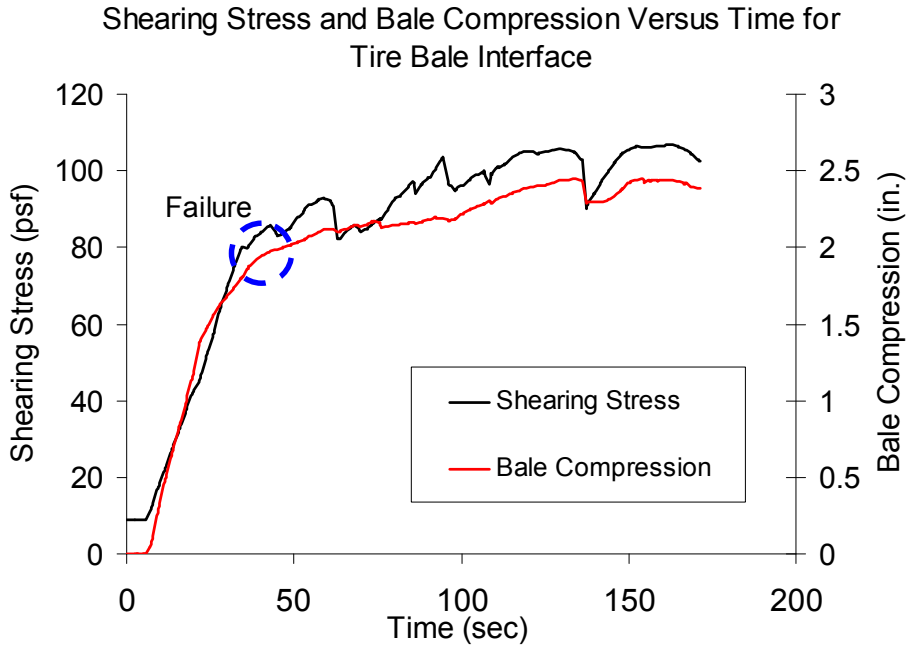

Figure D.17: Interface Shearing Resistance and Tire Bale Compression versus Elapsed Testing Time for the Dry Tire Bale Only Interface (Normal Stress = 102 psf)

Results for Partially Saturated (WAP) Tire Bale Interface Test #2: Normal Stress = 102 psf

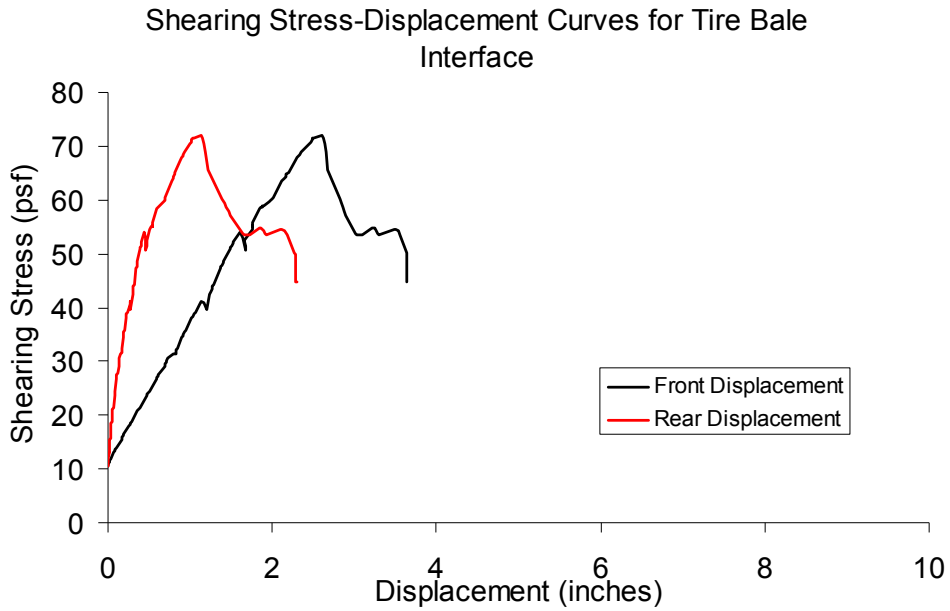

Figure D.18: Interface Shearing Resistance versus Displacement for the Partially Saturated (WAP) Tire Bale Only Interface (Normal Stress = 102 psf)

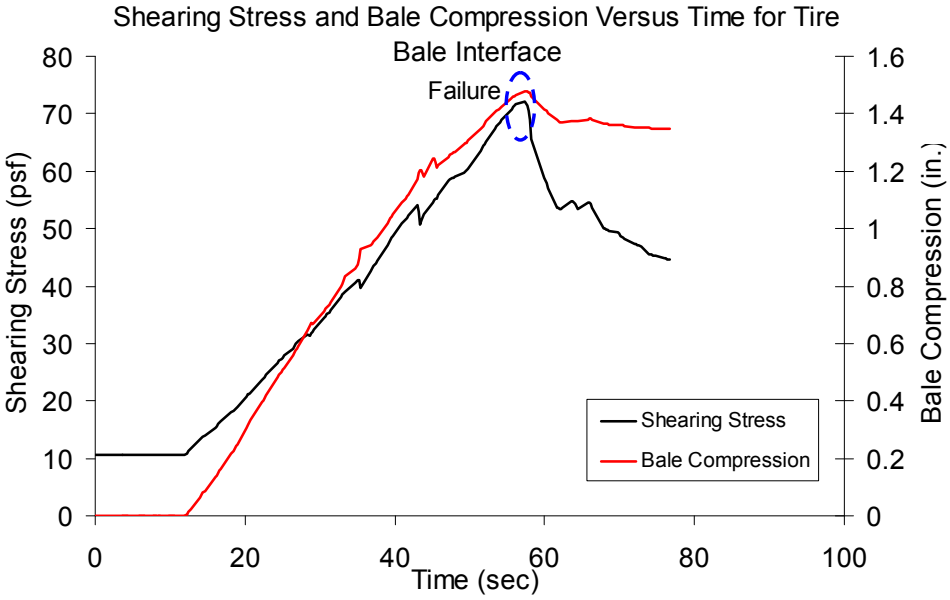

Figure D.19: Interface Shearing Resistance and Tire Bale Compression versus Elapsed Testing Time for the Partially Saturated (WAP) Tire Bale Only Interface (Normal Stress = 102 psf)

Results for Partially Saturated (WAP) Tire Bale Interface Test #3: Normal Stress = 102 psf

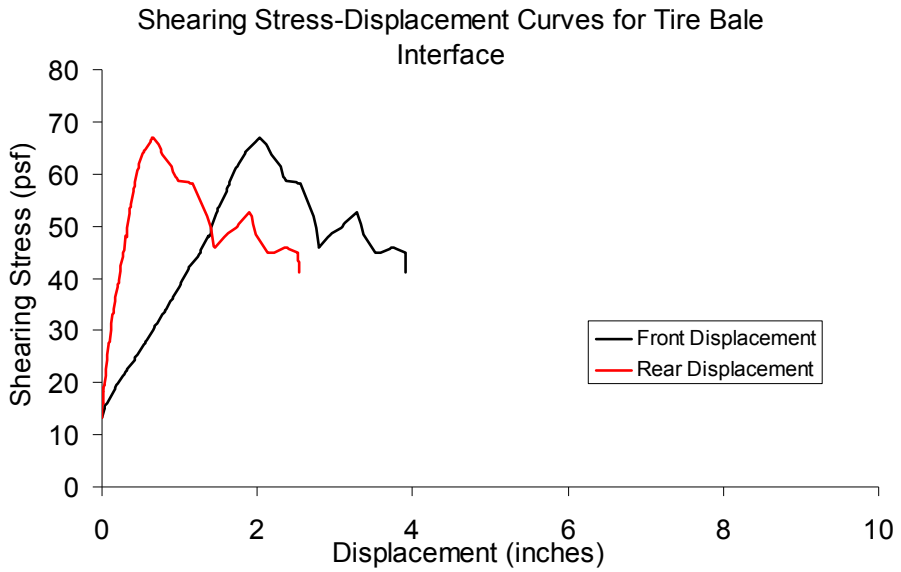

Figure D.20: Interface Shearing Resistance versus Displacement for the Partially Saturated (WAP) Tire Bale Only Interface (Normal Stress = 102 psf)

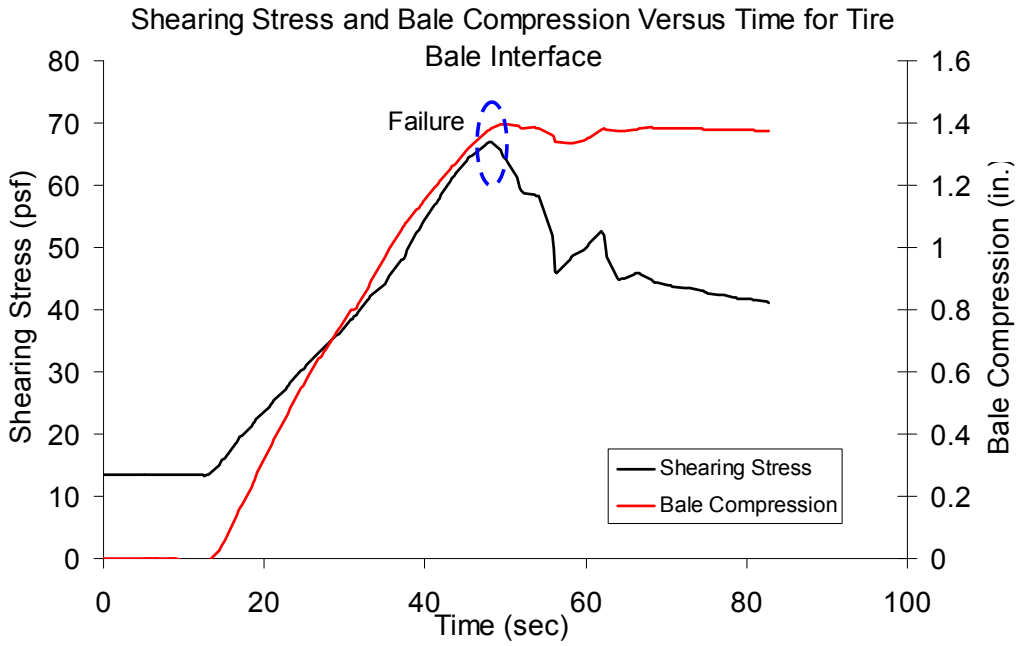

Figure D.21: Interface Shearing Resistance and Tire Bale Compression versus Elapsed Testing Time for the Partially Saturated (WAP) Tire Bale Only Interface (Normal Stress = 102 psf)

Results for Fully Saturated (WDP) Tire Bale Interface Test #3: Normal Stress = 102 psf

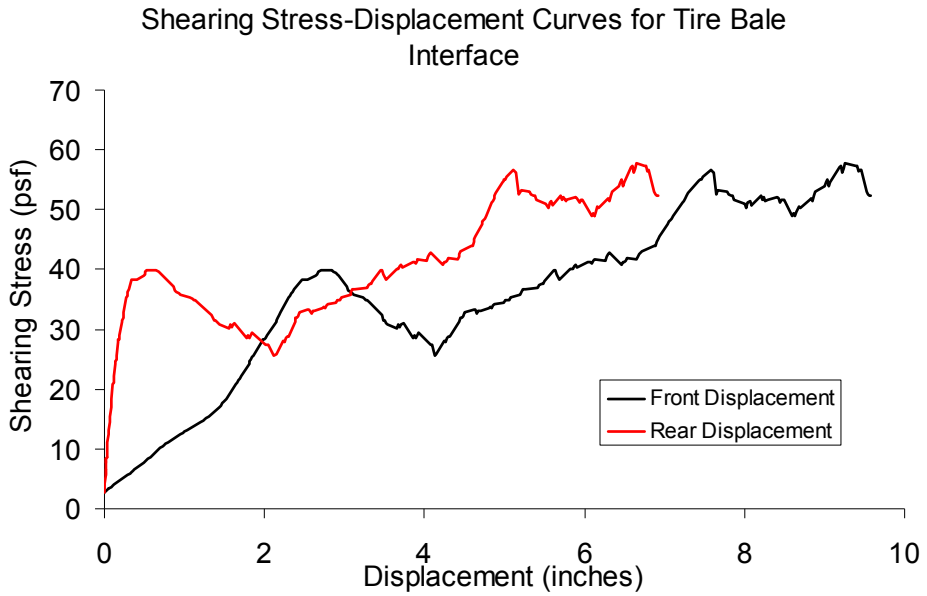

Figure D.22: Interface Shearing Resistance versus Displacement for the Fully Saturated (WBP) Tire Bale Only Interface (Normal Stress = 102 psf)

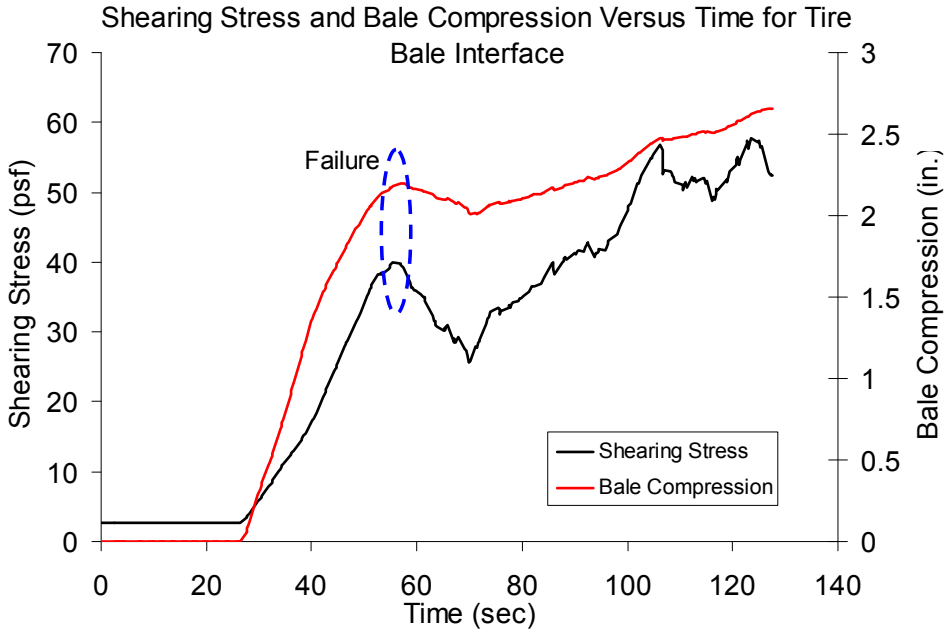

Figure D.23: Interface Shearing Resistance and Tire Bale Compression versus Elapsed Testing Time for the Fully Saturated (WBP) Tire Bale Only Interface (Normal Stress = 102 psf)

Results for Fully Saturated (WDP) Tire Bale Interface Test #4: Normal Stress = 102 psf

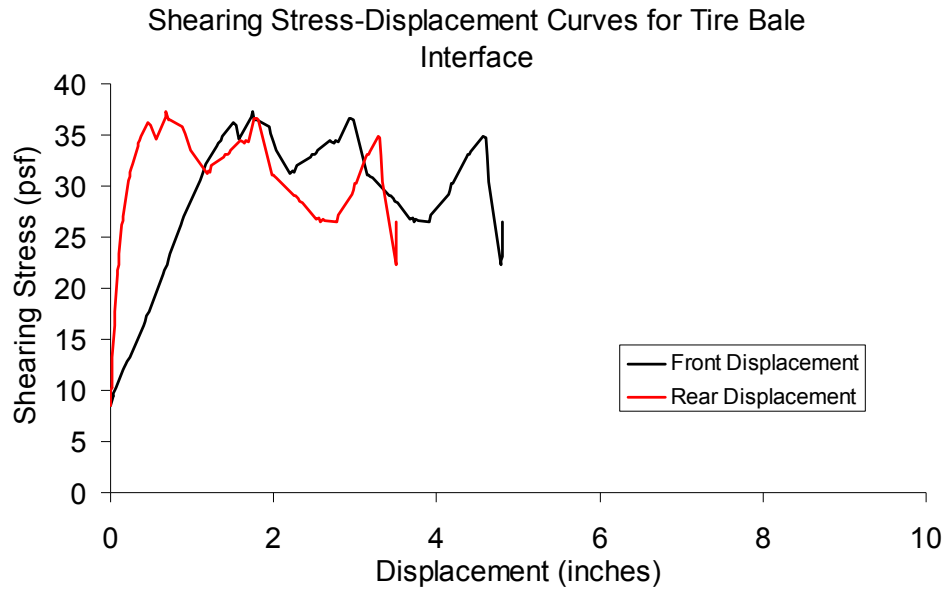

Figure D.24: Interface Shearing Resistance versus Displacement for the Fully Saturated (WBP) Tire Bale Only Interface (Normal Stress = 102 psf)

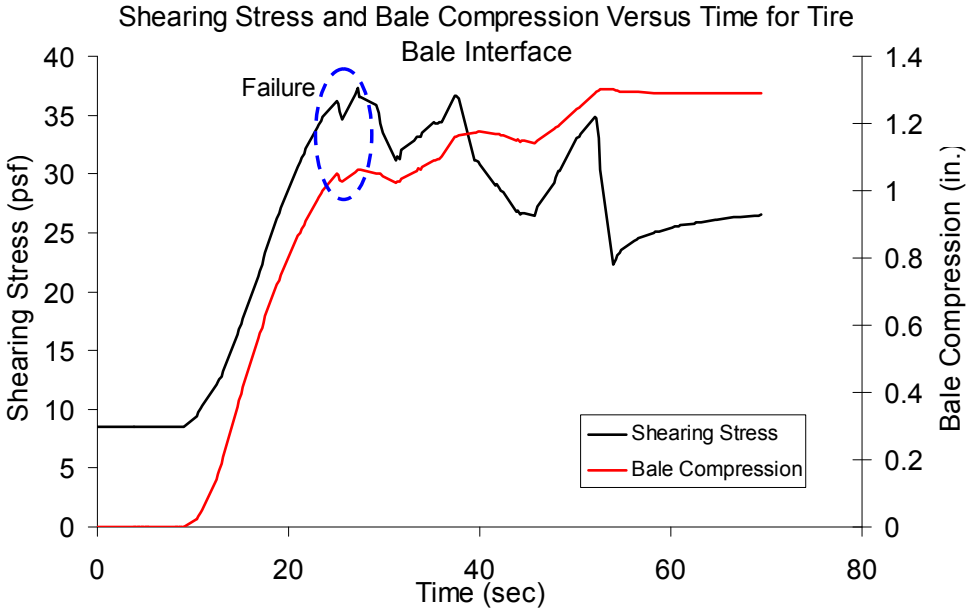

Figure D.25: Interface Shearing Resistance and Tire Bale Compression versus Elapsed Testing Time for the Fully Saturated (WBP) Tire Bale Only Interface (Normal Stress = 102 psf)

Results for Dry Tire Bale Interface Test #5: Normal Stress = 180 psf

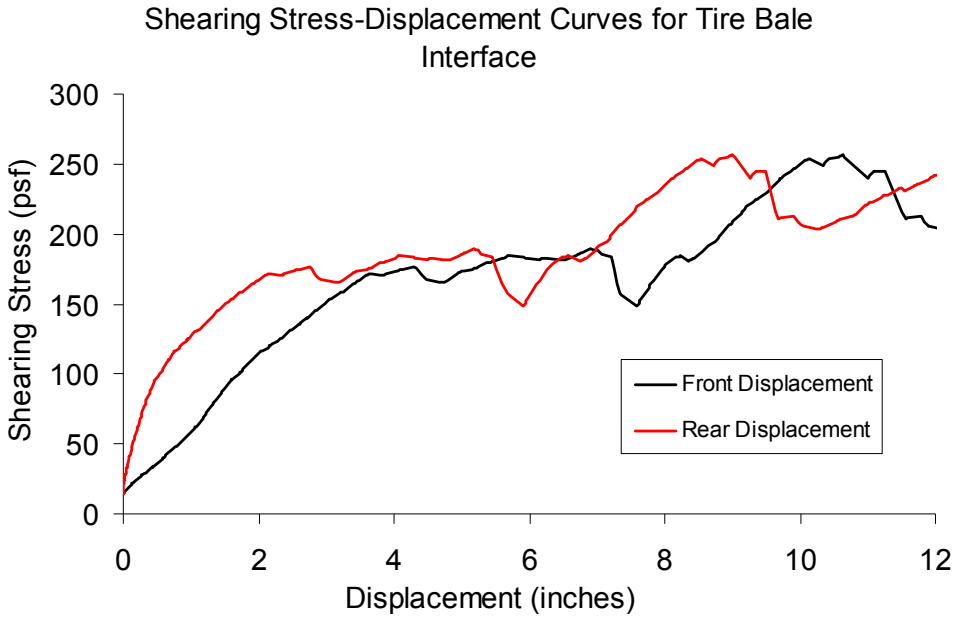

Figure D.26: Interface Shearing Resistance versus Displacement for the Dry Tire Bale Only Interface (Normal Stress = 180 psf)

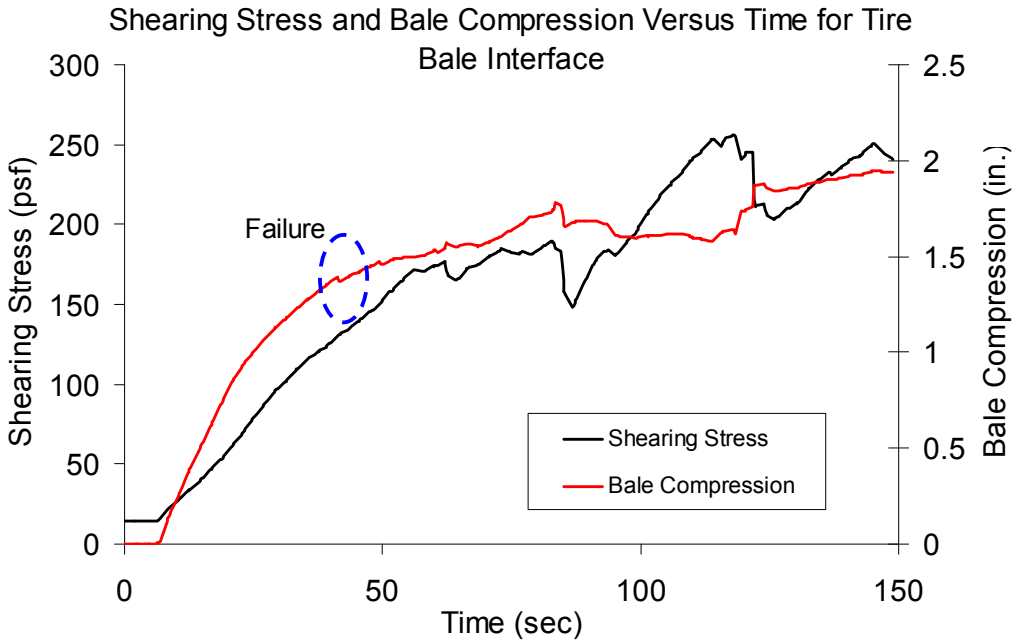

Figure D.27: Interface Shearing Resistance and Tire Bale Compression versus Elapsed Testing Time for the Dry Tire Bale Only Interface (Normal Stress = 180 psf)

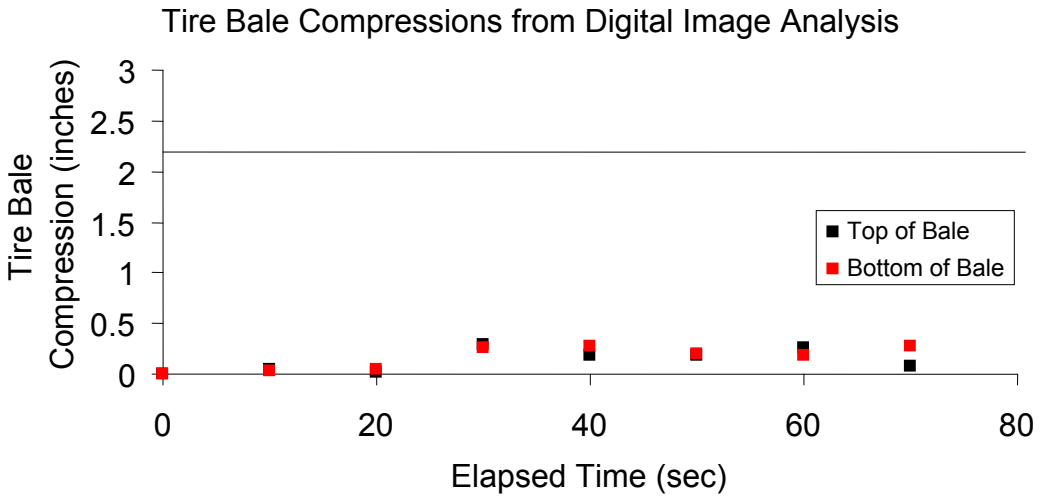

Figure D.28: Compressions of the Mobile Tire Bale Measured with Digital Image Analysis for the Dry Tire Bale Only Interface (Normal Stress = 180 psf)

Results for Dry Tire Bale Interface Test #6: Normal Stress = 180 psf

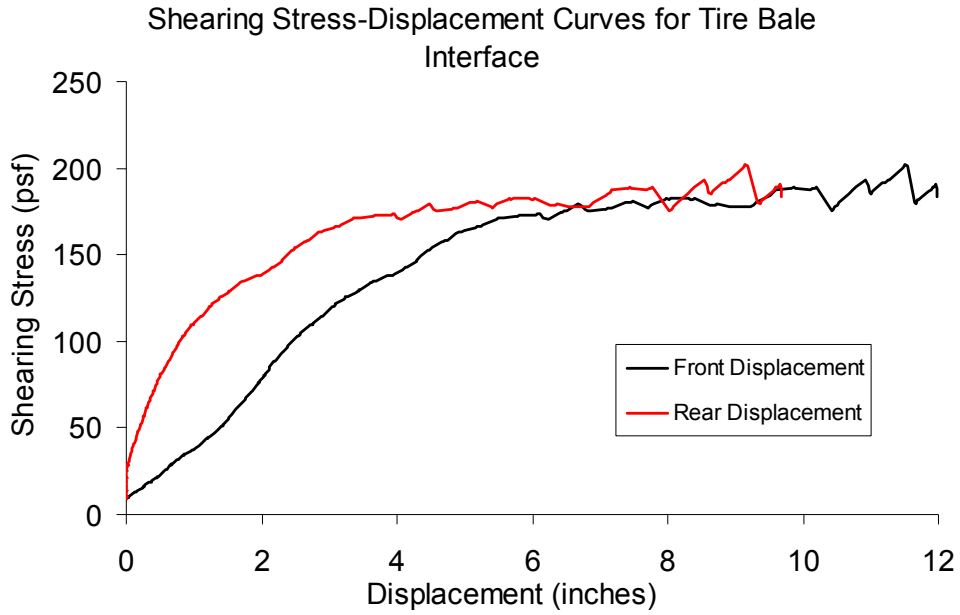

Figure D.29: Interface Shearing Resistance versus Displacement for the Dry Tire Bale Only Interface (Normal Stress = 180 psf)

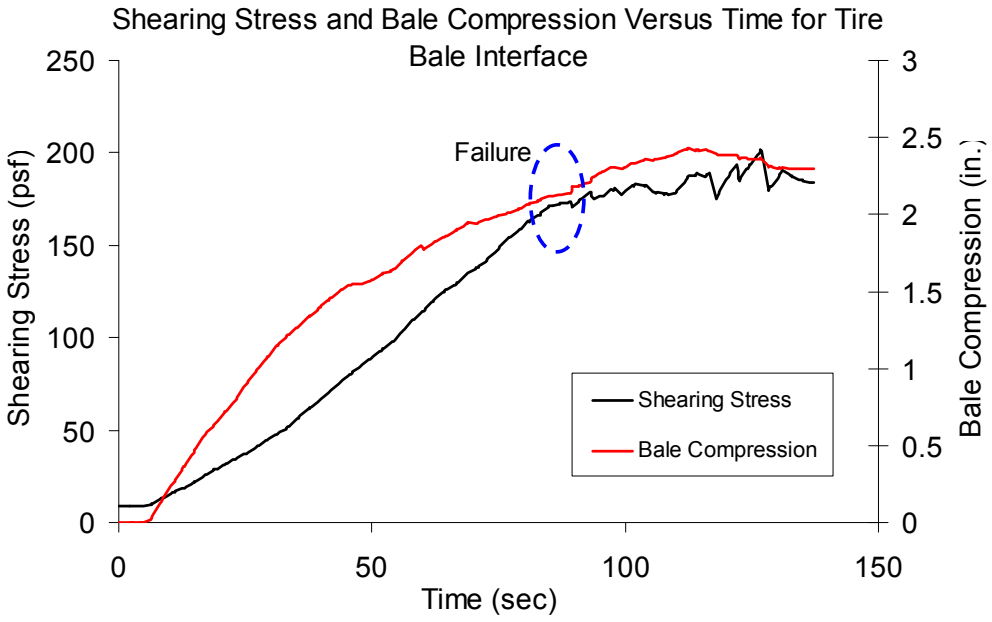

Figure D.30: Interface Shearing Resistance and Tire Bale Compression versus Elapsed Testing Time for the Dry Tire Bale Only Interface (Normal Stress = 180 psf)

Results for Partially Saturated (WAP) Tire Bale Interface Test #4: Normal Stress = 216 psf

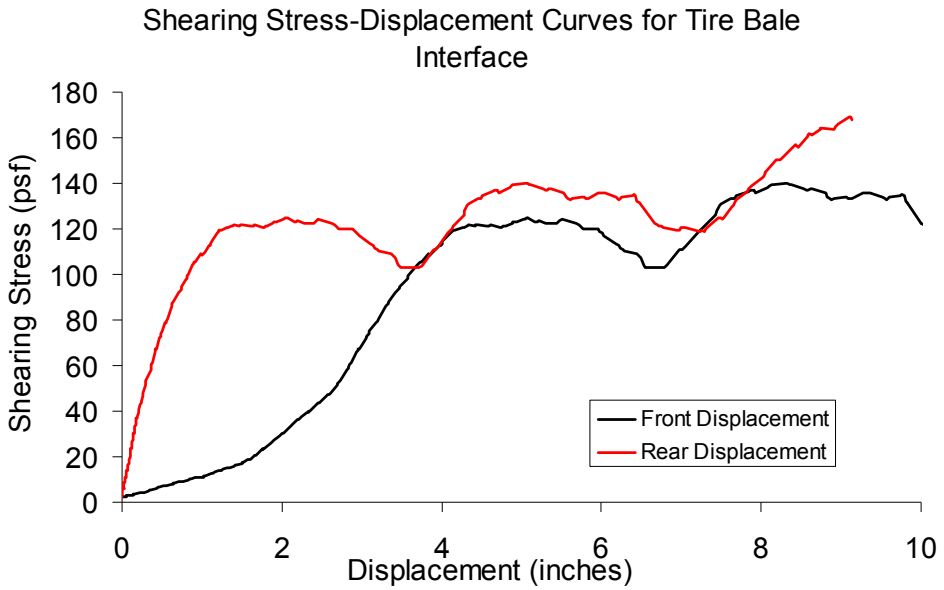

Figure D.31: Interface Shearing Resistance versus Displacement for the Partially Saturated (WAP) Tire Bale Only Interface (Normal Stress = 216 psf)

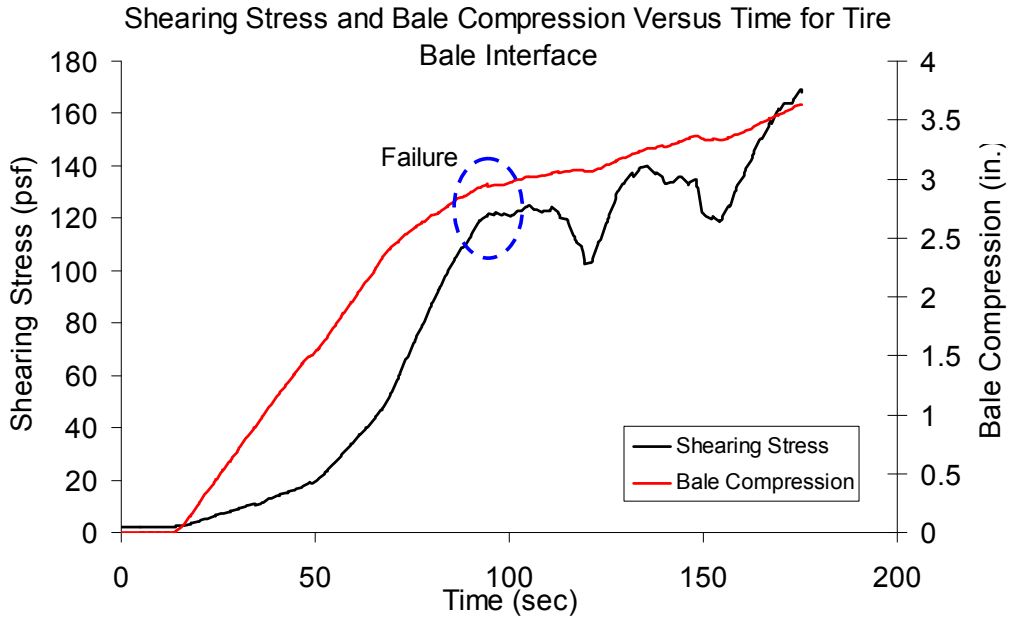

Figure D.32: Interface Shearing Resistance and Tire Bale Compression versus Elapsed Testing Time for the Partially Saturated (WAP) Tire Bale Only Interface (Normal Stress = 216 psf)

Results for Partially Saturated (WAP) Tire Bale Interface Test #5: Normal Stress = 216 psf

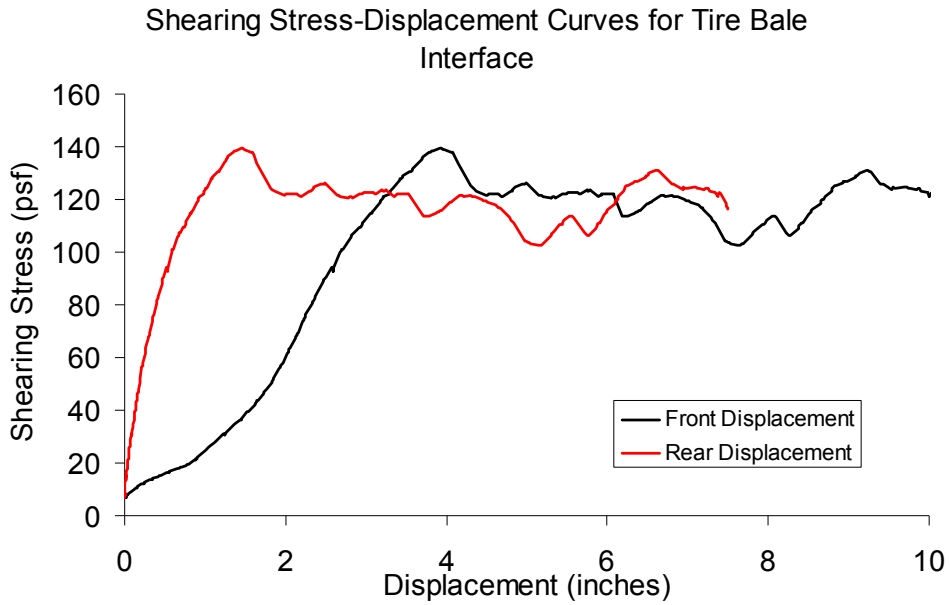

Figure D.33: Interface Shearing Resistance versus Displacement for the Partially Saturated (WAP) Tire Bale Only Interface (Normal Stress = 216 psf)

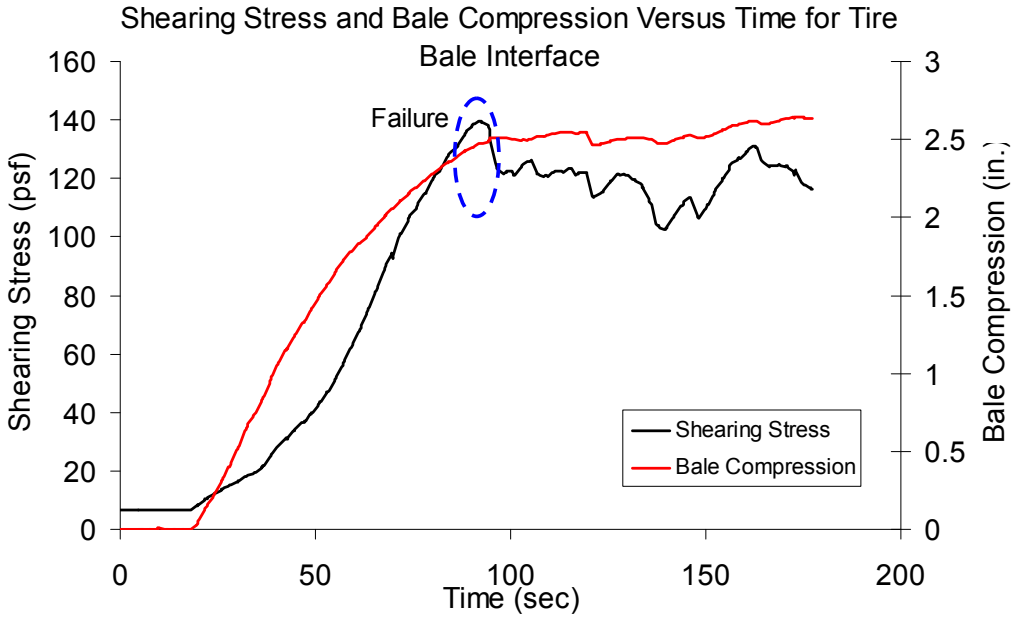

Figure D.34: Interface Shearing Resistance and Tire Bale Compression versus Elapsed Testing Time for the Partially Saturated (WAP) Tire Bale Only Interface (Normal Stress = 216 psf)

Results for Fully Saturated (WBP) Tire Bale Interface Test #5: Normal Stress = 216 psf

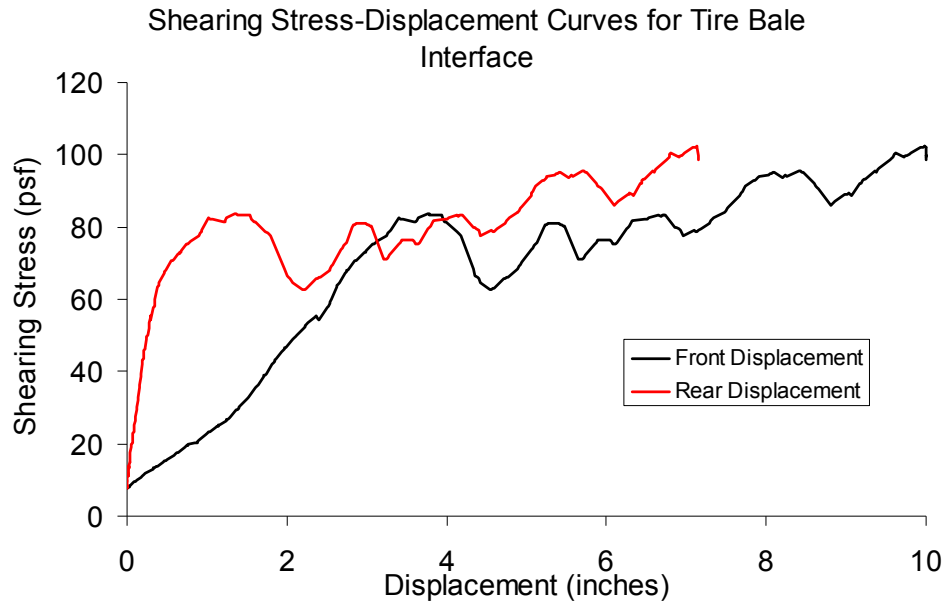

Figure D.35: Interface Shearing Resistance versus Displacement for the Fully Saturated (WBP) Tire Bale Only Interface (Normal Stress = 216 psf)

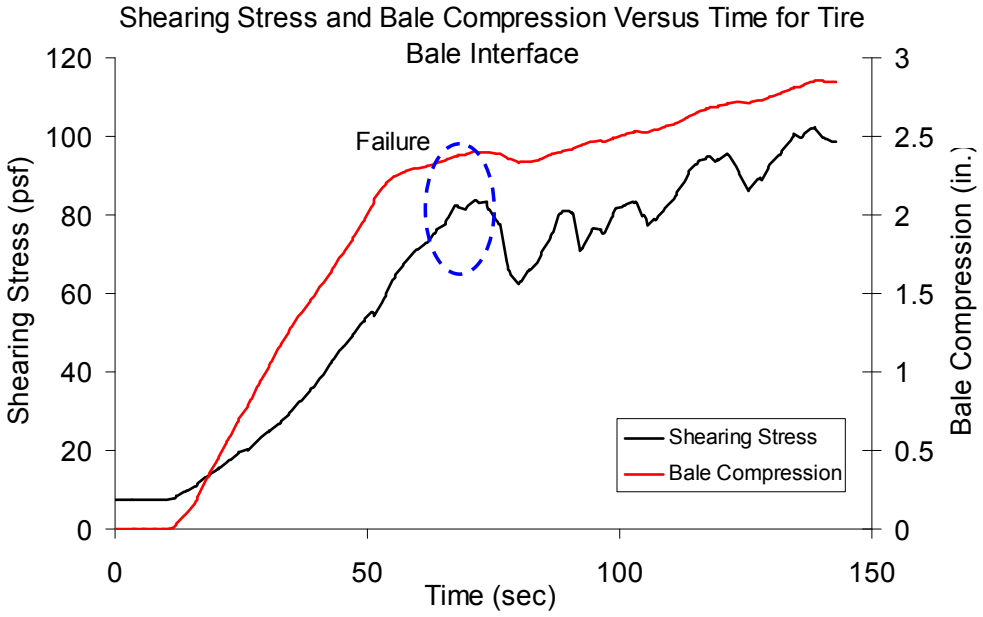

Figure D.36: Interface Shearing Resistance and Tire Bale Compression versus Elapsed Testing Time for the Fully Saturated (WBP) Tire Bale Only Interface (Normal Stress = 216 psf)

Results for Fully Saturated (WBP) Tire Bale Interface Test #6: Normal Stress = 216 psf

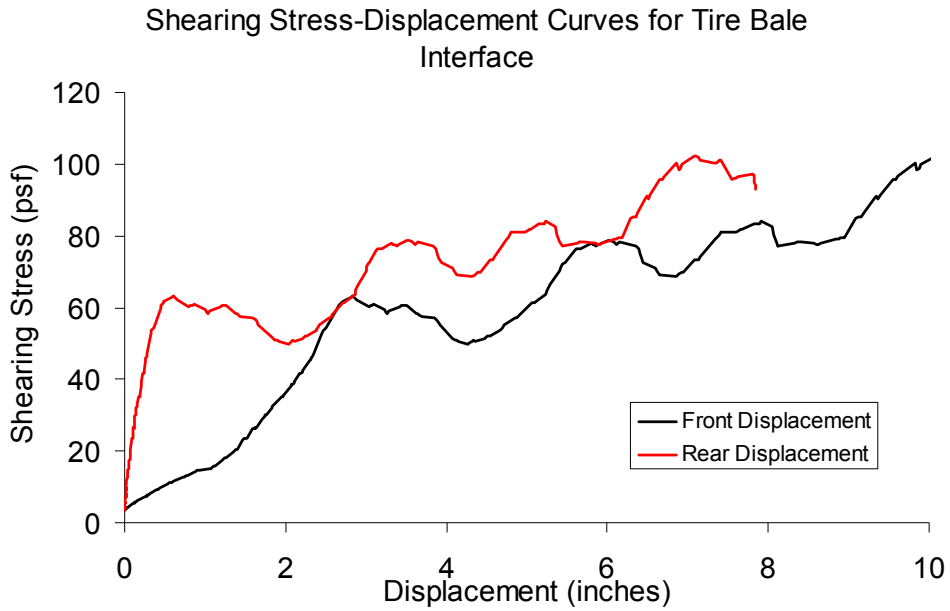

Figure D.37: Interface Shearing Resistance versus Displacement for the Fully Saturated (WBP) Tire Bale Only Interface (Normal Stress = 216 psf)

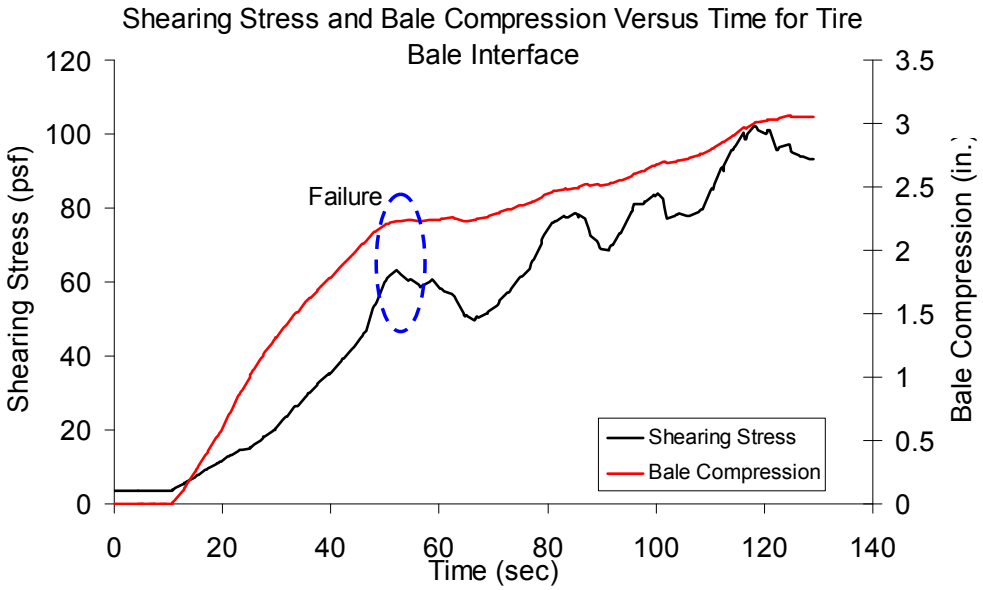

Figure D.38: Interface Shearing Resistance and Tire Bale Compression versus Elapsed Testing Time for the Fully Saturated (WBP) Tire Bale Only Interface (Normal Stress = 216 psf)

Results for Dry Tire Bale Interface Test #7: Normal Stress = 252 psf

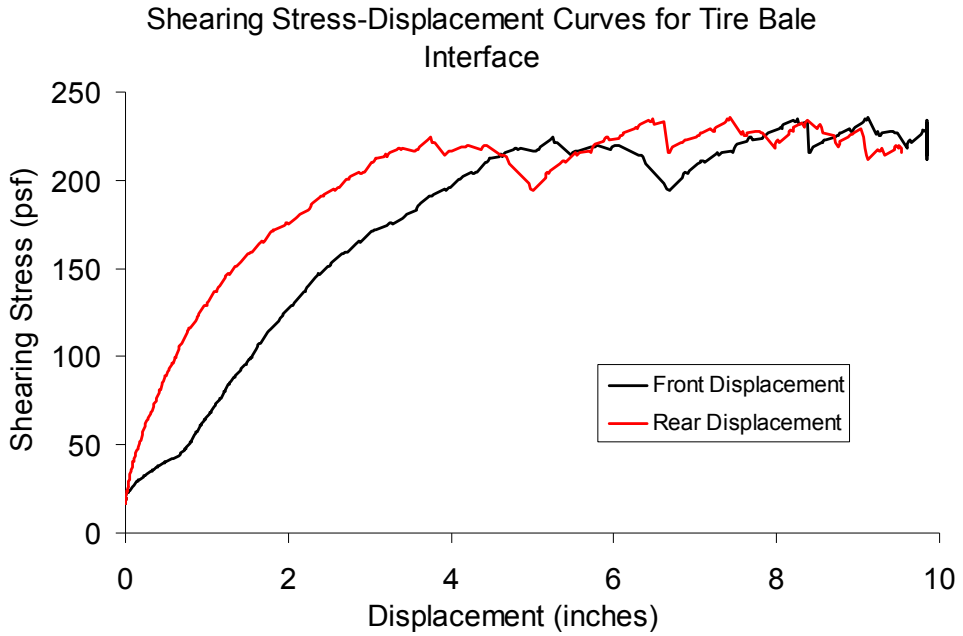

Figure D.39: Interface Shearing Resistance versus Displacement for the Dry Tire Bale Only Interface (Normal Stress = 252 psf)

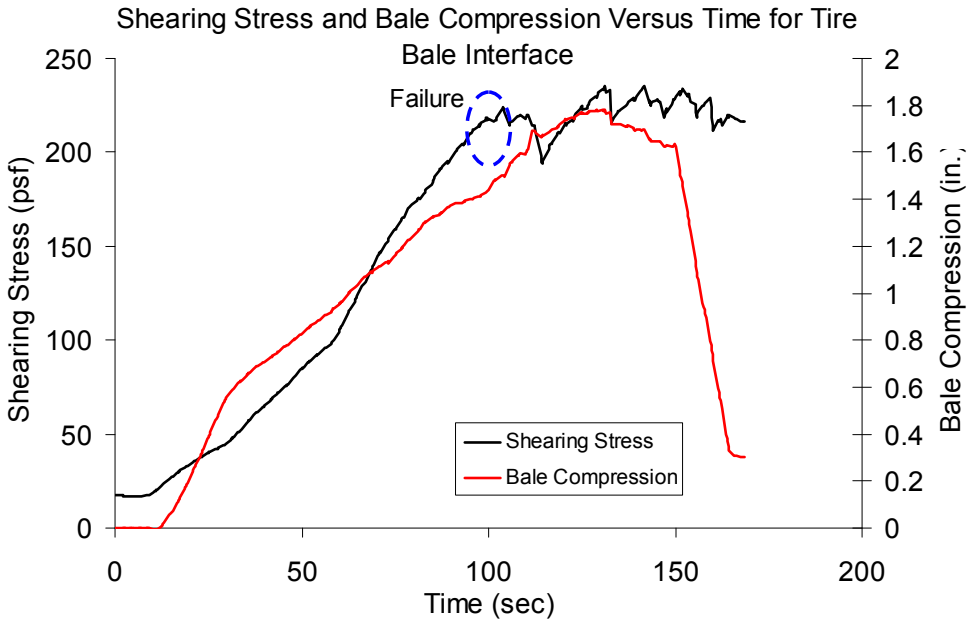

Figure D.40: Interface Shearing Resistance and Tire Bale Compression versus Elapsed Testing Time for the Dry Tire Bale Only Interface (Normal Stress = 252 psf)

Results for Dry Tire Bale Interface Test #8: Normal Stress = 252 psf

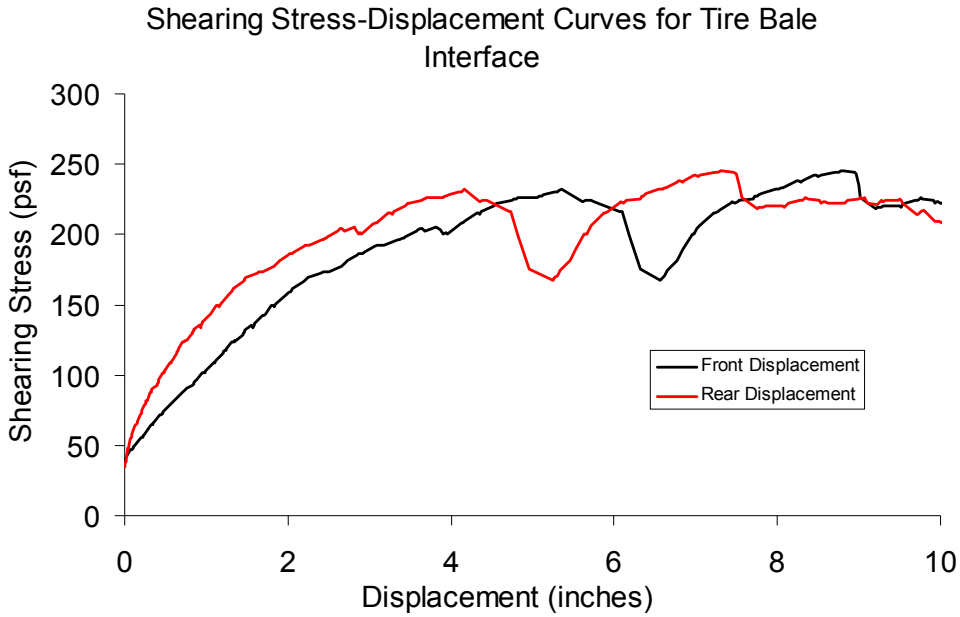

Figure D.41: Interface Shearing Resistance versus Displacement for the Dry Tire Bale Only Interface (Normal Stress = 252 psf)

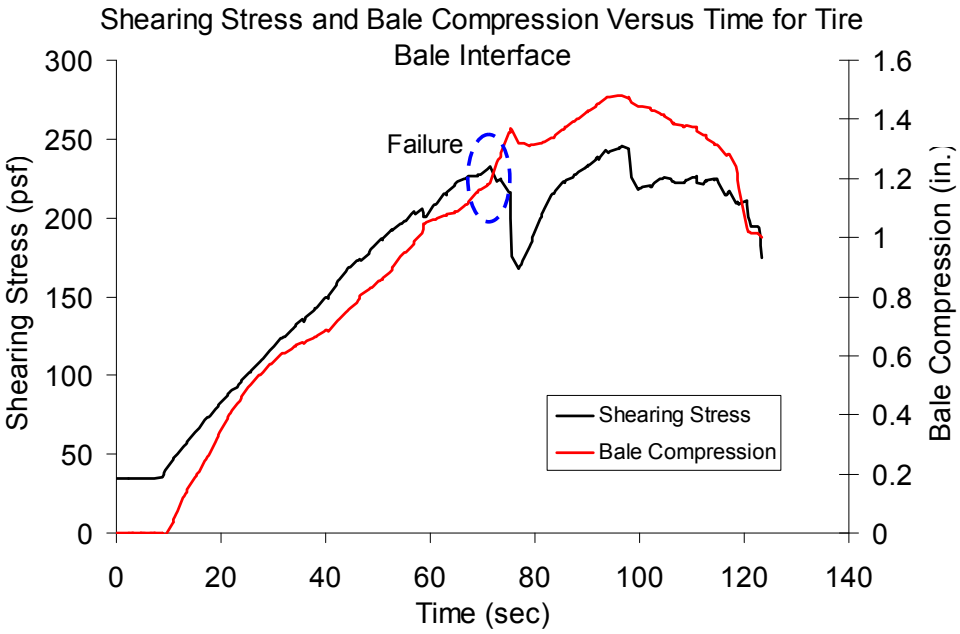

Figure D.42: Interface Shearing Resistance and Tire Bale Compression versus Elapsed Testing Time for the Dry Tire Bale Only Interface (Normal Stress = 252 psf)

Results for Dry Tire Bale Interface Test #9: Normal Stress = 288 psf

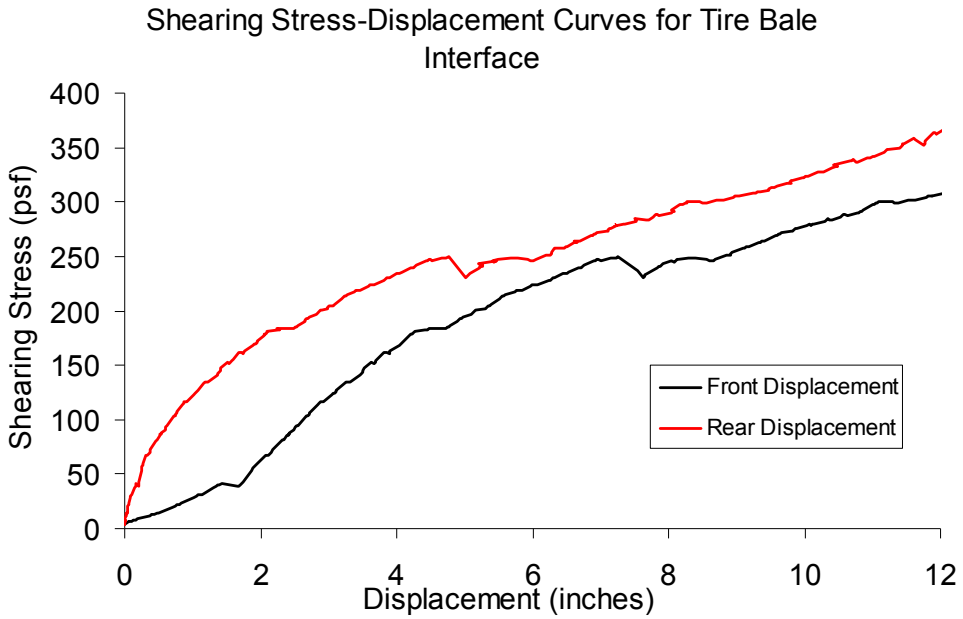

Figure D.43: Interface Shearing Resistance versus Displacement for the Dry Tire Bale Only Interface (Normal Stress = 288 psf)

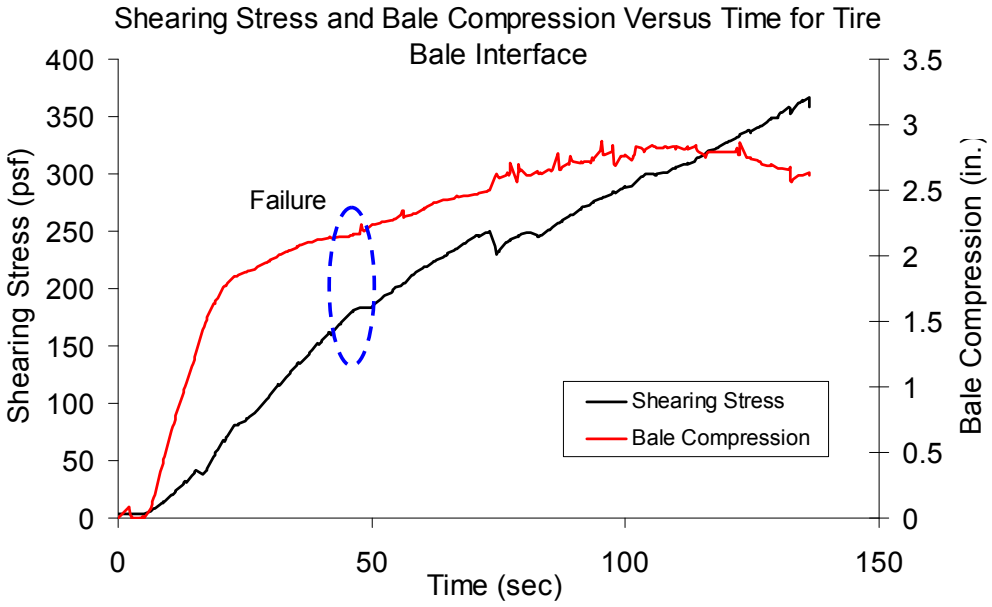

Figure D.44: Interface Shearing Resistance and Tire Bale Compression versus Elapsed Testing Time for the Dry Tire Bale Only Interface (Normal Stress = 288 psf)

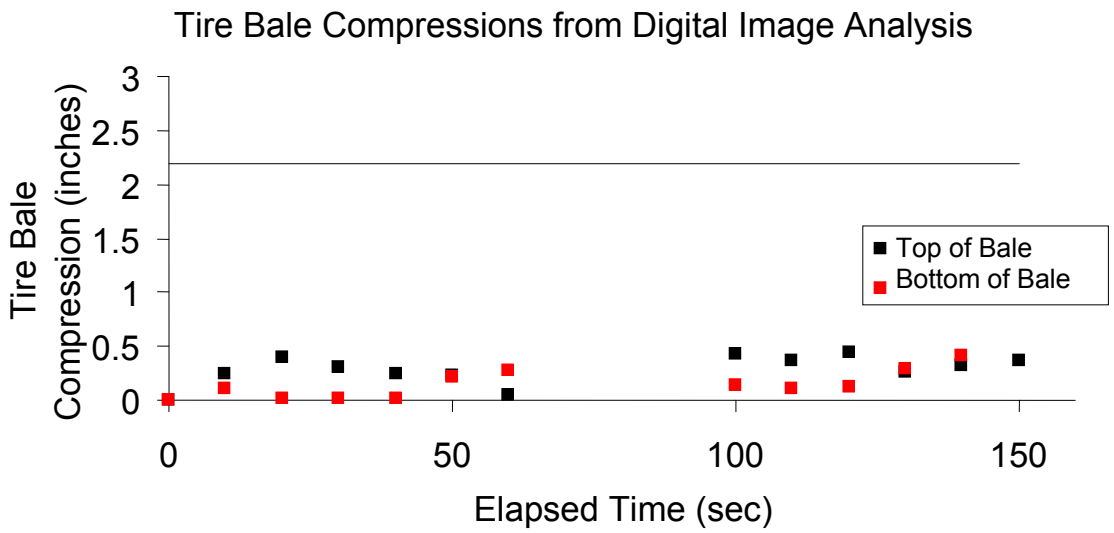

Figure D.45: Compressions of the Mobile Tire Bale Measured with Digital Image Analysis for the Dry Tire Bale Only Interface (Normal Stress = 288 psf)

Results for Dry Tire Bale Interface Test #10: Normal Stress = 288 psf

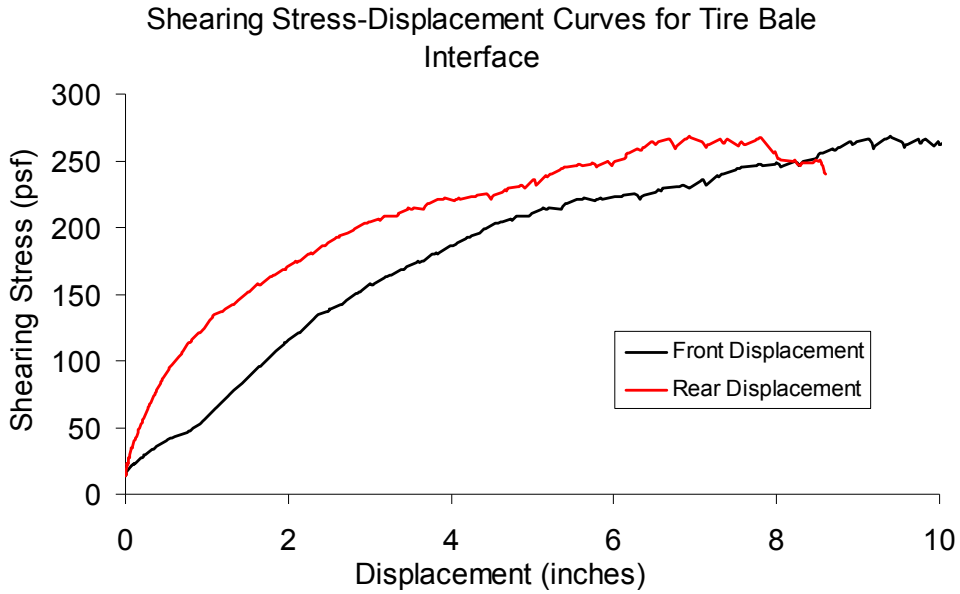

Figure D.46: Interface Shearing Resistance versus Displacement for the Dry Tire Bale Only Interface (Normal Stress = 288 psf)

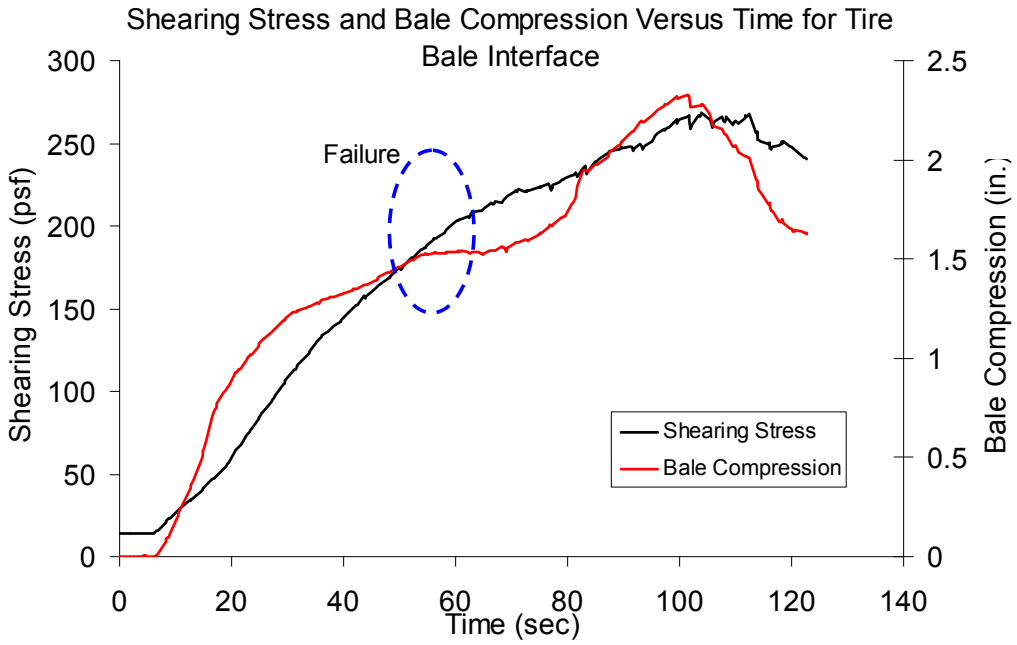

Figure D.47: Interface Shearing Resistance and Tire Bale Compression versus Elapsed Testing Time for the Dry Tire Bale Only Interface (Normal Stress = 288 psf)

Results for Dry Tire Bale Interface Test #11: Normal Stress = 361 psf

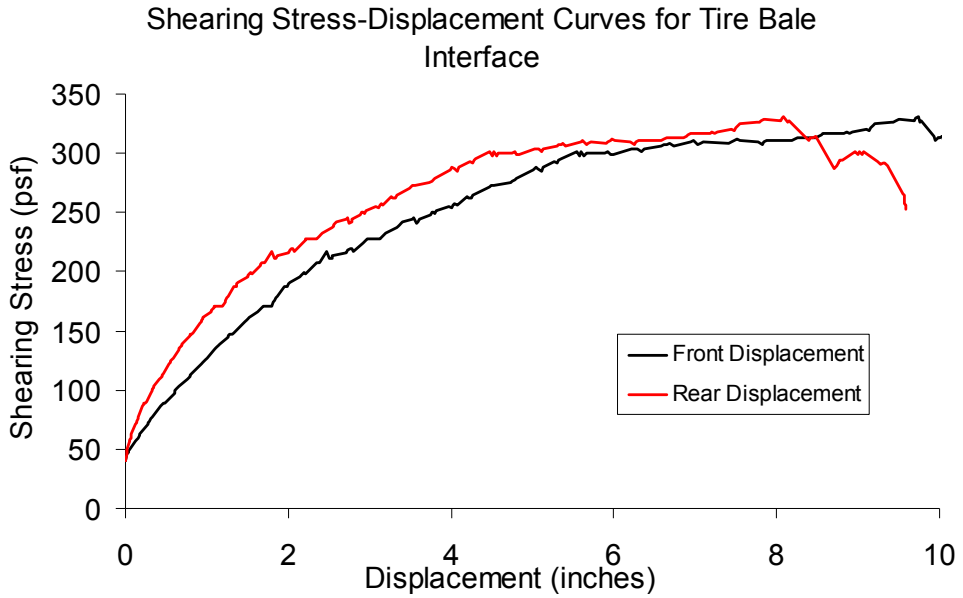

Figure D.48: Interface Shearing Resistance versus Displacement for the Dry Tire Bale Only Interface (Normal Stress = 361 psf)

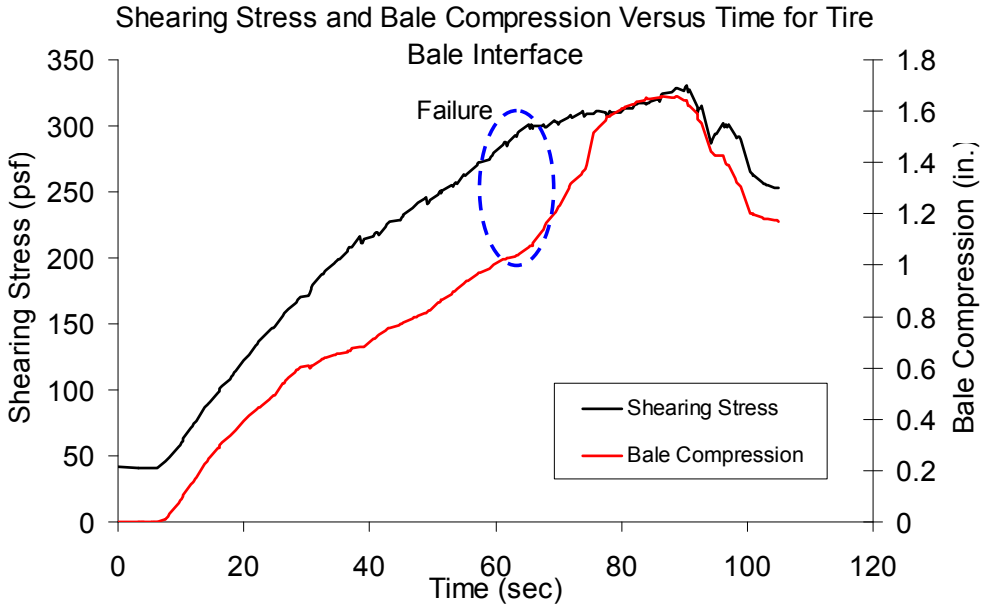

Figure D.49: Interface Shearing Resistance and Tire Bale Compression versus Elapsed Testing Time for the Dry Tire Bale Only Interface (Normal Stress = 361 psf)

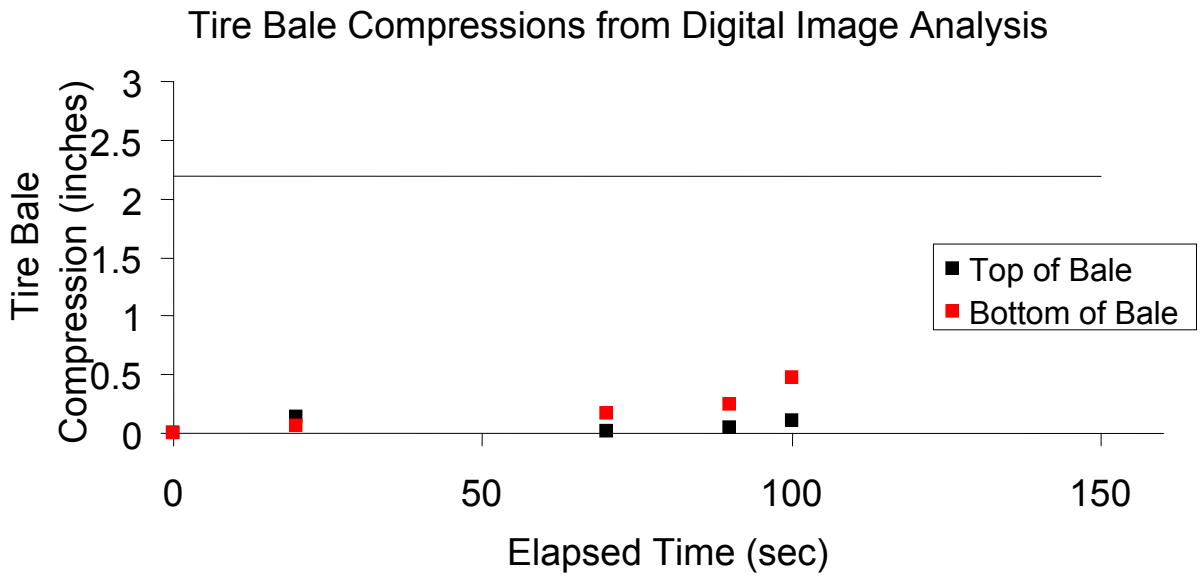

Figure D.50: Compressions of the Mobile Tire Bale Measured with Digital Image Analysis for the Dry Tire Bale Only Interface (Normal Stress = 361 psf)

Results for Dry Tire Bale Interface Test #12: Normal Stress = 361 psf

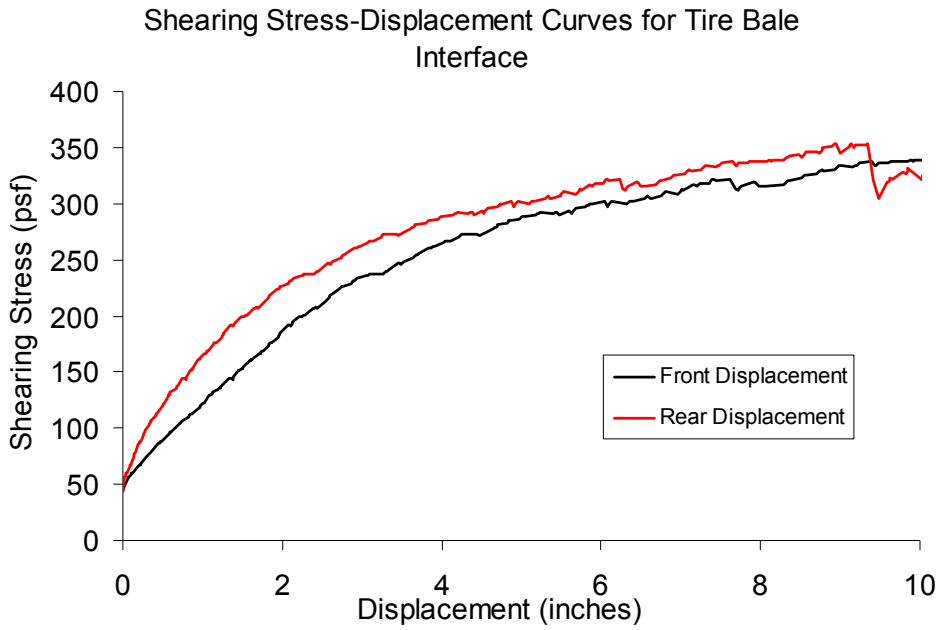

Figure D.51: Interface Shearing Resistance versus Displacement for the Dry Tire Bale Only Interface (Normal Stress = 361 psf)

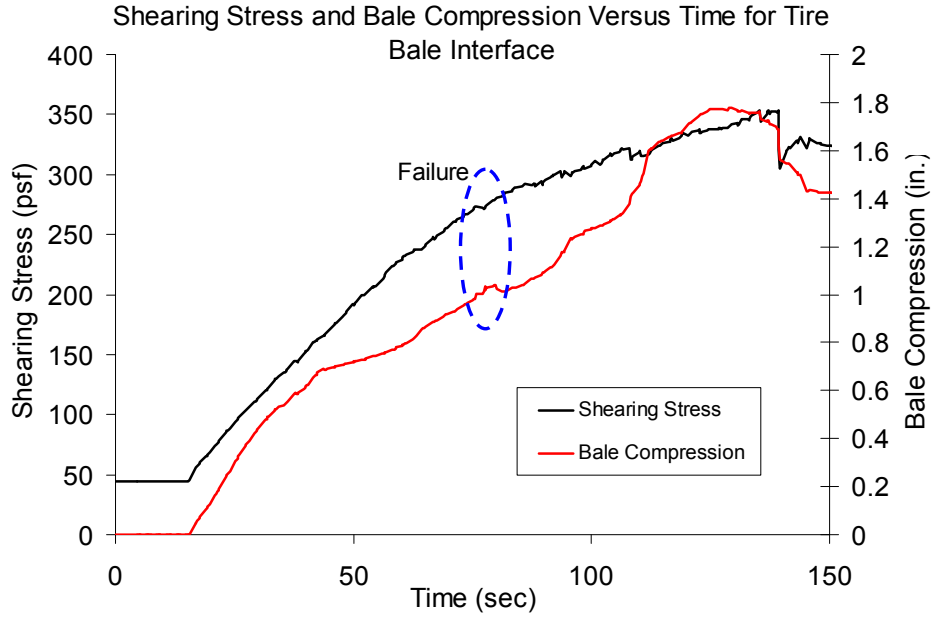

Figure D.52: Interface Shearing Resistance and Tire Bale Compression versus Elapsed Testing Time for the Dry Tire Bale Only Interface (Normal Stress = 361 psf)

Results for Partially Saturated (WAP) Tire Bale Interface Test #6: Normal Stress = 361 psf

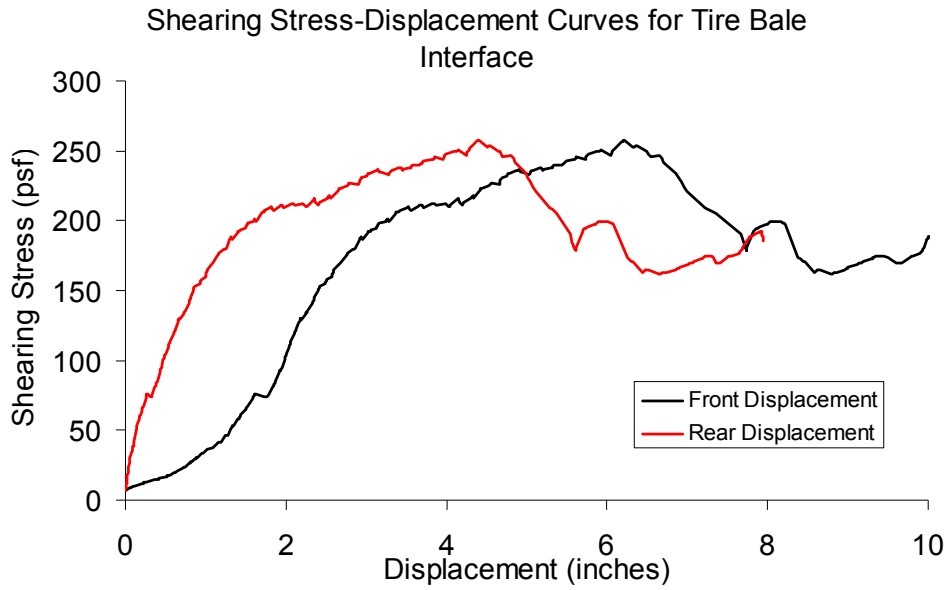

Figure D.53: Interface Shearing Resistance versus Displacement for the Partially Saturated (WAP) Tire Bale Only Interface (Normal Stress = 361 psf)

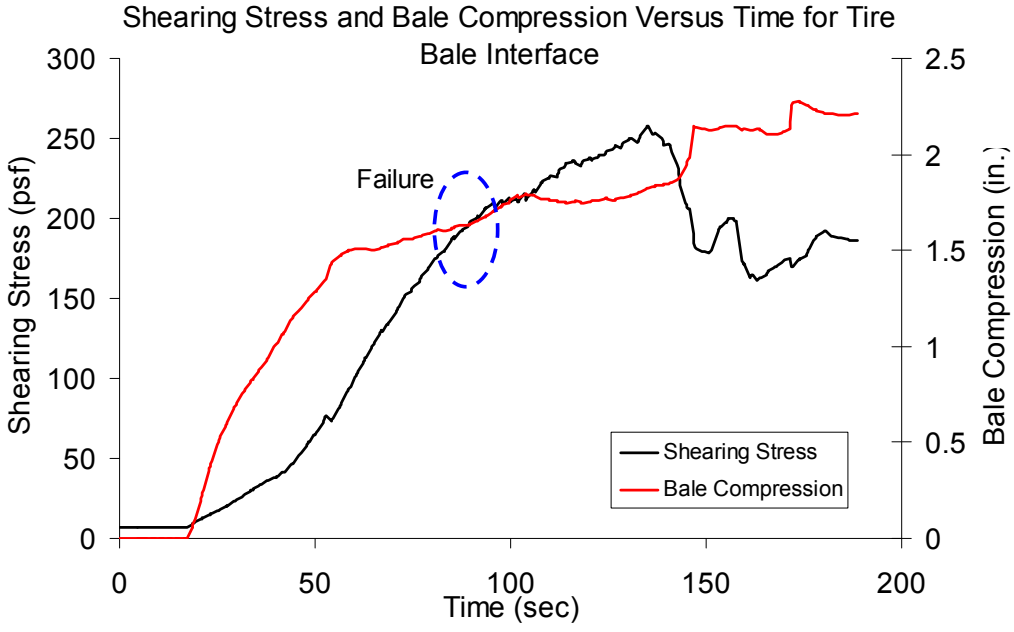

Figure D.54: Interface Shearing Resistance and Tire Bale Compression versus Elapsed Testing Time for the Partially Saturated (WAP) Tire Bale Only Interface (Normal Stress = 361 psf)

Results for Fully Saturated (WAP) Tire Bale Interface Test #7: Normal Stress = 361 psf

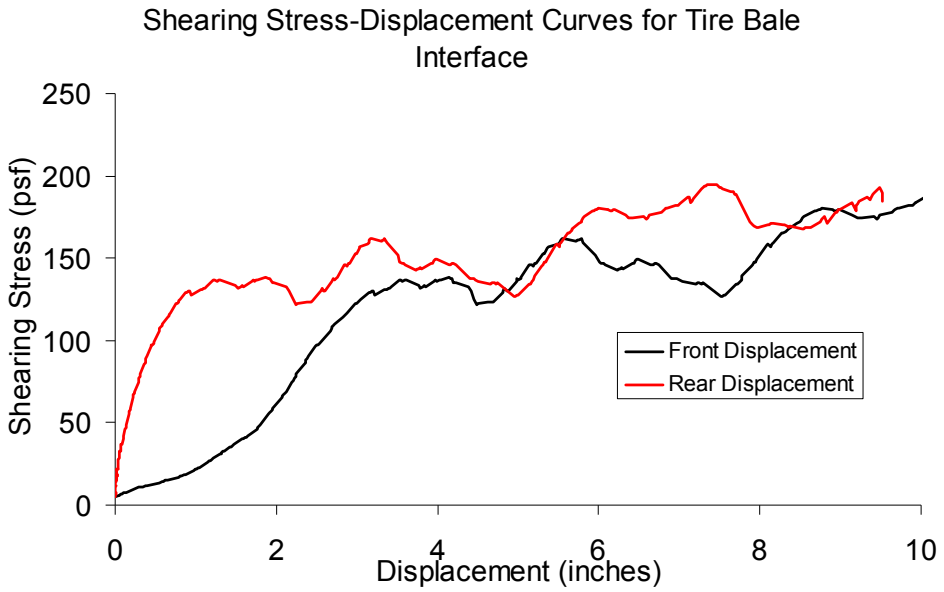

Figure D.55: Interface Shearing Resistance versus Displacement for the Fully Saturated (WBP) Tire Bale Only Interface (Normal Stress = 361 psf)

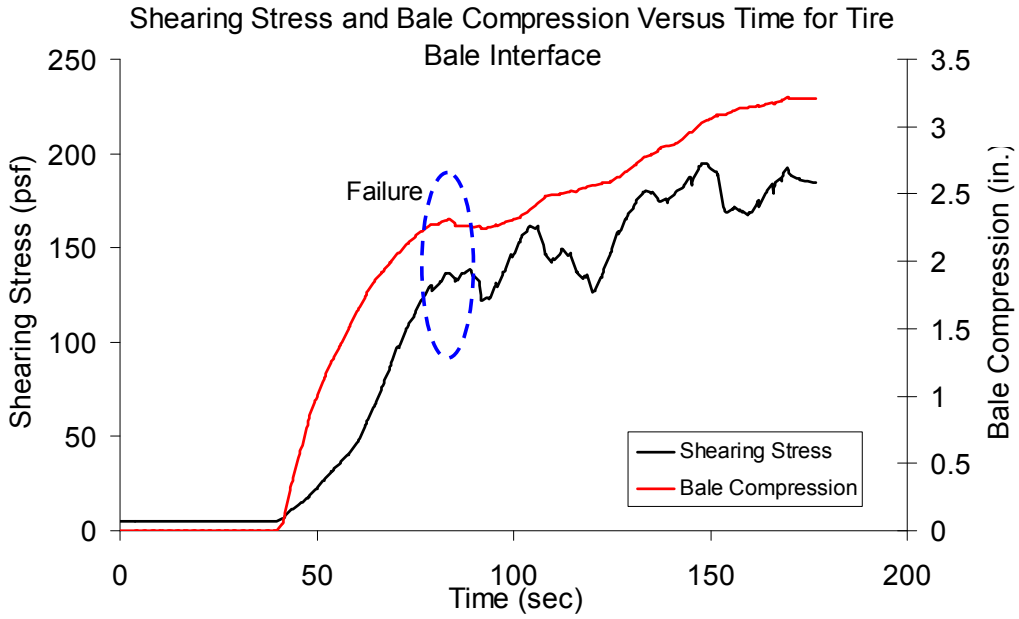

Figure D.56: Interface Shearing Resistance and Tire Bale Compression versus Elapsed Testing Time for the Fully Saturated (WBP) Tire Bale Only Interface (Normal Stress = 361 psf)

Results for Fully Saturated (WAP) Tire Bale Interface Test #8: Normal Stress = 361 psf

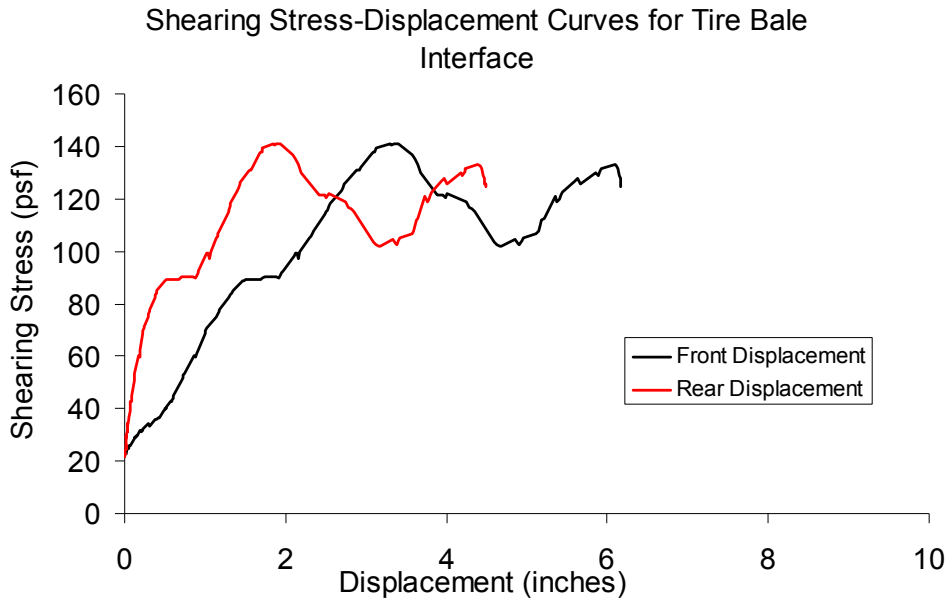

Figure D.57: Interface Shearing Resistance versus Displacement for the Fully Saturated (WBP) Tire Bale Only Interface (Normal Stress = 361 psf)

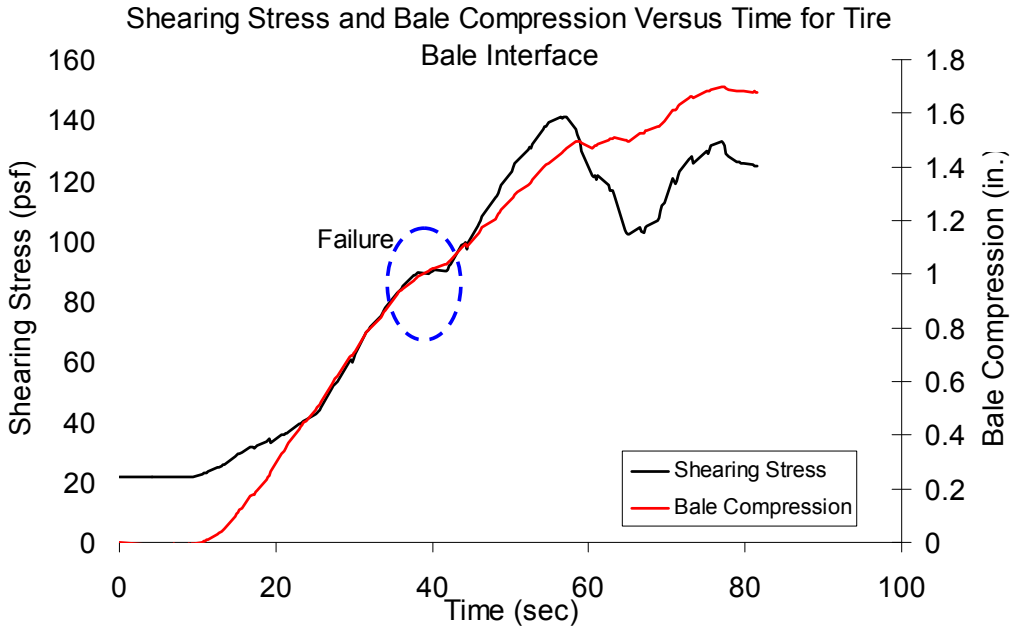

Figure D.58: Interface Shearing Resistance and Tire Bale Compression versus Elapsed Testing Time for the Fully Saturated (WBP) Tire Bale Only Interface (Normal Stress = 361 psf)

Appendix E: Testing Data from the Large Scale Direct Shear Testing of the Anisotropic Tire Bale Only Interface

The following appendix section provides the data obtained for each of the large scale direct shear tests conducted for the dry and wet anisotropic tire bale interfaces that was not specifically reported in Chapter 6. A detailed analysis of the data is provided in Chapter 6.4.

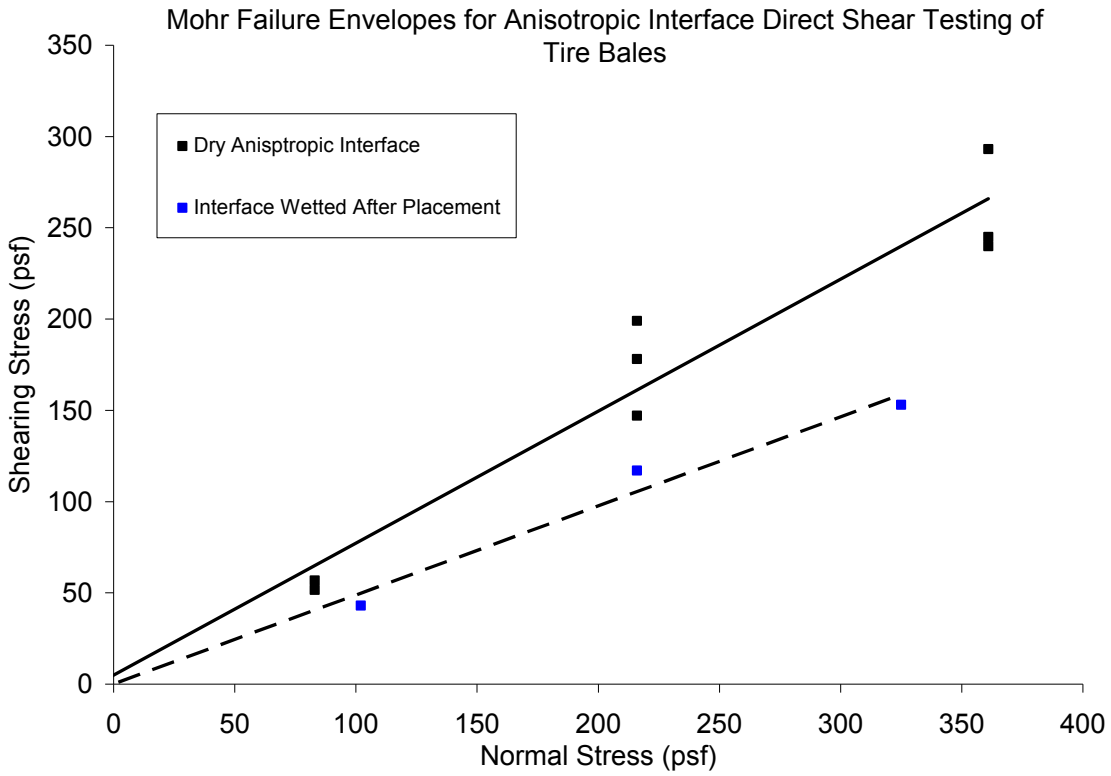

Figure E.1: Shear Strength Envelopes for the Dry and Wet Anisotropic Tire Bale Only Interfaces

Results for Anisotropic Dry Tire Bale Interface Test #1: Normal Stress = 83 psf

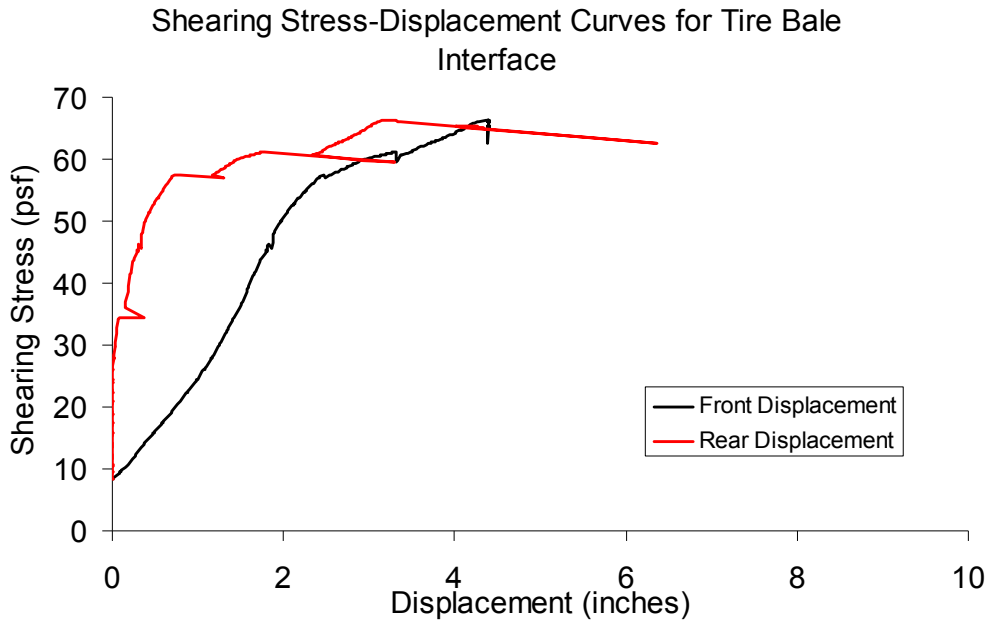

Figure E.2: Interface Shearing Resistance versus Displacement for the Dry Anisotropic Tire Bale Only Interface (Normal Stress = 83 psf)

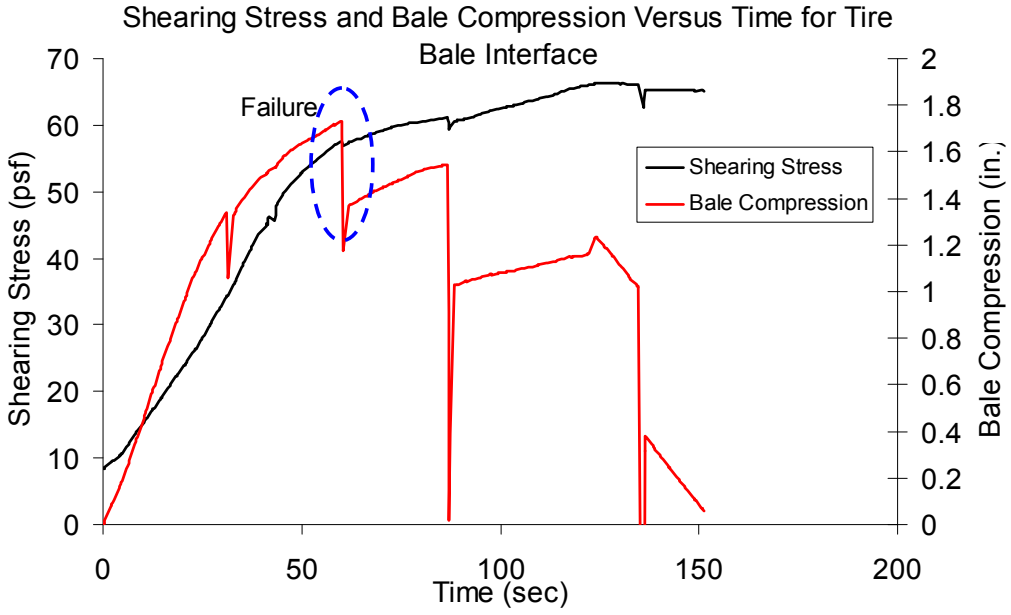

Figure E.3: Interface Shearing Resistance and Tire Bale Compression versus Elapsed Testing Time for the Dry Anisotropic Tire Bale Only Interface (Normal Stress = 83 psf)

Results for Anisotropic Dry Tire Bale Interface Test #2: Normal Stress = 83 psf

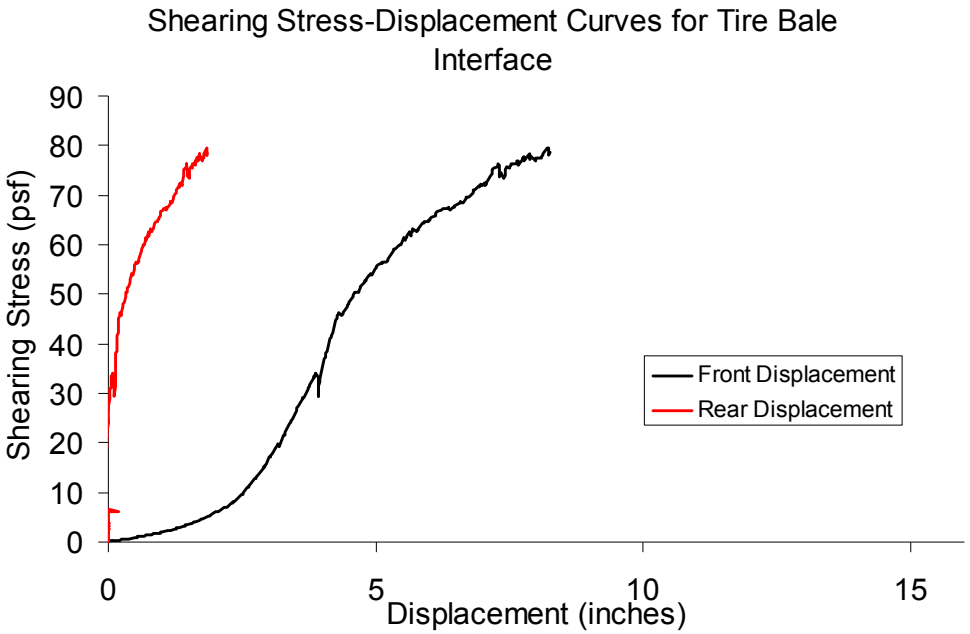

Figure E.4: Interface Shearing Resistance versus Displacement for the Dry Anisotropic Tire Bale Only Interface (Normal Stress = 83 psf)

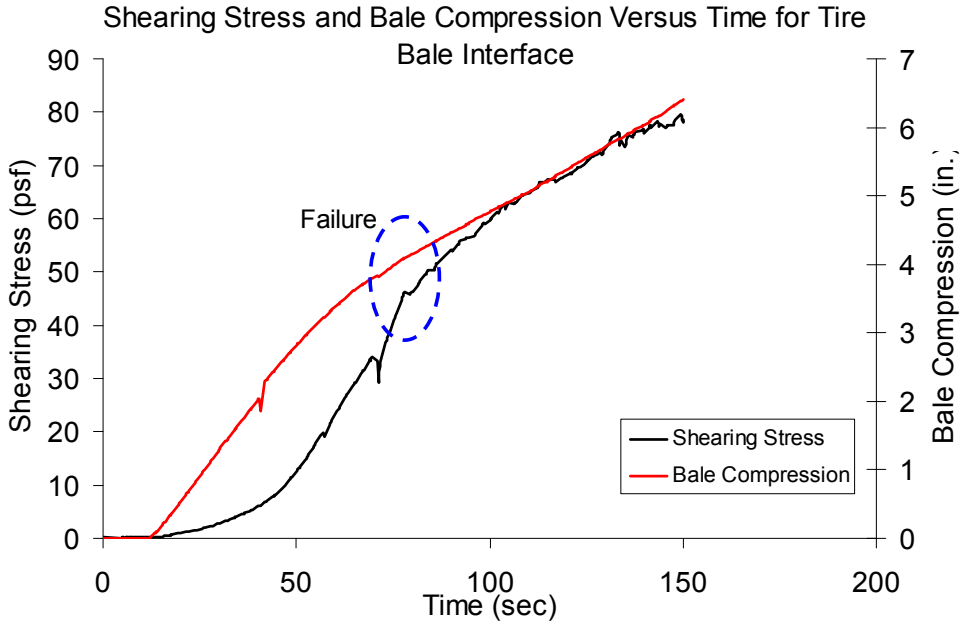

Figure E.5: Interface Shearing Resistance and Tire Bale Compression versus Elapsed Testing Time for the Dry Anisotropic Tire Bale Only Interface (Normal Stress = 83 psf)

Results for Anisotropic Wet Tire Bale Interface Test #1: Normal Stress = 102 psf

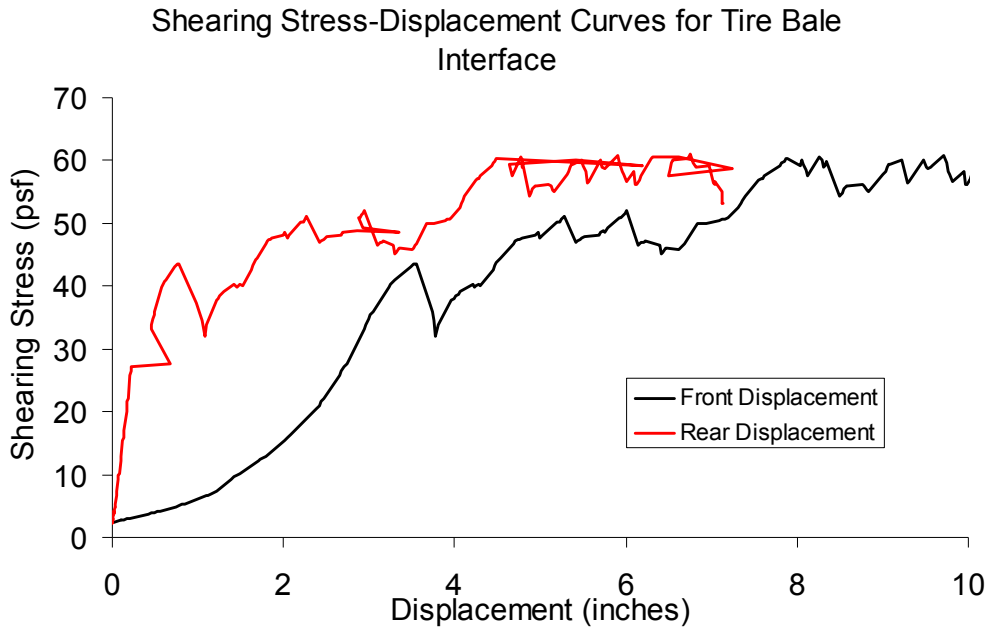

Figure E.6: Interface Shearing Resistance versus Displacement for the Wet Anisotropic Tire Bale Only Interface (Normal Stress = 102 psf)

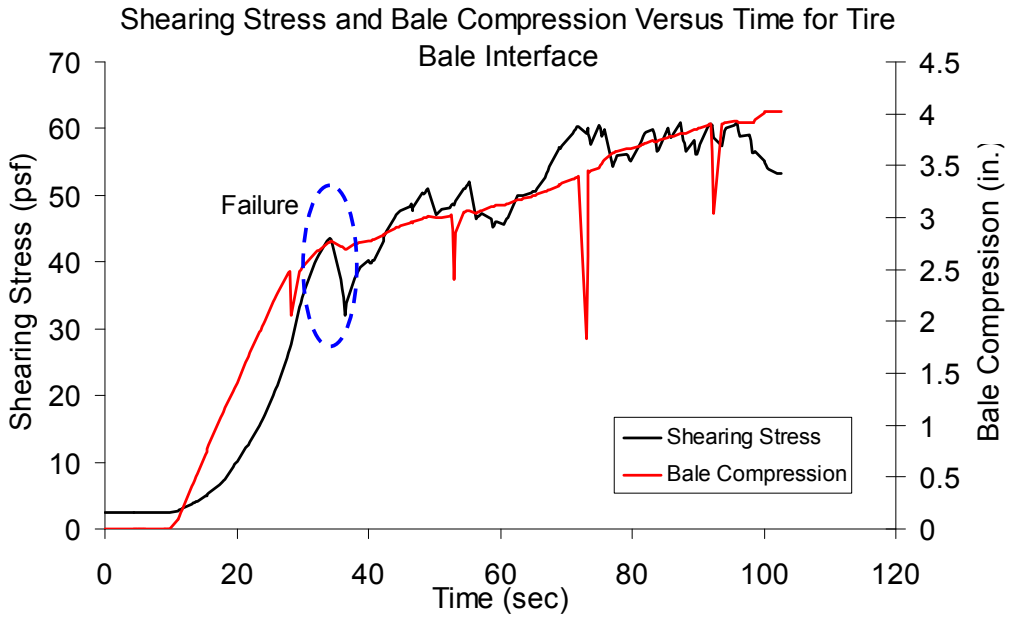

Figure E.7: Interface Shearing Resistance and Tire Bale Compression versus Elapsed Testing Time for the Wet Anisotropic Tire Bale Only Interface (Normal Stress = 102 psf)

Results for Anisotropic Dry Tire Bale Interface Test #3: Normal Stress = 216 psf

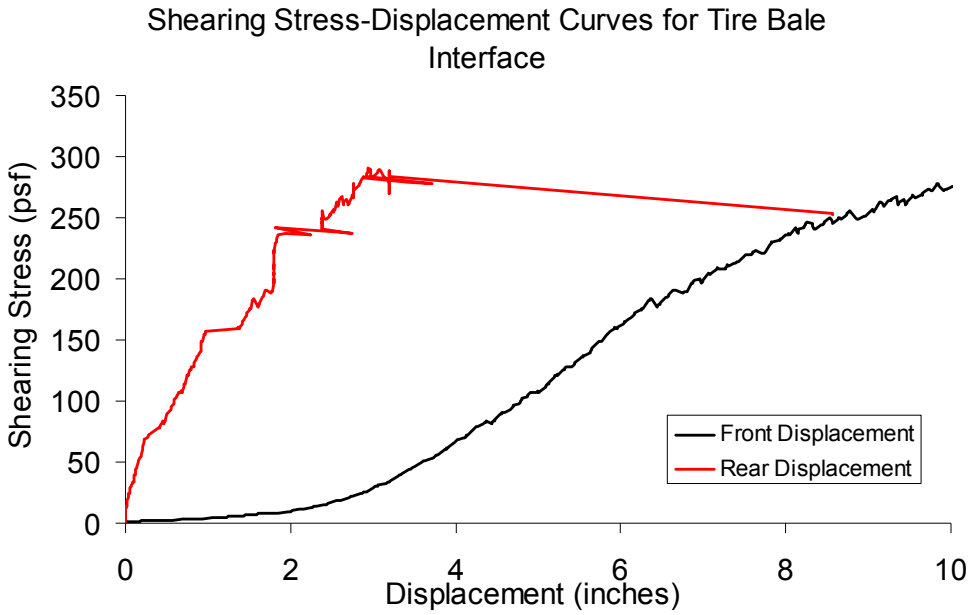

Figure E.8: Interface Shearing Resistance versus Displacement for the Dry Anisotropic Tire Bale Only Interface (Normal Stress = 216 psf)

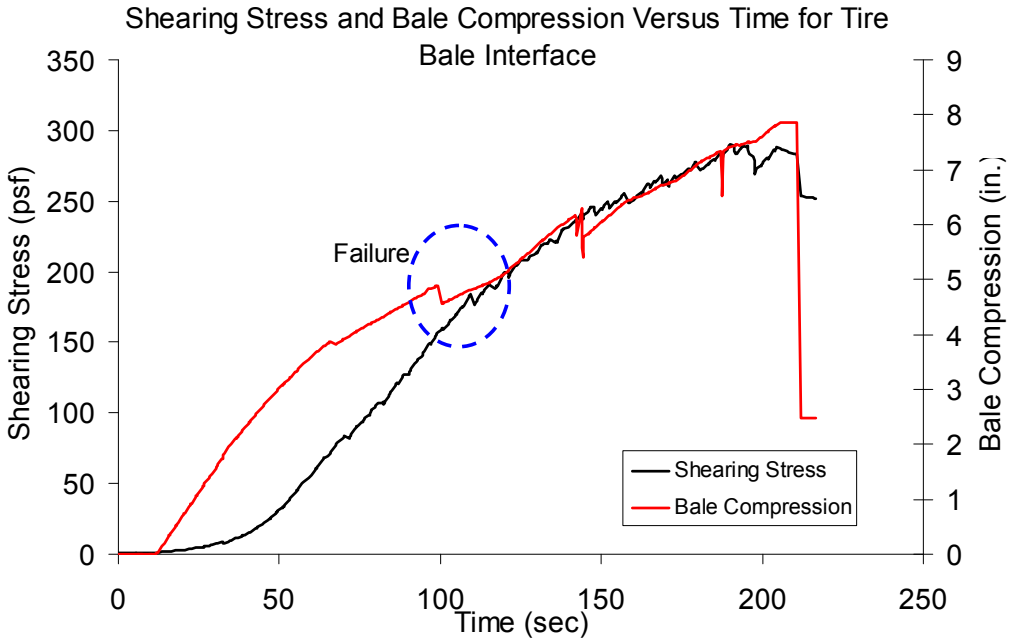

Figure E.9: Interface Shearing Resistance and Tire Bale Compression versus Elapsed Testing Time for the Dry Anisotropic Tire Bale Only Interface (Normal Stress = 216 psf)

Results for Anisotropic Dry Tire Bale Interface Test #4: Normal Stress = 216 psf

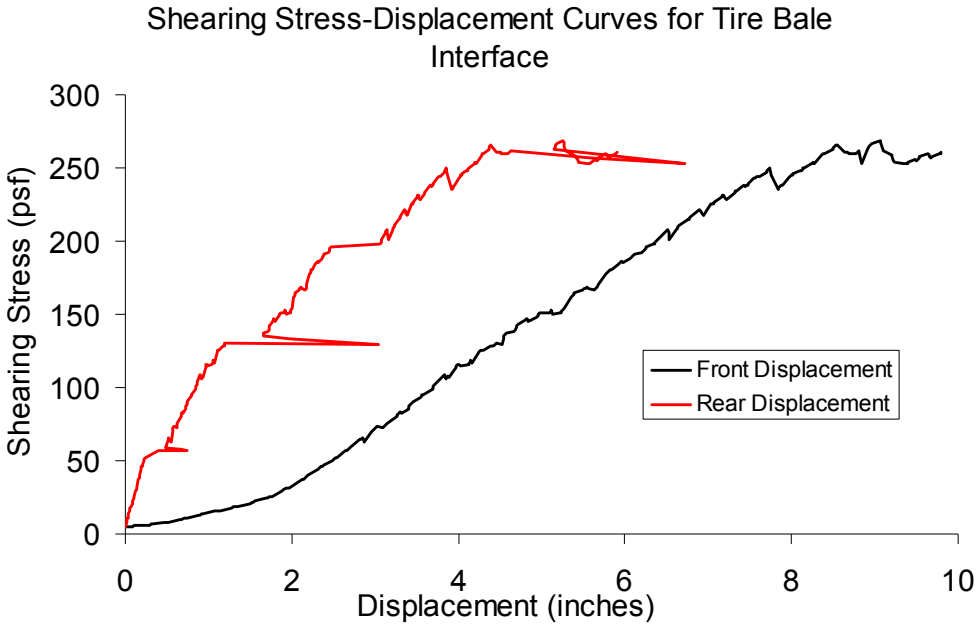

Figure E.10: Interface Shearing Resistance versus Displacement for the Dry Anisotropic Tire Bale Only Interface (Normal Stress = 216 psf)

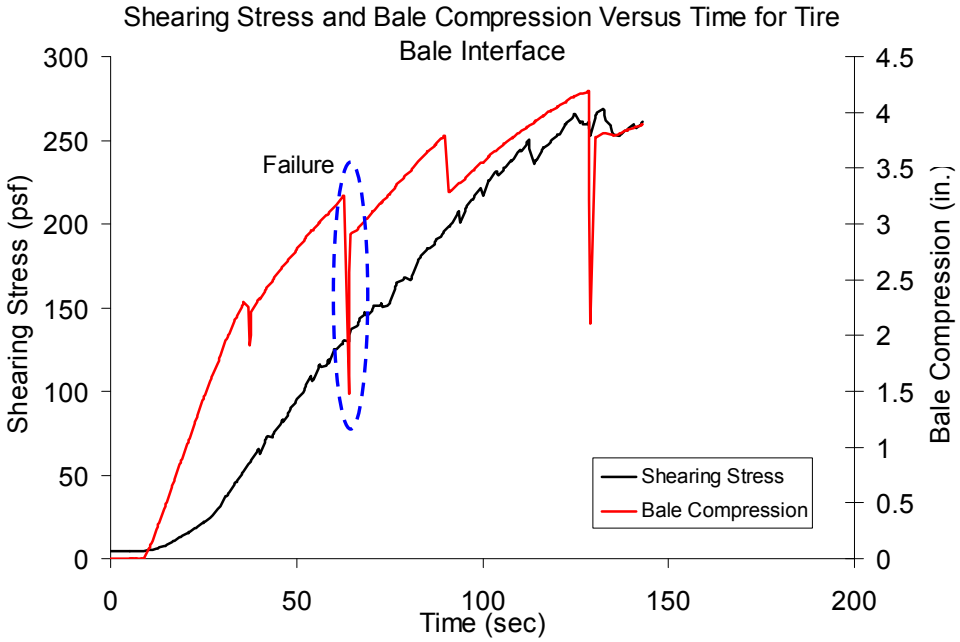

Figure E.11: Interface Shearing Resistance and Tire Bale Compression versus Elapsed Testing Time for the Dry Anisotropic Tire Bale Only Interface (Normal Stress = 216 psf)

Results for Anisotropic Wet Tire Bale Interface Test #2: Normal Stress = 216 psf

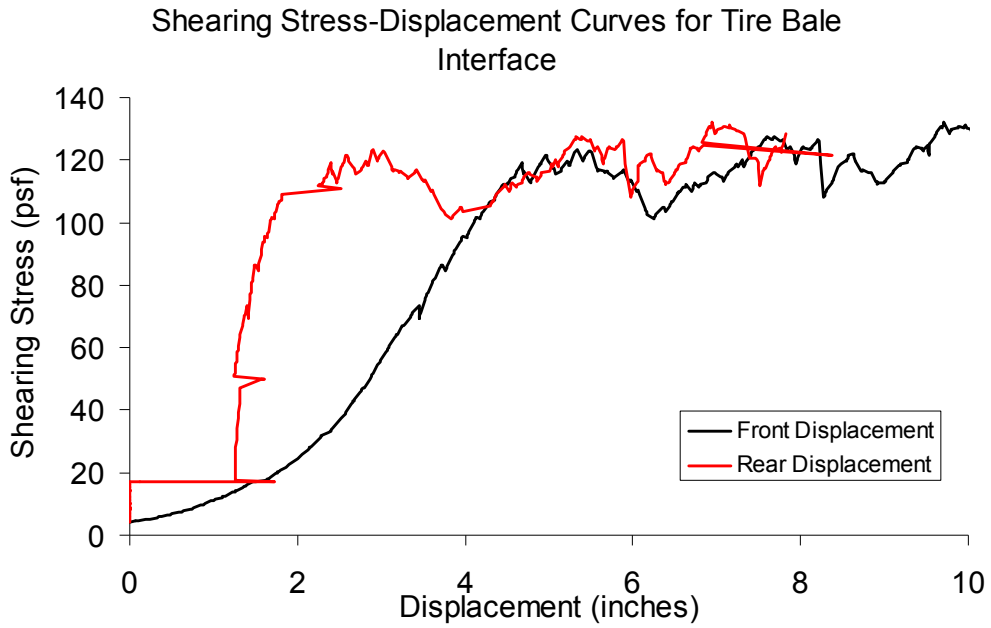

Figure E.12: Interface Shearing Resistance versus Displacement for the Wet Anisotropic Tire Bale Only Interface (Normal Stress = 216 psf)

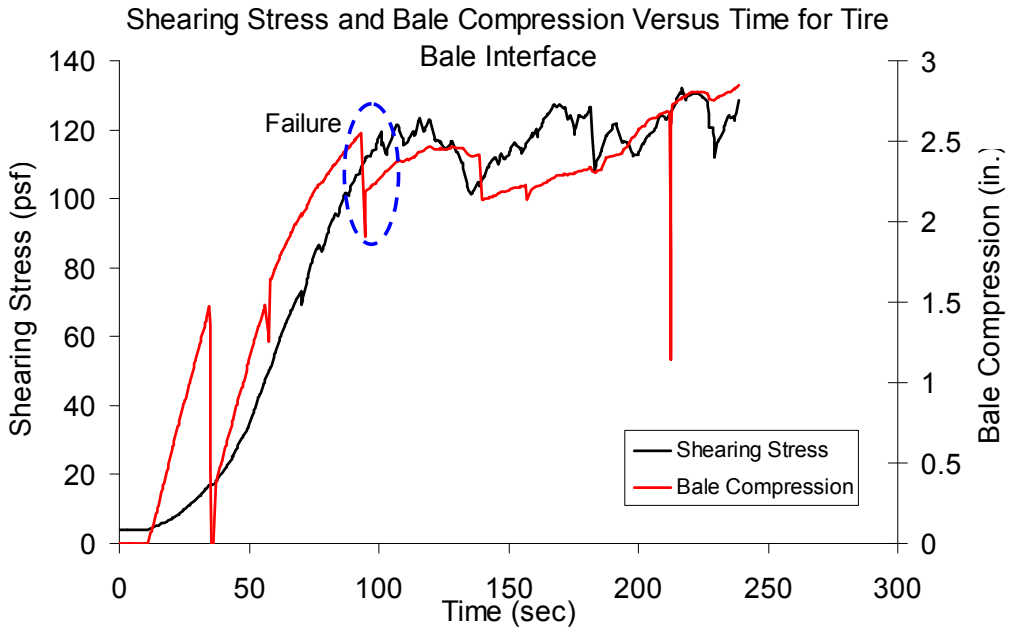

Figure E.13: Interface Shearing Resistance and Tire Bale Compression versus Elapsed Testing Time for the Wet Anisotropic Tire Bale Only Interface (Normal Stress = 216 psf)

Results for Anisotropic Wet Tire Bale Interface Test #3: Normal Stress = 325 psf

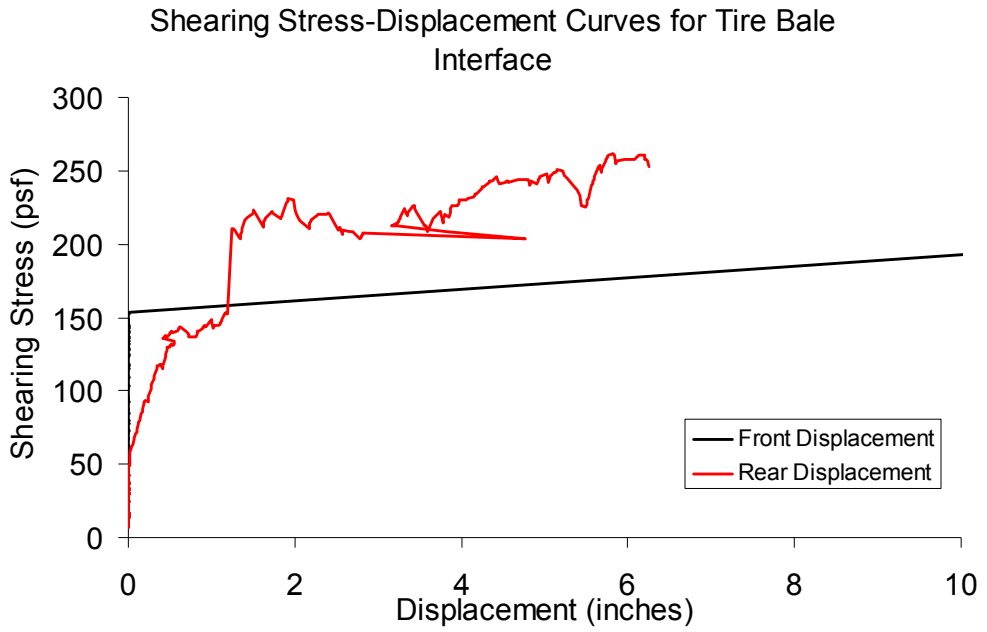

Figure E.14: Interface Shearing Resistance versus Displacement for the Wet Anisotropic Tire Bale Only Interface (Normal Stress = 325 psf)

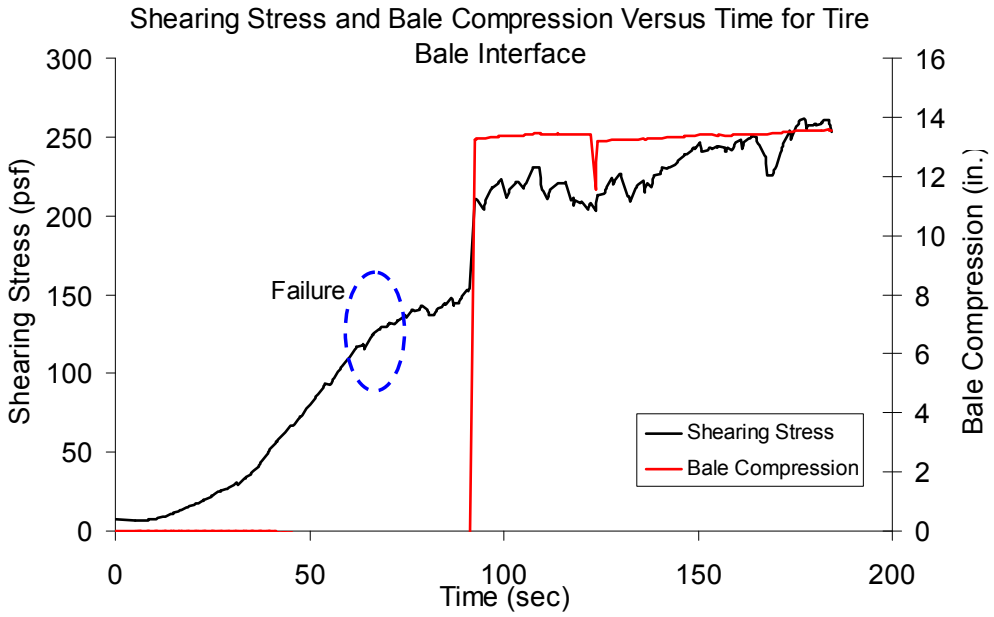

Figure E.15: Interface Shearing Resistance and Tire Bale Compression versus Elapsed Testing Time for the Wet Anisotropic Tire Bale Only Interface (Normal Stress = 325 psf)

Results for Anisotropic Dry Tire Bale Interface Test #5: Normal Stress = 361 psf

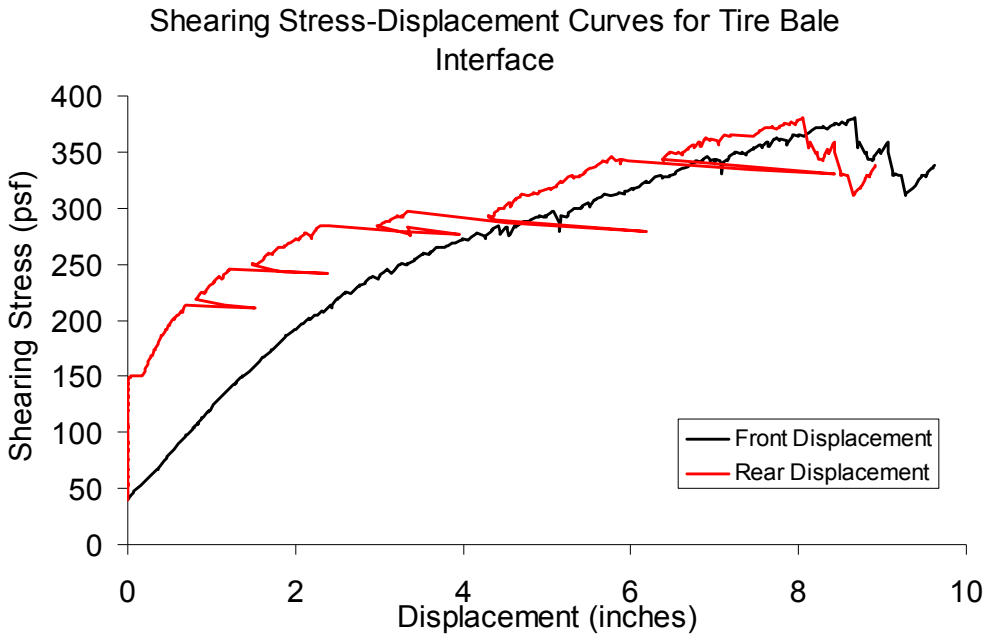

Figure E.16: Interface Shearing Resistance versus Displacement for the Dry Anisotropic Tire Bale Only Interface (Normal Stress = 361 psf)

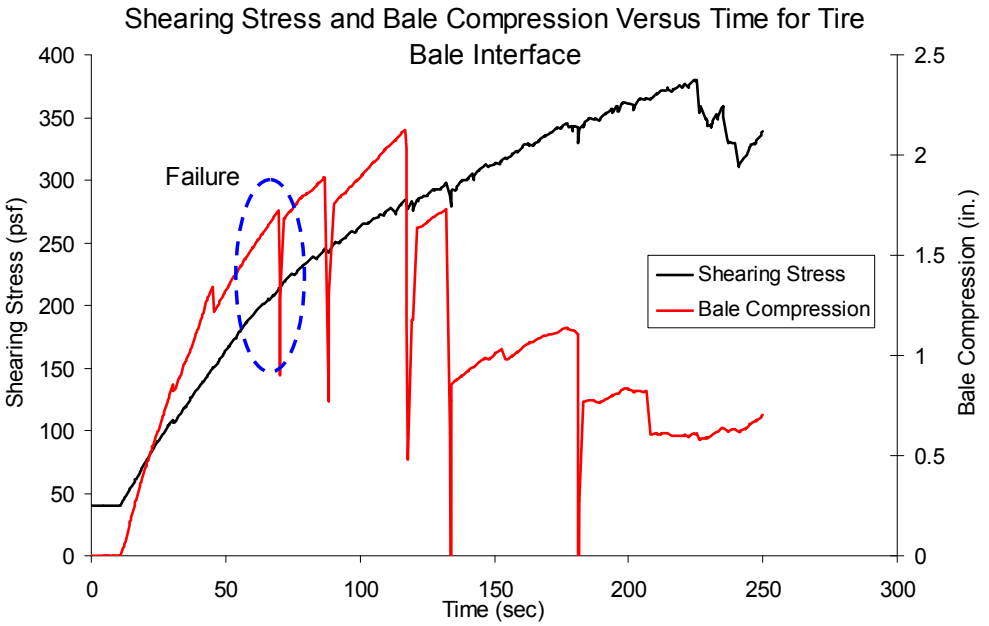

Figure E.17: Interface Shearing Resistance and Tire Bale Compression versus Elapsed Testing Time for the Dry Anisotropic Tire Bale Only Interface (Normal Stress = 361 psf)

Results for Anisotropic Dry Tire Bale Interface Test #6: Normal Stress = 361 psf

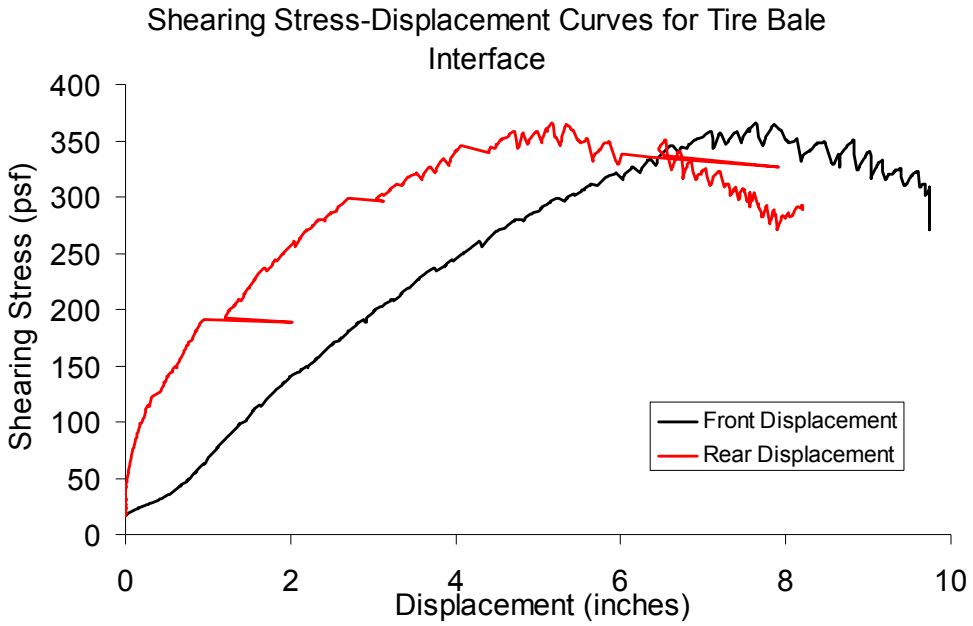

Figure E.18: Interface Shearing Resistance versus Displacement for the Dry Anisotropic Tire Bale Only Interface (Normal Stress = 361 psf)

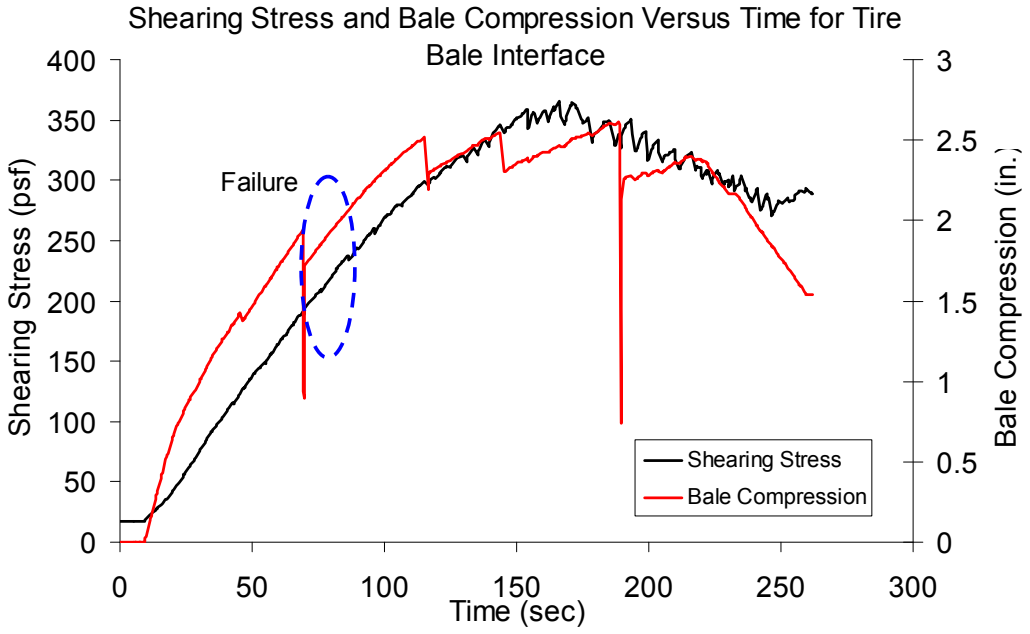

Figure E.19: Interface Shearing Resistance and Tire Bale Compression versus Elapsed Testing Time for the Dry Anisotropic Tire Bale Only Interface (Normal Stress = 361 psf)

Appendix F: Testing Data from the Large Scale Direct Shear Testing of the Tire Bale-Soil Interfaces

The following appendix section provides the data obtained for each of the large scale direct shear tests conducted for the tire bale-soil interfaces that was not specifically reported in Chapter 6. A detailed analysis of the data is provided in Chapter 6.5.

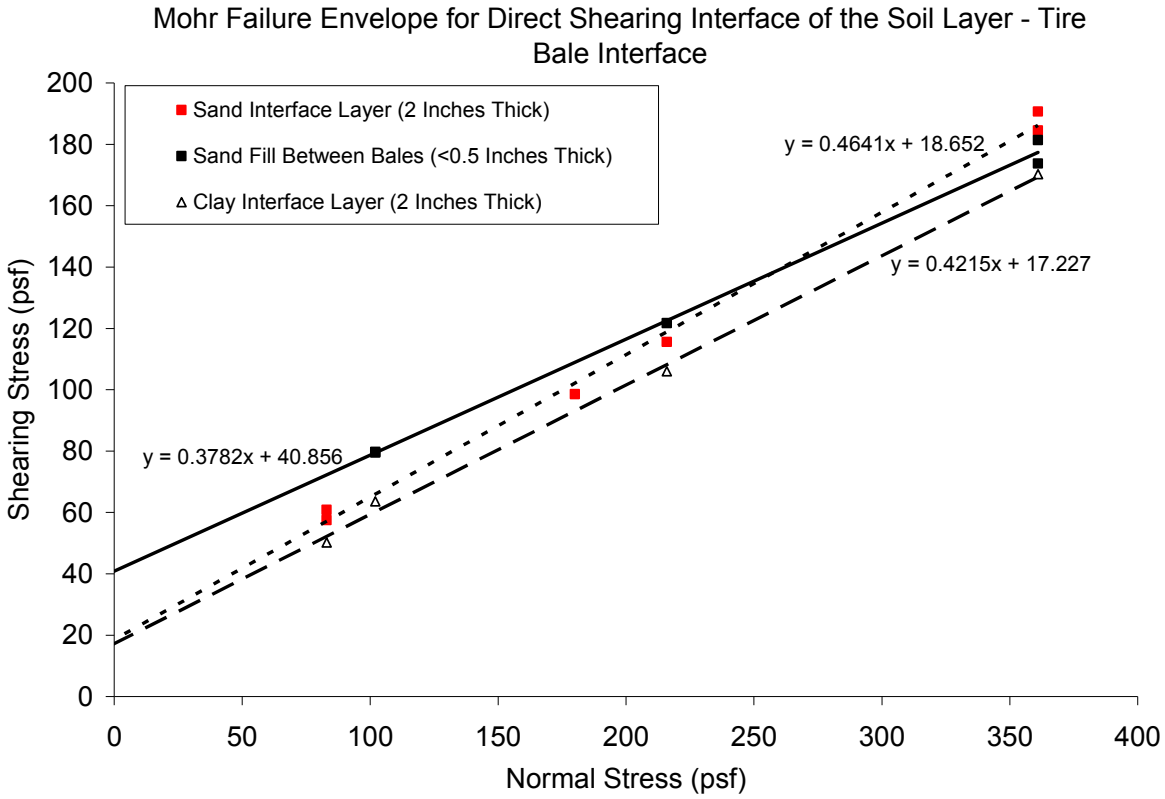

Figure F.1: Shear Strength Envelopes for the Thin Sand, Thick Sand and Thick Clay Interfaces

Results for Thick Sand-Tire Bale Interface Test #1: Normal Stress = 83 psf

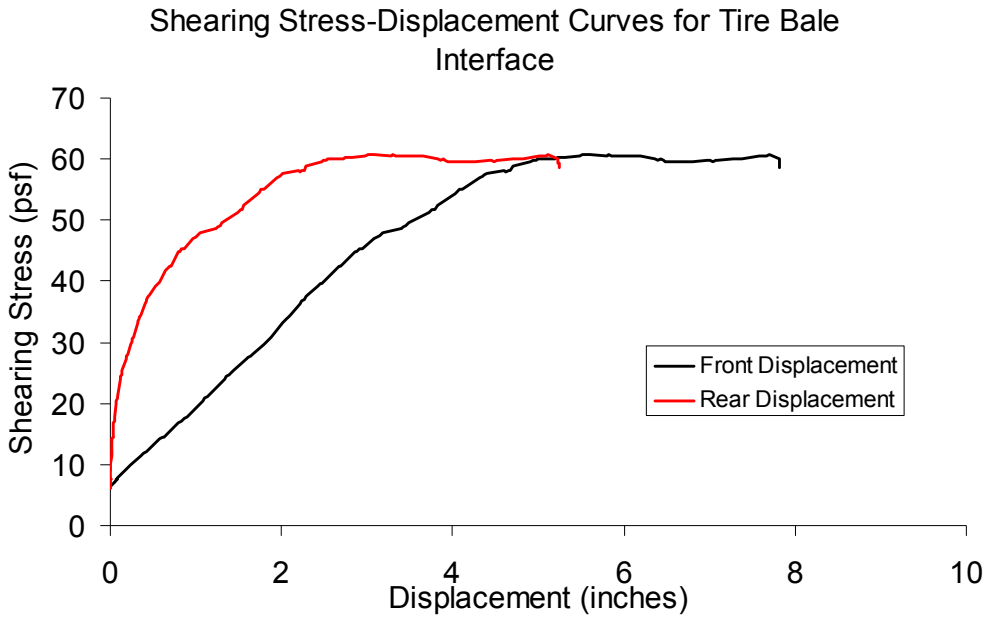

Figure F.2: Interface Shearing Resistance versus Displacement for the Thick Sand-Tire Bale Interface (Normal Stress = 83 psf)

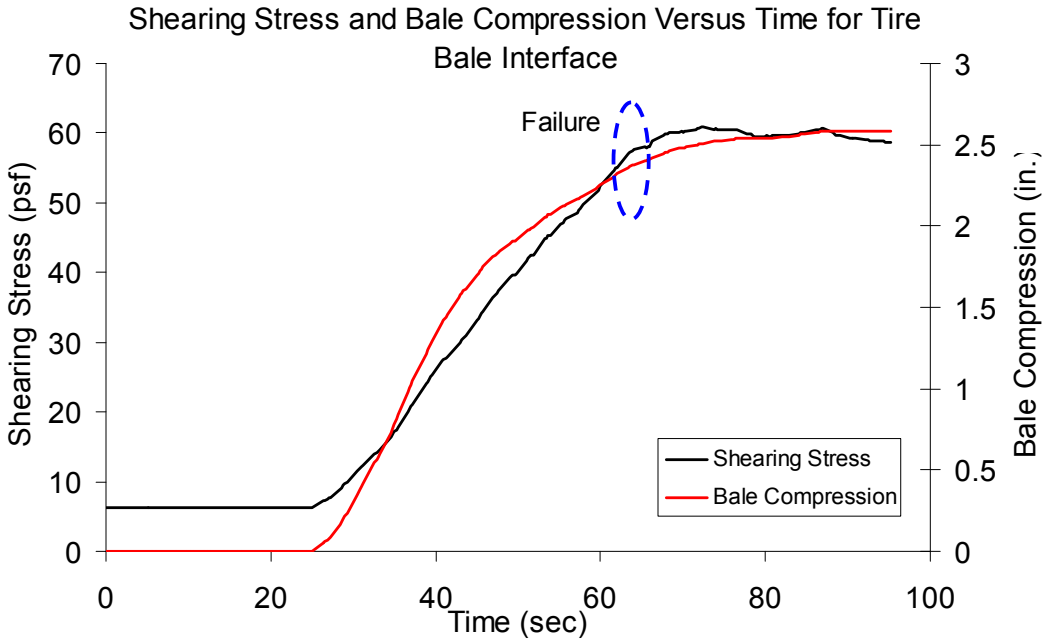

Figure F.3: Interface Shearing Resistance and Tire Bale Compression versus Elapsed Testing Time for Thick Sand-Tire Bale Interface (Normal Stress = 83 psf)

Results for Thick Sand-Tire Bale Interface Test #2: Normal Stress = 83 psf

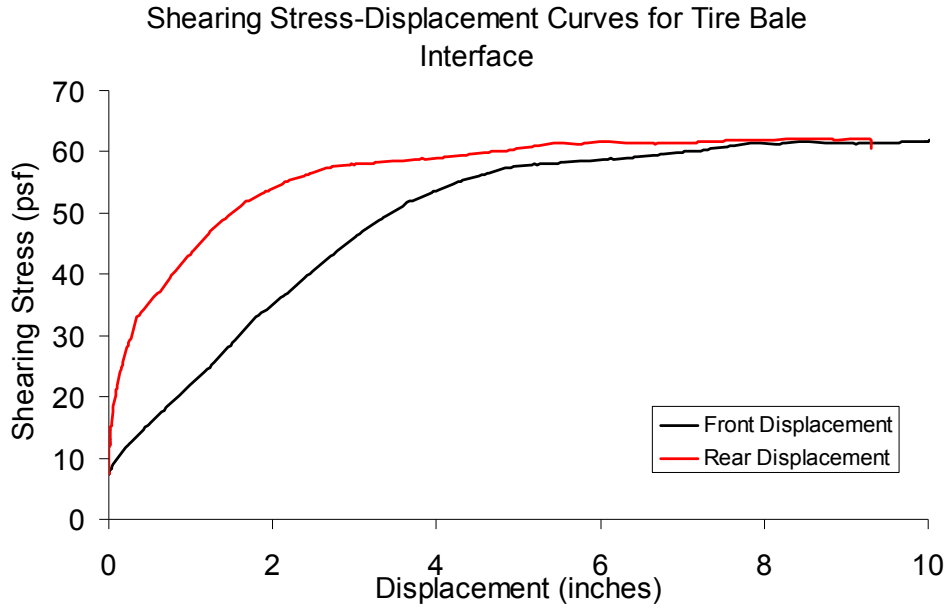

Figure F.4: Interface Shearing Resistance versus Displacement for the Thick Sand-Tire Bale Interface (Normal Stress = 83 psf)

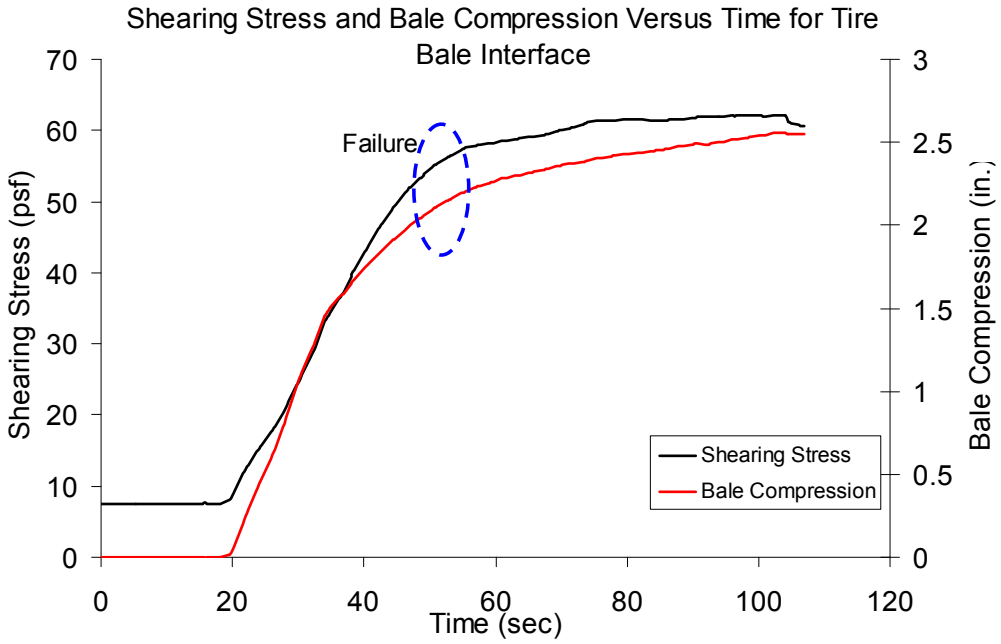

Figure F.5: Interface Shearing Resistance and Tire Bale Compression versus Elapsed Testing Time for Thick Sand-Tire Bale Interface (Normal Stress = 83 psf)

Results for Thick Clay-Tire Bale Interface Test #1: Normal Stress = 83 psf

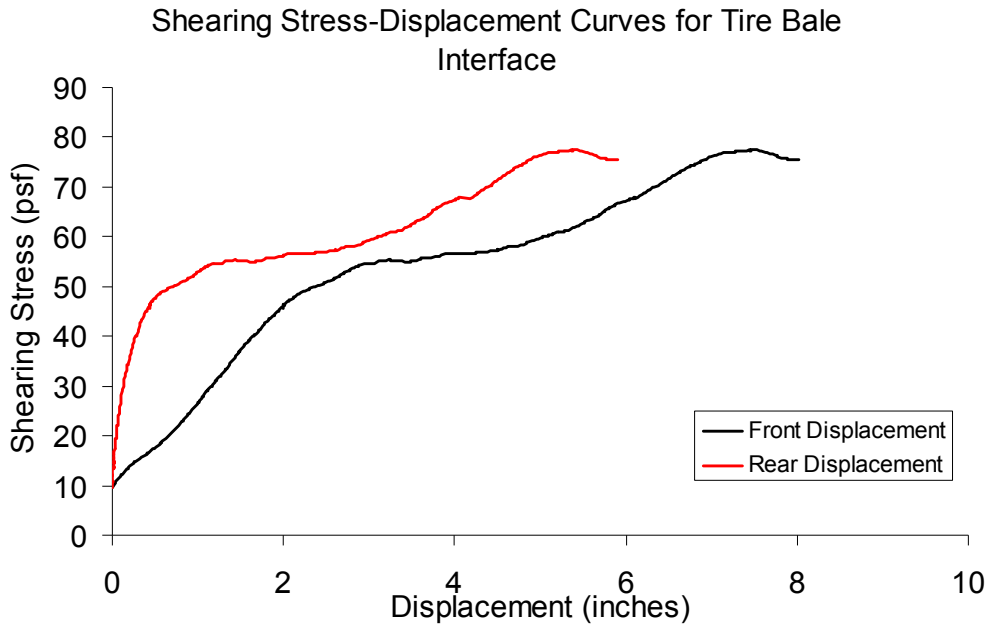

Figure F.6: Interface Shearing Resistance versus Displacement for the Thick Clay-Tire Bale Interface (Normal Stress = 83 psf)

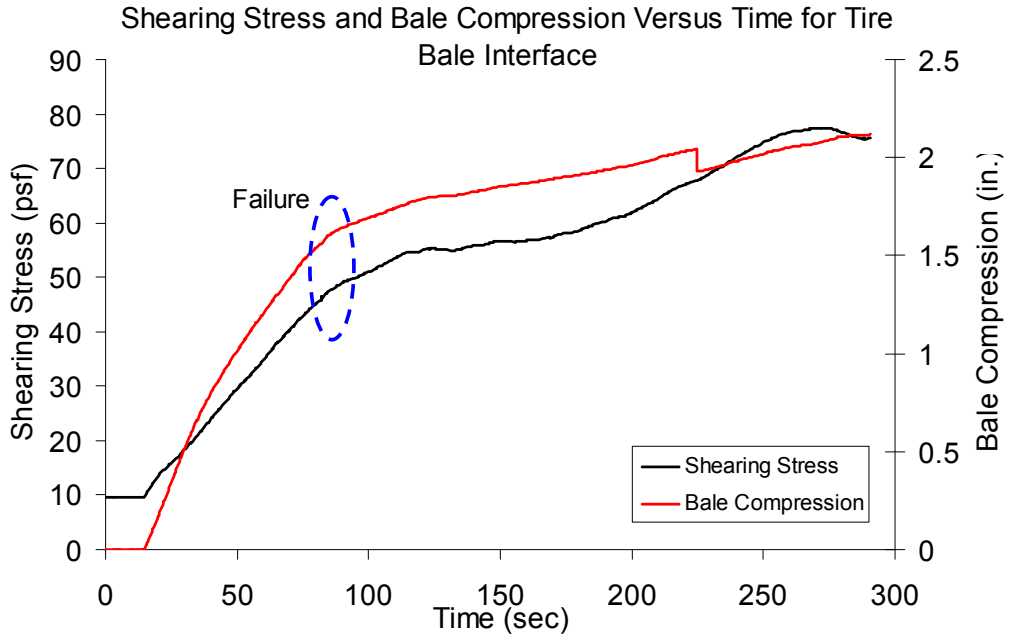

Figure F.7: Interface Shearing Resistance and Tire Bale Compression versus Elapsed Testing Time for Thick Clay-Tire Bale Interface (Normal Stress = 83 psf)

Results for Thin Sand-Tire Bale Interface Test #1: Normal Stress = 102 psf

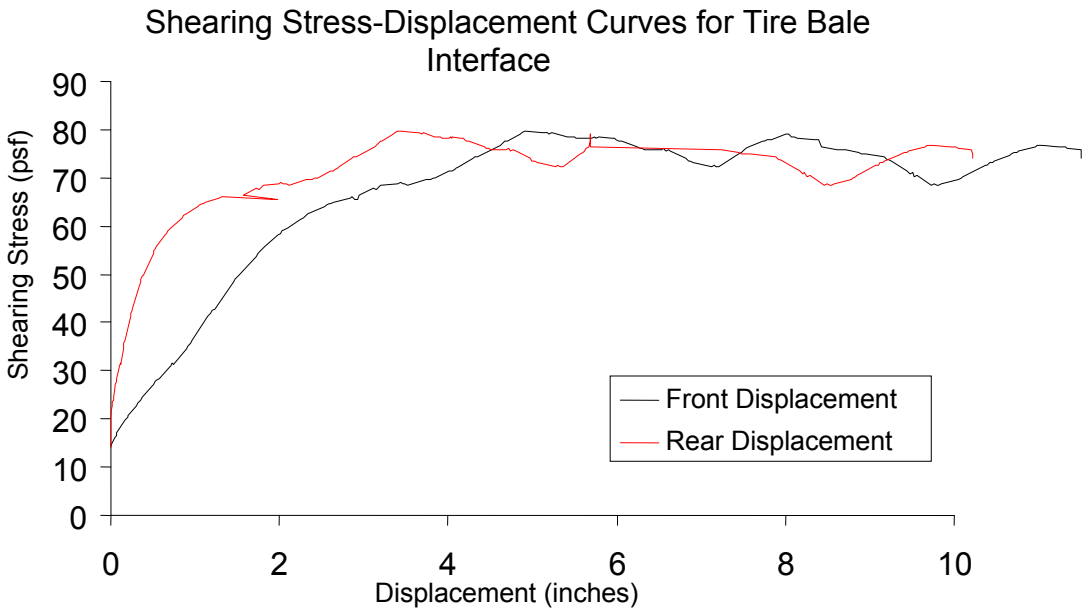

Figure F.8: Interface Shearing Resistance versus Displacement for the Thin Sand-Tire Bale Interface (Normal Stress = 102 psf)

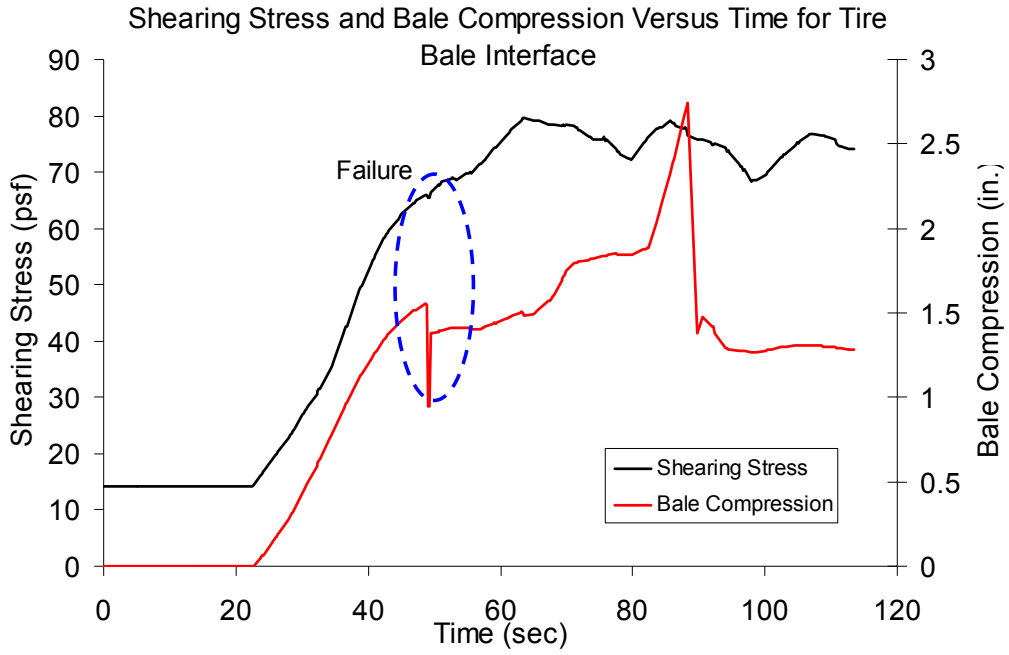

Figure F.9: Interface Shearing Resistance and Tire Bale Compression versus Elapsed Testing Time for Thin Sand-Tire Bale Interface (Normal Stress = 102 psf)

Results for Thin Sand-Tire Bale Interface Test #2: Normal Stress = 102 psf

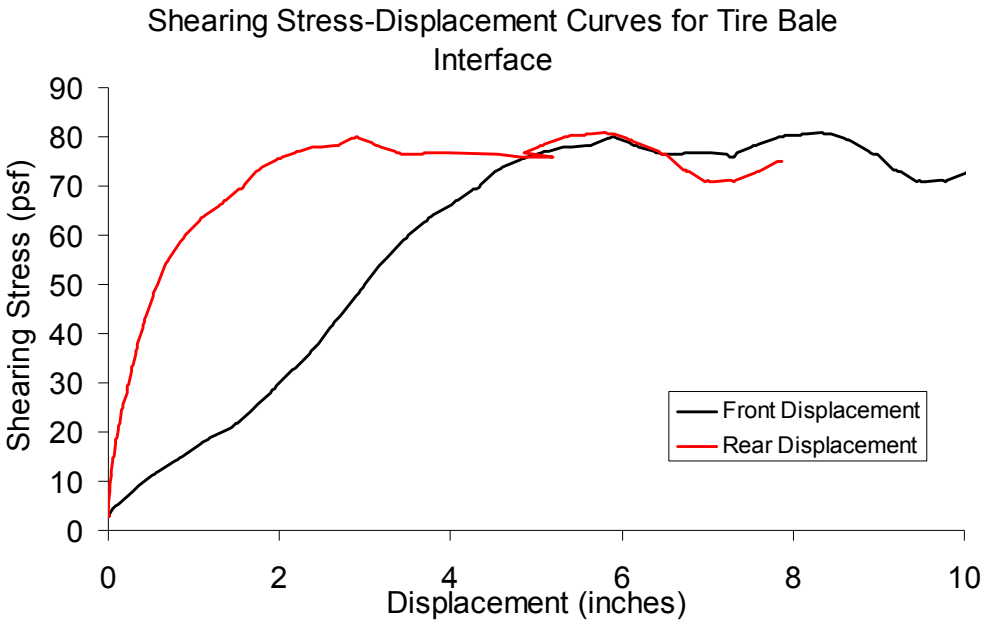

Figure F.10: Interface Shearing Resistance versus Displacement for the Thin Sand-Tire Bale Interface (Normal Stress = 102 psf)

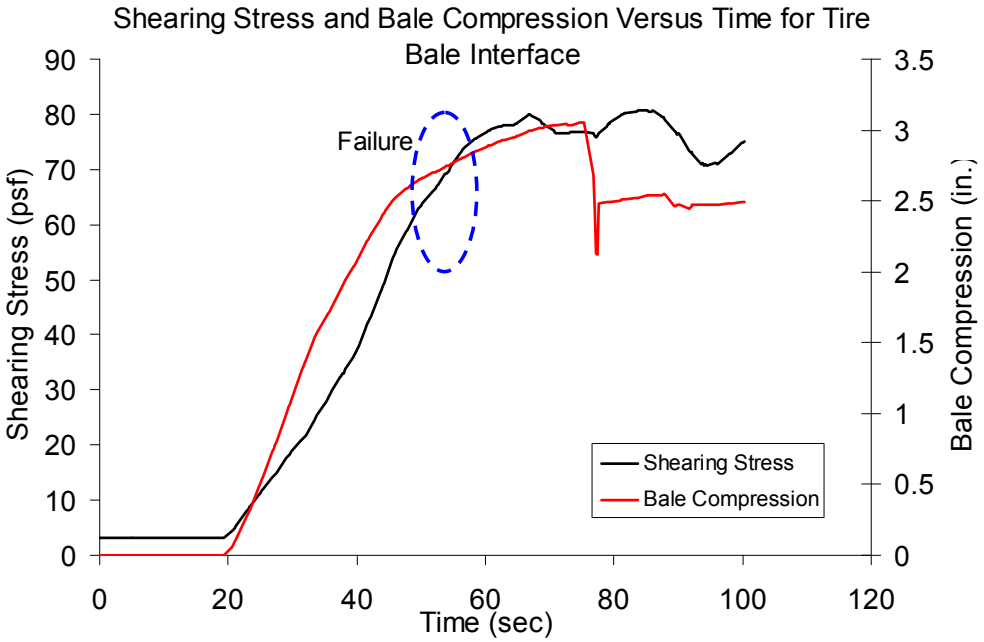

Figure F.11: Interface Shearing Resistance and Tire Bale Compression versus Elapsed Testing Time for Thin Sand-Tire Bale Interface (Normal Stress = 102 psf)

Results for Thick Clay-Tire Bale Interface Test #2: Normal Stress = 102 psf

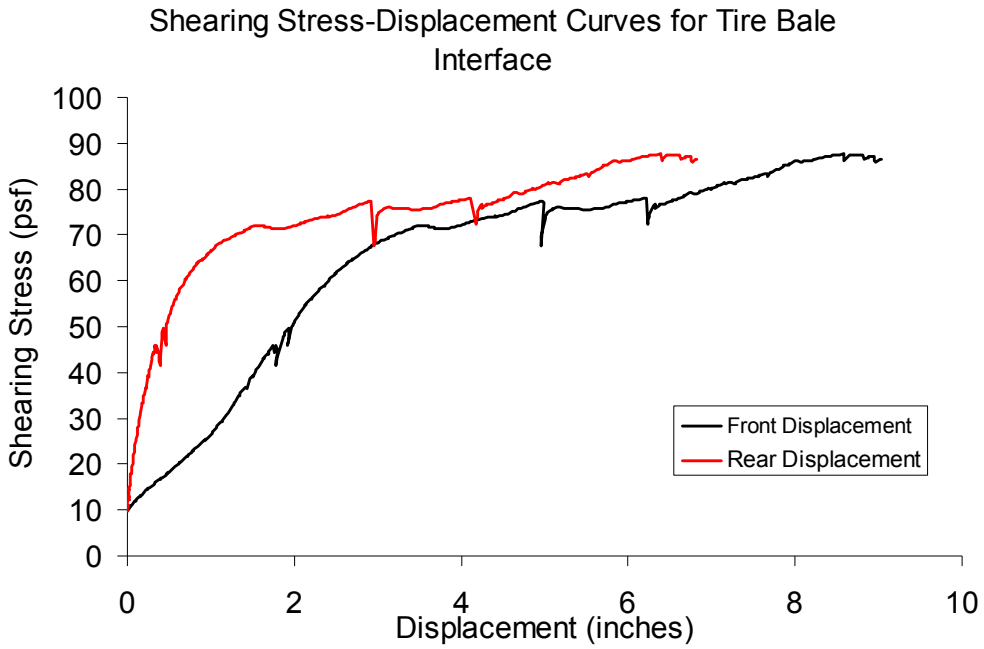

Figure F.12: Interface Shearing Resistance versus Displacement for the Thick Clay-Tire Bale Interface (Normal Stress = 102 psf)

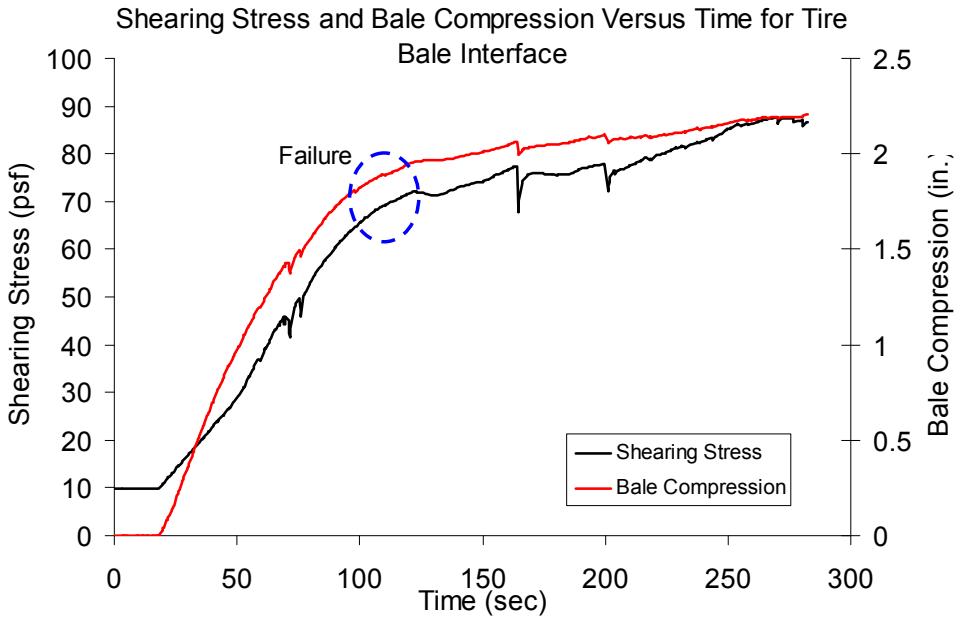

Figure F.13: Interface Shearing Resistance and Tire Bale Compression versus Elapsed Testing Time for Thick Clay-Tire Bale Interface (Normal Stress = 102 psf)

Results for Thick Sand-Tire Bale Interface Test #3: Normal Stress = 180 psf

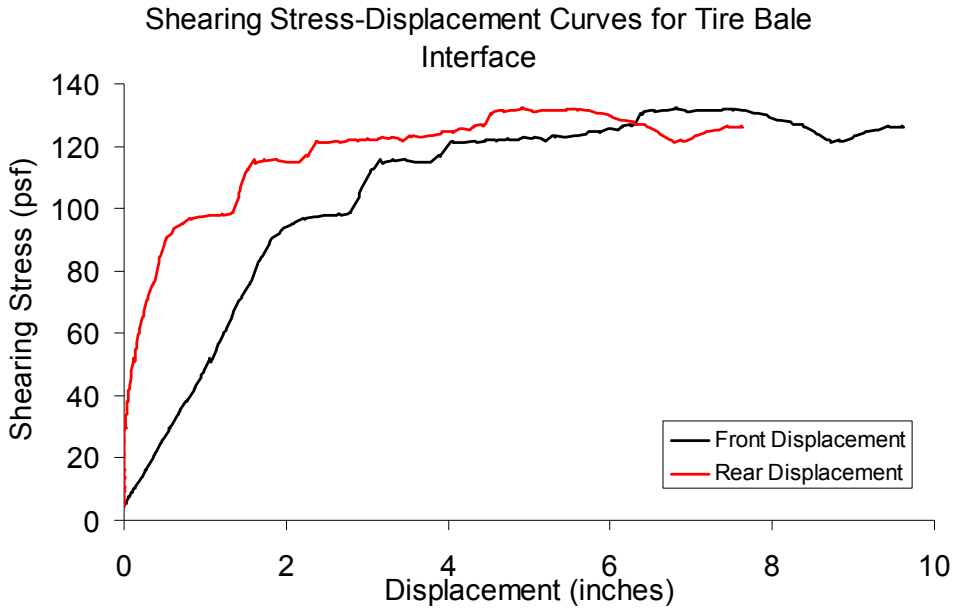

Figure F.14: Interface Shearing Resistance versus Displacement for the Thick Sand-Tire Bale Interface (Normal Stress = 180 psf)

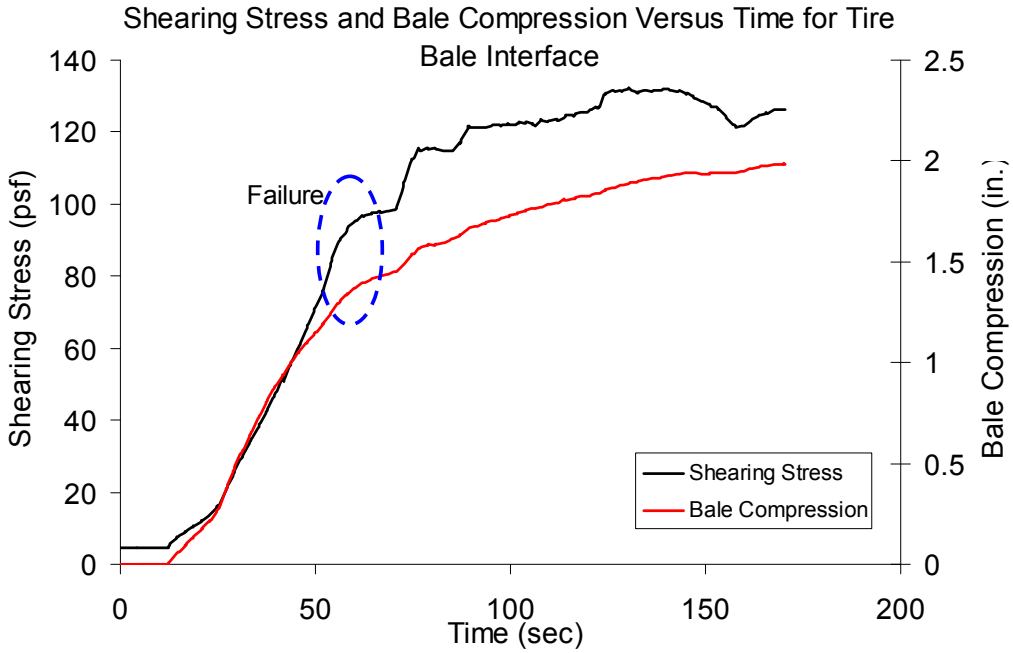

Figure F.15: Interface Shearing Resistance and Tire Bale Compression versus Elapsed Testing Time for Thick Sand-Tire Bale Interface (Normal Stress = 180 psf)

Results for Thick Sand-Tire Bale Interface Test #4: Normal Stress = 216 psf

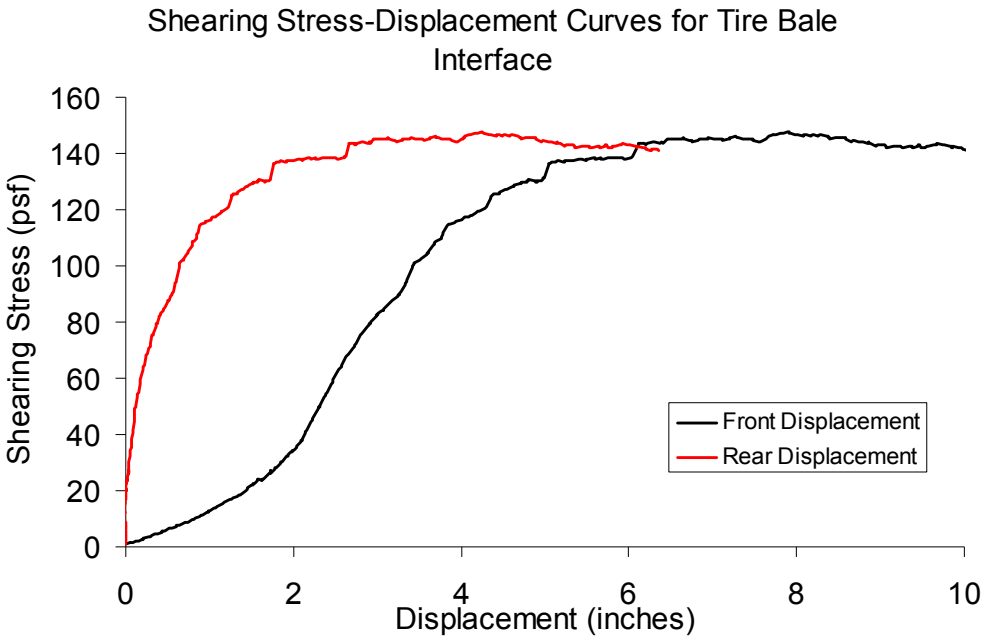

Figure F.16: Interface Shearing Resistance versus Displacement for the Thick Sand-Tire Bale Interface (Normal Stress = 216 psf)

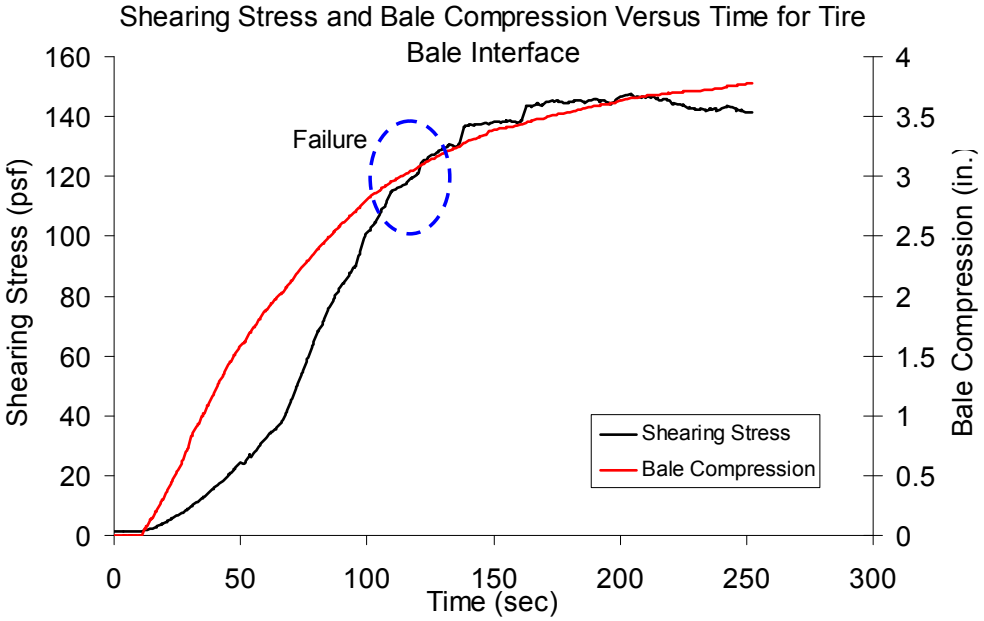

Figure F.17: Interface Shearing Resistance and Tire Bale Compression versus Elapsed Testing Time for Thick Sand-Tire Bale Interface (Normal Stress = 216 psf)

Results for Thin Sand-Tire Bale Interface Test #3: Normal Stress = 216 psf

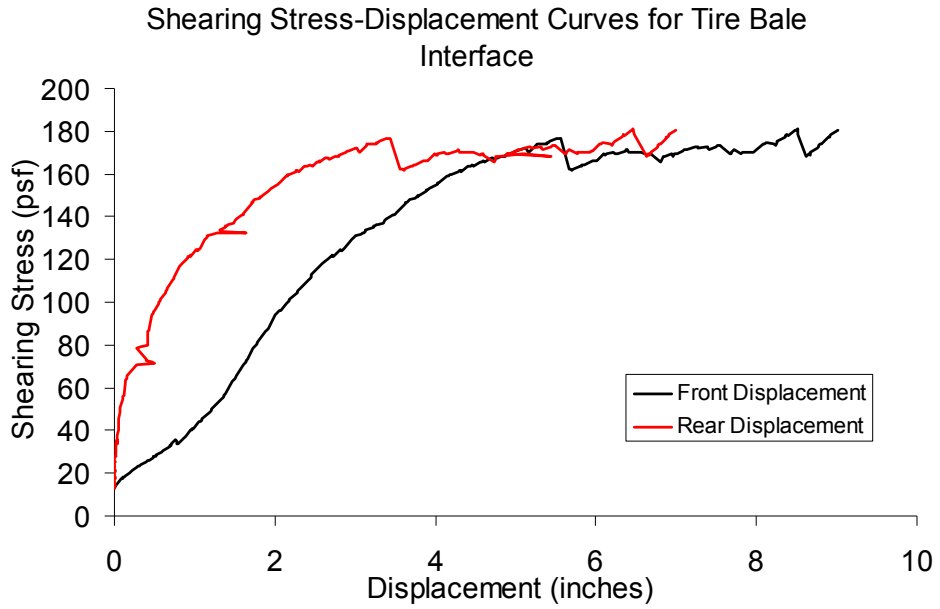

Figure F.18: Interface Shearing Resistance versus Displacement for the Thin Sand-Tire Bale Interface (Normal Stress = 216 psf)

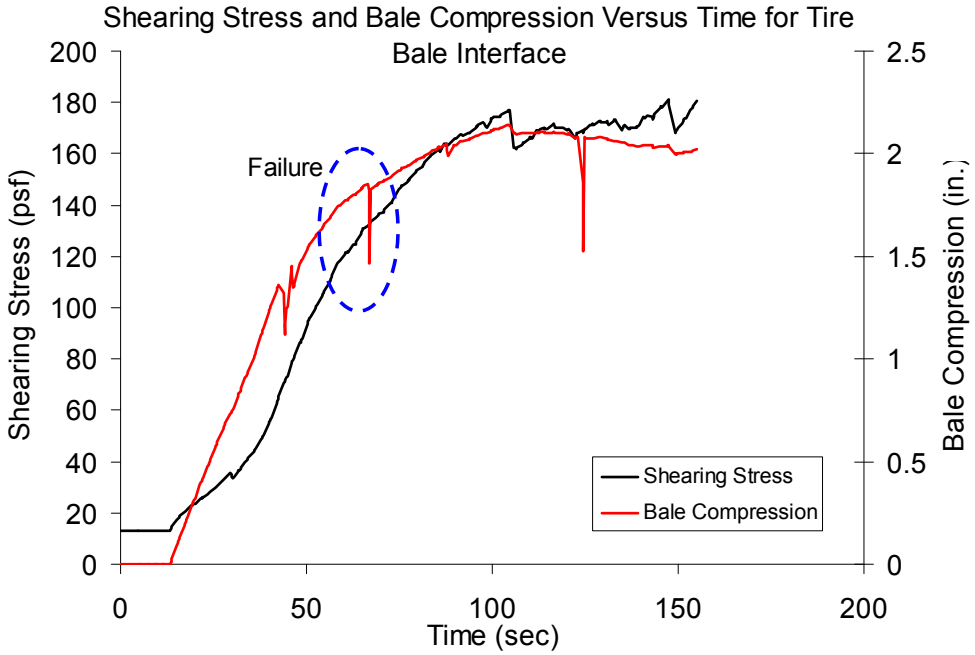

Figure F.19: Interface Shearing Resistance and Tire Bale Compression versus Elapsed Testing Time for Thin Sand-Tire Bale Interface (Normal Stress = 216 psf)

Results for Thick Clay-Tire Bale Interface Test #3: Normal Stress = 216 psf

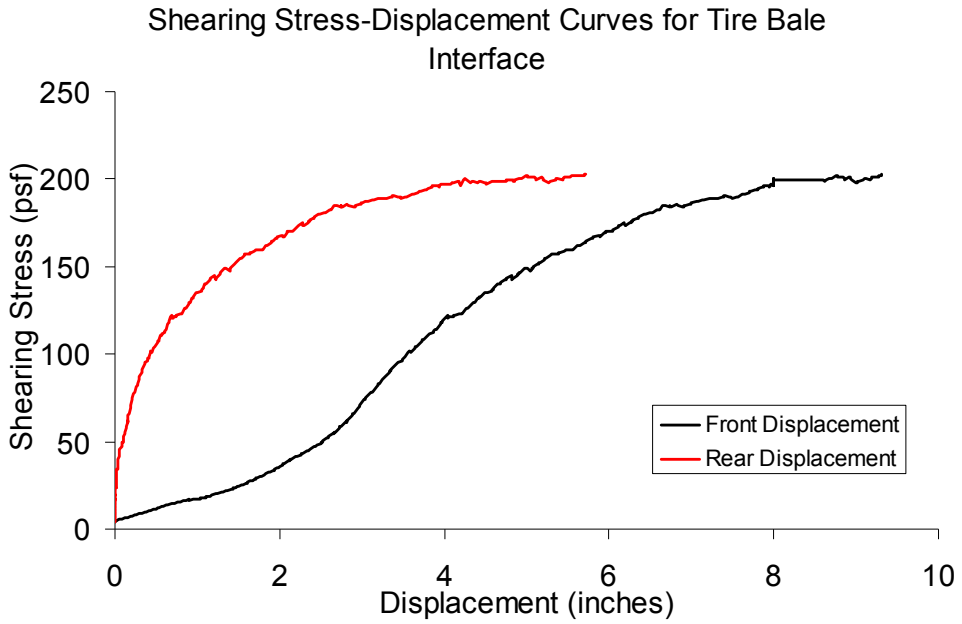

Figure F.20: Interface Shearing Resistance versus Displacement for the Thick Clay-Tire Bale Interface (Normal Stress = 216 psf)

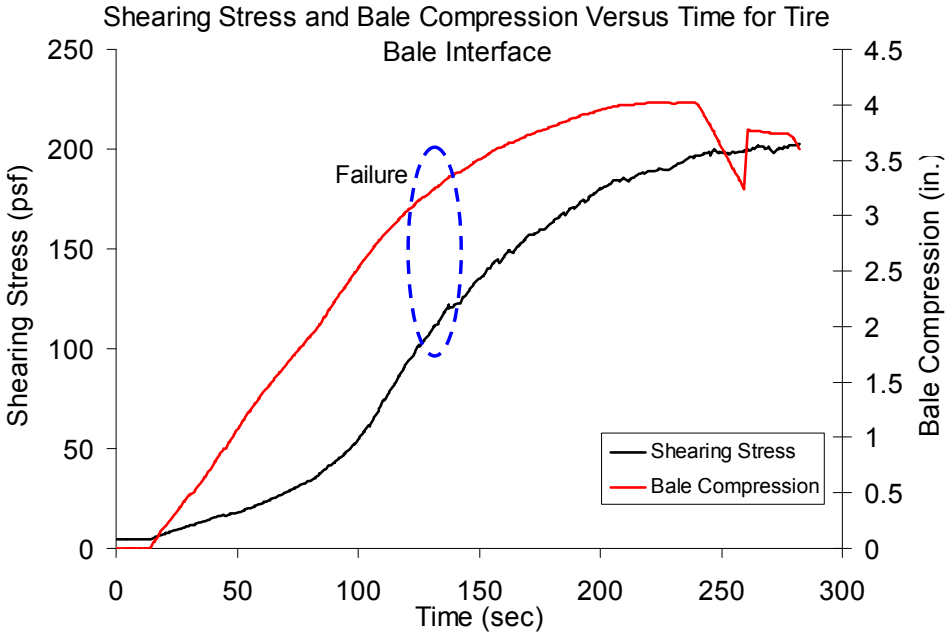

Figure F.21: Interface Shearing Resistance and Tire Bale Compression versus Elapsed Testing Time for Thick Clay-Tire Bale Interface (Normal Stress = 216 psf)

Results for Thick Sand-Tire Bale Interface Test #5: Normal Stress = 361 psf

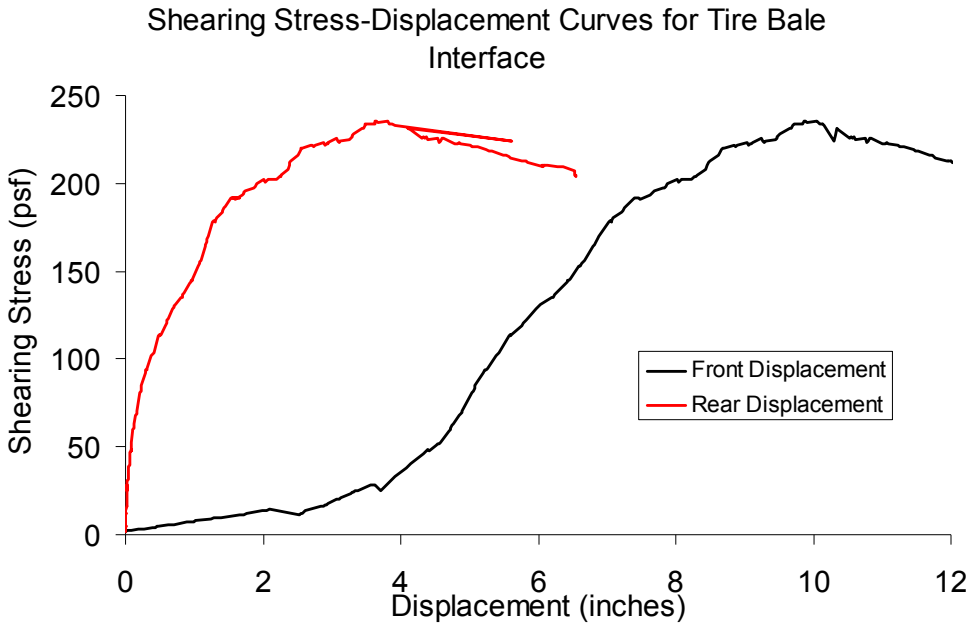

Figure F.22: Interface Shearing Resistance versus Displacement for the Thick Sand-Tire Bale Interface (Normal Stress = 361 psf)

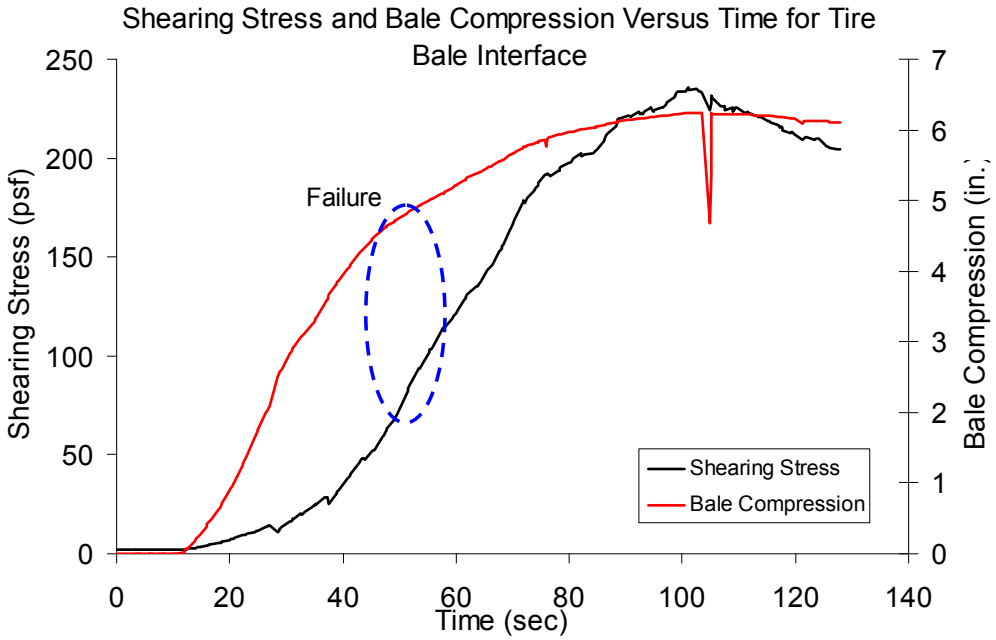

Figure F.23: Interface Shearing Resistance and Tire Bale Compression versus Elapsed Testing Time for Thick Sand-Tire Bale Interface (Normal Stress = 361 psf)

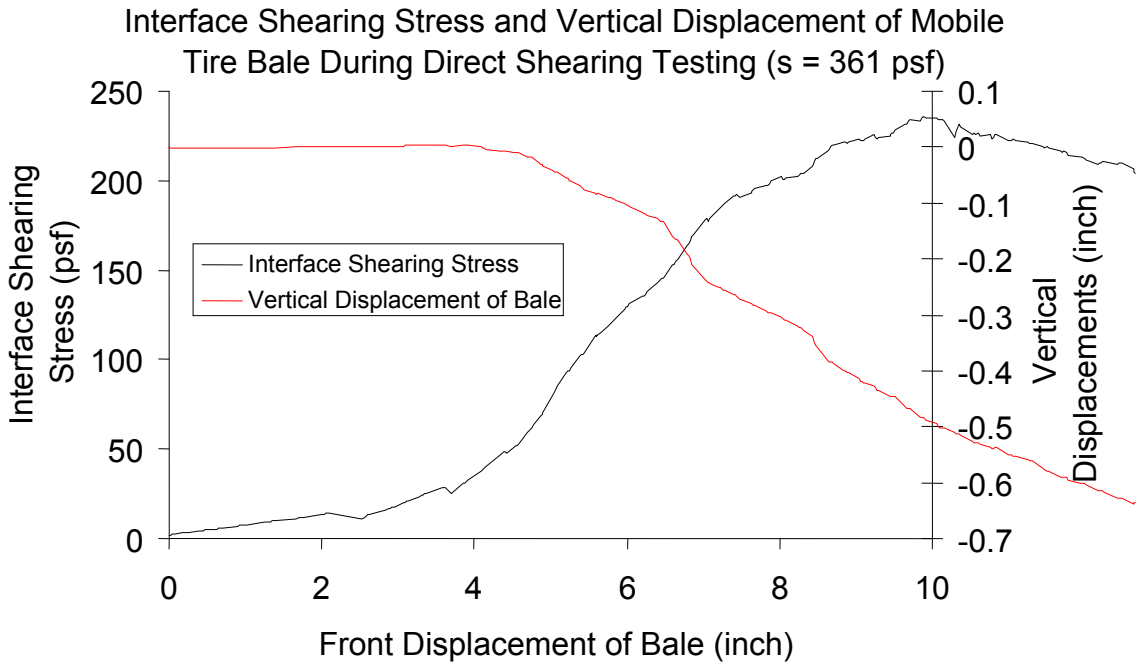

Figure F.24: Interface Shearing Resistance and Vertical Movement of the Tire Bale versus Front Displacement of the Bale for Thick Sand-Tire Bale Interface (Normal Stress = 361 psf)

Results for Thick Sand-Tire Bale Interface Test #6: Normal Stress = 361 psf

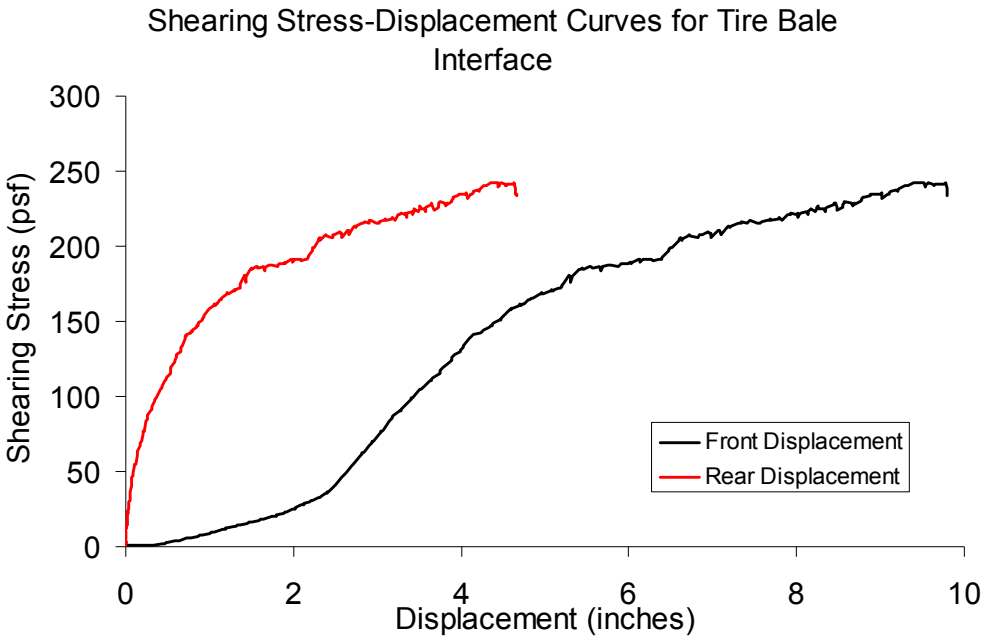

Figure F.25: Interface Shearing Resistance versus Displacement for the Thick Sand-Tire Bale Interface (Normal Stress = 361 psf)

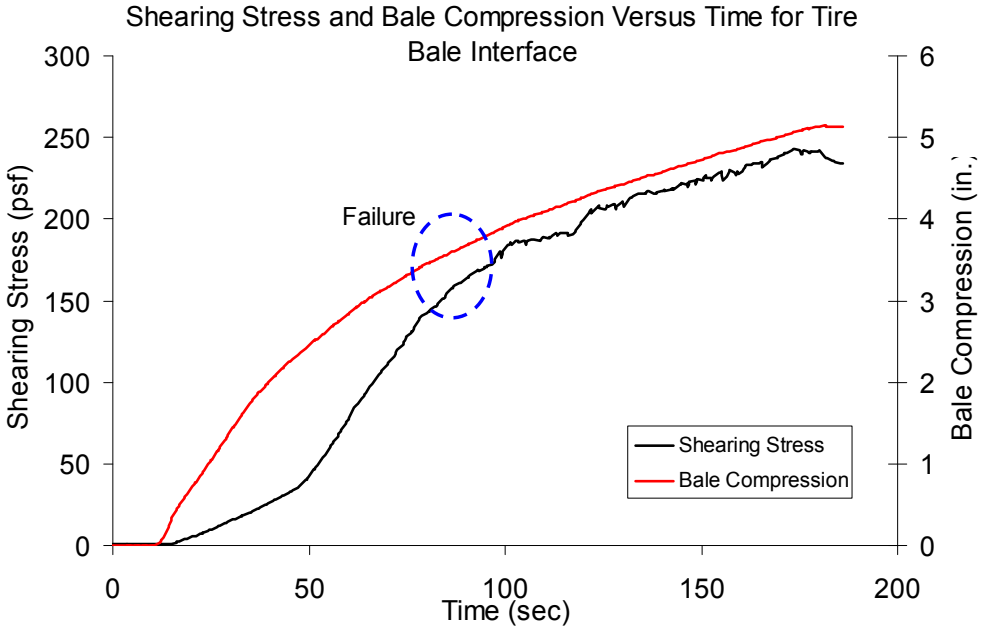

Figure F.26: Interface Shearing Resistance and Tire Bale Compression versus Elapsed Testing Time for Thick Sand-Tire Bale Interface (Normal Stress = 361 psf)

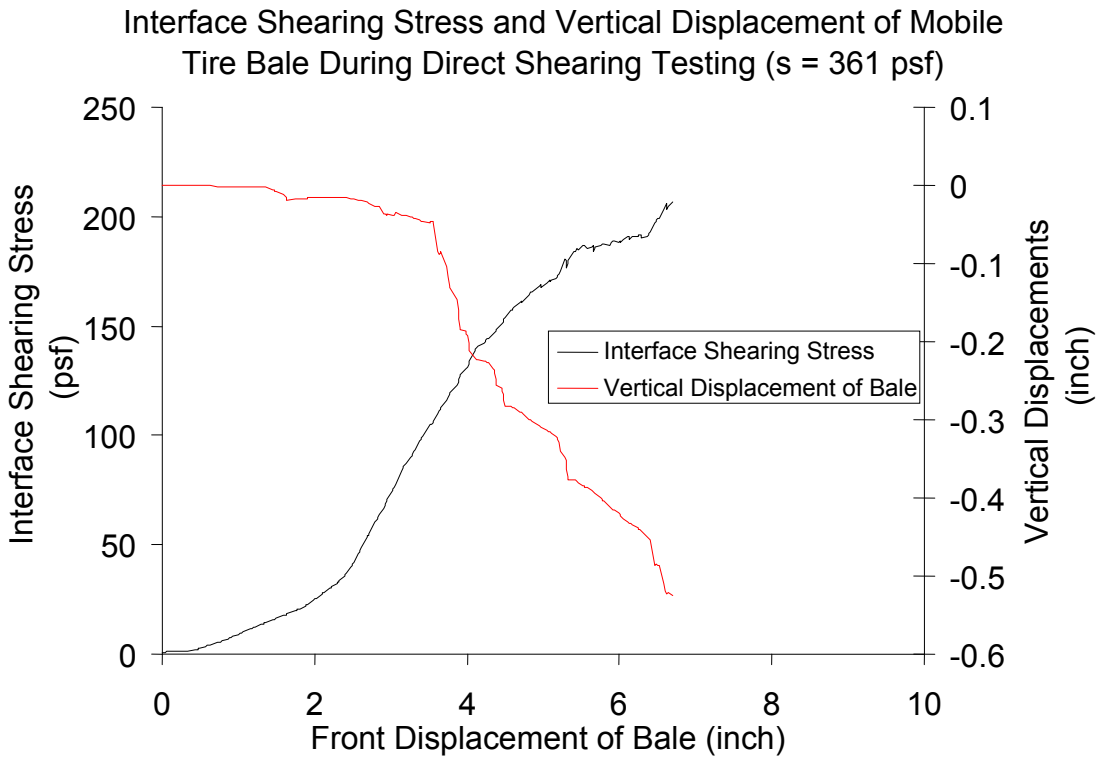

Figure F.27: Interface Shearing Resistance and Vertical Movement of the Tire Bale versus Front Displacement of the Bale for Thick Sand-Tire Bale Interface (Normal Stress = 361 psf)

Results for Thin Sand-Tire Bale Interface Test #4: Normal Stress = 361 psf

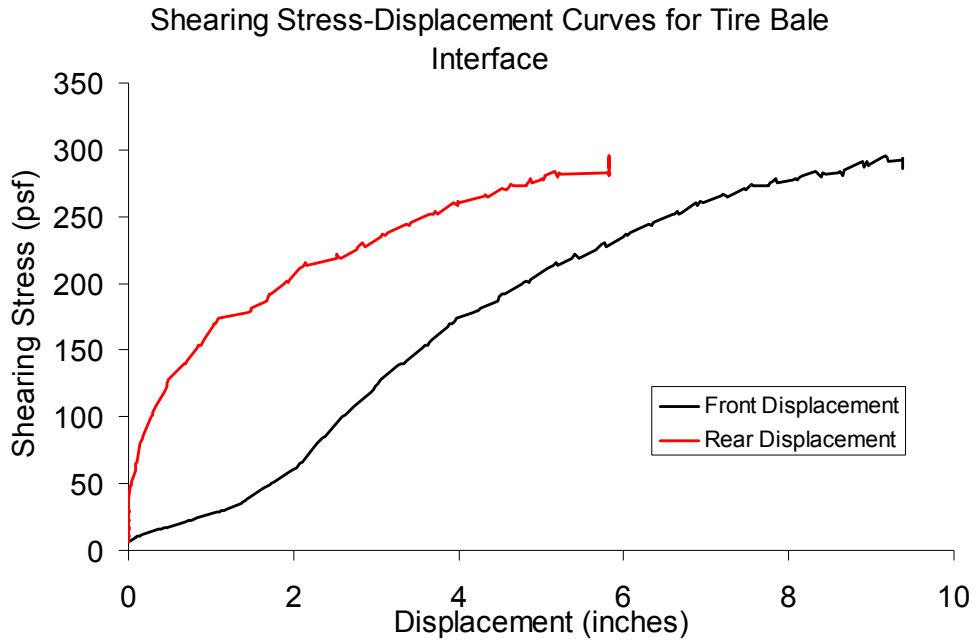

Figure F.28: Interface Shearing Resistance versus Displacement for the Thin Sand-Tire Bale Interface (Normal Stress = 361 psf)

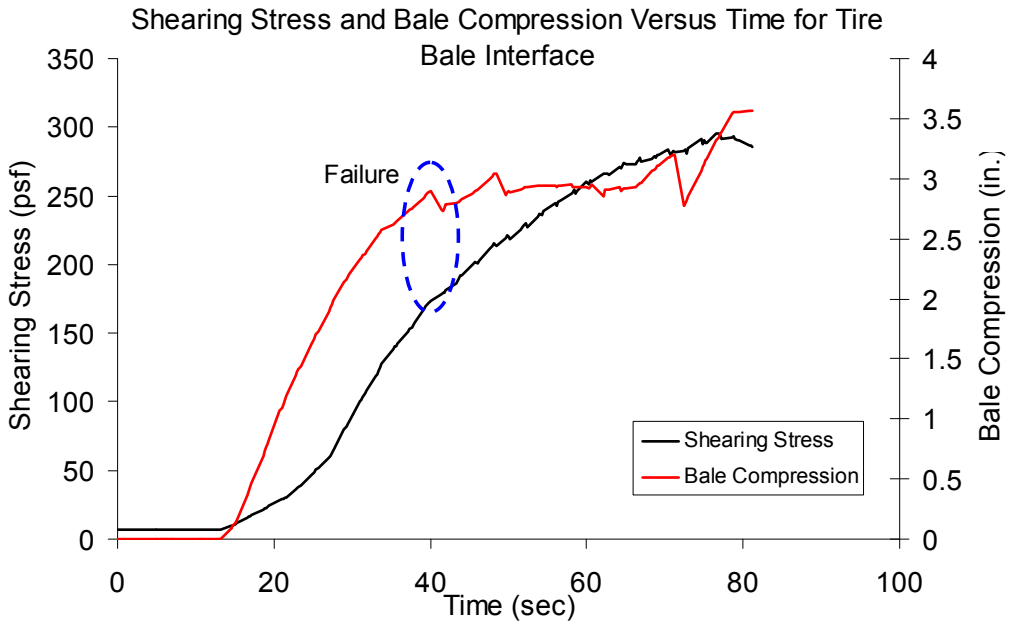

Figure F.29: Interface Shearing Resistance and Tire Bale Compression versus Elapsed Testing Time for Thin Sand-Tire Bale Interface (Normal Stress = 361 psf)

Results for Thin Sand-Tire Bale Interface Test #5: Normal Stress = 361 psf

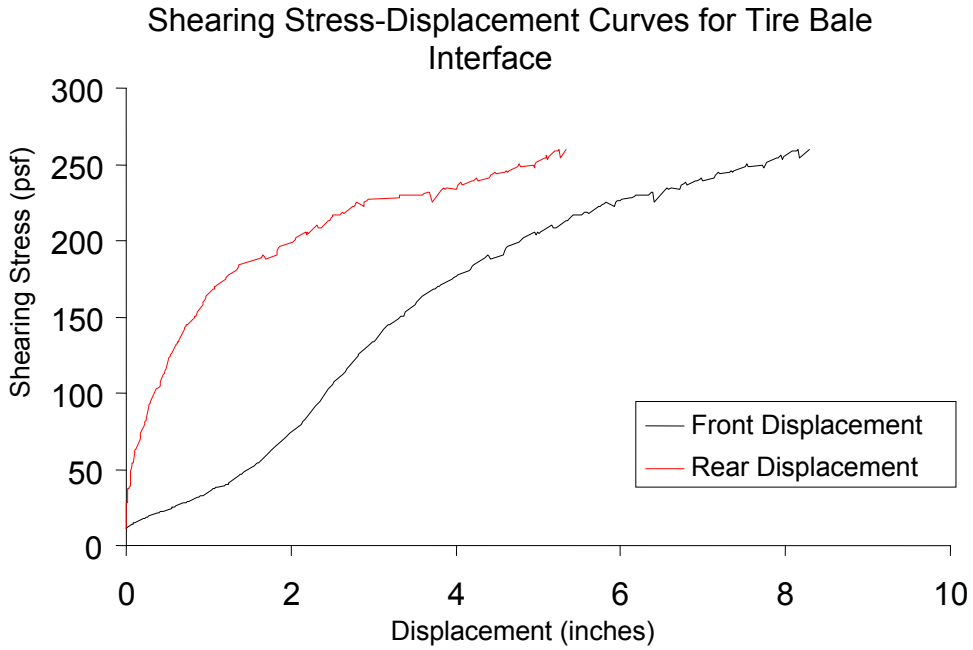

Figure F.30: Interface Shearing Resistance versus Displacement for the Thin Sand-Tire Bale Interface (Normal Stress = 361 psf)

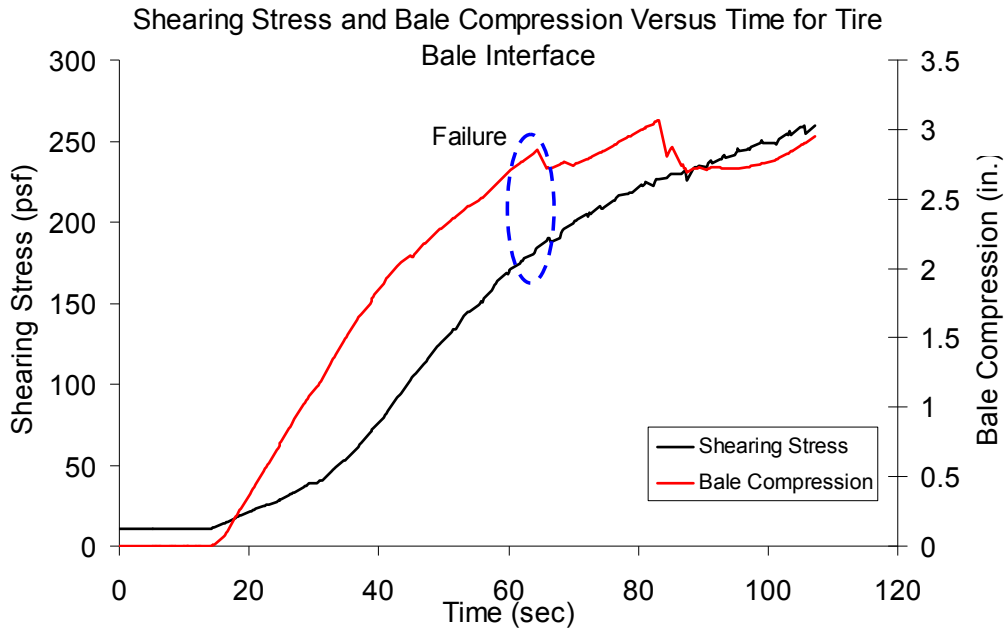

Figure F.31: Interface Shearing Resistance and Tire Bale Compression versus Elapsed Testing Time for Thin Sand-Tire Bale Interface (Normal Stress = 361 psf)

Results for Thick Clay-Tire Bale Interface Test #4: Normal Stress = 361 psf

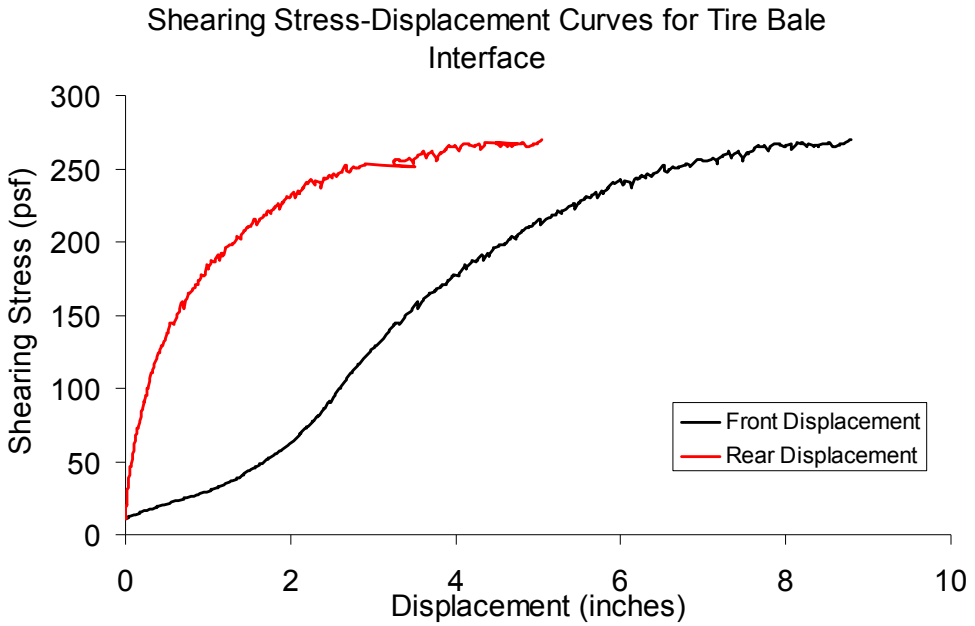

Figure F.32: Interface Shearing Resistance versus Displacement for the Thick Clay-Tire Bale Interface (Normal Stress = 361 psf).

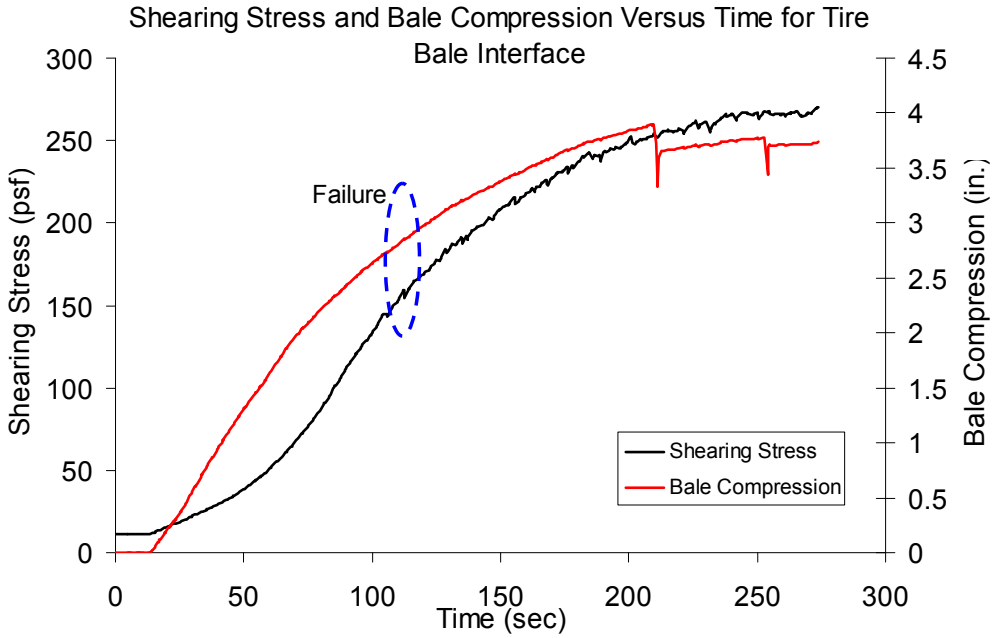

Figure F.33: Interface Shearing Resistance and Tire Bale Compression versus Elapsed Testing Time for Thick Clay-Tire Bale Interface (Normal Stress = 361 psf)

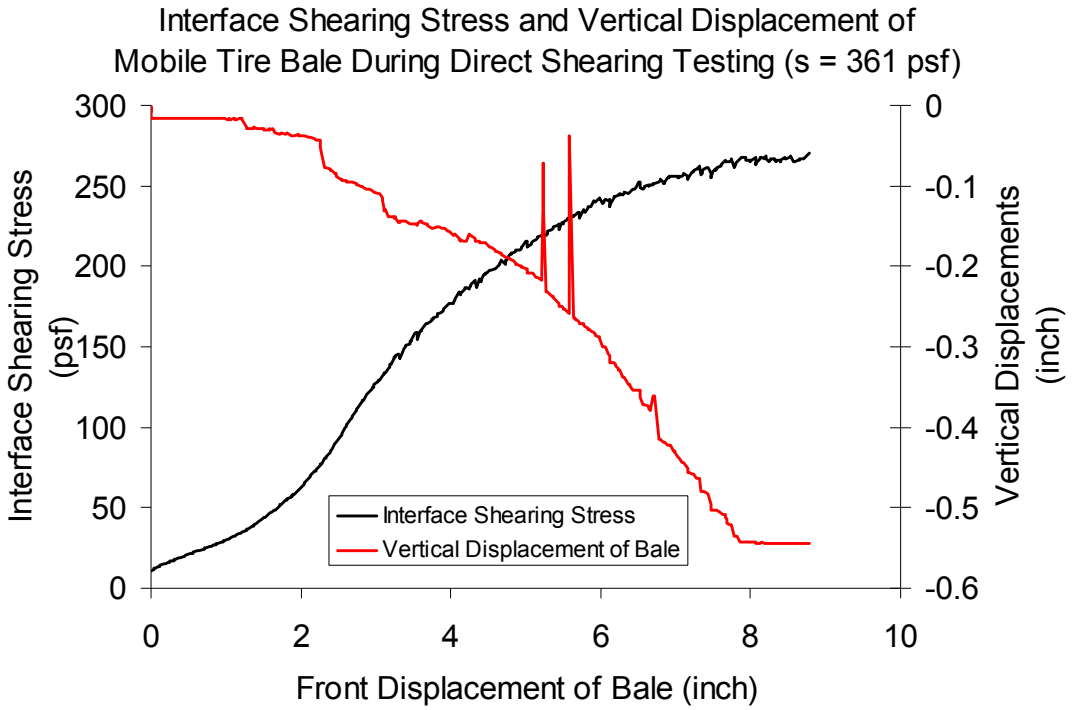

Figure F.34: Interface Shearing Resistance and Vertical Movement of the Tire Bale versus Front Displacement of the Bale for Thick Clay-Tire Bale Interface (Normal Stress = 361 psf)

Appendix G: Testing Data from the Compression Testing of the Tire Bale Structures

The following appendix section provides the data obtained for each of the compression tests conducted for the tire bale structures not specifically reported in Chapter 7. A detailed analysis of the data is provided in Chapter 7.

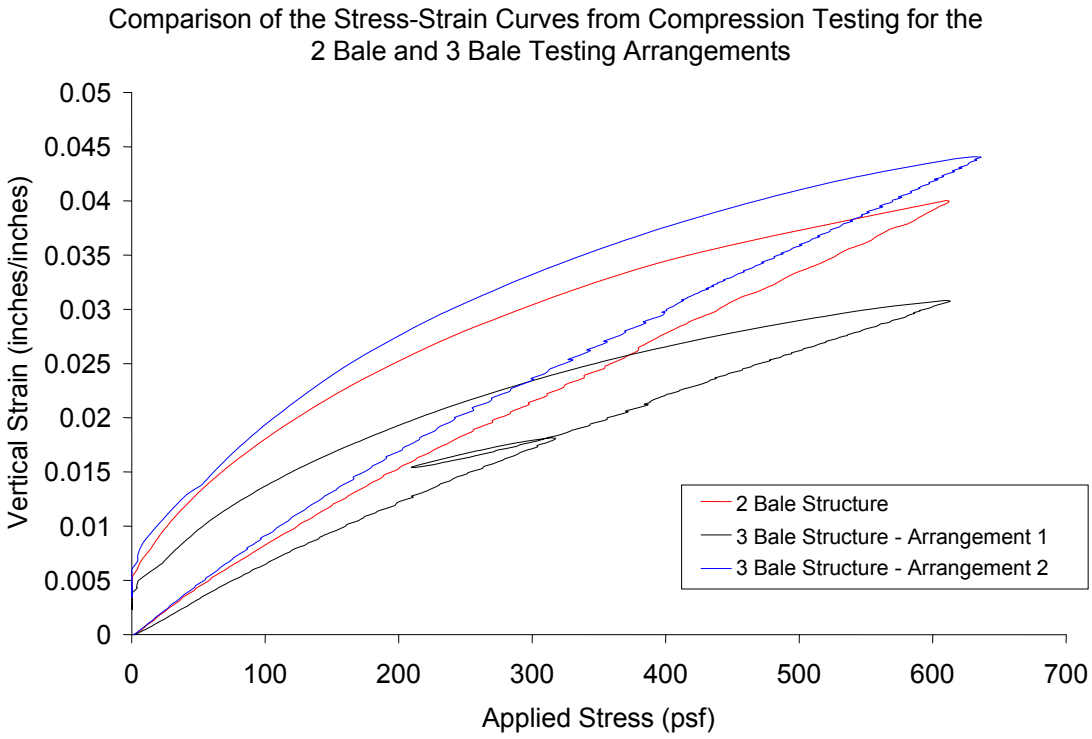

Figure G.1: Total Compressive Strain versus Applied Compressive Load for a Series of Compression Testing on Tire Bales under Different Testing Structures

Results for Arrangement 1 of the 3 Tire Bale Structure

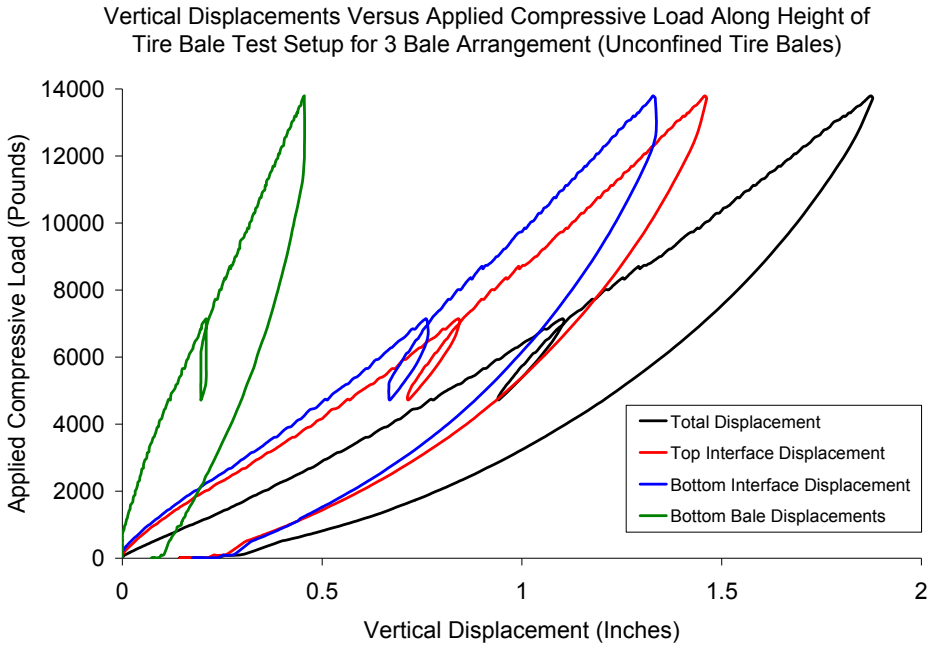

Figure G.2: Vertical Displacements of the Unconfined 3Bale Structure

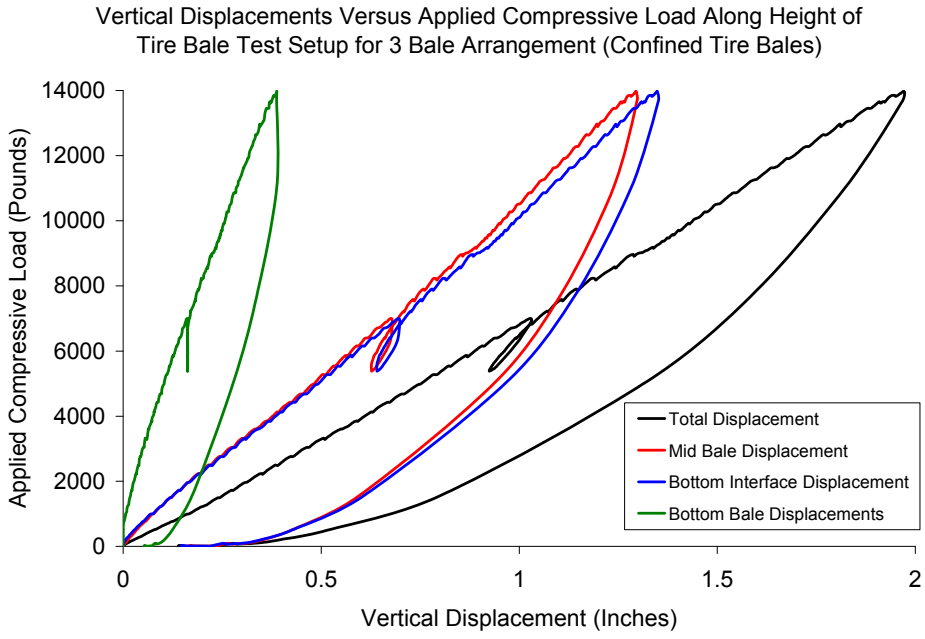

Figure G.3: Vertical Displacement of the Minimally Confined 3 Bale Structure

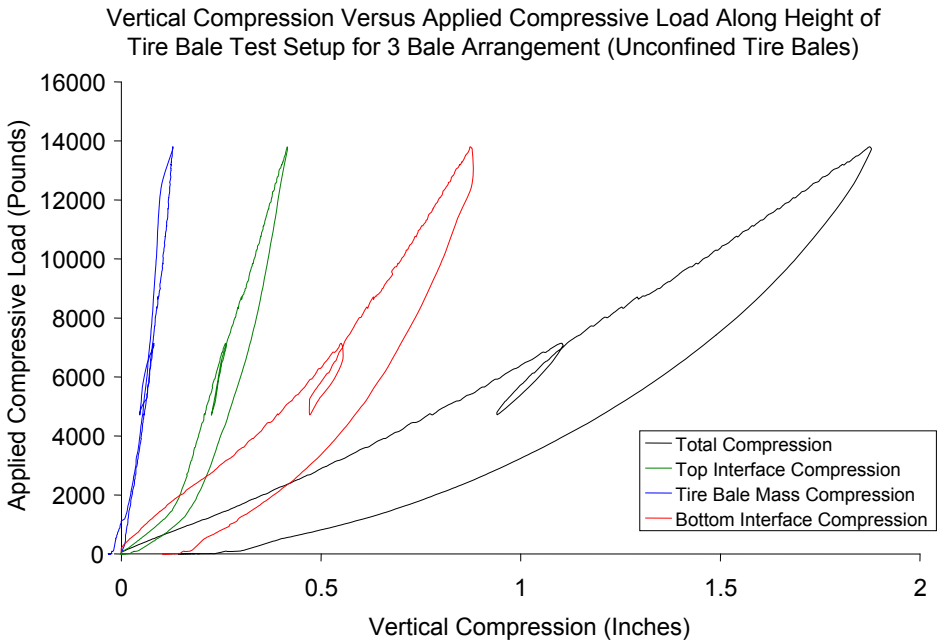

Figure G.4: Vertical Compressions of the Unconfined 3 Bale Structure

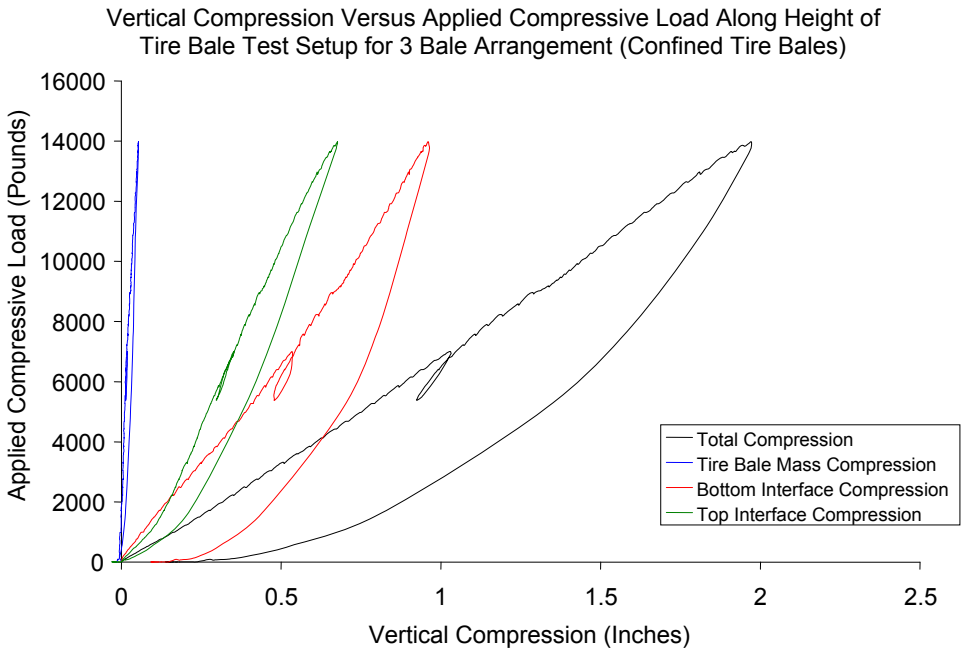

Figure G.5: Vertical Compressions of the Minimally Confined 3 Bale Structure

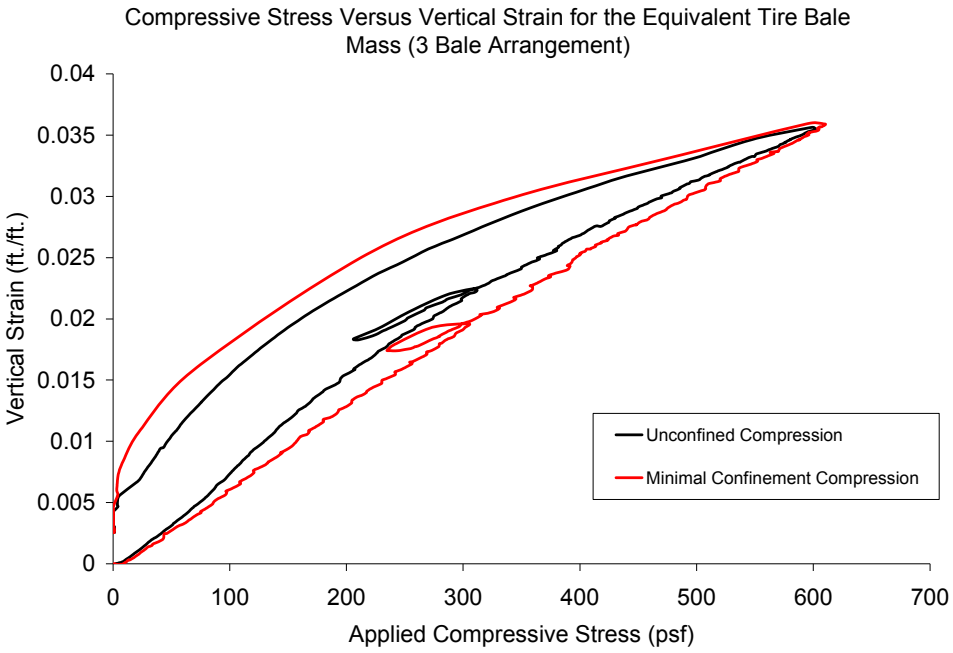

Figure G.6: Compression of the Equivalent Tire Bale Mass for the Unconfined and Minimally Confined 3 Bale Structure

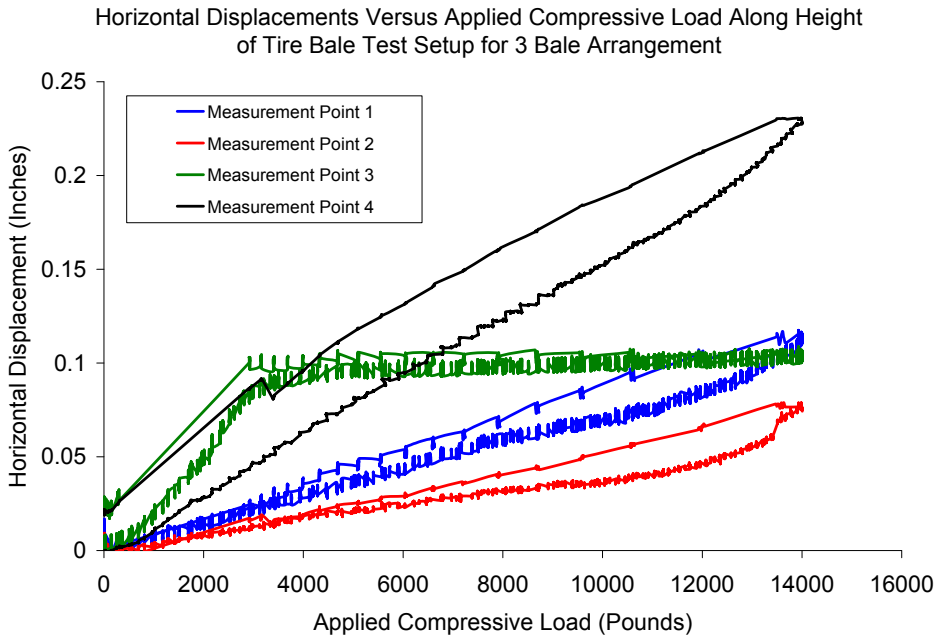

Figure G.7: Horizontal Deformation of the Tire Bale Structure during Unconfined Compression for the 3 Bale Structure

Results for Arrangement 2 of the 3 Tire Bale Structure

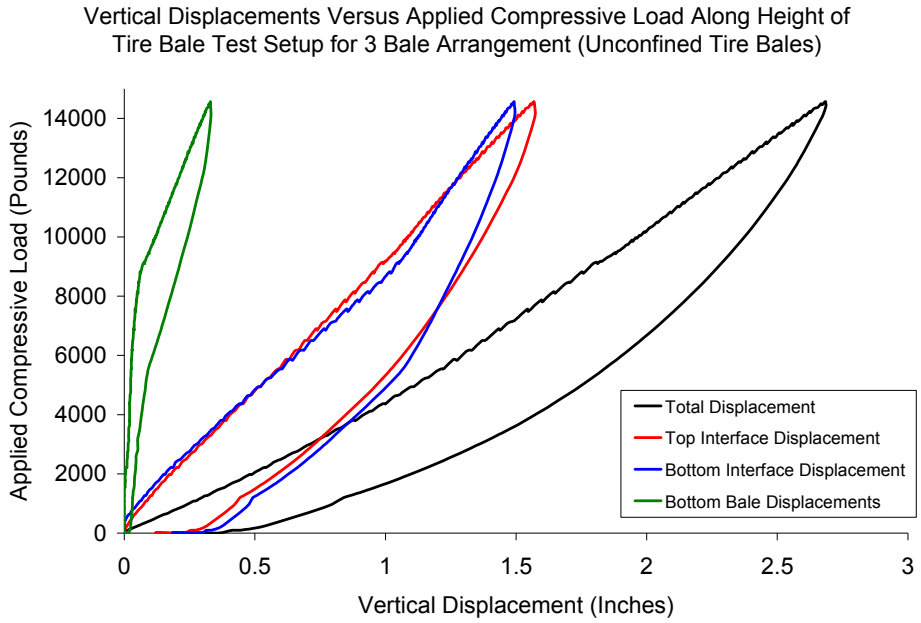

Figure G.8: Vertical Displacements of the Unconfined 3Bale Structure

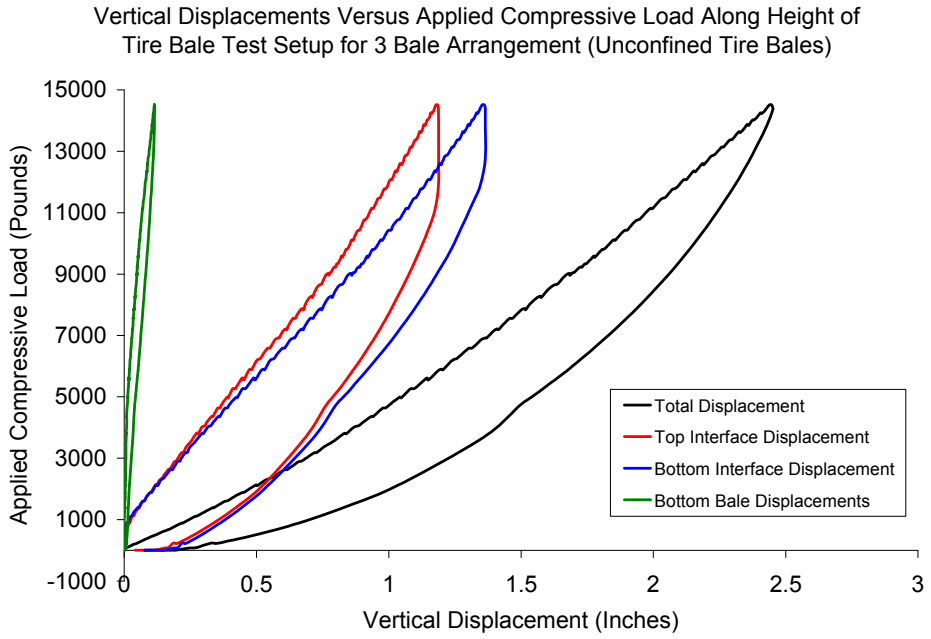

Figure G.9: Vertical Displacement of the Minimally Confined 3 Bale Structure

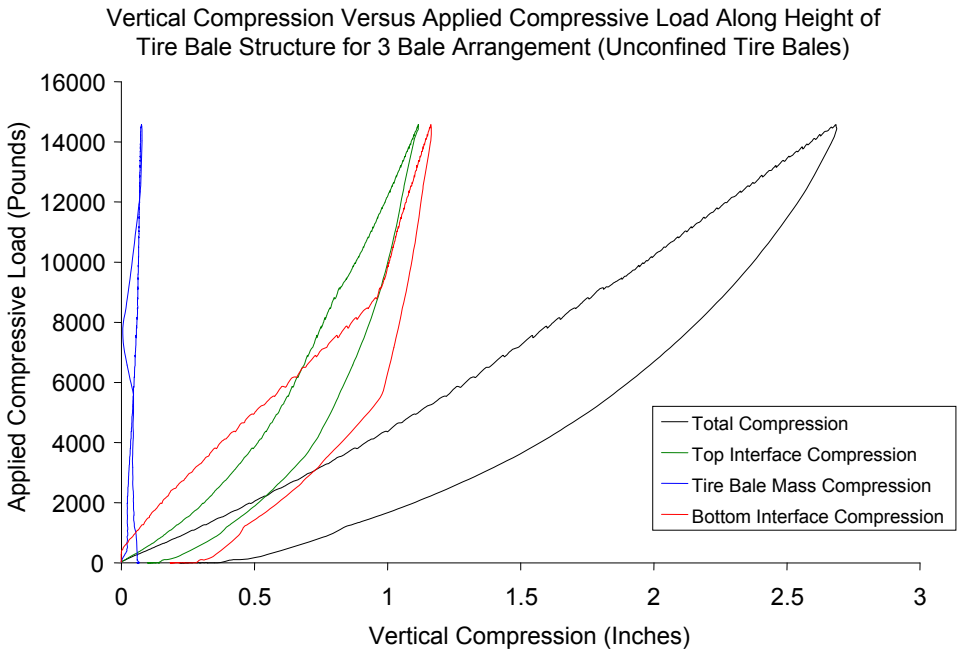

Figure G.10: Vertical Compressions of the Unconfined 3 Bale Structure

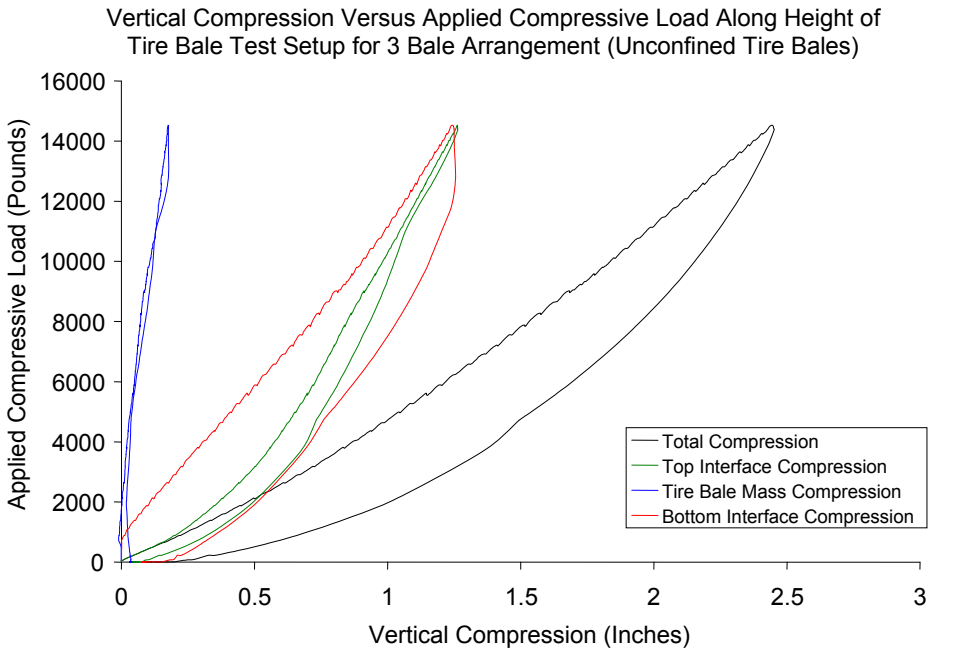

Figure G.11: Vertical Compressions of the Minimally Confined 3 Bale Structure

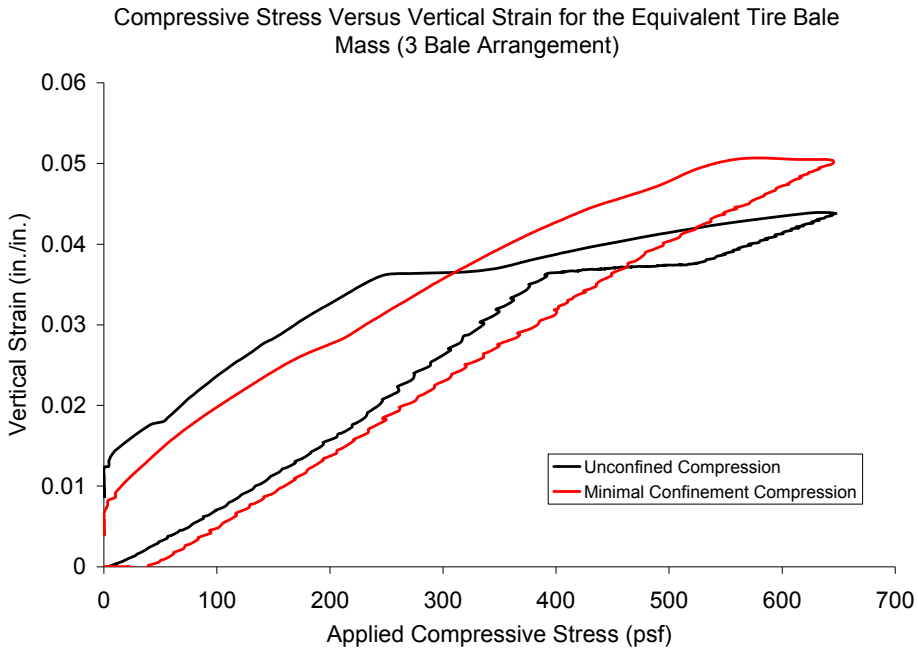

Figure G.12: Compression of the Equivalent Tire Bale Mass for the Unconfined and Minimally Confined 3 Bale Structure

Results for the 2 Tire Bale Structure

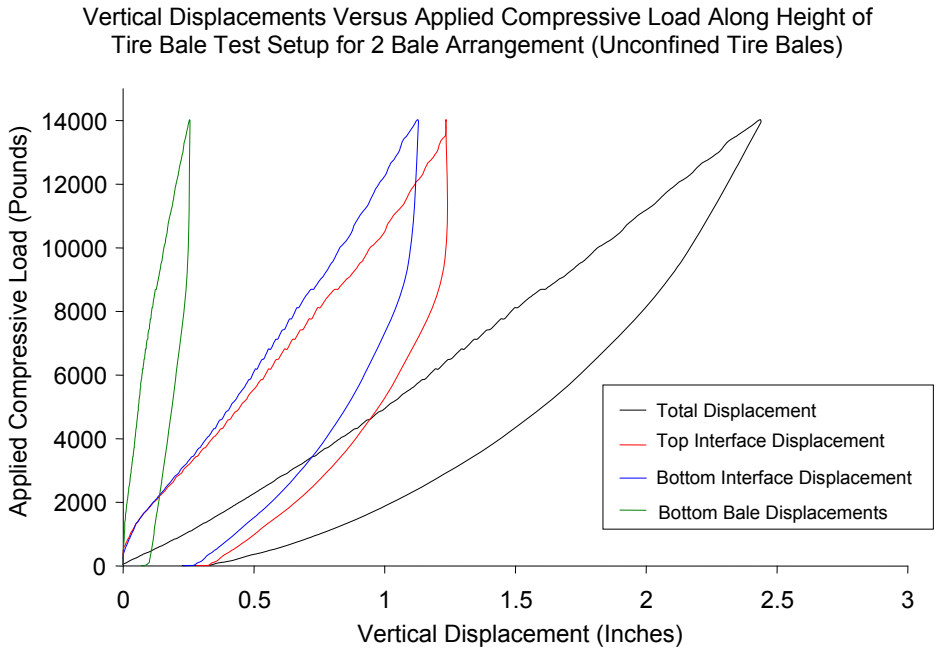

Figure G.13: Vertical Displacements of the Unconfined 2 Bale Structure

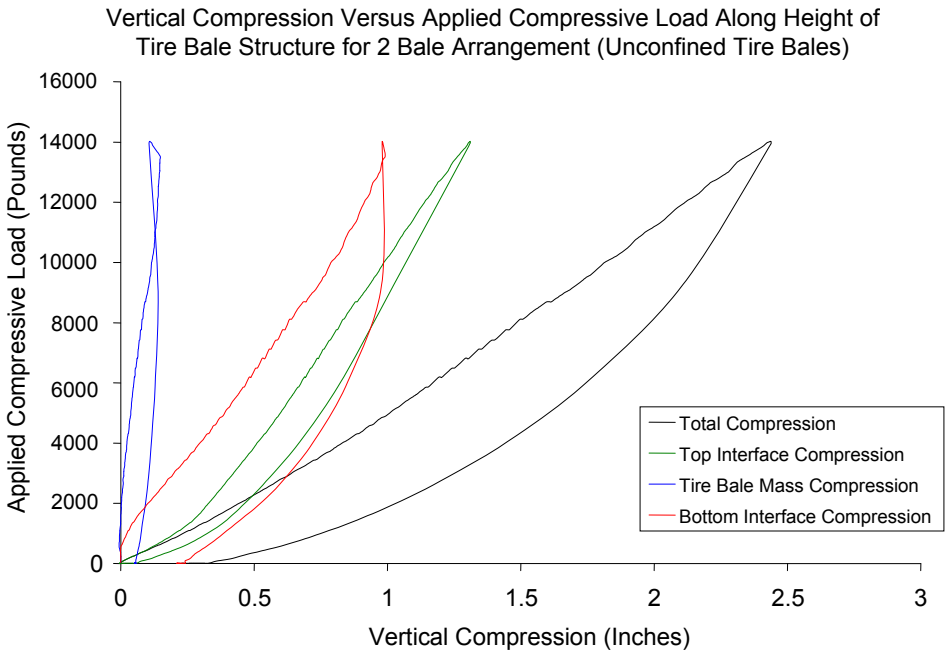

Figure G.14: Vertical Compressions of the Unconfined 2 Bale Structure